Terms and Conditions of Use of Digitised Theses from Trinity College Library Dublin

Copyright statement

All material supplied by Trinity College Library is protected by copyright (under the Copyright and Related Rights Act, 2000 as amended) and other relevant Intellectual Property Rights. By accessing and using a Digitised Thesis from Trinity College Library you acknowledge that all Intellectual Property Rights in any Works supplied are the sole and exclusive property of the copyright and/or other IPR holder. Specific copyright holders may not be explicitly identified. Use of materials from other sources within a thesis should not be construed as a claim over them.

A non-exclusive, non-transferable licence is hereby granted to those using or reproducing, in whole or in part, the material for valid purposes, providing the copyright owners are acknowledged using the normal conventions. Where specific permission to use material is required, this is identified and such permission must be sought from the copyright holder or agency cited.

Liability statement

By using a Digitised Thesis, I accept that Trinity College Dublin bears no legal responsibility for the accuracy, legality or comprehensiveness of materials contained within the thesis, and that Trinity College Dublin accepts no liability for indirect, consequential, or incidental, damages or losses arising from use of the thesis for whatever reason. Information located in a thesis may be subject to specific use constraints, details of which may not be explicitly described. It is the responsibility of potential and actual users to be aware of such constraints and to abide by them. By making use of material from a digitised thesis, you accept these copyright and disclaimer provisions. Where it is brought to the attention of Trinity College Library that there may be a breach of copyright or other restraint, it is the policy to withdraw or take down access to a thesis while the issue is being resolved.

Access Agreement

By using a Digitised Thesis from Trinity College Library you are bound by the following Terms & Conditions. Please read them carefully.

I have read and I understand the following statement: All material supplied via a Digitised Thesis from Trinity College Library is protected by copyright and other intellectual property rights, and duplication or sale of all or part of any of a thesis is not permitted, except that material may be duplicated by you for your research use or for educational purposes in electronic or print form providing the copyright owners are acknowledged using the normal conventions. You must obtain permission for any other use. Electronic or print copies may not be offered, whether for sale or otherwise to anyone. This copy has been supplied on the understanding that it is copyright material and that no quotation from the thesis may be published without proper acknowledgement.

Tissue engineering scaled-up anatomically shaped osteochondral constructs for joint resurfacing

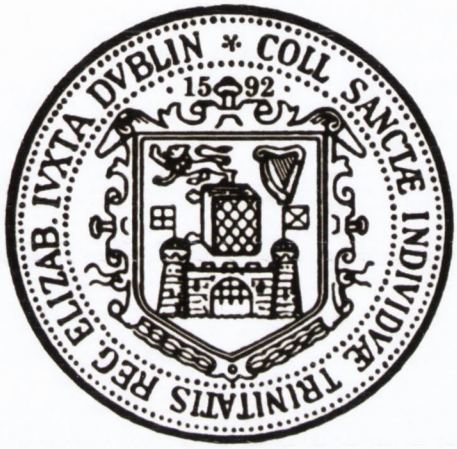

Tariq Mesallati BA BAI

A thesis submitted to the University of Dublin in partial fulfilment of the requirements for the degree of

Doctor in Philosophy

Trinity College Dublin

September 2014

Supervisor

Dr Daniel J. Kelly

External Examiner

Prof Manuela Gomes

Internal Examiner

Prof Garret O'Donnell

Declaration

I declare that this thesis has not been submitted as an exercise for a degree at this or any other university and it is entirely my own work.

I agree to deposit this thesis in the University's open access institutional repository or allow the library to do so on my behalf, subject to Irish Copyright Legislation and Trinity College Library conditions of use and acknowledgement.

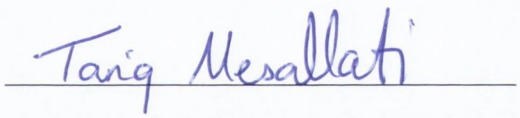

Tariq Mesallati

Summary

Partial and total joint replacements are the only surgical procedures currently available to treat articular cartilage degeneration associated with degenerative diseases such as osteoarthritis (OA). While these procedures are well established, they are not without limitations and failures are not uncommon. Joint replacement prostheses also have a finite lifespan making them unsuitable for the growing population of younger and more active patients requiring treatment for OA. In recent years there has been increased interest in the use of cell and tissue engineering based therapies for the treatment of focal cartilage defects. These therapies aim to regenerate or replace damaged tissues through a combination of cells, three-dimensional scaffolds and signalling molecules. While significant progress has been made in this field, realizing an efficacious therapeutic option for the treatment of OA remains elusive and is considered to be one of the greatest challenges in the field of orthopaedic medicine. The overall objective of this thesis, therefore, was to tissue engineer a scaled-up, anatomically shaped osteochondral construct that could potentially be used to replace the articulating surface of a synovial joint. Such a construct could be used as an alternative to, or delay the need for, unicompartmental or total joint arthroplasty.

To achieve this goal requires a number of challenges to be addressed. Given that OA affects multiple tissues in the diseased joint, including the articular cartilage and underlying subchondral bone, it is therefore essential to develop a scalable approach to simultaneously engineer both of these tissue types within an osteochondral construct using readily available cell sources. Generating anatomically shaped grafts mimicking the articulating surface of damaged joints is also essential to maintain proper joint mechanics during joint articulation.

This thesis began by investigating if dynamic compression in combination with modified scaffold architecture could result in enhanced, homogeneous cartilage formation, as a means of engineering scaled-up, functional cartilaginous constructs of a clinically relevant size. Dynamic compression was found to significantly increase sGAG synthesis in solid chondrocyte (CC) seeded agarose hydrogels, and preferentially increase collagen accumulation in regions of constructs where FE modelling predicted highest levels of fluid flow. The introduction of nutrient channels, however, was found to have a detrimental effect on cartilage formation within constructs. Cartilage extracellular matrix (ECM) accumulation was generally quite low in agarose hydrogels, at least when compared to typical native articular cartilage values.

In light of these results using agarose encapsulation, the next phase of this thesis compared a self-assembly (or scaffold-free) strategy to agarose encapsulation as a means of engineering functional cartilaginous grafts using culture expanded CCs. At high seeding densities, it was observed that total sGAG and collagen synthesis was greater with agarose encapsulation than self-assembly. When normalized to wet weight however, self-assembled constructs exhibited significantly higher levels of collagen accumulation compared to agarose hydrogels. Furthermore, self-assembly appeared to lead to the faster generation of a more hyaline-like tissue, with a tissue architecture and a ratio of collagen to sGAG content more closely resembling native articular cartilage.

The potential use of CCs for cartilage tissue engineering applications is severely limited due to the lack of available healthy donor cartilage for harvesting cells in older or diseased patients. Dedifferentiation of CCs during culture expansion is also a problem. Therefore, it was next investigated if cartilage-like grafts could be engineered by self-assembly of infrapatellar fat pad-derived mesenchymal stem cells (FPSCs). Self-assembly of FPSCs led to the formation of a dense cartilaginous tissue, with cartilage ECM accumulation approaching native cartilage values.

An alternative strategy to using CCs or mesenchymal stems cells (MSCs) alone is to use a co-culture of CCs and MSCs to generate cartilage. This was next investigated with the results showing that mixed co-culture can lead to increased proliferation and cartilage matrix synthesis compared to monoculture controls. In addition, structured co-culture was shown to specifically lead to increased proliferation and matrix synthesis of CCs.

In the final part of the thesis, the generation of scaled-up anatomically shaped osteochondral constructs was investigated. Tissue engineered osteochondral grafts (~2 cm diameter) mimicking the geometry of the medial femorotibial joint were generated from moulds fabricated by rapid prototyping. It was found that a chondrogenically primed MSC seeded alginate hydrogel could support endochondral bone formation *in vivo*, and furthermore, that a phenotypically stable layer of articular cartilage could be engineered over this bony tissue using self-assembly of CCs and MSCs.

To conclude, this thesis provides a novel framework for tissue engineering biological joint replacement prostheses that could potentially regenerate damaged/diseased joints. If certain challenges can be overcome, it opens up the potential of a therapeutic solution for the millions of people suffering from OA worldwide.

Acknowledgements

I would like to first sincerely thank my supervisor, Dr. Danny Kelly, for his incredible support, guidance, motivation and positivity over my entire time in Trinity College, and his invaluable help in preparing and writing this thesis.

I would also like to thank all of the professors and staff within the Trinity Centre for Bioengineering (TCBE) for all of their help over the years. In particular, I would especially like to thank Dr. Conor Buckley, both for his hands-on help in the lab in the early days of the PhD, to sound advice and deeply appreciated help with papers in the later years.

To all the guys and girls in the TCBE postgrad and postdoc offices, I'd like to really thank everyone for all of the brilliant events and holidays away over the years, not to mention the crazy nights out in Dublin unavoidably ending in coppers! Special mention to Darren, Eamon and Alanna for the months writing up the theses together, making the process much more bearable.

I'd also like to thank IRCSET for 3 years of PhD funding, and last but not least, my family and friends outside of Trinity for all their support and love!

Table of Contents

List of Figures

List of Tables

Nomenclature

The nomenclature contains some of the abbreviations used in this thesis. It is not a full list of all abbreviations and symbols used - they will be explained in the text whenever used.

%w/w	% wet weight
ACI	Autologous chondrocyte implantation
ALP	Alkaline phosphatase
ANOVA	Analysis of variance
BMP	Bone morphogenetic protein
BMSC	Bone marrow derived mesenchymal stem cell
B-TCP	β-tri calcium phosphate
$CaCl_2$	Calcium chloride
CC	Chondrocyte
CFU-F	Colony forming unit-fibroblast
DC	Dynamic compression
DMSO	Dimethyl sulphoxide
ECM	Extracellular matrix
EDTA	Ethylenediaminetetraacetic acid
FBS	Fetal bovine serum
FGF	Fibroblast growth factor
FPSC	Infrapatellar fat pad derived stem cell
FS	Free swelling

H&E	Haematoxylin and Eosin
HA	Hydroxyapatite
HCL	Hydrochloric acid
Ihh	Indian hedgehog
IL	Interleukin
MACI	Matrix-induced autologous chondrocyte implantation
MNC	Mononuclear cell
MSC	Mesenchymal stem cell
PBS	Phosphate buffered saline
PCL	Polycaprolactone
PDMS	Polydimethylsiloxane
PEG	Polyethylene-glycol
PLGA	Poly (lactic-co-glycolic acid)
pO_2	Partial pressure oxygen
PTFE	Polytetrafluoroethylene
PTHrP	Parathyroid hormone-related protein
RGD	Arginine-glycine-aspartic acid
sGAG	Sulphated glycosaminoglycan
TGF-β	Transforming growth factor-β
TMJ	Temporomandibular joint
μCT	Micro-computed tomography
VEGF	Vascular endothelial growth factor

Publications

Journal Articles

T. Mesallati, C. T. Buckley, T. Nagel, D. J. Kelly, Introducing microchannels into chondrocyte-seeded agarose hydrogels influences matrix accumulation in response to dynamic compression and TGF-β3 stimulation. 8th International Conference on Cell & Stem Cell Engineering (ICCE), Dublin, Ireland. International Federation for Medical and Biological Engineering (IFMBE) Proceedings, 30, 26-30 (2011).

T. Mesallati, C. T. Buckley, T. Nagel, D. J. Kelly, Scaffold architecture determines chondrocyte response to externally applied dynamic compression. Biomechanics and Modeling in Mechanobiology (BMMB), 12, 889-899 (2013); published online EpubOct (10.1007/s10237-012-0451-2).

T. Mesallati, C. T. Buckley, D. J. Kelly, A comparison of self-assembly and hydrogel encapsulation as a means to engineer functional cartilaginous grafts using culture expanded chondrocytes. Tissue Engineering Part C, Methods, 20, 52-63 (2014); published online EpubJan (10.1089/ten.TEC.2013.0118).

T. Mesallati, C. T. Buckley, D. J. Kelly, Engineering articular cartilage-like grafts by self-assembly of infrapatellar fat pad-derived stem cells. Biotechnology and Bioengineering, 111, 1686-1698 (2014); published online EpubAug (10.1002/bit.25213).

Conference Abstracts

T. Mesallati, C. T. Buckley, T. Nagel, D. J. Kelly. The effect of introducing micro-channels into dynamically compressed chondrocyte-seeded hydrogels. 8th International Conference on Cell & Stem Cell Engineering (ICCE), Trinity College Dublin, Ireland, 11th-12th June 2010.

T. Mesallati, C. T. Buckley, T. Nagel, D. J. Kelly. Scaffold architecture determines chondrocyte response to externally applied dynamic compression. 57th Annual Meeting of the Orthopaedic Research Society, Long Beach, California, USA, Paper 0232/Poster 0232, 13th-16th January 2011.

T. Mesallati, C. T. Buckley, D. J. Kelly. A comparison of the functional properties of cartilage tissues engineered with fat pad derived MSCs using either self-assembly or agarose encapsulation. Proceedings of the 17th Annual Conference of the Section of Bioengineering of the Royal Academy of Medicine in Ireland, National University of Ireland, Galway, Ireland, January 2011.

T. Mesallati, C. T. Buckley, D. J. Kelly. Is self-assembly using progenitor cells a better approach to engineering functional cartilage tissue than hydrogel encapsulation? Tissue Engineering and Regenerative Medicine International Society (TERMIS), Granada, Spain, Histology and Histopathology, Cellular and Molecular Biology, Volume 26 (supplement 1), page 81 (paper 8.010), 7th-10th June 2011.

T. Mesallati, C. T. Buckley, D. J. Kelly. Engineering functional cartilaginous grafts using chondrocyte-agarose constructs supported by a superficial layer of stem cells. Proceedings of the 18th Annual Conference of the Section of Bioengineering of the Royal Academy of Medicine in Ireland, Queens University, Belfast, Northern Ireland, January 2012.

T. Mesallati, C. T. Buckley, D. J. Kelly. Engineering functional cartilaginous grafts using chondrocyte agarose constructs supported by a superficial layer of stem cells. Tissue Engineering and Regenerative Medicine International Society (TERMIS), 3rd

World Congress, Hofburg Congress Centre, Vienna, Austria, 5th-8th September 2012.

T. Mesallati, C. T. Buckley, D. J. Kelly. An evaluation of mesenchymal stem cell seeded alginate hydrogels for generating scaled-up, anatomically accurate constructs suitable for total joint regeneration. Proceedings of the 19th Annual Conference of the Section of Bioengineering of the Royal Academy of Medicine in Ireland, Trinity College Dublin, Dublin, Ireland, January 2013.

T. Mesallati, E.J. Sheehy, T. Vinardell, C. T. Buckley, D. J. Kelly. Tissue engineering scaled-up, anatomically accurate, osteochondral constructs for joint resurfacing. The Anatomical Society Summer Meeting, Royal College of Surgeons in Ireland (RCSI), Dublin, Ireland, Journal of Anatomy, Volume 224, Issue 2, page 228, 4th-5th July 2013.

T. Mesallati, E.J. Sheehy, C. T. Buckley, D. J. Kelly. Tissue engineering scaled-up, anatomically accurate osteochondral constructs for joint resurfacing. Proceedings of the 20th Annual Conference of the Section of Bioengineering of the Royal Academy of Medicine in Ireland, Limerick, Ireland, January 2014.

T. Mesallati, E.J. Sheehy, T. Vinardell, C. T. Buckley, D. J. Kelly. Tissue engineering scaled-up, anatomically accurate, osteochondral constructs for joint resurfacing. 60th Annual Meeting of the Orthopaedic Research Society, Hyatt Regency, New Orleans, Louisiana, USA, 15th-18th March 2014.

T. Mesallati, E.J. Sheehy, T. Vinardell, C. T. Buckley, D. J. Kelly. Tissue engineering scaled-up, anatomically accurate, osteochondral constructs for joint resurfacing. Tissue Engineering and Regenerative Medicine International Society (TERMIS), Genova, Italy, 10th-13th June 2014.

1 Introduction

1.1 Cell Based Therapies for Cartilage Repair

Articular cartilage is a dense connective tissue which, by providing a bearing surface with low friction and wear, helps distribute the loads between opposing bones in a synovial joint. The cartilage cells, chondrocytes, maintain the extracellular matrix (ECM) in healthy tissue, but when injured, cartilage has a poor intrinsic capacity for healing. The avascular nature of the tissue and the tight network of ECM limit cell migration to the injury site, thereby contributing to the tissue's poor regenerative potential (Mankin, 1982). Damage to articular cartilage can occur through trauma or joint disease. If articular cartilage defects are left untreated, they can lead to joint disorders, such as osteoarthritis (OA) (Schinhan et al., 2011).

OA is the most common joint disorder, commonly affecting the hands, feet, spine, and large weight-bearing joints, such as the hips and knees. The disease, characterized by joint pain and dysfunction, is a major cause of disability in all parts of the world. It is caused by joint degeneration, a process involving the progressive loss of articular cartilage and mechanical integrity of the joint. Although increasing age and excessive articular surface contact stress increase the risk of degeneration in all joints, the pathophysiology of the joint degeneration remains poorly understood (Buckwalter and Martin, 2006). During the course of OA, structural lesions typically develop within the articular cartilage layer (Hunziker, 2002). The lesions increase in size over time, potentially destroying the entire thickness of the cartilage. If the lesions reach the subchondral bone, local bleeding may occur, encouraging the formation of repair tissue. This repair tissue however is more similar to fibrous tissue than to the hyaline cartilage it has replaced (Furukawa et al., 1980), with inferior mechanical properties (Heath and Magari, 1996), and is found to degenerate over time. Although there are no current treatments to prevent or cure OA, the standard procedure for treating the symptoms of the disease is total joint

replacement. This involves surgically replacing the arthritic articular surface with an artificial metal and polyethylene prosthesis. While this procedure can provide pain relief and improved function to patients, it does not restore the articular cartilage and subchondral bone, and the replacement joint can fail over time (Elisseeff et al., 2005). Joint replacement prostheses also have a finite lifespan, making them unsuitable for the growing population of younger and more active patients requiring treatment for OA (Kurtz et al., 2009, Guilak, 2010, Keeney et al., 2011).

Cell and tissue engineering based therapies have demonstrated significant potential for treating focal cartilage defects in recent years (Brittberg et al., 1994, Temenoff and Mikos, 2000b). The general premise of tissue engineering is to provide a functional biological tissue equivalent to replace tissue lost by disease or traumatic events (Elisseeff et al., 2005), with cartilage engineering focusing on cell-based therapies for cartilage repair. Cartilage tissue engineering involves seeding cells onto a three dimensional scaffold, and cultivating the resulting construct under conditions that promote chondrogenesis (Hung et al., 2004). The autologous chondrocyte implantation (ACI) technique is often considered to be the first example of clinical cartilage tissue engineering, with the technique now firmly established for the treatment of focal cartilage defects (Brittberg, 2008). The first step of the technique involves harvesting healthy cartilage from the patient (usually from the femoral condyle), isolating chondrocyte cells from the harvested tissue, and subsequently culturing these cells *in vitro*. The cells are expanded for approximately 2 weeks, after which they are trypsinised, resuspended and transferred to the operating theatre. The second step of ACI involves opening up the damaged joint of the patient, suturing a flap of periosteum over the defect, and implanting the culture expanded cells into the defect site. The procedure has evolved over the years, with second and third generation ACI involving implanting cell-seeded membranes (MACI®), and cell-seeded 3D scaffolds (Hyalograft-C®) into the defect site.

These ACI techniques have successfully been used in repairing small, isolated cartilage defects (Brittberg, 2008), however they are not suitable for treating larger defects or OA joints. In fact, no tissue engineered product currently exists to repair large defects, such as those associated with OA. Defects associated with OA

typically affect multiple tissues in the diseased joint, including the articular cartilage and underlying subchondral bone. There is therefore an essential need to scale-up current tissue engineering based approaches to successfully engineer suitably sized, osteochondral constructs. Generating anatomically shaped grafts mimicking the articulating surface of damaged joints is also essential to maintain proper joint mechanics during joint articulation. If such scaled-up anatomically shaped osteochondral constructs were successfully engineered, they could be used to partially or totally resurface the bones of damaged or diseased synovial joints, and if successful could be used as an alternative to partial or total joint replacement.

1.2 Challenges with Scaling-Up Osteochondral Constructs

The generation of scaled-up cartilaginous grafts with clinically relevant dimensions remains a significant challenge. Engineering such grafts requires either high cell numbers or the use of cells with a high proliferative capacity. Chondrocytes may not be suitable for this reason, due to their limited availability, and restricted proliferative capacity (Gelse et al., 2008, Kock et al., 2012). Mesenchymal stem cells (MSCs) could be used as a potential alternative. MSCs possess the ability to proliferate extensively *in vitro* while maintaining their multipotent differentiation potential (Pittenger et al., 1999), making them an almost ideal cell type for engineering scaled-up cartilaginous constructs large enough to resurface an entire joint. However, cartilage tissue engineered using MSCs can become hypertrophic and undergo endochondral ossification *in vivo* (Farrell et al., 2009, Scotti et al., 2010, Janicki et al., 2010, Farrell et al., 2011, Scotti et al., 2013, Yang et al., 2013), so care must be taken when using this cell type for cartilage tissue engineering purposes. Regardless of the cell source chosen, another key challenge when engineering large constructs *in vitro* is fully meeting the nutritional requirements of the cells. Previous attempts to engineer larger tissue grafts have generally led to the formation of inhomogeneous constructs, with superior tissue formation in the periphery of constructs, surrounding a hypoxic, necrotic core (Martin et al., 2004a). Nutrient transfer limitations to the centre of the construct are believed to be responsible for this problem. Bioreactors are one potential tool for achieving a more homogeneous construct. They enhance nutrient transport and waste removal from

the core, and supply the necessary regulatory signals needed by the cells to differentiate, such as dynamic compressive loading for cartilage formation (Chao et al., 2007). Altering the architecture of the constructs is another possible way to overcome nutrient transport limitations. It has been shown that the introduction of macroscopic channels throughout the depth of the construct can result in the formation of a more homogeneous cartilaginous tissue (Bian et al., 2009b).

Engineering osteochondral tissues (comprised of cartilage and bone) is highly desirable for treating damaged joints, as injuries or diseases of the joint often affect both the articular cartilage and underlying subchondral bone. Also, the use of osteochondral constructs can circumvent the troublesome issue of cartilage to host integration. Poor integration of implanted cartilage with the host tissue is a major problem, but osteochondral constructs can enhance this integration, with the bone region anchoring the cartilage implant to the host tissue. Perhaps the most important aspect of designing osteochondral constructs is obtaining successful integration between the cartilaginous and osseous components. This can be approached via suturing, cell-mediated ECM formation or by the use of fibrin glues (Grayson et al., 2008), however, maintaining the stability of this cartilage-bone union still remains a challenge.

A further challenge in developing tissue engineered therapies to resurface part or all of a joint is generating anatomically shaped grafts, with the graft mimicking the geometry of the joint it is replacing. This is necessary for the implant to maintain the intended joint mechanics during articulation with adjacent surfaces (Grayson et al., 2008). There are examples in the literature of engineered scaffolds and grafts mimicking the geometrical form of articular surfaces (Hung et al., 2003, Alhadlaq et al., 2004, Alhadlaq and Mao, 2005, Lee et al., 2009, Lee et al., 2010, Ding et al., 2013), however tissue engineering anatomically accurate osteochondral constructs of scale remains a significant challenge in the field.

1.3 Objectives of Thesis

The overall objective of this thesis is to tissue engineer a scaled-up, anatomically shaped osteochondral construct that could potentially be used to replace the

articulating surface of a synovial joint. To achieve this goal requires a number of challenges to be addressed:

1. As a means of scaling-up to engineer functional cartilaginous constructs of a clinically relevant size, this thesis will first investigate if the introduction of nutrient channels throughout a cell seeded hydrogel, in combination with dynamic compression, can result in enhanced, homogeneous cartilage formation.
2. This thesis will next compare a self-assembly (or scaffold-free) strategy to agarose hydrogel encapsulation as a means to engineer functional cartilaginous grafts using culture expanded chondrocytes (CCs).
3. Having identified self-assembly as a means of engineering scalable cartilage grafts, but acknowledging the inherent limitations associated with the use of chondrocytes for cartilage tissue engineering, this thesis will next attempt to engineer cartilage-like grafts through self-assembly of infrapatellar fat pad-derived mesenchymal stem cells.
4. As an alternative strategy to using CCs or mesenchymal stems cells (MSCs) alone, this thesis will investigate if a co-culture of CCs and MSCs can be used to generate a more cartilaginous graft *in vitro*.
5. The final part of the thesis will attempt to generate scaled-up anatomically shaped osteochondral constructs. It is hypothesised that scaled-up chondrogenically primed bone marrow-derived MSC (BMSC) seeded alginate hydrogels can support endochondral bone formation *in vivo*, and furthermore, that a phenotypically stable layer of articular cartilage can be engineered over this bony tissue using a self-assembled co-culture of CCs and BMSCs. Furthermore, it is hypothesised that anatomically shaped constructs mimicking the geometry of medial femorotibial joint replacement prostheses can be generated from moulds fabricated by rapid prototyping.

A tissue engineered construct such as this could be used as an alternative to, or delay the need for unicompartmental or total joint arthroplasty, which would be of huge benefit to patients suffering from degenerated cartilage worldwide.

2 Literature Review

2.1 Introduction

The premise of generating scaled-up, anatomically shaped osteochondral constructs (suitable for treating a diseased joint) can be first simplified by considering the independent generation of cartilage and bone. This literature review will therefore begin by describing the composition, structure and function of articular cartilage and bone. A brief discussion of the well-established clinical strategies used when attempting to repair damaged cartilage and bone tissue will be included.

The field of tissue engineering offers the hope of successful cartilage and bone regeneration. Therefore, a review of cartilage and bone tissue engineering strategies will be presented, describing how cells, scaffolds and diverse signals are being integrated for therapeutic effect in this exciting field. Finally, this chapter will review key papers attempting to engineer osteochondral constructs, ranging from those suitable in treating small focal defects, to recent advances in generating scaled-up, clinically relevant scaffolds potentially suitable for treating large defects. Anatomically-accurate osteochondral constructs currently being generated in the field of joint condyle repair will also be examined.

2.2 Composition, Structure and Function of Articular Cartilage

2.2.1 Articular Cartilage

Articular cartilage is a highly organized avascular tissue composed of an extensive extracellular matrix synthesized by cartilage cells, or chondrocytes. This hyaline cartilage covers the subchondral bone in diarthrodial joints (Figure 2-1), where, in conjunction with synovial fluid, it provides a smooth lubricated surface for joint movement by distributing load evenly, whilst also protecting the articular surface of bone from abrasion (Kheir and Shaw, 2009). The joint is surrounded by a dense fibrous membrane, known as the perichondrium (Buckwalter, 1983). Articular cartilage in adults is a relatively acellular tissue, with cell volume averaging

approximately 2% of the total cartilage volume in human adults (Poole et al., 2001). The majority of the tissue is composed of extracellular matrix (ECM).

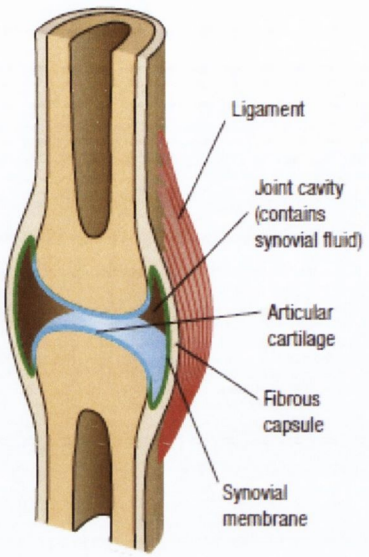

Figure 2-1: Cross-sectional diagram through a synovial joint (Setton, 2008).

2.2.2 Zones of Organisation

Articular cartilage is typically divided into four zones: superficial, middle, deep, and the calcified cartilage zone (Newman, 1998). Chondrocyte phenotype, shape and organization vary through the depth of articular cartilage; see Figure 2-2(A). In the superficial tangential zone (STZ) chondrocytes are flattened and aligned parallel to the articular surface. Chondrocytes at the articular surface produce a protein known as superficial zone protein (Schumacher et al., 1999). This protein is also known as lubricin, and it has a significant role in the smooth articulation provided by articular cartilage in joints (Warman, 2000). Below the superficial zone is the middle zone, which has a lower cell density with more rounded and randomly distributed chondrocytes. Chondrocytes in the deep zone are spheroidal, and are arranged in a columnar orientation, perpendicular to the joint surface. The lowest cell density is found in this zone (Mitrovic et al., 1983). Finally, a thin zone of calcified cartilage separates the cartilage from the subchondral bone, with the boundary separating the

calcified and non-calcified cartilage known as the tidemark. The cells in this calcified zone usually express the hypertrophic phenotype, and the calcified matrix they produce helps provide excellent structural integration between the cartilage and the subchondral bone (Poole et al., 2001).

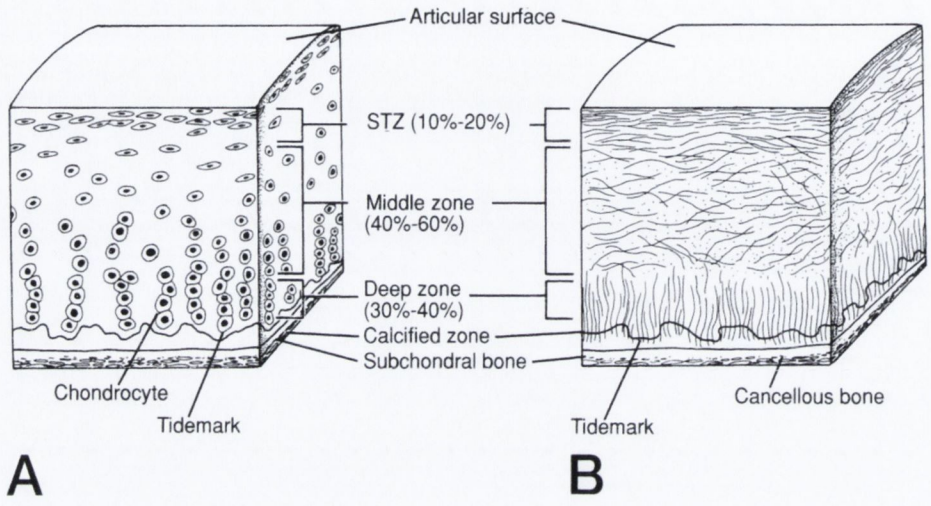

Figure 2-2: Structure of articular cartilage. (A) schematic representation of the chondrocyte organization throughout the depth of articular cartilage; (B) schematic representation of the collagen fibre architecture throughout the depth of articular cartilage (Buckwalter et al., 1994).

During embryogenesis stem cells in the developing limb differentiate into chondrocytes, which in turn secrete a specialised cartilaginous extracellular matrix (ECM). These cartilage cells are distributed either singularly, or in clusters known as isogeneous groups (Kheir and Shaw, 2009). Each chondrocyte is surrounded by a thin, pericellular matrix that provides hydrodynamic protection for the chondrocyte (Kheir and Shaw, 2009). The chondrocyte and its pericellular matrix are collectively known as a chondron (Poole, 1997). In each chondron, the chondrocyte is linked to a high pericellular concentration of proteoglycans, as well as hyaluronan, biglycans and matrix glycoproteins (Poole et al., 1987).

The chondrocytes are embedded within the extracellular matrix that they, themselves produce and maintain. This matrix is saturated with fluid (60% to 80% of wet weight of cartilage), and consists of a highly organized framework of structural macromolecules, including collagens (70% of dry weight of cartilage),

proteoglycans (15% to 25%), and non-collagenous proteins and glycoproteins (Buckwalter and Mankin, 1997).

Many different types of collagen can be found in articular cartilage, namely types II, VI, IX, X, and XI, although type II accounts for approximately 90% to 95% of the total collagen present in the matrix. Collagen content is highest at the articular surface (Figure 2-3), and decreases toward the deep zone (Ateshian, 2009). Types IX and XI, along with type II, form fibrils that interweave to form a mesh (Temenoff and Mikos, 2000b).

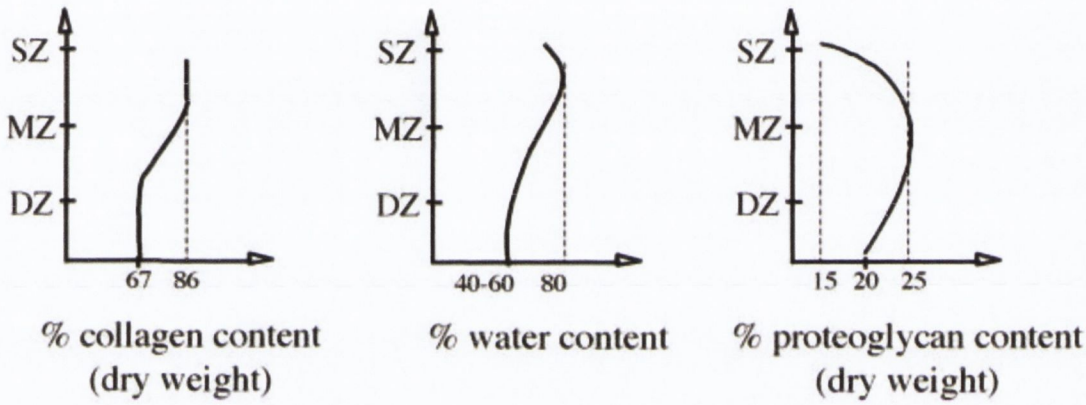

Figure 2-3: Distribution of collagen, water and proteoglycan content as a function of depth from the articular surface (Mow and Guo, 2002).

Collagen fibre architecture varies quite dramatically throughout the depth of articular cartilage, as shown in Figure 2-2(B). In the STZ, collagen fibres are arranged parallel to the articular surface. In the middle zone, the fibres have a random and oblique orientation, and are less densely packed to accommodate the high density of proteoglycans and tissue fluid. The collagen fibrils run vertically to the articular surface in the deep zone, anchoring the tissue to the calcified zone. The organization of the collagen fibrils into a tight meshwork provides cartilage with its most significant property, its tensile strength (

Figure 2-4A). It also contributes to the cohesiveness of the tissue by mechanically entrapping large proteoglycans (Buckwalter and Mankin, 1997). The highest tensile properties are found in the superficial zone of articular cartilage, allowing it to accommodate the shear, tensile, and compressive forces encountered during articulation (Poole et al., 2001). Although strong in tension, collagen fibres offer little resistance to compression (

Figure 2-4B) (Mow and Hung, 2001).

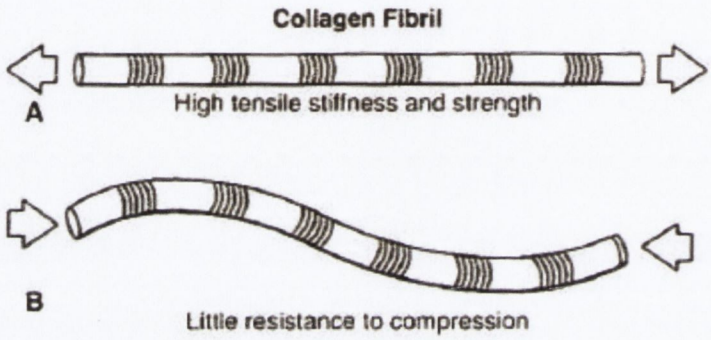

Figure 2-4: Illustration of the mechanical properties of collagen fibrils; (A) stiff and strong in tension, but (B) weak and buckling easily with compression (Mow and Hung, 2001).

Cartilage proteoglycans exist either as monomers or as aggregates. The proteoglycan monomers consist of a central protein core, with one or more glycosaminoglycan (GAG) chain (long unbranched polysaccharide chains, which consist of repeating disaccharides that contain an amino sugar) bound to it (Buckwalter and Mankin, 1997). There are four main types of GAGs found in cartilage, namely hyaluronic acid, chondroitin sulphate, keratan sulphate, and dermatan sulphate (Buckwalter and Mankin, 1997). Within each GAG chain, each unit of disaccharide has at least one negatively charged carboxylate or sulphate group, resulting in GAG chains with a negative overall charge. These negatively charged GAGs give proteoglycans their hydrophilic properties, thus allowing cartilage to retain water, which is essential to its proper function (Kheir and Shaw, 2009). The most important proteoglycan monomer is aggrecan (Figure 2-5), as it

fills most of the interfibrillar space of the articular cartilage matrix. It consists of chondroitin sulphate and keratan sulphate chains covalently bound to the central protein core, with the core containing three globular regions, G1, G2, and G3. Aggrecan may be visualised as having a "bottle-brush" like structure (Mow and Hung, 2001).

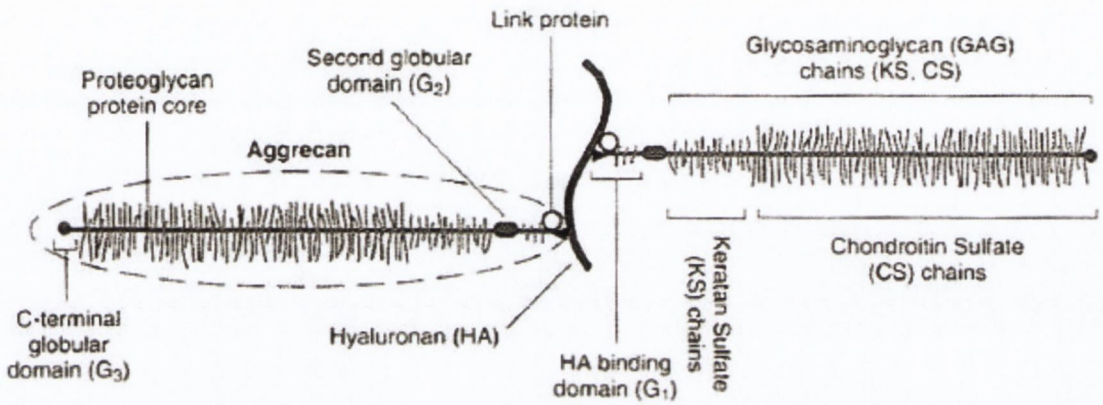

Figure 2-5: Schematic depiction of aggrecan (Mow and Hung, 2001).

The proteoglycan aggregates (Figure 2-6) are composed of a central hyaluronic acid chain, to which proteoglycan monomers are attached by means of specialised link proteins (Newman, 1998). These aggregates can have up to several hundred monomers non-covalently attached to their central chain, via a specific hyaluronic acid binding region (HABR). The formation of aggregates helps to anchor proteoglycans within the cartilage matrix, which is crucial to prevent their movement during deformation of the tissue (Buckwalter and Mankin, 1997). This, in turn, helps add structural stability and rigidity to the ECM (Mow and Hung, 2001).

In contrast to collagen, the proteoglycan content is lowest at the articular surface (Figure 2-3), increases in the middle zone, then remains constant or decreases slightly in the deep zone (Ateshian, 2009).

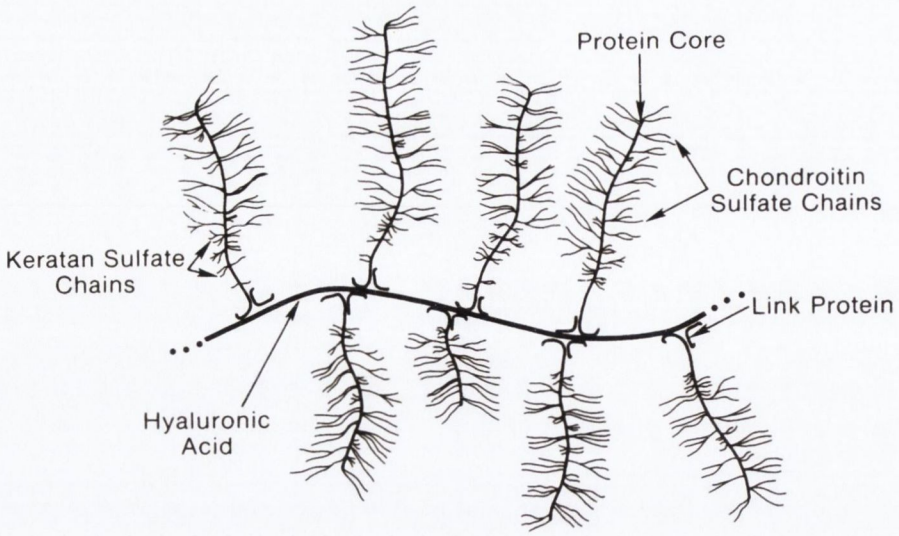

Figure 2-6 Illustration of a proteoglycan aggregate (Buckwalter, 1982) .

The most abundant component of articular cartilage is tissue fluid. This fluid contains gases, metabolites and a large amount of positively charged cations, to balance the negatively charged GAGs in the ECM (Temenoff and Mikos, 2000b). It is the exchange of this fluid with synovial fluid in the joint, through diffusion, which supplies the avascular cartilage with essential nutrients and oxygen. Interstitial fluid content is highest in the superficial region (Figure 2-3), and decreases with increasing depth (Ateshian, 2009). In the tissues, the collagen intrafibrillar space contains approximately 30% of the water, with the majority of the water (70%) residing in the proteoglycan solution domain. This interfibrillar water is free to move when a load or pressure gradient is applied to the tissue (Gu et al., 1998). The movement of the interstitial fluid is important in controlling cartilage mechanical behaviour and joint lubrication (Mow and Hung, 2001).

The chemical structure of proteoglycan aggregates, and their physical interaction with collagen and the interstitial fluid, determines in part the structural organization of the ECM and its swelling properties (Mow and Hung, 2001). The negative electrical charges of the GAG chains create strong intramolecular and intermolecular charge-charge repulsion forces. In a structural sense, these repulsion forces extend and stiffen the proteoglycan macromolecules into the interfibrillar space formed by the surrounding collagen network, allowing the macromolecules to

occupy a large solution domain (Figure 2-7A) (Mow and Hung, 2001). In an effort to balance this negative electrical charge, and maintain tissue electroneutrality, the interstitial fluid attempts to attract more cations than anions into the tissue. This results in a net imbalance in electrolyte concentration between the interstitial fluid and surrounding tissue bath, thus producing an osmotic pressure difference, known as Donnan osmotic pressure (Ateshian, 2009). This osmotic pressure causes swelling of the solid matrix of the tissue, which is resisted and balanced by the tensile stress of the collagen network (Ateshian, 2009). Under this swelling pressure, the collagen network is subjected to a pre-stress of significant magnitude (Setton et al., 1998).

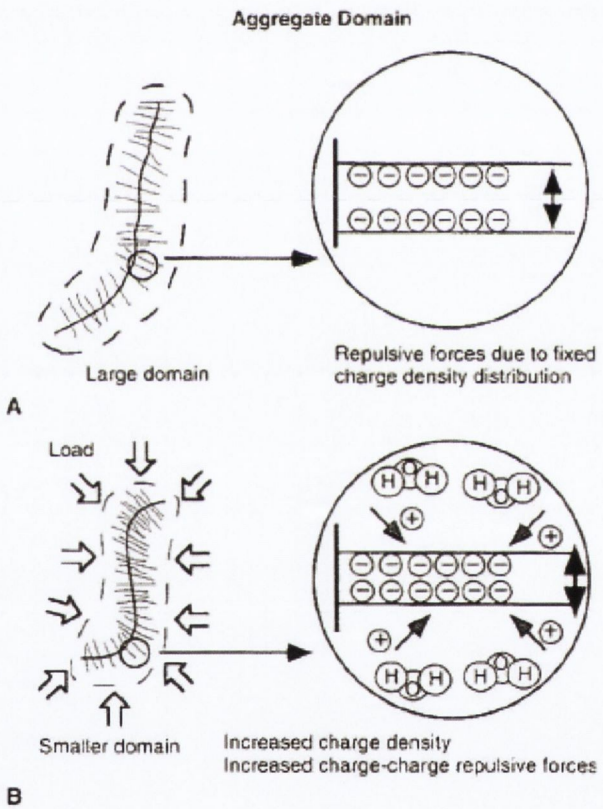

Figure 2-7: (A) Schematic representation of a proteoglycan (PG) aggregate solution domain (left) and repelling forces associated with the fixed negative charge groups on the GAGs of the monomer (right); (B) Applied compressive stress decreases the aggregate solution domain (left), thus increasing charge density and intermolecular charge repulsive forces (right) (Mow and Hung, 2001).

When a compressive stress is applied to the cartilage surface, there is an instantaneous deformation, which is caused by a change in the proteoglycan (PG) molecular domain (Figure 2-7B) (Mow and Hung, 2001). The internal pressure in the matrix increases and fluid is forced out of the tissue. Interstitial fluid pressurization has been shown to support more than 90% of the load applied to the cartilage surface immediately after loading (Soltz and Ateshian, 1998), with the fluid essentially shielding the solid matrix from the high stresses frequently experienced by diarthrodial joints (Mow and Guo, 2002). As the interstitial fluid exudes out of the tissue, the PG concentration increases, which in turn increases the charge-charge repulsive forces within the tissue. The ability of proteoglycans and hence cartilage to resist compression can be attributed to the Donnan osmotic swelling pressure associated with the GAGs, and also to the bulk compressive stiffness of the PG aggregates entangled in the collagen network (Mow and Hung, 2001).

Collagen and PGs also interact, with PGs helping to maintain the structure and mechanical functionality of the collagen fibrils (Muir, 1983). This interaction is crucial in the formation of cartilage; a porous-permeable, fibre-reinforced composite matrix possessing the essential mechanical characteristics of a solid, which can interact with water to resist large forces associated with joint articulation (Mow and Hung, 2001). The structural arrangement of the important components of cartilage can be seen below (Figure 2-8).

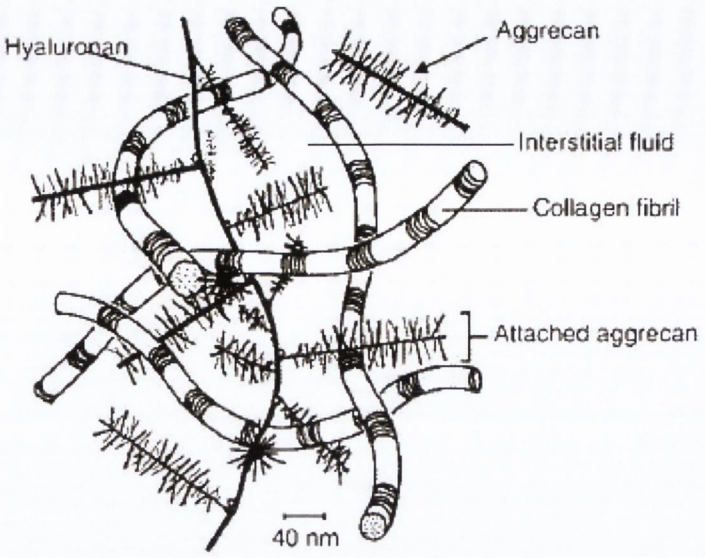

Figure 2-8: Schematic representation of the molecular organization of cartilage (Mow and Hung, 2001).

2.2.3 Biomechanical Behaviour of Articular Cartilage

Articular cartilage can be viewed as a biphasic tissue consisting of a solid collagen and proteoglycan matrix phase, and an interstitial fluid phase, with the fluid free to move through the solid matrix. Each phase plays an important role in the functional behaviour of the tissue (Mow and Hung, 2001). This biphasic nature contributes to the viscoelastic properties of the tissue; a material which when it is subjected to the action of a constant (time-independent) load or a constant deformation, exhibits a variable response with time. The response of such a material can be modelled as a combination of the response of a viscous fluid and an elastic solid (Mow and Hung, 2001).

The two fundamental responses of a viscoelastic material to loading are creep and stress relaxation (Mow and Hung, 2001). Creep occurs when a constant load is applied to a viscoelastic material. The material deforms under this constant load, but the deformation is not instantaneous, as it would be in a single-phase elastic material. The displacement of the material is a function of time, with rapid

displacement initially, followed by a slow, progressively increasing displacement (creep) until equilibrium is reached.

Stress relaxation occurs when a viscoelastic material is subjected to a constant deformation. The material typically responds with a rapid, high initial stress, followed by a slowly (time-dependent) decreasing stress until an equilibrium state is reached (Mow and Hung, 2001).

The response of articular cartilage to these two phenomena, creep and stress relaxation, arises from the flow of interstitial fluid through the solid matrix. Due to the low permeability of the cartilage, this movement of fluid through the matrix generates large frictional drag forces, and high pressures within the solid matrix (Mow and Guo, 2002). As cartilage is compressed, its pores decrease in size, making it more difficult for fluid to flow through them due to these frictional drag forces. This results in a self-protective mechanical feedback mechanism within cartilage, limiting rapid fluid flow in response to high loads (Kheir and Shaw, 2009). The component of cartilage viscoelasticity caused by interstitial fluid flow is known as the biphasic viscoelastic behaviour, while the component of viscoelasticity caused by macromolecular motion is known as the intrinsic viscoelastic behaviour of the solid matrix (Mow and Hung, 2001).

A confined compression test (Figure 2-9) is one of the most commonly used methods for investigating the behaviour of cartilage subjected to a load, and for determining its mechanical properties. This test involves inserting a cylindrical cartilage specimen into a cylindrical, impermeable, smooth-walled confining rig that prevents deformation and fluid flow in the radial direction. A rigid porous-permeable loading platen is used to compress the tissue, causing fluid to flow from the tissue vertically upwards through the platen. The advantage of this test is that it generates a uniaxial flow which does not depend on tissue anisotropy, thus simplifying the calculations required in determining mechanical properties of the tissue. The compression test is carried out in either creep mode, or stress relaxation mode.

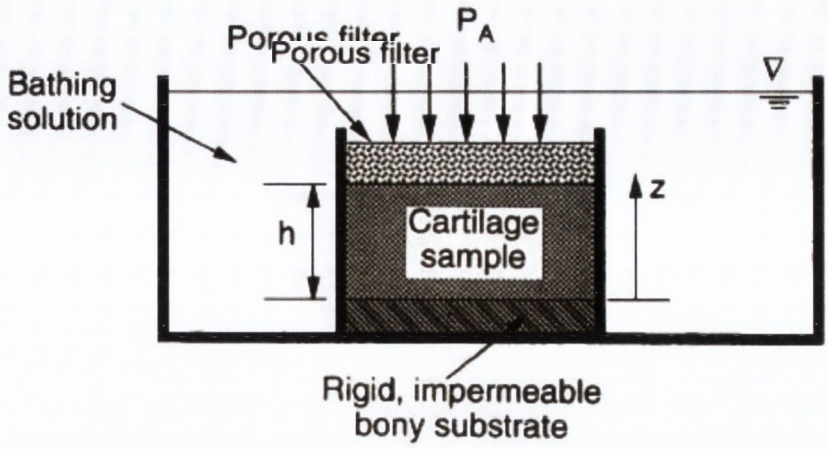

Figure 2-9: Schematic of confined compression configuration (Mow and Guo, 2002).

When a constant compressive load is applied to the cartilage, creep deformation occurs, as shown in Figure 2-10. The tissue is subjected to the constant load (point A), and allowed to creep to its final equilibrium strain (point C). The creep is caused by the exudation of the interstitial fluid from the tissue, with rapid exudation initially (matching the early rapid rate of increased deformation), followed by progressively diminishing fluid flow until it stops completely. During creep, the load applied at the surface is balanced by the compressive stress developed within the matrix and the frictional drag generated by the interstitial fluid flow during exudation (Mow and Hung, 2001). Creep stops when the compressive stress within the solid matrix can fully balance the applied stress, at which point the equilibrium strain is reached (point C). As no fluid flow occurs at this point, the equilibrium deformation can be used to determine the intrinsic compressive modulus (H_a) of the solid matrix. It is also possible to determine the permeability coefficient of the tissue from this creep experiment. The aggregate modulus of native human articular cartilage is typically in the range of 0.5 to 0.9 MPa (Athanasiou et al., 1991).

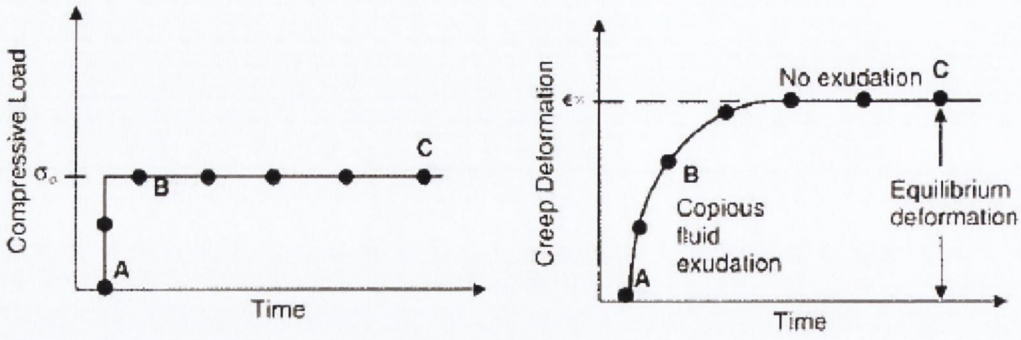

Figure 2-10: The creep response of articular cartilage (right) under a constantly applied stress (left) (Mow and Hung, 2001).

A stress-relaxation response involves compressing the cartilage at a constant rate until a desired displacement is reached (Figure 2-11). Once this strain level is reached (point B in Figure 2-11), the strain is maintained at the same level until the end of the response (E). During the compression phase (O-B), the stress rises continuously until the peak stress is reached (B), corresponding to the same time point at which the desired final displacement is reached. This stress rise in the compression phase is associated with fluid exudation and the compaction of the solid matrix near the surface. During the stress-relaxation phase (B-E), the stress continuously decays until the equilibrium stress is reached (Mow and Hung, 2001). This stress relaxation is associated with fluid redistribution within the porous solid matrix and the relief of the high compaction region near the surface of the matrix. At this point the compressive stress developed within the solid matrix is equal to the stress generated by the intrinsic compressive modulus of the solid matrix corresponding to that displacement. Once the load is removed, the cartilage will fully recover from the deformation due to the inherent elasticity of the solid matrix and fluid imbibition (Mow and Guo, 2002).

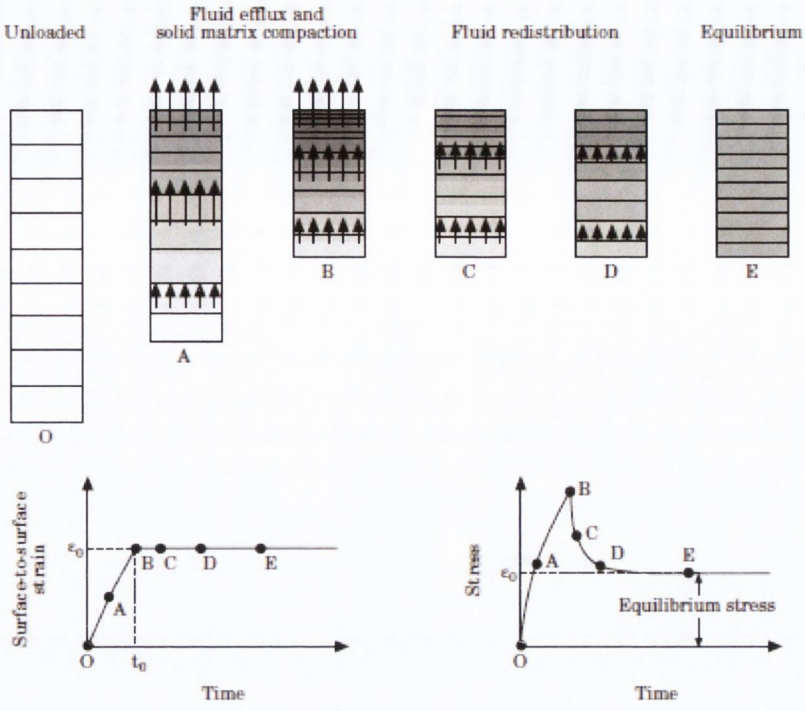

Figure 2-11: Schematic representation of fluid exudation and redistribution within cartilage during a confined compression, stress-relaxation experiment. The horizontal bars in the upper figures indicate the distribution of strain in the cartilage, with interstitial fluid flow represented by arrows. Lower left figure depicts controlled ramp displacement curve. Lower right figure depicts stress response curve during compression phase (O,A,B) and relaxation phase (B,C,D,E) (Mow et al., 1999).

In addition to confined compression tests, unconfined compression tests can be used to determine the mechanical properties of cartilage (Figure 2-12). In an unconfined compression test, the cartilage is compressed between two impermeable platens, with the tissue free to bulge in the transverse direction. The ratio of stress to strain at equilibrium is the Young's Modulus (E). By using determined values of the aggregate modulus and Poisson's ratio of cartilage (Athanasiou et al., 1991), the Young's Modulus can be estimated as approximately 0.45 to 0.85 MPa. It is interesting to note that cartilage has a much lower stiffness than most engineering materials; for example the Young's modulus of steel is approximately 200GPa.

Indentation tests (Figure 2-12) provide an attractive alternative to the other compression tests, as the cartilage being tested can remain attached to its underlying

bone, thus providing a more natural environment for testing. From this test, one is able to determine the aggregate modulus, permeability, and Poisson's ratio of the tissue.

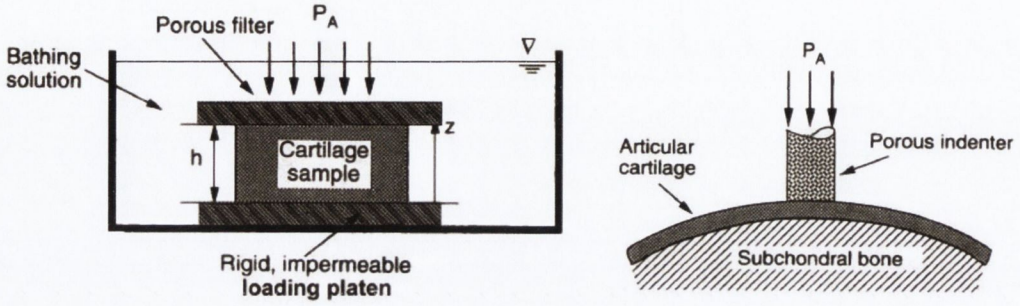

Figure 2-12: Schematic of unconfined compression configuration (left), and apparatus used to perform indentation test on articular cartilage (Mow and Guo, 2002).

The relationship between the mechanical properties of cartilage and water content can help explain early cartilage changes in animal models of osteoarthritis. The proteoglycan content and equilibrium stiffness decrease in these models, with the rate of deformation and water content found to increase (McDevitt and Muir, 1976). As proteoglycan content decreases, more space is available in the tissue for fluid to flow, thereby resulting in an increase in water content. This correlates with an increase in permeability, which causes more fluid to flow out of the tissue, and hence a more rapid rate of deformation. This ultimately increases the stress experienced by the solid matrix of the cartilage.

When performing mechanical tests such as those mentioned above, it is important to remember that as the composition and structure of cartilage varies throughout its depth, so too do the mechanical properties. This natural inhomogeneity of mechanical properties in normal articular cartilage may play a significant role in augmenting the signal transduction mechanisms to the chondrocytes in order to maintain the integrity of the ECM of the cartilage (Mow and Guo, 2002). From a bioengineering perspective, it is therefore highly likely that in order to fully restore the load-bearing functions of damaged articular cartilage,

the natural, spatially-varying distribution of the biochemical composition, structural organisation, and mechanical properties of the tissue will have to be reproduced.

2.3 Articular Cartilage Damage

2.3.1 Classic healing

The response of the body to injury is usually described as consisting of three phases (Newman, 1998). The first phase is cell death, or necrosis, which begins at the time of injury. In this phase, damaged blood vessels will release blood to subsequently form a clot. Platelets trapped within the clot will release various growth factors, inducing the migration of multipotent MSCs into the injury site, as well as initiating the vascularisation process (Newman, 1998). The second phase is inflammation, with the blood vessels increasing in width and permeability. This results in the formation of a dense fibrous tissue network. The last and longest phase is the remodelling phase. It leads to the formation of a vascular granulation tissue, which in some organs creates a scar, and in others is capable of restoring the function and structure of the original damaged tissue.

2.3.2 Injuries to Articular Cartilage

The response of cartilage to injury differs significantly from this classic healing model, due to its avascular nature, and the fact that its cells, the chondrocytes, are trapped in the collagen-proteoglycan mesh they create, and thus are unable to migrate to the injury site from adjacent healthy cartilage (Newman, 1998). The three main types of cartilage injury are matrix disruption, partial thickness defects, and full thickness defects (Temenoff and Mikos, 2000b). Matrix disruption occurs from blunt trauma to the body. The ECM is damaged, but remaining cells can repair the tissue, provided the injury is not too extreme. Partial-thickness defects disrupt the cartilage surface, but do not extend to the subchondral bone, and arise as a result of trauma, mechanical injury, or wear and tear (Spiller et al., 2011). With these defects there is a brief period of matrix synthesis by the chondrocytes adjacent to the injury, but this ceases before the defect can be significantly healed. Full thickness defects damage the entire cartilage zone, whilst also penetrating the subchondral bone

beneath (Temenoff and Mikos, 2000b). As the defect penetrates the bone, a more classical healing response occurs, with the formation of a fibrin clot. Progenitor cells from the bone marrow migrate into the defect causing the fibrin clot to be replaced with tissue intermediate between hyaline cartilage and fibrocartilage (Temenoff and Mikos, 2000b). This tissue is not as stiff as native cartilage, and is often found to degenerate over time. The size of the defect and the age of the patient will also influence the healing response of the cartilage, with decreasing size and age improving healing potential. It has been shown in a horse model that small defects (less than 3mm) can completely heal, while larger defects are more difficult to repair (Convery et al., 1972).

2.3.3 Osteoarthritis

If left untreated, partial and full thickness cartilage defects can lead to joint disorders such as osteoarthritis (Schinhan et al., 2011). OA is the most common joint disorder, and is one of the most frequent health concerns for older people. It is also a major burden on the economy, with medical costs relating to OA estimated to be as much as $65 billion in the United States alone (Little et al., 2011). Approximately 714,000 people in Ireland currently suffer from this degenerative disease, with 18% of patients less than 55 years old (Source: Arthritis Ireland). OA has long been considered as being the result of age or trauma (Martel-Pelletier, 2004), and commonly affects the hands, feet, spine, and large weight-bearing joints, such as the hips and knees. It is characterised by joint pain and dysfunction, and in its advanced stages, joint contractures, muscle atrophy and limb deformity. The disease results from the progressive proteolytic breakdown and erosion of articular cartilage in synovial joints, causing structural lesions to develop within the cartilage layer, followed by the attempted repair of the cartilage, remodelling and sclerosis of subchondral bone. This is sometimes accompanied by subchondral bone cysts and marginal osteophytes (Buckwalter and Martin, 2006). OA usually develops in the absence of a known cause of joint degeneration; this is known as primary or idiopathic OA. Secondary OA is less common and develops due to joint degeneration caused by injuries or a variety of inflammatory and developmental disorders.

There are no current treatments to prevent or cure OA; the standard procedure for treating the disease is surgical replacement of the diseased joint with a metal and polyethylene prosthesis (Guilak, 2010). While this procedure can provide pain relief and improved function to patients, it does not completely restore the articular cartilage and subchondral bone, and the replacement joint can degenerate over time (Pavone et al., 2001, Ma et al., 2005, Browne et al., 2010, Kerin et al., 2011, Seil and Pape, 2011). Joint replacement prostheses also have a finite lifespan, making them unsuitable for the growing population of younger and more active patients requiring treatment for OA (Kurtz et al., 2009, Guilak, 2010, Keeney et al., 2011). Osteotomies can be used as a means to decrease symptoms due to OA, and relieve pain. The surgery involves mechanically realigning the joint so the joint reaction force is directed away from the diseased articular cartilage, and toward the remaining healthy cartilage surface in the joint. Although the technique can provide pain relief to patients, again the solution is only temporary, with satisfactory results usually only lasting between 3 and 12 years (Newman, 1998). The procedure is usually carried out on patients thought to be too young for joint replacement.

Despite these limited and inadequate solutions to osteoarthritic injuries, there are a number of surgical procedures that aim to induce the healing of articular cartilage defects. These procedures will be discussed in the following section.

2.4 Articular Cartilage Repair

There are two traditional strategies employed in the attempt to repair and restore articular cartilage and its underlying subchondral bone. The first is to use marrow stimulation techniques to enhance the intrinsic capacity of the cartilage and the subchondral bone to heal themselves. The second approach is to regenerate a new joint surface by transplanting an osteochondral graft to the defect site. Other, less sophisticated techniques, simply attempt to reduce the clinical symptoms of cartilage damage through procedures such as lavage and debridement.

2.4.1 Lavage, Shaving and Debridement

The irrigation or lavage of a joint using the closed-needle-hole procedure (Chang et al., 1993) has been shown to relieve pain in osteoarthritic or trauma patients. It has

been suggested that the rinsing extracts proteoglycans and aggrecans from the superficial cartilage matrix region, perhaps promoting the adhesion of repair cells and a subsequent anti-inflammatory response (Hunziker and Kapfinger, 1998). Some studies have suggested that any benefits due to lavage can be attributed to a placebo effect of the procedure, although overall, it does appear that the procedure has a beneficial effect for a limited amount of time (Hunziker, 2002).

Chondral shaving is used to remove diseased chondral tissue arthroscopically. The occurrence of this procedure has diminished greatly over the years, with the procedure mainly recommended for chondromalacia patellae or patello-femoral pain (Hunziker, 2002). Debridement combines the shaving procedure with lavage, providing temporary relief to patients.

Most attempts to enhance the intrinsic healing potential of cartilage have traditionally focused on recruiting pluripotent cells from the bone marrow, thus encouraging the natural repair response of the body to attempt to heal and rebuild the cartilage tissue.

2.4.2 Marrow stimulation

Penetration of the subchondral bone is one technique used to repair partial or full thickness articular cartilage injuries. A variety of techniques have been employed, including multiple drill holes, microfractures, spongialization, and abrasion arthroplasty. All of these techniques introduce the vascular-mediated elements necessary for the classic healing response, such as fibrin clot, blood and marrow cells, cytokines, growth factors, and vascular invasion (Newman, 1998).

Pridie drilling involves drilling therapeutic holes into the subchondral bone-marrow spaces underlying regions of damaged articular cartilage, promoting the formation of fibrocartilaginous repair tissue. The microfracture technique is similar to the Pridie drilling technique, but the microfracture holes are considerably smaller. The advantage of this technique is that it can be performed by a minimally invasive arthroscopic approach. Spongialization is mainly applied in patellar surgery, and involves complete removal of the subchondral bone plate at the lesion site (Hunziker, 2002).

2.4.3 Autologous/Allogeneic tissue transplantation

A more recent approach in treating cartilage defects is to regenerate a new joint surface by transplanting chondrogenic tissue to the defect site. Perichondrial and periosteal grafts are an example of such a treatment. Perichondrial grafts involve taking perichondrium from the rib, and placing it into the cartilage defect site, with the hope that the undifferentiated perichondrium cells will be induced to form chondrocytes in the new environment. Periosteal grafts have the same principle, with the periosteal tissue obtained from an adjacent area to the defect site (Temenoff and Mikos, 2000b). In studies comparing periosteal and perichondrium transplants, enhanced chondrogenesis was observed in periosteal grafts (O'Driscoll, 1998). These procedures have proven to be effective for some patients; however they do result in donor site morbidity, and add complications to surgery when obtaining the draft tissue (Temenoff and Mikos, 2000b).

An alternative to regenerating a new joint surface is to replace it with a substitute. Mosaicplasty, or autograft osteochondral transplantation (Figure 2-13), involves the transplantation of at least one cylindrical osteochondral plug from a relatively non-weight bearing region of the patient's own joint, into the defect site. For articular cartilage defects in the knee, the plug is usually taken from the edge of the patellar groove, or the area proximal to the intercondylar notch (O'Driscoll, 1998). A disadvantage of this treatment is that the transplantation of the tissue from a low-weight bearing area to a high-weight bearing one will invariably lead to its degeneration, as a result of mechanical overloading (Hunziker, 2002).

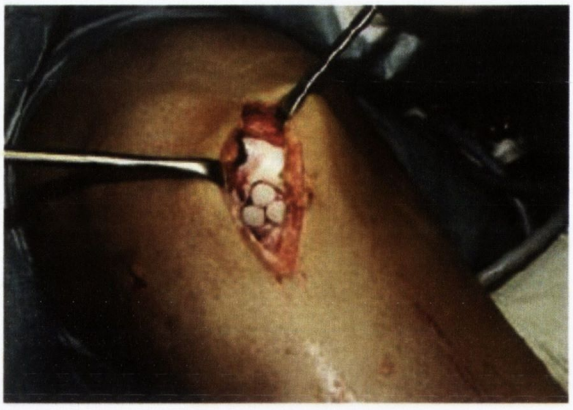

Figure 2-13: Mosaicplasty on the medial femoral condyle for the treatment of a chondral defect. Three osteochondral plugs can be seen implanted in the defect (Kalson et al., 2010).

Allogeneic osteochondral grafts can also be used, with the transplanted tissue often supplied by cadavers. Studies have shown a 95% rate of survival of such grafts at 5 years, and a 66% rate at 20 years (O'Driscoll, 1998). Issues with this treatment involve immunological problems, as associated with all allogeneic transplants. Frozen grafts may reduce this problem, but freezing can also reduce tissue viability (Hunziker, 1999).

Overall, the above techniques provide an unsatisfactory solution to articular cartilage repair. They all share certain limitations, namely reduced biocompatibility, donor site limitation and morbidity, dislocation, wear and potential pathogen transmission (Haasper et al., 2008). Driven by these limitations, present researchers have focused their resources on attempting to consistently regenerate damaged cartilage tissue through tissue engineering principles. This will be discussed in section 2.6.

2.5 Bone

2.5.1 Structure and Composition

Bone tissue is a dense connective tissue in the body. This tissue importantly supports and protects the various organs within the body, produces red and white blood cells and stores minerals. Calcified bone contains approximately 25% organic matrix and 70% inorganic mineral (hydroxyapatite), with the remainder of the tissue

composed of cells and water (Sommerfeldt and Rubin, 2001). Prior to mineralization, the organic matrix (osteoid) consists primarily of collagen type I.

The skeleton consists of two main types of structural bone, cortical bone and trabecular bone (Figure 2-14). Cortical bone (80% of total bone) is dense and is formed from Haversian systems, systems consisting of concentric lamellae of bone tissue surrounding a central canal of blood vessels (Ralston, 2009). Trabecular (or cancellous) bone is less dense, and fills the centre of long bones, flat bones and vertebrae. This bone consists of an interconnecting meshwork of bone trabeculae, separated by bone marrow filled spaces, and is remodelled more rapidly than cortical bone (Ralston, 2009).

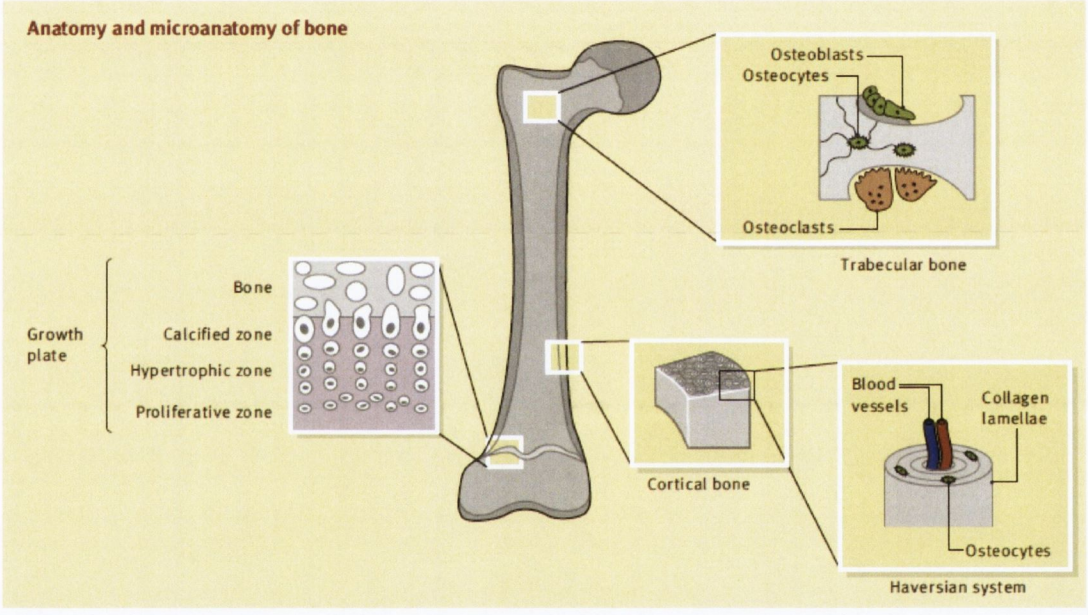

Figure 2-14: Anatomy and microanatomy of bone (Ralston, 2009).

Three different cell types can be found within bone. The first, the osteoblast, lays down the extracellular matrix of bone and regulates mineralization within the tissue (Sommerfeldt and Rubin, 2001). Osteoblasts are derived from mesenchymal osteoprogenitor cells found in bone marrow and periosteum (Mackie, 2003). These cells regulate mineralization by helping to initiate it through production of phosphate-containing proteins (such as bone sialoprotein), and by simultaneously providing enzymes that regulate phosphoprotein phosphorylation (such as alkaline phosphatase). Some osteoblasts ultimately become embedded in bone matrix to

form the second bone cell type, the osteocyte (Mackie, 2003). Osteocytes are the most abundant cell type in bone. When embedded in bone matrix, these cells remain connected with other osteocytes and also with bone-lining cells at the bone's surface, resulting in an extensive network of intercellular communication (Sommerfeldt and Rubin, 2001). These osteocytes are thought to be responsible for sensing the effects of mechanical strain on the skeleton (Ralston, 2009). The third cell type, osteoclasts, are derived from haematopoietic stem cells. The main feature of these cells is their ability to resorb fully mineralized bone at sites known as Howship's lacunae (Sommerfeldt and Rubin, 2001).

Healthy bone undergoes a constant cycle of renewal and repair throughout the life of a human, often termed bone remodelling. Bone remodelling is a balanced process involving osteoblasts depositing new bone, and osteoclasts resorbing old bone by secreting hydrochloric acid and proteolytic enzymes into the extracellular space. Once bone resorption has occurred, osteoclasts undergo apoptosis, triggering the beginning of the bone formation cycle (involving osteoblasts). Bone diseases generally occur as a result of abnormalities in bone remodelling, leading to clinical symptoms such as pain, fracture and calcium/phosphate homeostasis abnormalities (Ralston, 2009).

The bones of the skeleton develop via two main processes. Flat bones (like those in the skull) develop by a process known as intramembranous ossification. This involves differentiation of mesenchymal cells directly into bone-forming osteoblasts (Kronenberg, 2003). However, the majority of bones are formed through a more complicated process, known as endochondral ossification.

2.5.2 Endochondral Ossification

Endochondral ossification is the process by which the embryonic cartilaginous model of most bones contributes to longitudinal growth, and involves the gradual transformation of cartilage to bone (Mackie et al., 2008). The process begins with MSCs proliferating and differentiating into chondrocytes that synthesize a hyaline matrix (Figure 2-15). The chondrocytes mature and eventually undergo terminal

differentiation (hypertrophy), where they mineralize the ECM by depositing hydroxyapatite (Mackie et al., 2008). The hypertrophic cells secrete the hypertrophic marker collagen type X and the enzyme alkaline phosphatase (ALP) during this stage. The cells also release metalloproteases which degrade the cartilaginous ECM (Mackie et al., 2008). This degradation allows for vascular invasion (aided by the hypertrophic cells producing vascular endothelial growth factor), resulting in oxygenation of the tissue, and recruitment of chondroclasts, which remove apoptotic chondrocytes (Sundelacruz and Kaplan, 2009, Kronenberg, 2003). Vascular invasion also leads to the recruitment of new MSCs, which differentiate into osteoblasts that secrete bone matrix (Merceron et al., 2010). Bone lengthening then occurs through proliferating chondrocytes forming secondary ossification centres (Kronenberg, 2003).

Studies have shown that endochondral ossification is enhanced by motion and mechanical stimulation, and is inhibited by fixation (McKibbin, 1978, Dimitriou et al., 2005, Sundelacruz and Kaplan, 2009).

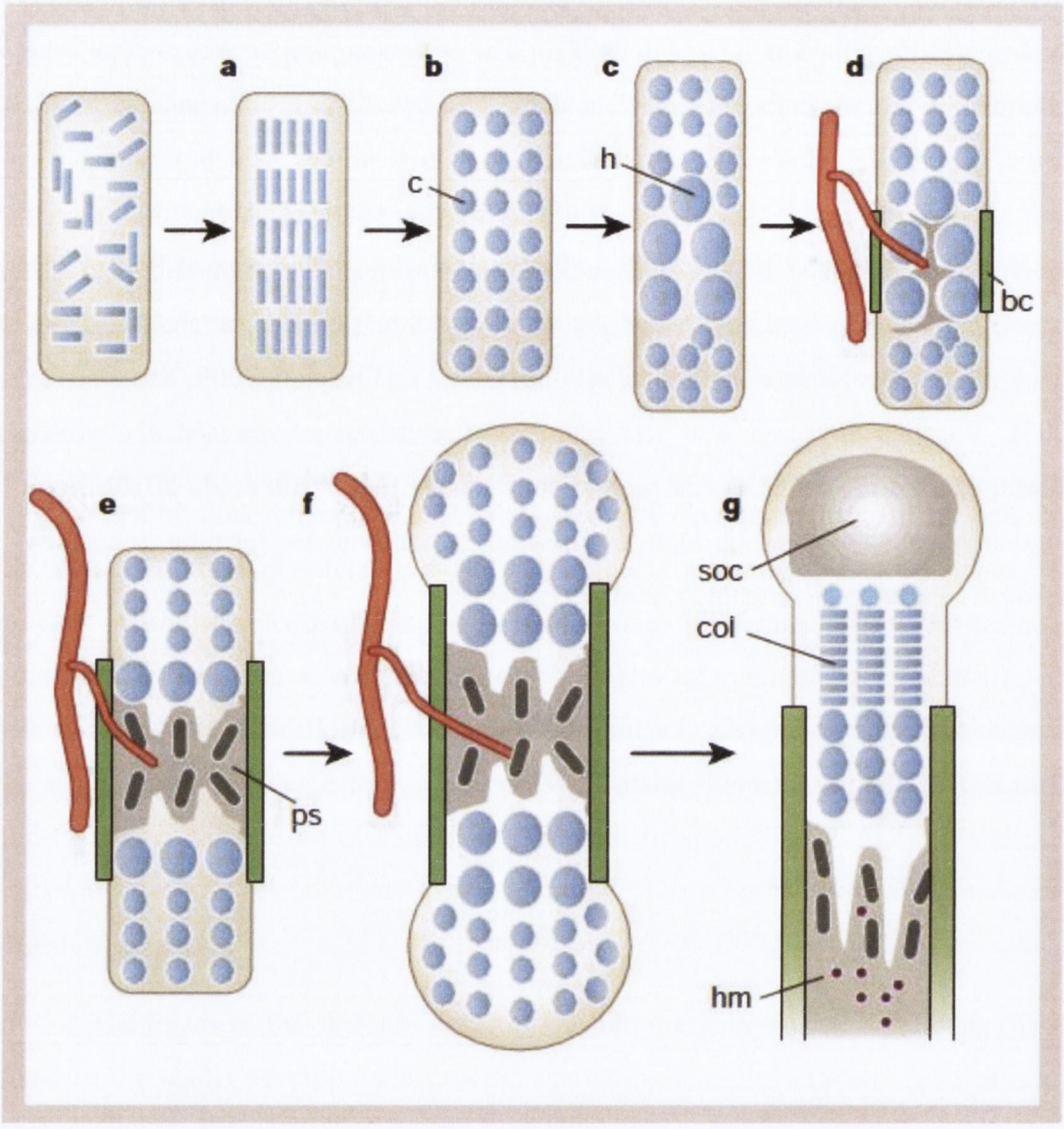

Figure 2-15: Endochondral bone formation. (A) Condensation of MSCs. (B) MSCs differentiate into chondrocytes (c). (C) Chondrocytes undergo hypertrophy (h). (D) Perichondrial cells adjacent to hypertrophic chondrocytes become osteoblasts, forming the bone collar (bc). (E) Vascular invasion occurs, forming the primary spongiosa (ps). (F) Chondrocytes proliferate, lengthening the bone. (G) Secondary ossification centres (soc) form. A growth plate forms consisting of columns of proliferating chondrocytes (col). Haematopoietic marrow (hm) expands in marrow space along with MSCs (Kronenberg, 2003).

2.5.3 Bone Repair

Bone repair occurs by two mechanisms. The first, primary fracture healing, occurs when there is no movement between the fracture surfaces. When there is movement, secondary fracture healing occurs, resulting in the formation of a callus. This can be described by the four-stage model (Schindeler et al., 2008).

Stage 1 involves inflammation of the tissue. Damage to the bone activates wound healing pathways, and the secretion of cytokines and growth factors (such as VEGF) by inflammatory cells advance clotting into a fibrinous thrombus (Gerstenfeld et al., 2003, Einhorn, 1998). MSCs migrate to the inflammation site. In stage 2 of the fracture repair model MSC derived chondrocytes replace fibrous and granulation tissue with cartilage; this forms a semi-rigid soft callus that is able to provide mechanical support to the fracture (Schindeler et al., 2008). The chondrocytes then undergo hypertrophy and mineralise the cartilaginous matrix before undergoing apoptosis. Stage 3 involves gradual removal of the soft callus and revascularisation of the fracture site. A new hard callus is formed to bridge the fracture surfaces. The final stage of fracture repair, stage 4, involves remodelling of the woven bone hard callus into cortical and/or trabecular bone.

Tissue engineering based strategies used to regenerate bone will be discussed later, but first a review of current cartilage tissue engineering based therapies will be reviewed.

2.6 Cartilage Tissue Engineering

Tissue engineering has demonstrated significant potential for cartilage repair in recent years. The science aims to regenerate damaged tissues by developing biological substitutes that restore, maintain or improve tissue function (O'Brien, 2011). The standard approach of tissue engineering is to seed cells on a three-dimensional (3D) biomaterial scaffold. The scaffold is used to create a 3D environment that promotes tissue development of the cells that are placed within it (Elisseeff et al., 2005). The scaffolds can also be seeded with growth factors, or

subjected to biophysical stimuli (bioreactor) to encourage cell deformation and production of ECM. The combination of cells, scaffolds, and environmental factors (mechanical/chemical signals) is often referred to as the tissue engineering triad (Figure 2-16).

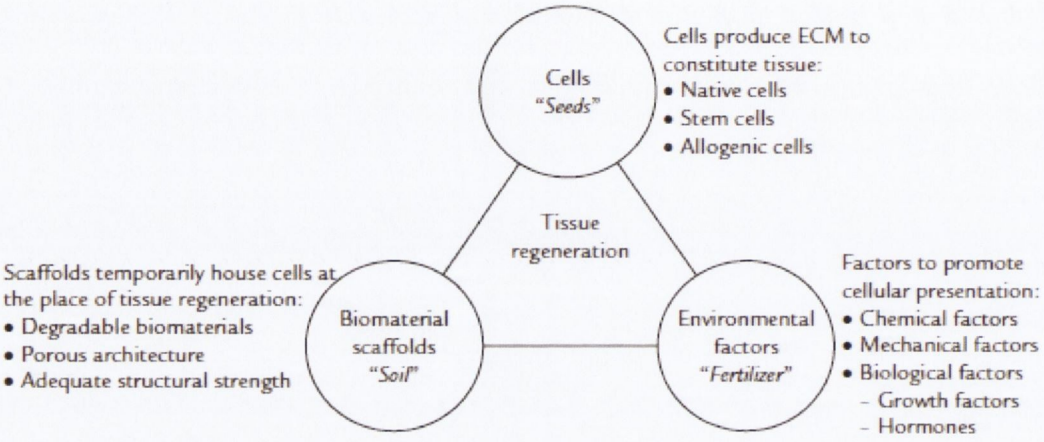

Figure 2-16: The tissue engineering triad of cells, biomaterial scaffolds and environmental factors (Chiang and Jiang, 2009).

The cell-seeded scaffolds are either cultured *in vitro*, to synthesize tissues which can be subsequently implanted into a defect site, or they can be implanted directly into the defect site, where tissue synthesis is induced *in vivo* (O'Brien, 2011). Although the *in vitro* strategy is more controllable (and hence in certain ways is more straightforward), the optimal environmental parameters required for engineering constructs with native cartilage biological and mechanical properties are still unknown. The *in vivo* strategy treats the intra-articular environment as a naturally suitable condition for the cultivation of regenerated cartilage (Chiang and Jiang, 2009). It involves implanting a scaffold, growth factors, and cells (can be a combination of some or all) directly into the defect site to repair the cartilage lesion. It is important with this strategy that a sufficient number of chondrogenic cells are implanted, and that they are fully capable of producing the required ECM. It is also important that the cells remain in the cartilage defect site, and that any repair tissue generated integrates firmly with the surrounding tissue. First generation autologous chondrocyte implantation (ACI) is an example of both culture strategies in action.

2.6.1 Autologous Chondrocyte Implantation

The ACI technique (Figure 2-17) could be considered as the first example of clinical cartilage tissue engineering, with the procedure being firmly established in the treatment of focal cartilage defects. The ideal patient for the treatment suffers from a full thickness chondral or osteochondral defect surrounded by healthy, normal cartilage in an otherwise healthy knee, although often, this is not the case. The first step of the technique involves harvesting healthy cartilage from the patient. This is usually a full thickness biopsy down to the subchondral bone, with an arthroscopic gouge or ring curette used to obtain the tissue samples. Common sites for biopsy include the superomedial and superlateral edge of the femoral condyle. The next step involves isolating the chondrocytes from the harvested tissue, and subsequently culturing these cells *in vitro*. The purpose of this step is to increase the cell number to an adequate level, and lasts approximately 2 weeks, after which the cells are trypsinised and transferred to the operating theatre. At this stage, the damaged joint is opened by a surgeon, and the cartilage injury is debrided to healthy cartilage. A flap of periosteum is sutured over the defect and the expanded cells are implanted into the defect with a typical treatment dose of 2 million cells/cm^2 of defect area (Brittberg, 2008).

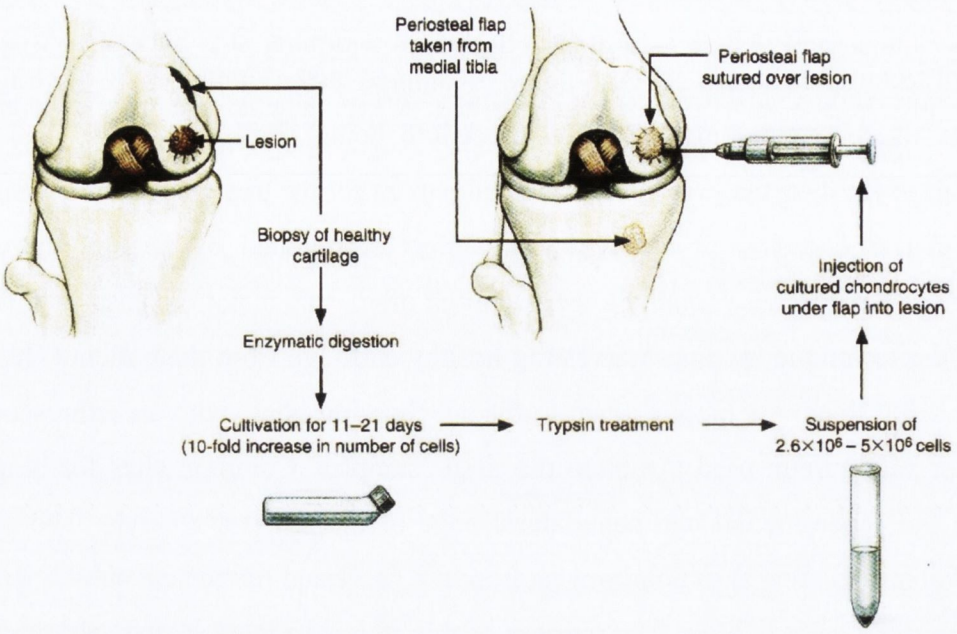

Figure 2-17: Schematic diagram of autologous chondrocyte implantation in the right femoral condyle (Brittberg et al., 1994).

Studies have demonstrated that this first-generation cell based therapy results in significant improvement in function, reduction in symptoms, and the generation of hyaline-like cartilage in patients (Jones and Peterson, 2006, Brittberg, 2008). The technique also has several limitations related to technical aspects of the surgery, including the invasiveness of the procedure, cost, and postoperative complications such as hypertrophy associated with the periosteal patch. To overcome some of these limitations, including hypertrophy of the periosteal patch, the procedure was modified to include the use of a bioabsorbable collagen membrane cover instead of a periosteal cover. This collagen-covered ACI (CACI) technique reduced postoperative complications, but still required an open surgery with sutures (Brittberg, 2010). This led to developments of second and third generation ACI.

Matrix-induced ACI (MACI) is an example of second generation ACI, and involves seeded chondrocytes onto a type I/III collagen membrane *in vitro*, before the cell seeded membrane is implanted directly into the chondral defect. The MACI cell-seeded membrane may be implanted via mini-arthrotomy or arthroscopy, less invasive procedures than with earlier ACI techniques. Additional advantages include a reduced surgical time to implant the MACI membrane, as the procedure

does not require a periosteum or collagen membrane cover, the need for microsuturing, or the harvest of the periosteal flap (Brittberg, 2010).

Third generation ACI involves seeding chondrocytes in 3D-matrices. Hyalograft-C® is an example of this, where the cells are seeded onto a scaffold based on hyaluronic acid. This scaffold has be shown to provide good physical support to allow cell-cell contact, cluster formation, and ECM deposition (Kon et al., 2009).

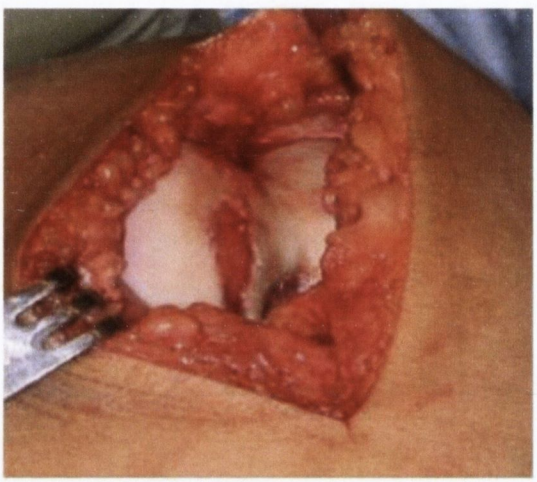

Figure 2-18: Femoral condyle lesion treated by chondrocytes cultured in a hyaluronic acid scaffold (Brittberg, 2008).

Although these ACI techniques have found some success in repairing small focal cartilage defects, they are not suitable for treating larger defects, such as those associated with OA. They are limited by the amount of healthy cartilage that can be harvested from the patient, as well as donor site morbidity. To overcome this limitation, chondrocytes are expanded *in vitro*, to obtain sufficient cell numbers for constructing a clinically useful implant (Elisseeff et al., 2005). However, when chondrocytes are removed from their native environment and expanded *in vitro*, they dedifferentiate and lose their chondrogenic phenotype (Schnabel et al., 2002). Despite this fact, many studies have, and still use chondrocytes in other tissue engineering investigations, as will be discussed in the following sections.

2.6.2 Cell Sources for Cartilage Tissue Engineering

Cells are the most important component of tissue engineering, with a variety of cell types presently available to generate cartilage. When deciding on the ideal cell source to use, there are a few considerations to be made. For example, the cells should be immunocompatible, ideally coming from the patient themselves (like autologous chondrocytes in ACI). This will also minimise the risk of disease transmission. Ease of tissue harvesting and expansion are also important factors to consider, when choosing cell source. The main cell sources used in cartilage tissue engineering studies are chondrocytes and MSCs.

2.6.2.1 Chondrocytes (CCs)

The majority of the early cartilage tissue engineering work, including first generation ACI involved chondrocytes (CCs). This is a logical choice, as it is these cells that are responsible for secretion of cartilaginous ECM within the body. The first disadvantage of using this cell source is the lack of available donor tissue. Taking a cartilage biopsy also creates further lesions in the joint surface, leading to donor site morbidity. The lack of available healthy cartilage leads to the second problem of these cells. When the cells are expanded in monolayer culture to increase cell number, they dedifferentiate towards a fibroblastic phenotype producing collagen type I instead of the desired collagen type II (Benya and Shaffer, 1982, Temenoff and Mikos, 2000b, Diaz-Romero et al., 2005). When these dedifferentiated cells are subsequently implanted *in vivo*, a consequence of their loss of phenotype is a progressive loss of cell ability to form hyaline cartilage. As is often the case with first generation ACI, these dedifferentiated cells may form fibrous tissue instead of the required hyaline tissue (Pelttari et al., 2008a).

To give an idea of the typical number of CCs available for ACI procedures, the average cartilage biopsy from a patient contains ~ 280 mg of cartilage (Brittberg, 2008), with the average CC yield from a human cartilage digest being ~ 2.5 million cells/g of tissue (Jakob et al., 2003). If we assume these CCs undergo 4 population doublings during a single expansion passage, then this equates to approximately 11 million CCs available after one passage, or 180 million CCs available after 2 passages (Santoro et al., 2010).

CCs need a 3D environment to maintain or reexpress their chondrogenic phenotype. If dedifferentiated chondrocytes are subsequently cultured in such a 3D environment, they can reexpress the chondrogenic phenotype (Benya and Shaffer, 1982), and synthesize a mechanically functional cartilage-like ECM (Buschmann et al., 1992a). However, it still remains difficult to produce a tissue with ECM accumulation levels matching those of native articular cartilage (Buschmann et al., 1995b). Some studies have even shown that dedifferentiated chondrocytes maintained in 3D culture never fully revert back to pre-expansion gene expression levels for cartilage-specific molecules (Benz et al., 2002).

CCs have been shown to suffer from an age related loss in yield, proliferation and post-expansion chondrogenic capacity (Barbero et al., 2004). This raises many issues when considering that the majority of patients requiring cartilage repair are elderly. It has also been shown that CCs isolated from OA patients exhibit reduced collagen synthesis when redifferentiated in a 3D pellet model (Tallheden et al., 2005). Furthermore, CCs in OA cartilage typically produce cartilage-degrading enzymes such as MMP13 and aggrecanases (Van der Kraan and Van den Berg, 2012), obviously undesirable when trying to engineer cartilage. Generating cartilage using CCs clearly has many drawbacks, and with future research aimed at developing tissue engineering based methods to treat large lesions in patients with OA, the use of this cell source may become completely unfeasible. For such reasons much current research is aimed at an alternative cell type, the MSC.

2.6.2.2 Mesenchymal Stem Cells (MSCs)

Stem cells are undifferentiated cells capable of undergoing self-renewal and differentiating into many tissue-specific cell lineages when provided with the appropriate cues. These properties are very useful for the purpose of tissue engineering, as the cells are capable of both proliferating to achieve the substantial cell number required to make new tissue, and differentiating into multiple cell types to engineer new repair tissue (Elisseeff et al., 2005). This fact that stem cells can be expanded extensively in culture and still maintain their multipotent differentiation potential is hugely appealing to cartilage tissue engineers, especially when

considered to the alternative of expanded dedifferentiated chondrocytes (Pittenger et al., 1999).

Stem cells can be isolated from embryonic and postnatal tissues. Embryonic stem cells (ESCs) come from the inner mass of the blastocyst, and are described as pluripotent, meaning that a single cell has the capability of differentiating into cells of all germ layers (endoderm, ectoderm, and mesoderm) and generate all tissues of the body (Duplomb et al., 2007). This cell source seems ideal for tissue engineering purposes. Much controversy surrounds the use of human ESCs however, with many social, ethical and legal concerns restricting the use of these cells in many labs and hospitals around the world. Other factors limiting their application to human cell therapy include immunological incompatibilities, potential for malignant tumour growth, and an insufficient understanding and control over ESC differentiation (Sundelacruz and Kaplan, 2009).

Adult mesenchymal stem cells are a very attractive alternative as they can also differentiate into distinctive end-stage cell types, such as those that fabricate specific mesenchymal tissues including bone, cartilage, muscle, bone marrow stroma, tendon/ligament, fat, dermis and other connective tissues as shown in Figure 2-19 (Caplan, 2007). These multipotent progenitor cells also secrete a range of bioactive macromolecules that are both immunoregulatory, and serve to structure regenerative microenvironments in fields of tissue injury (Caplan, 2007). Mesenchymal stem cells are present in many adult mesenchymal tissues, such as bone marrow, adipose tissue, muscle and synovial membrane. Perhaps the best characterised population of MSCs are those originating from the bone marrow.

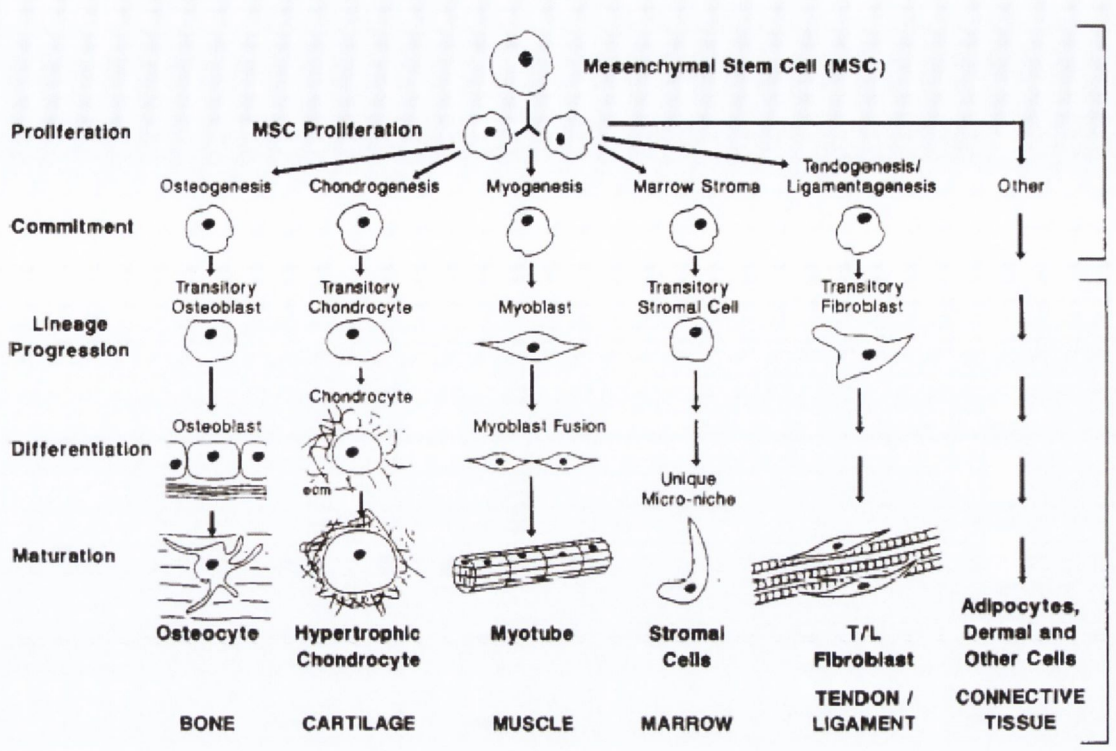

Figure 2-19: The mesengenic process. Adult MSCs have the capacity to differentiate into bone, cartilage, muscle, marrow stroma, tendon/ligament, fat, and other connective tissues. The sequence of this differentiation involves multistep lineages controlled by growth factors and cytokines. This figure is structured in a manner comparable to hematopoietic lineage progression (Caplan, 2005).

Bone marrow-derived MSCs (BMSCs) were first identified by Friedenstein (Friedenstein et al., 1970), where he observed that upon plastic adherence of bone marrow cells, a rare cell population developed into colony forming units that were fibroblastic [CFU-F] (Friedenstein et al., 1992). It has been stated that only 0.001 to 0.01% of cells resident in adult bone marrow are MSCs (Pittenger et al., 1999). These cells are distinguished from other cells by their ability to proliferate with an attached well-spread morphology and by the presence of a consistent set of marker proteins on their surface (Pittenger et al., 1999). These cells have been shown to have a strong proliferative potential, and can differentiate into a range of tissues (Pittenger et al., 2000), and it is for this reason that many studies have used BMSCs in the attempt to generate cartilage (Huang et al., 2004b, Thorpe et al., 2008, Vinardell et al., 2009, Thorpe et al., 2010a, Thorpe et al., 2013).

There are some interesting studies comparing BMSCs to chondrocytes (CCs). When bovine CCs and BMSCs from the same animal are cultured under identical conditions, CCs not only create a significantly more functional tissue than BMSCs, but they also maintain the improvement in biosynthetic and mechanical properties after 10 weeks of culture, by which time the BMSCs have reached a plateau (Mauck et al., 2006, Chao et al., 2007). More recent animal studies, however, have demonstrated that matrix-associated implantation of predifferentiated human BMSCs leads to superior histological results in repairing chronic osteochondral defects, when compared with articular CCs (Marquass et al., 2011). In addition, recent clinical studies comparing different cell sources for ACI therapy have shown that human BMSCs are just as effective as CCs for articular cartilage repair (Nejadnik et al., 2010). The fact that the ACI procedure using BMSCs requires one less knee surgery, costs less, and minimises donor-site morbidity clearly shows the huge potential that these cells have in the future of cartilage tissue engineering.

When using BMSCs for articular cartilage repair, a central challenge is to generate chondrocytes that do not undergo hypertrophy when implanted *in vivo*. If such chondrocytes become hypertrophic, the cartilage they have formed may be transformed to bone, through the natural process of endochondral ossification (as discussed in section 2.5.2). The natural tendency of chondrogenically primed BMSCs to undergo hypertrophy and mineralize *in vivo* may limit their use clinically for cartilage repair (Pelttari et al., 2006, Dickhut et al., 2008, Dickhut et al., 2009, Lee et al., 2011, Vinardell et al., 2012b). On the other hand, this tendency of BMSCs to undergo endochondral ossification *in vivo* can be manipulated for the purposes of bone regeneration (Farrell et al., 2009, Scotti et al., 2010, Janicki et al., 2010, Farrell et al., 2011, Scotti et al., 2013). Using BMSCs to engineer endochondral bone will be discussed further in section 2.7.2.

From a patient perspective, it can be argued that the isolation of stem cells from other sources in the body is preferable, given that their isolation from bone marrow can be a painful and risk-containing sampling procedure (Pelttari et al., 2008a). To this effect, recent studies have provided new insights into alternative sources of stem cells (Marsano et al., 2007). Adipose tissue is considered to be an

attractive stem cell source, as it is easily accessible in large quantities (Dragoo et al., 2003), and adipose-derived stem cells show a proliferation and multilineage capacity comparable to BMSCs (De Ugarte et al., 2003). Stem cells can be found in the infrapatellar fat pad (IFP) of the knee and the synovial tissue of the joint capsule. Interestingly, IFP and synovium derived stem cells have been shown to be more phenotypically similar to chondrocytes than other sources such as bone marrow, making them an attractive stem cell source for cartilage repair studies (English et al., 2007).

The IFP found in the human knee is a structure composed of adipocytes and connective tissues containing collagen and GAGs. Its proximal end is attached to the distal end of the patella, and its distal end is attached to the anterior portions of the medial and lateral menisci. The surface of the fat pad articulates with distal femur, and it is thought the fat pad also has an important function as a shock absorber (Nakano et al., 2004). Studies have shown that IFP derived stem cells (FPSCs) can proliferate and undergo robust chondrogenesis when cultured in the presence of pro-chondrogenic factors (Wickham et al., 2003b, English et al., 2007, Khan et al., 2007, Lee et al., 2008, Jurgens et al., 2009, Buckley et al., 2010a, Buckley et al., 2010c, Buckley and Kelly, 2012). It has also been suggested that these FPSCs could be a useful autologous source for cellular therapy development in the treatment of OA (English et al., 2007). FPSCs have even been shown to synthesize higher amounts of sGAG and collagen compared to BMSCs alone (Vinardell et al., 2011, Vinardell et al., 2012b), making them a very promising cell source for cartilage tissue engineering.

2.6.2.3 Co-culture of Chondrocytes and Stem Cells

Recent studies have begun to investigate the effects of co-culturing chondrocytes and stem cells for cartilage repair strategies (Hendriks et al., 2007, Leijten et al., 2013). Of these studies, one of the first investigated the co-culture of expanded articular CCs with BMSCs (Tsuchiya et al., 2004), showing upregulation of cell proliferation, cartilaginous extracellular matrix (ECM) production and type II collagen gene expression in mixed pellet culture compared to monoculture controls. A more recent study found similar results, demonstrating that structured co-culture

pellets of BMSCs and CCs (3:1 ratio) produce significantly more proteoglycan than either CC or MSC pellets, when cultured in hypoxic and inflammatory conditions intended to mimic an injured joint microenvironment (Cooke et al., 2011). From a clinical perspective, studies have shown that co-culture of BMSCs and CCs leads to increased cartilage matrix formation and furthermore, can provide better macroscopic cartilage regeneration within focal cartilage lesions, when compared with microfracture (Bekkers et al., 2013a, Bekkers et al., 2013b). Increased cartilage matrix production has also been reported in the co-culture of adipose-derived stem cells (ASCs) and CCs (Hildner et al., 2009, Lee and Im, 2010, Acharya et al., 2012).

Although the majority of reported co-culture studies involve pellet culture (Giovannini et al., 2010, Wu et al., 2011, Acharya et al., 2012, Wu et al., 2012, Wu et al., 2013b), mixed co-culture of BMSCs and CCs within larger hydrogels and other 3D scaffolds has also been reported (Mo et al., 2009, Yang et al., 2009, Miao et al., 2009, Liu et al., 2010, Meretoja et al., 2012, Sabatino et al., 2012, Meretoja et al., 2013, Dahlin et al., 2014b). One such study demonstrated that a mixed co-culture of MSCs and CCs (4:1 ratio) in hyaluronic acid hydrogels leads to significantly higher Young's modulus, glycosaminoglycan levels, and collagen content than single cell only controls *in vitro* (Bian et al., 2011). The synergistic cartilage forming effect of co-culture has also been shown *in vivo* with BMSC-CC mixed co-culture collagen scaffolds accumulating higher amounts of GAG than corresponding single cell only controls, when implanted subcutaneously in nude mice (Sabatino et al., 2012).

In attempting to separate out the effects of the two cell types, it has been shown that in co-culture of stem cells and CCs, the former cells secrete factors that drive proliferation of the CC population (Wu et al., 2011, Wu et al., 2012, Acharya et al., 2012, Wu et al., 2013b). Interestingly, adipose-derived stem cells and BMSCs have a similar proliferative effect on these co-cultured CCs (Wu et al., 2012, Acharya et al., 2012). The concept of MSCs secreting a variety of cytokines and growth factors that have both paracrine and autocrine activities is well established (Caplan and Dennis, 2006). MSC-secreted bioactive molecules are known to have trophic effects on cells in their vicinity, influencing the regeneration of cells or tissue. The term trophic can also relate to the effect of these MSC-secreted bioactive

molecules on the proliferation and matrix production of surrounding cells (Wu et al., 2012, Wu et al., 2013a). Recent studies have shown that one of the trophic factors released by MSCs is fibroblast growth factor-1 (FGF-1) which leads to increased proliferation of co-cultured CCs (Wu et al., 2013b). Other soluble factors detected in the supernatant of MSC-CC co-culture constructs include TGF-β1, IGF-1 and BMP-2 (Liu et al., 2010) which have been shown to affect cell proliferation (Richter, 2009, Shu et al., 2011, Li et al., 2011). Indeed, BMP-2 has been shown to promote chondrocyte proliferation *via* the Wnt/β-catenin signalling pathway (Li et al., 2011).

Co-culture studies have also shown that factors released by CCs can enhance MSC chondrogenesis (Ahmed et al., 2007, Hwang et al., 2007, Lettry et al., 2010, Aung et al., 2011, Acharya et al., 2012). In addition, co-culture of CCs and BMSCs has been shown to suppress markers of BMSC hypertrophy (such as type X collagen expression) *in vitro* (Fischer et al., 2010, Cooke et al., 2011, Aung et al., 2011, Acharya et al., 2012, Kang et al., 2012). This phenomenon is demonstrated in Figure 2-20, where hyaluronic acid hydrogels containing co-cultured CCs and BMSCs (shown on the left) exhibit much weaker type X collagen immunohistochemical staining than BMSC only controls (Bian et al., 2011).

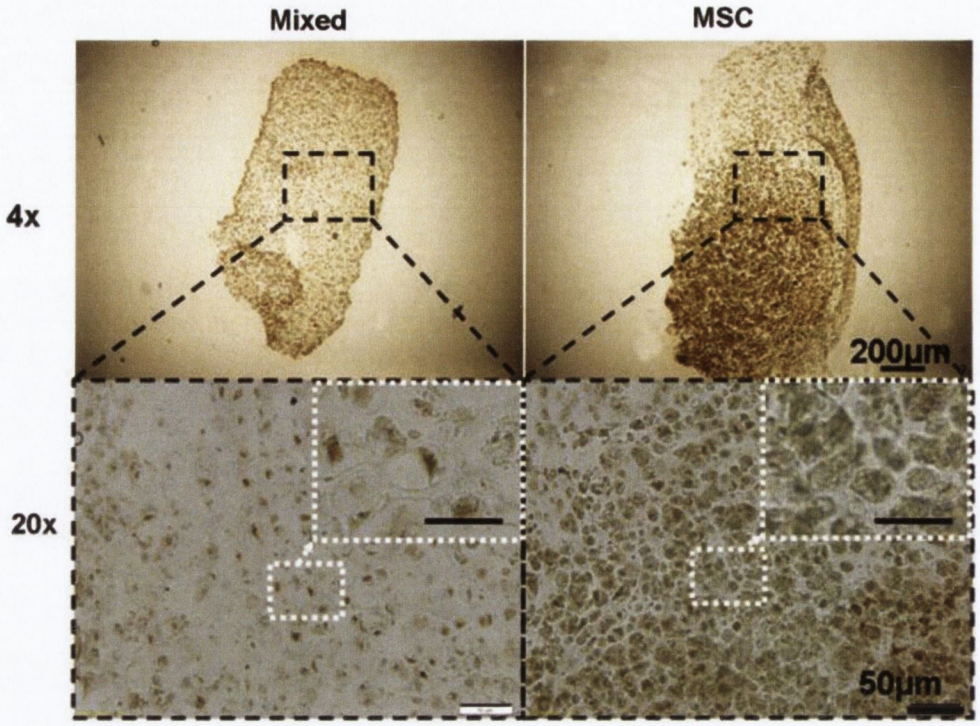

Figure 2-20: Immunohistochemical staining of type X collagen for MSC & CC co-culture constructs (left) and MSC only controls (right) (Bian et al., 2011).

It has been speculated in BMSC & CC co-culture, that suppression of hypertrophy is mediated by CCs secreting parathyroid hormone-related protein (PTHrP) (Fischer et al., 2010). In addition, it has been reported that in co-culture of BMSCs and CCs, the former cells die off over time (Wu et al., 2011, Meretoja et al., 2012); this would reduce hypertrophy in the resultant tissue. In conclusion, co-culture appears to be a very promising strategy for cartilage tissue engineering, and is one method that can be used in preventing MSCs from undergoing hypertrophy in culture, possibly leading to the generation of phenotypically stable cartilage *in vivo*.

2.6.3 Biomaterial Scaffolds for Cartilage Tissue Engineering

It is well established that cells reside within a 3D environment within the body (Vinatier et al., 2009). We have seen that isolated chondrocytes will lose their differentiated phenotype in 2D culture (Darling and Athanasiou, 2005), and will partially regain their differentiated phenotype if they are maintained in a 3D environment (Benya and Shaffer, 1982, Malda et al., 2003). This indicates that the 3D environment has a significant role in supporting the chondrocytic phenotype,

and it is for this reason that 3D scaffolds are often used for culturing chondrocytes or promoting the chondrogenic differentiation of MSCs (Vinatier et al., 2009). When choosing an appropriate scaffold, there are five main considerations to be made when determining its suitability for cartilage engineering purposes (O'Brien, 2011).

1) The scaffold must be biocompatible. Cells must be able to adhere to the scaffold, and function normally. After the construct is implanted *in vivo*, it must not provoke any immune reaction from the body.

2) The scaffold must be biodegradable. This is to allow the body's own cells, and the cells within the scaffold, produce their own ECM, and eventually replace the implanted scaffold over time. The degradation particles should also be non-toxic and be free to exit the body without difficulty.

3) The scaffold should have mechanical properties consistent with the anatomical site it is being implanted into. Producing scaffolds with adequate mechanical properties is one of the greatest challenges faced when attempting to engineer cartilage. The implanted scaffold must have sufficient mechanical integrity to function as soon as it is implanted in the body.

4) Scaffold architecture is of huge importance. Scaffolds should have an interconnected pore structure and a suitable porosity to ensure cellular penetration and adequate diffusion of nutrients to the cells and to the ECM. Successful waste removal also depends on a porous interconnected structure. The mean pore size of the scaffold must also be considered.

5) Manufacturing technology is important, as the scaffold must be clinically and commercially viable.

A wide variety of biomaterials are used to construct these 3D scaffolds. Hydrogels are an example of such a material, and include for example, alginate, agarose, poly (ethylene glycol), poly (vinyl alcohol), pluronics, chitosan, collagen, and fibrin (Buckley et al., 2009b). Hydrogels are composed of a viscous polymer made of hydrophilic macromolecules which are able to from a hydrogel after physical, ionic or covalent crosslinking (Drury and Mooney, 2003, Vinatier et al.,

2009). Their hydrophilic polymer network becomes highly swollen in water, giving hydrogels properties similar to cartilage. These gels therefore mimic the 3D environment of cells in cartilage, and have been shown to promote chondrocyte attachment in a similar manner to cartilage ECM (Cushing and Anseth, 2007), maintain the chondrogenic phenotype (Yamaoka et al., 2006), and through their viscoelastic properties, permit the transfer of loads to chondrocytes, which depend on mechanical signals for their survival (Mauck et al., 2000a). There are several design variables that can be altered to modify the potential of a hydrogel to function as a cartilage substitute as shown in Figure 2-21 (Spiller et al., 2011).

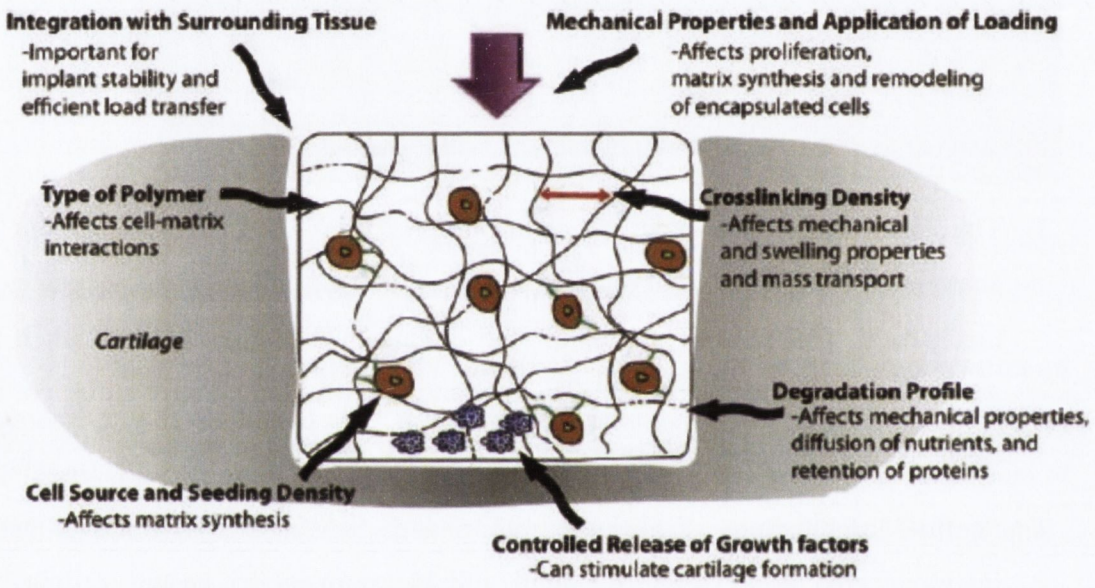

Figure 2-21: Illustration of how design variables can affect hydrogel properties and response of encapsulated cells (Spiller et al., 2011).

Hydrogels can be composed of naturally derived materials, or of synthetic polymers. Hydrogels formed from naturally derived polymers, such as agarose, alginate and collagen, are attractive biomaterials because they can be degraded by cell-secreted enzymes (Spiller et al., 2011). Such hydrogels are used in MACI including collagen type I/III and hyaluronan (Marcacci et al., 2005).

2.6.3.1 Agarose

Agarose, a linear polysaccharide derived from marine red algae, was one of the first hydrogels studied for tissue engineering purposes, due to its ease of gelation and cell

encapsulation (Spiller et al., 2011). Chondrocyte (CC) seeded agarose hydrogels have been shown to support the chondrogenic phenotype (Benya and Shaffer, 1982, Sun et al., 1986), support the synthesis of functional cartilaginous ECM (Aulthouse et al., 1989, Buschmann et al., 1992a, Mauck et al., 2000a, Mauck et al., 2002a, Mauck et al., 2003c), and have been shown to be biocompatible (Cook et al., 2003). Studies have used CC seeded agarose hydrogels to form cartilage tissue with similar mechanical properties to native cartilage (Lima et al., 2006, Lima et al., 2007, Byers et al., 2008), in combination with transforming growth factor-β3 (TGF-β3) and delayed mechanical loading. Agarose hydrogels have also been used as scaffolds for chondrogenically primed stem cells (Mouw et al., 2007, Erickson et al., 2009, Buckley et al., 2010c, Vinardell et al., 2011, Vinardell et al., 2012b). For example, bone marrow-derived MSC (BMSC) encapsulated agarose has been used for cartilage tissue engineering purposes (Mauck et al., 2006, Mauck et al., 2007, Thorpe et al., 2008, Huang et al., 2009, Thorpe et al., 2010a, Huang et al., 2010a, Thorpe et al., 2013). More recently, infrapatellar fat pad-derived stem cells (FPSCs) have been shown to possess a strong chondrogenic capacity when encapsulated in agarose hydrogels (Buckley et al., 2010a, Buckley et al., 2010c, Buckley and Kelly, 2012). A study comparing agarose to other hydrogel types, including alginate and type I collagen, has shown that MSC seeded agarose gels express the highest aggrecan and collagen type II gene expression (Diduch et al., 2000), demonstrating the importance of the hydrogel in cartilage engineering. Hydrogels based on agarose (and alginate) are commercially available as CARTIPATCH (Selmi et al., 2007, Selmi et al., 2008).

2.6.3.2 Alginate

Alginate is a naturally occurring anionic polymer typically obtained from brown seaweed (*Phaeophyceae*). The structure of alginate consists of blocks of (1, 4)-linked β-D-mannuronate (M) and α-L-guluronate (G) residues. Only the G blocks of alginate are believed to participate in intermolecular cross-linking with divalent cations (e.g. Ca^{2+}) to form hydrogels; therefore the M/G ratio, sequence and G-block

length are critical factors affecting the physical properties of alginate hydrogels (George and Abraham, 2006, Lee and Mooney, 2012).

Alginate has been investigated and used for many biomedical applications, due to its attractive characteristics of:

1. Biocompatibility
2. Low toxicity
3. Low cost
4. Mild gelation by addiction of divalent cations such as Ca^{2+} (Gombotz and Wee, 1998).

Due to these properties alginate has a lot of applications in:

- Wound healing - Alginate wound dressings can maintain a physiologically moist environment, minimize bacterial infection and encourage significant wound healing (Lee and Mooney, 2012).
- Delivery of bioactive agents - Drugs and macromolecular proteins can be released from alginate hydrogels in a gradual, controlled manner (Simmons et al., 2004).
- Cell transplantation and tissue engineering.

For tissue engineering based therapies, alginate is often used in the form of a hydrogel. As stated earlier, these hydrogels are three-dimensionally cross-linked networks made up of hydrophilic polymers. They are usually biocompatible, as they are structurally similar to the macromolecular-based components in the body (Sakiyama-Elbert and Hubbell, 2001).

The most common technique used for preparing alginate hydrogels is the ionic cross-linking method. This method involves combining an aqueous alginate solution with ionic cross-linking agents, such as divalent cations i.e. Ca^{2+} from $CaCl_2$, $CaSO_4$, or $CaCO_3$, or Sr^{2+} from $SrCl_2$ (Lee and Mooney, 2012). The divalent cations bind to the guluronate blocks of the alginate chains, and these blocks form junctions with the guluronate blocks of adjacent polymer chains in what is called the

egg-box model of cross-linking, resulting in a gel structure (Grant et al., 1973). This process can be seen in Figure 2-22 below.

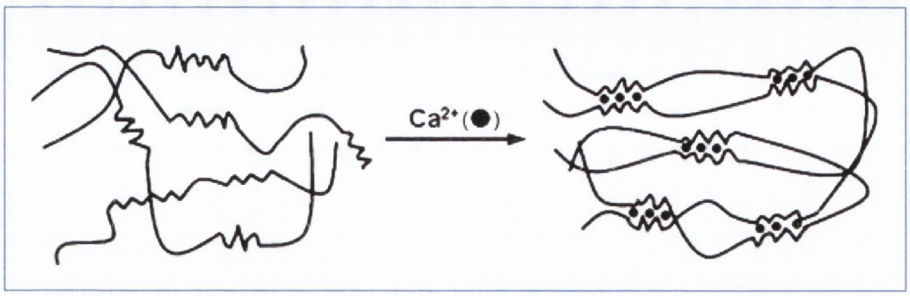

Figure 2-22: Egg-box model of ionic cross-linking of alginate hydrogels (Lee and Yuk, 2007, Lee and Mooney, 2012).

The gelation rate is a critical factor in controlling gel uniformity and strength when using divalent cations like Ca^{2+}, and slower gelation rates result in more uniform, ordered structures with greater mechanical integrity (Kuo and Ma, 2001). The temperature at which gelation occurs can affect the gelation rate; lower temperatures reduce the diffusion rate of divalent cations leading to slower cross-linking (Augst et al., 2006).

One drawback of the ionic cross-linking technique is the limited long-term stability of alginate hydrogels in physiological conditions; the gels can dissolve due to the release of the divalent ions cross-linking the gels into the surrounding culture media, due to exchange reactions with monovalent cations (such as sodium ions) (Lee and Mooney, 2012). Supplementing the culture medium with $CaCl_2$ is one way of preventing this temporal degradation of alginate.

There are, however, some situations where degradation of alginate is desirable, such as implantation of alginate hydrogels *in vivo*. In these cases, degradation of the alginate can be controlled through manipulation of the polymer molecular weight (MW) and composition (Augst et al., 2006). Gamma-irradiation of high MW alginate can yield polymers of various molecular weights and structures. Using gamma-irradiation to decrease the size of the polymer chains (and decrease the MW) can lead to increased degradation rates *in vivo* (Simmons et al., 2004). The more rapidly degrading gels typically lead to increased bone formation, both in terms of quality and quantity (Alsberg et al., 2003). Alginate hydrogel degradation

can also be accelerated through the process of partial oxidation (Jeon et al., 2012), as alginate can be made susceptible to hydrolysis *via* reaction with sodium periodate (Augst et al., 2006).

MSC seeded alginate has been used successfully in the past for *in vitro* cartilage tissue engineering (Ma et al., 2003, Mehlhorn et al., 2006, Shen et al., 2009, Igarashi et al., 2010, Lee and Mooney, 2012, de Vries-van Melle et al., 2014). It has also been used extensively in the field of bone tissue engineering (see section 2.7 for some examples).

2.6.3.3 Scaffold Architecture

Scaffold architecture can be modified to overcome issues such as nutrient transport and waste removal limitations. This would be a significant when engineering large constructs, where nutrients could not diffuse to the core of the scaffold, perhaps leading to core necrosis. Bian et al. obtained a more homogeneous cartilaginous tissue upon the introduction of macroscopic channels throughout the depth of the construct (Bian et al., 2009a). Buckley et al. found that the introduction of microchannels, in addition to rotational culture, resulted in sGAG accumulation levels in the core similar to those relatively high values measured in the periphery of solid constructs (Buckley et al., 2009b). Modifying scaffold architecture therefore could be an important step when attempting to engineer large functional tissues, suitable for treating OA lesions.

2.6.3.4 Self-Assembly method

Self-assembly is a relatively new technique involving the culturing of cells without any initial scaffold. The self-assembly (SA) process itself typically involves the aggregation of cells within transwell inserts (Yu et al., 1997, Naumann et al., 2004, Murdoch et al., 2007, Hayes et al., 2007) or custom made agarose molds (Hu and Athanasiou, 2006a, Elder and Athanasiou, 2008a), allowing the cells to secrete their own ECM which collectively acts as a scaffold forming a cohesive construct. It is one of many scaffold-free techniques currently being investigated in the field of cartilage engineering. These scaffold-free techniques began with the observation that chondrocytes cultured in high density monolayer form matrices that increase in

thickness over time (Adkisson Iv et al., 2001), and that small non-adherent clusters of chondrocytes can retain the chondrocytic phenotype (Tacchetti et al., 1987). The early SA studies mainly focused on the use of chondrocytes for engineering cartilaginous grafts (Reginato et al., 1994, Dodge et al., 1998, Estrada et al., 2001, Novotny et al., 2006).

From a tissue engineering perspective, the SA method has many advantages compared to cell culturing techniques involving scaffolds. SA can circumvent many scaffold-related issues, such as stress shielding of cells from biophysical stimulation, poor cell attachment, toxic scaffold degradation products, inflammatory response to the implanted material, poorly controlled biodegradability and a reduction in cell to cell communication, amongst others (Temenoff and Mikos, 2000a, Hutmacher, 2000, Bryant et al., 2004a, Liu and Ma, 2004, Hu and Athanasiou, 2006b, Elder et al., 2009, Tran et al., 2011, Athanasiou et al., 2013, Kharkar et al., 2013). The following table compares scaffold use to the self-assembling process (Hu and Athanasiou, 2006b).

Table 2-1: Comparison of scaffold use to self-assembling process (Hu and Athanasiou, 2006b).

	Possible scaffold problems	Self-assembling solutions
1	Stressful seeding processes such as cross-linking process	No seeding stress
2	Loss of phenotype associated with some solid scaffolds	Phenotype retained in self-assembling process
3	Inhibition of cell migration and cell to cell communication	Cells initially in direct contact with each other
4	Stress shielding of cells from mechanotransduction	Entirety of neotissue fully exposed to mechanical stimuli
5	Scaffold obstructs cell growth and ECM remodelling	Unobstructed ECM production and remodelling
6	Toxic degradation products	No degradation products
7	Inflammatory response towards scaffold	No scaffold for body to react to
8	Invasion of other cell types into scaffold	Cells form cohesive construct with no space for other cells

Numerous approaches to forming scaffold-free constructs have been described, including pellet culture, active tissue contraction, transwells, custom moulds, and agarose wells (Tran et al., 2011). Pellet culture involves centrifuging cells in microtubes, and allowing the mass of cells to aggregate. This culture is

commonly used to investigate chondrocyte and MSC responses to various stimuli. Pellet culture is particularly suited for studying MSCs, as the cell-cell interactions are similar to those observed in pre-cartilage condensations found during embryonic development (Zhang et al., 2010). Studies have shown that MSCs are capable of chondrogenic differentiation in pellet culture (Johnstone et al., 1998). However, some studies have raised concerns about this approach, witnessing undifferentiated and necrotized central regions of the pellet, with chondrogenic differentiation found only in the outer layers (Kafienah et al., 2007). The self-assembly method was found to be superior to the pellet culture system with human bone marrow derived MSCs (Zhang et al., 2010). The self-assembly method in this instance involved suspending cells in chondrogenic medium, and covering the plastic surface of a tissue culture plate with the cell suspension; SA constructs were found to accumulate higher levels of sGAG and type II collagen than pellet culture. In addition, the deposition of ECM was more homogenous with the SA method.

The self-assembly method is often performed in agarose moulds (Zhang et al., 2011), particularly when investigating the self-assembly of chondrocytes (Hu and Athanasiou, 2006a, Elder and Athanasiou, 2008a). In one such study, chondrocytes allowed to self-assemble in agarose coated 96-well plates formed tissue-engineered constructs that were hyaline-like in appearance with histological, biochemical, and biomechanical properties approaching those of native articular cartilage (Hu and Athanasiou, 2006b). The constructs reached one third the stiffness of native tissue. Coating the plates in agarose avoided the problem of chondrocytes dedifferentiating on the plastic surface of the tissue culture plate. Radial confinement has also been shown to be beneficial for chondrocyte self-assembly, increasing the aggregate modulus and improving the collagen organization in the engineered construct (Elder and Athanasiou, 2008a). Studies have investigated the optimal seeding density for self-assembly using chondrocytes (Revell et al., 2008). When comparing seeding densities ranging from 0.25-11 million cells per construct, the optimal initial seeding density was found to be 3.75 million cells, with no functional constructs formed when seeded with less than 2 million cells. Higher seeding density contributed to thicker constructs with larger diameters and had a significant effect on biochemical and mechanical properties.

Transwells are also used for self-assembly, as they provide a surface for cell attachment while minimally inhibiting diffusion of nutrients and waste products to and from the cells (Elder et al., 2009). They also laterally confine the tissue as it forms, giving the user control over the tissue's shape and dimensions. Chondrocyte self-assembled constructs engineered on a PET membrane have been shown to result in the generation of hyaline cartilage (Naumann et al., 2004). The experimental set-up is illustrated in Figure 2-23.

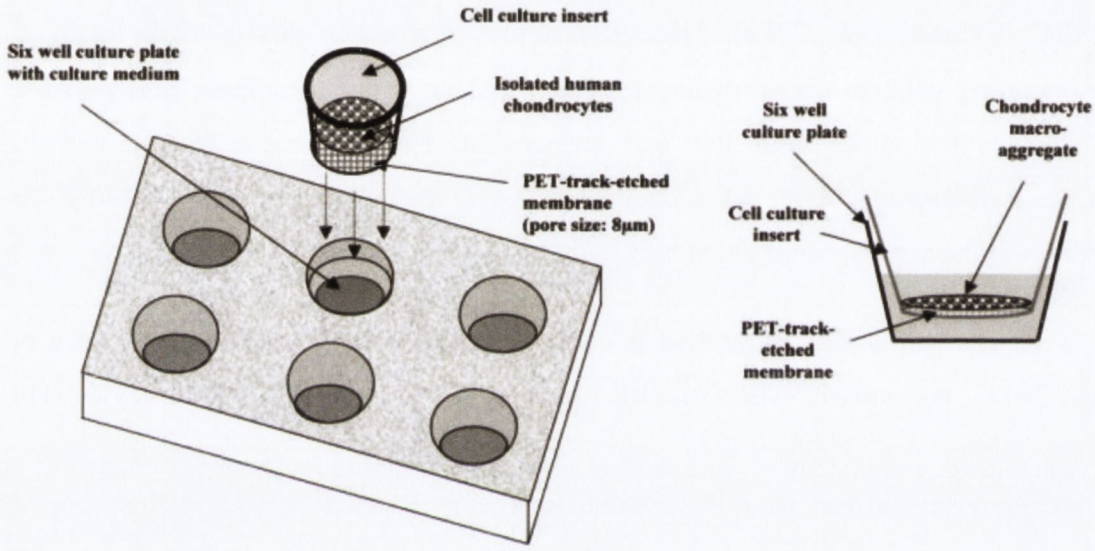

Figure 2-23: Experimental set-up for transwell culture. Cells are seeded on bottom of membrane for culture in 6 well plate (Naumann et al., 2004).

Transwells are more commonly used for BMSCs (Lee et al., 2011), with one study using 6.5 mm diameter, 0.4 μm pore size polycarbonate transwells to culture human BMSCs (Murdoch et al., 2007). Within 2 weeks, these BMSCs were found to differentiate and produce translucent, flexible discs 1mm in thickness (seeded at 0.5 million cells) (Murdoch et al., 2007). When compared to pellets, it was also found that self-assembly was superior in terms of ECM production, with more homogenous deposition of matrix. Polyethylene terephthalate membrane transwell inserts (3 μm pores) have also been used with neonatal porcine bone

marrow MSCs to generate functional hyaline-like cartilage through self-assembly (Elder et al., 2009).

Porcine synovial-derived stem cells have also been used to engineer cartilaginous constructs using self-assembly (Ando et al., 2007). In this example, MSCs were cultured at high density in monolayer, forcibly detached from the substratum, and the cell/matrix complex was allowed to spontaneously contract into a construct. Implantation of the construct into a porcine chondral defect was found to initiate repair with a chondrogenic like tissue. The repair tissue exhibited mechanical properties similar to native porcine cartilage in static compression and friction tests. The study was repeated using human synovial-derived stem cells (Ando et al., 2008), and the resulting construct was found to possess self-supporting mechanical properties, with evidence of chondrogenesis.

Despite a significant interest in self-assembly in recent years, remarkably, no studies have been undertaken to determine if functional cartilage-like grafts can be engineered through self-assembly of infrapatellar fat pad-derived stem cells. In addition, one question which remains unanswered in the literature is whether the self-assembly approach is superior to hydrogel/scaffold encapsulation of cells as a means to engineer functional cartilaginous grafts (determined by direct experimental comparison).

The scaffold-free constructs reported in the literature typically range from 0.071 to 0.785 cm^2 in size (Tran et al., 2011). This is equivalent to a diameter of approximately 3 to 10mm. It has been shown in a study of 25,124 knee arthroscopies that the majority of chondral defects are at least 0.5 cm^2 (8mm diameter), over a third of which are at least 1cm^2 (11 mm diameter) (Widuchowski et al., 2007, Tran et al., 2011). If scaffold free constructs are to be used in the treatment of such defects, or in treating larger defects (such as those associated with OA), additional stimuli may be required to construct suitably sized constructs with adequate mechanical properties. Stimuli may include mechanical cues generated using bioreactors, or a variety of growth factors.

2.6.4 Environmental Factors important in Cartilage Tissue Engineering

The last member of the tissue engineering triad, environmental factors include mechanical factors, chemical factors, and biological growth factors. Bioreactors can provide a biomimetic environment to cells and scaffolds to optimise cell function (Chao et al., 2007). They enhance nutrient transport and waste removal and supply the necessary regulatory signals to the cells, such as dynamic compressive loading for cartilage. Bioreactors can aid seeding of scaffolds, when homogeneous distribution of cells is difficult (Freed et al., 1998).

2.6.4.1 Chondrocytes & Mechanical Factors

Some of the early bioreactor studies investigated dynamic compression of cartilage disks (Kim et al., 1994, Buschmann et al., 1999), showing compression stimulated cartilage-specific ECM production. Dynamic compressive loading has also been shown to improve the mechanical and biochemical properties of chondrocyte seeded agarose hydrogels (Mauck et al., 2000a, Mauck et al., 2003b, Hung et al., 2004, Kelly et al., 2004, Ng et al., 2006). Hydrostatic pressure has also been shown to enhance the biosynthetic activity of chondrocytes seeded into hydrogels (Toyoda et al., 2002, Toyoda et al., 2003, Elder et al., 2006). The temporal application of loading may also be important. Delayed loading has been beneficial for chondrocytes maintained in a chemically defined media supplemented with TGF-β3 (Lima et al., 2007), allowing the cartilage cells to first develop a substantial pericellular and extracellular matrix before loading commences.

2.6.4.2 MSCs & Mechanical Factors

Dynamic compressive loading of MSC seeded agarose gels has also been investigated (Huang et al., 2004a, Mauck et al., 2007). It has been demonstrated that dynamic compressive loading in the absence of TGF-β members can increase chondrogenic gene expression (Huang et al., 2005, Campbell et al., 2006, Mauck et al., 2007). In the presence of TGF-β3, some studies have shown increases in chondrogenic gene expression and ECM secretion with loading (Angele et al., 2004, Terraciano et al., 2007). Other studies however have shown decreases in

chondrogenic gene expression (Campbell et al., 2006) and ECM secretion (Thorpe et al., 2008, Kisiday et al., 2009, Thorpe et al., 2010a) with loading. It has recently been shown that delayed dynamic compression, initiated after a sufficient period of chondroinduction, can enhance matrix distribution and the mechanical properties of MSC seeded agarose constructs (Huang et al., 2010a).

Perfusion bioreactors have been designed to improve mass transport and to provide shear stimuli to MSCs as a means to enhance osteogenesis, as shear flow has been shown to promote osteopontin and osteocalcin gene expression in these cells (Li et al., 2004).

2.6.4.3 Self-Assembly & Mechanical Factors

Passive axial compression has been shown to significantly increase the Young's modulus and ultimate tensile strength of bovine chondrocyte self-assembled constructs, as well as increasing collagen production (Elder and Athanasiou, 2008a). Intermittent hydrostatic pressure (10 MPa, 1 Hz, 4h/day) has also been shown to increase collagen production for chondrocyte self-assembly (Hu and Athanasiou, 2006a). Tran *et al.* investigated the effects of perfusion and dynamic compression using a commercial bioreactor (C9-x Cartigen bioreactor) on similar constructs (Tran et al., 2011). Constructs cultured in the bioreactor exhibited an increase in total GAG content, equilibrium compressive modulus, and dynamic modulus compared to constructs maintained in free swelling conditions.

2.6.4.4 Growth Factors

The transforming growth factor (TGF)–β family of polypeptides includes the various TGF-β isoforms and bone morphogenetic proteins (BMPs). The TGF-β family include five members. Active TGF-β1, 2, and 3 are generally considered to be potent stimulators of proteoglycans and of type II collagen synthesis in chondrocytes (Vinatier et al., 2009). They can also induce chondrogenic differentiation of MSCs *in vitro* (Grimaud et al., 2002).

BMPs have essential roles in chondrogenesis and osteogenesis during skeletal development. Several BMPs can stimulate chondrogenic differentiation of MSCs and enhance synthesis of collagen II and aggrecan by chondrocytes *in vitro*. These include BMP-2, 4, 6, 7, 13 and 14 (Vinatier et al., 2009).

Fibroblast growth factors (FGF) are important in skeletal development. In adult chondrocytes, FGF-2 encourages proliferation. Furthermore, it has been observed that MSCs expanded in FGF-2 supplemented media not only proliferate more rapidly, but subsequently undergo more robust chondrogenic differentiation (Stewart et al., 2007).

2.6.4.5 Oxygen tension

Articular chondrocytes typically experience an oxygen concentration varying from 1 to 7% (Vinatier et al., 2009). The adaptation of the cells to this low oxygen tension is mediated by transcription factors, such as hypoxia inducible factor (Fedele et al., 2002). Hypoxia has been shown to increase the synthesis of ECM proteins in cultured chondrocytes *in vitro* (Domm et al., 2002). Hypoxia has also been shown to promote chondrogenic differentiation of MSCs derived from bone marrow (Robins et al., 2005) and adipose tissue (Wang et al., 2005). This suggests that hypoxia is a key regulator of the differentiation and biosynthetic activity of chondrocytes and chondroprogenitor cells. It has also been suggested that hypoxia can inhibit collagen X expression, the marker of chondrocyte hypertrophy, during chondrogenesis of epiphyseal chondrocytes (Chen et al., 2006), adipose derived MSCs (Betre et al., 2006) and BMSCs (Sheehy et al., 2012).

2.7 Bone Tissue Engineering

Current therapies to treat large bone defects often require the use of bone grafts. Bone tissue can be taken from the patient to treat these defects, but availability is very limited (Meijer et al., 2008, Farrell et al., 2011). There is, therefore, a huge interest and need to develop new strategies for bone replacement. Tissue engineering based therapies attempting to regenerate damaged bone typically form bone tissue through the process of intramembranous ossification. This strategy will

be briefly reviewed next, along with the limitations associated with such an approach.

2.7.1 Intramembranous Bone Tissue Engineering

Attempts to regenerate bone typically involve seeding BMSCs within 3D scaffolds and culturing the resultant constructs in osteogenic medium *in vitro*, followed by implantation into the patient (Santos and Reis, 2010). This strategy attempts to recapitulate the intramembranous (ossification) bone formation process in the body, where MSCs differentiate directly into bone-forming osteoblasts and lay down new bone. When the tissue engineered construct is implanted into an avascular region however, the implanted cells have a limited capacity to uptake substrate molecules (such as oxygen and glucose) and to clear waste products (Santos and Reis, 2010). Cell and construct viability can be hugely impaired by these limitations derived from a lack of vasculature, often leading to core degradation /necrosis and implant failure (Sieminski and Gooch, 2000, Muschler et al., 2004). Using this intramembranous approach for bone formation has a further limitation in that the *in vitro* culture of a tissue engineered construct (in osteogenic conditions) can lead to significant mineralisation of the matrix contained within the scaffold. This can subsequently seal the pores of the scaffold and further restrict vascularisation once the construct is implanted *in vivo*. In fact, it has been shown that both acellular collagen-GAG and collagen-calcium phosphate scaffolds can lead to greater bone healing (in rat cranial defects) than that observed in otherwise identical (osteogenically primed) MSC seeded scaffolds (Lyons et al., 2010). Immunological analysis revealed that this was due to MSCs depositing excess matrix during *in vitro* culture, which then acted as a barrier to macrophage-led remodelling, vascularisation and bone formation when implanted *in vivo*, resulting in avascular core necrosis of osteogenically primed MSC seeded implants (O'Brien, 2011). Numerous other studies have demonstrated how a major obstacle to clinical success in bone tissue engineering is this problem of core degradation (Goldstein et al., 2001, Tremblay et al., 2005, Ko et al., 2007, Phelps and Garcia, 2009, O'Brien, 2011).

The intramembranous approach for bone tissue engineering has been attempted with alginate. Osteogenically primed bone marrow-derived MSCs (BMSCs), in combination with calcium cross-linked alginate gels, have had some success in engineering bone tissue and repairing alveolar bone defects in dogs (Weng et al., 2006). One promising study has shown that alginate/chitosan gels in combination with BMSCs and bone morphogenetic protein-2 (BMP-2) can stimulate trabecular bone formation in nude mice (Park et al., 2005).

Looking at the literature as a whole, a large number of bone tissue engineering studies attempting to recapitulate the intramembranous ossification process demonstrate the significant limitations of this approach; namely, the difficulty for vasculature to reach the centre of tissue engineered constructs, and the difficulty in providing cells with the necessary nutrients and oxygen required for survival. For these reasons, bone tissue engineers have started moving away from this approach, and have begun looking at the process of endochondral ossification for inspiration and guidance in forming whole bones *in vivo*.

2.7.2 Endochondral Bone Tissue Engineering

There are several rationales behind the hypothesis that endochondral bone formation is more promising in a bone tissue engineering context than the more traditional method of intramembranous ossification (Farrell et al., 2011). For a start, chondrocytes in the body normally reside in an avascular tissue and are therefore naturally programmed for optimal functionality in a low oxygen environment (Coyle et al., 2009, Farrell et al., 2011). This is almost the exact environment chondrogenically primed MSCs would be subjected to upon implantation into an avascular area of tissue. In addition, chondrogenically primed MSCs cultured *in vitro* have a natural tendency to become hypertrophic, which is an important step in the endochondral ossification pathway (Pelttari et al., 2006, Hellingman et al., 2010, Farrell et al., 2011). Furthermore, it has been suggested that the factors released by chondrogenically primed MSCs progressing along the endochondral pathway *in vivo* would be considerably more complex and controlled spatiotemporally than any

growth factor combination one could propose when attempting to optimise vascularisation and bone formation in the body (Farrell et al., 2011).

An early bone tissue engineering study attempting to recapitulate endochondral ossification was also one of the first studies showing that whole-bone reconstruction can be performed using MSCs (Huang et al., 2006). This study found that chondrogenically primed MSC seeded hyaluronan scaffolds can lead to abundant bone formation and neovascularisation within the carpal bone when implanted *in vivo* for 12 weeks (Huang et al., 2006). Histological analysis at 6 weeks showed filling of the carpal space with islands of cartilage with interspersed bone ossicles, indicating bone formation was due to endochondral ossification. Importantly, osseous tissue was formed in the central portions of the tissue engineered constructs. Endochondral bone tissue engineering has also been achieved using embryonic stem cells (ESCs) (Jukes et al., 2008). In this study chondrogenically primed ESCs seeded within ceramic scaffolds were shown to form efficient endochondral bone when implanted orthotopically into critical-size cranial defects in rats.

There have been studies directly comparing the endochondral approach to the traditional intramembranous approach for bone tissue engineering. One such study tested how *in vitro* priming of human BMSCs along osteogenic and chondrogenic lineages influenced cell survival and bone formation *in vivo* (Farrell et al., 2009). Vessel ingrowth was reported in chondrogenically primed MSC seeded collagen-GAG scaffolds, whereas osteogenically primed MSC seeded scaffolds (recapitulating the intramembranous ossification approach) led to a poorly mineralized matrix with few surviving cells and no vascularisation. Chondrogenically primed MSCs were also found to produce vascular endothelial growth factor (VEGF) and matrix metalloproteinases (MMPs) during culture, factors known to be crucial for the induction of vascularisation. A follow-up study (with a longer *in-vivo* culture period) reported that after 8 weeks of subcutaneous implantation, chondrogenically primed MSC seeded scaffolds successfully formed (endochondral) bone and bone marrow (Farrell et al., 2011). Osteogenically primed constructs did not form any bone *in vivo*, highlighting the superiority of the

endochondral approach for bone tissue engineering. In agreement with this work, chondrogenic priming of MSCs on β-TCP scaffolds *in vitro* can also result in endochondral bone formation *in vivo*, with formation of haematopoietic marrow reported using this approach (Janicki et al., 2010). Again, endochondral bone formation was superior to the intramembranous approach in this study, with no haematopoietic marrow formed in intramembranous bone. Furthermore, in a study attempting to develop tissue engineered bone through endochondral and intramembranous ossification (using MSCs and osteoblasts respectively), it was shown that MSC seeded ceramic scaffolds undergoing endochondral ossification *in vivo* permitted greater vascularisation (both in terms of organisation and quantity) than osteoblast seeded implants undergoing intramembranous ossification (Tortelli et al., 2010). The authors postulated that increased vascularisation in MSC seeded implants (undergoing endochondral ossification) was due to a higher capacity of MSCs in recruiting host CD31+ endothelial cells.

One study using chondrogenically primed self-assembled MSCs to engineer endochondral bone *in vivo* reported some interesting results (Scotti et al., 2010). Implants displayed two distinct regions 4 weeks after implantation; an outer osteoid tissue, resembling a bony collar, and an inner cartilaginous region. After 8 weeks of implantation, the central cartilaginous region was almost completely resorbed, and bone ossicles appeared in its place. The implanted constructs were quite small; therefore, a follow-up study investigated the engineering of scaled-up bone (8 mm diameter) through endochondral ossification (Scotti et al., 2013). MSCs were seeded onto type I collagen meshes and cultured for 3 weeks in chondrogenic medium, followed by 2 weeks in hypertrophic medium (supplemented with IL-1β to accelerate remodelling) . After subcutaneous implantation, the cartilage tissue was effectively remodelled into bone and bone marrow. The implant was divided into 2 regions; an outer cortical-like perichondral bone region, and an inner trabecular-like endochondral bone area. Cartilage remodelling was accompanied by blood vessel ingrowth, displaying sinusoid-like structures and stabilised by pericytic cells (Scotti et al., 2013). In addition, marrow cavities of the ossicles contained native like levels of haematopoietic stem cells. The construct core, however, did include areas devoid of cells and matrix, demonstrating the challenges in generating scaled-up engineered

bone, and highlighting the importance of employing an appropriate scaffold material when attempting to engineer such large constructs.

Chondrogenically primed poly(lactic-co-glycolic acid)/poly(ε-caprolactone) MSC seeded scaffolds have also been used to successfully form endochondral bone *in vivo* (Yang et al., 2013). Finally, looking at alginate, BMSC seeded alginate hydrogels incorporated with BMP-2 and TGF-β3 have been shown to result in significant bone formation (occurring by endochondral ossification) after 15 weeks *in vivo* (Simmons et al., 2004). The alginate in that study was subjected to gamma-irradiation to accelerate the degradation rate *in vivo*, and covalently modified with RGD-containing peptides to control cell behaviour.

In conclusion, recapitulating the process of endochondral ossification for bone tissue engineering would appear to be quite superior to the more traditional intramembranous approach, although additional work is needed in generating scaled-up engineered bone of a clinically relevant size.

2.8 Osteochondral Tissue Engineering

Engineering osteochondral tissues comprised of articular cartilage and underlying subchondral bone is necessary to replace large defects (consisting of both damaged cartilage and bone) within synovial joints. Osteochondral tissues can also aid the integration between engineered constructs and host cartilage, with the osseous layer (of osteochondral constructs) acting as an anchor between engineered cartilage implants and host cartilage. The different approaches to engineering osteochondral constructs will be briefly discussed in this section.

One approach to osteochondral tissue engineering involves seeding chondrocytes directly onto an osseous scaffold base. Scaffold-free CCs have been combined with cell-free calcium polyphosphate bases, leading to bilayered implants which can withstand loading *in vivo* for up to 9 months with evidence of fusion to adjacent native cartilage, and fixation by bone ingrowth into the osseous base (Waldman et al., 2003a, Kandel et al., 2006). Self-assembled CCs have also been combined with cell-free poly(lactic acid) (PLA) or collagen/hydroxyapatite bases

(Wang et al., 2004) to form osteochondral constructs. After 7 weeks of culture, the CCs produced a layer of cartilage integrated with the subchondral scaffold. An *in vivo* study also using this strategy consisted of self-assembled CCs combined with β-tricalcium phosphate (β-TCP) for the subchondral base (Guo et al., 2004). Hyaline-like cartilage was observed 24 weeks post-implantation, but the authors recommended that further long-term studies would be required to justify the efficacy of the ceramic base.

Perhaps the most widely explored strategy for osteochondral tissue engineering involves the use of individual scaffolds for the bone and the cartilage regions that are subsequently joined together either before or during surgical implantation (O'Shea and Miao, 2008). One of the first osteochondral constructs formed in this manner consisted of 2 different regions sutured together (Schaefer et al., 2000, Schaefer et al., 2002). Chondrocyte (CC) seeded polyglycolic acid (PGA) meshes (the chondral layer) were sutured to periosteal cell seeded poly(lactic-co-glycolic acid)/polyethylene glycol (PLGA/PEG) sponges (the osseous bone forming layer) in one example (Schaefer et al., 2000). A follow-up study sutured CC seeded PGA meshes to collagen hydroxyapatite sponges (cell-free or with absorbed bone marrow) (Schaefer et al., 2002) with some success. Osteochondral constructs have been formed combining CC seeded PGA/PLA scaffolds (chondral layer) with natural or synthetic calcium carbonate osseous bases, using a fibrin cell solution to aid integration (Kreklau et al., 1999). In addition, CC seeded gelatin scaffolds have been combined with (cell-free) bone-derived calcium-phosphate blocks (Chang et al., 2004). Furthermore, chondrogenically primed BMSC seeded hyaluronic acid sponges have been combined with osteogenically primed BMSC seeded calcium phosphate bases, with the 2 components sealed together using a fibrin sealant (Gao et al., 2001). However, the cartilage formed in the chondral layer of osteochondral constructs in this study was found to be of a fibrous nature.

Instead of generating composite osteochondral grafts by crudely combining the separate chondral and osseous layers, heterogeneous osteochondral constructs composed of 2 distinct but integrated layers can be fabricated (Martin et al., 2007). This approach has been utilised in PLGA based scaffolds (Niederauer et al., 2000)

with one such study generating a composite scaffold consisting of CC seeded PLGA/PLA in one region, and PLGA/TCP in the other osseous region (Sherwood et al., 2002). Schek *et al.* also made use of synthetic polymers and ceramics to form a bilayered scaffold. In this study, a PLA sponge was seeded with porcine articular CCs and attached to a hydroxyapatite scaffold using biodegradable polymer fixation (Schek et al., 2004). The osteochondral scaffold was found to promote bone and cartilage growth, with a mineralised interface tissue. Novel chitosan/hydroxyapatite bilayered scaffolds have also been formed (Oliveira et al., 2006). In this study chitosan was allowed to partially penetrate the top region of the hydroxyapatite osseous base to allow proper integration of the two layers.

Generating a single homogenous scaffold using 2 cell types (with chondrogenic and osteogenic capacities) has been shown to be an effective osteochondral strategy also. One study implemented this approach by generating a PCL scaffold through fused deposition modelling (Cao et al., 2003). CCs were cultured in one half of the scaffold with MSCs cultured in the other half, and the composite construct was cultured *in vitro* in medium containing osteogenic supplements. In another study, a single poly(ethylene glycol) diacrylate (PEGDA) scaffold was seeded with either chondrogenically or osteogenically primed MSCs to form an osteochondral construct (Alhadlaq et al., 2004). The cells were loaded in two stratified and integrated hydrogel layers that were sequentially photopolymerised in a human condylar mould. After 4 weeks *in vivo*, the MSC derived CCs and osteoblasts had synthesised some cartilage and bone tissue.

The most sophisticated model for osteochondral tissue engineering makes use of an integrated structure allowing for both a cartilage and bone region, with a complete transition between the two scaffold components. More recent studies have targeted their efforts at generating these continuous stratified constructs. The main challenges facing these constructs include maintaining the stability of the cartilage and bone regions, and recapitulating the osteochondral interface (consisting of a thin layer of mineralized cartilage), critical for establishing long term functionality. Jiang *et al.* successfully generated an osteochondral scaffold comprised of 3 distinct, yet continuous regions of cartilage, calcified cartilage, and bone (Jiang et al., 2010). The

scaffold was based on an agarose hydrogel and composite microspheres of PLGA and 45S5 bioactive glass, seeded with chondrocytes and osteoblasts. The PLGA/bioactive glass component helped to promote CC mineralisation and a calcified interface.

In addition to generating osteochondral constructs by way of multi-layered scaffolds (Gao et al., 2001, Oliveira et al., 2006, Mano and Reis, 2007, Martin et al., 2007, Theodoropoulos et al., 2011, St-Pierre et al., 2012, Rodrigues et al., 2012, Sheehy et al., 2013), physical conditioning of tissues through the use of novel bioreactors can also be implemented to generate such tissues (Wang et al., 2004, Wendt et al., 2005, Mahmoudifar and Doran, 2005, Grayson et al., 2010, Rodrigues et al., 2011). Spatial growth factor or gene delivery systems can also be implemented to create desirable biological microenvironments that promote optimised osteochondral tissue regeneration (Mason et al., 1998, Saraf and Mikos, 2006, O'Shea and Miao, 2008, Guo et al., 2009, Guo et al., 2010, Chen et al., 2011, Re'Em et al., 2012, Santo et al., 2013a, Santo et al., 2013b).

There have been promising advances in the field of osteochondral tissue engineering of late, but overall, many tissue engineered osteochondral grafts suffer from poor tissue formation and compromised integration at the interface between the cartilage and bone layers (Schaefer et al., 2000, Gao et al., 2001, Schaefer et al., 2002, Fedorovich et al., 2012). Poor integration between the osteochondral graft and the host tissue is also a problem (Theodoropoulos et al., 2011), suggesting that further research into this area is required. In addition, many studies utilise CCs when forming the chondral layer of osteochondral constructs. This approach would be unfeasible when attempting to generate scaled-up constructs, where the availability of healthy CCs would be limited (especially in OA patients, for example). In addition, studies using MSCs to form cartilage (within osteochondral constructs) can lead to the formation of fibrocartilage as opposed to hyaline cartilage (Gao et al., 2001). Future studies investigating different cell sources for the chondral layer of osteochondral constructs are required.

2.9 Engineering Anatomically Shaped, Large-Scale Constructs

There have been several approaches pursued in the attempt to recapitulate the complex, anatomically accurate shapes of various chondral and osteochondral tissues in the body (Chao et al., 2007). The temporomandibular joint condyle is one such structure, due to its relatively small size and highly complex structure (Alhadlaq et al., 2004, Alhadlaq and Mao, 2005). As previously described, Alhadlaq *et al.* successfully generated an osteochondral construct through the photopolymerisation of 2 stratified and integrated PEGDA hydrogel layers in the shape of a human mandibular condyle (11 x 6 x 7 mm) (Alhadlaq et al., 2004). After 12 weeks *in vivo* culture, two stratified layers of cartilaginous and osseous tissues were formed, with the osseous portion containing bone trabeculae-like structures (Alhadlaq and Mao, 2005).

Photopolymerisation is a type of rapid prototyping. In the last decade, researchers have turned to other rapid prototyping techniques for producing scaffolds for tissue engineering applications (Hutmacher, 2000, Hutmacher et al., 2001, Zein et al., 2002, Huang et al., 2002, Sun and Lal, 2002, Woodfield et al., 2004), with great potential for creating anatomically accurate constructs. Rapid prototyping can allow for the formation of highly complex, but reproducible structures, generally constructed one layer at a time *via* computer-aided design (CAD) models and computer-controlled tooling processes (CAM) (Woodfield et al., 2004). These techniques allow researchers to design-in certain properties, such as porosity, pore size and interconnectivity. One of these rapid prototyping techniques is fused deposition modelling (FDM). This process uses rollers to feed a pre-formed fibre through a heated nozzle onto a computer-controlled table in a layer by layer process (Hutmacher, 2000, Hutmacher, 2001, Hutmacher et al., 2001, Zein et al., 2002, Huang et al., 2002, Woodfield et al., 2004). The designed object is fabricated as a 3D part based solely on the precise deposition of thin layers of the extrudate (Zein et al., 2002).

One significant study using rapid prototyping techniques to generate scaled-up, anatomically accurate osteochondral constructs successfully created anatomically shaped human tibial condyles (20 x 15 x 15 mm) (Lee et al., 2009). A

composite of poly-ε-caprolactone and hydroxyapatite (PCL/HA) was fabricated using layer deposition of 3D interlaid strands (Figure 2-24). Briefly, the anatomical contour of a human proximal tibial joint condyle was acquired from CT scans and manipulated using computer aided design software for 3D reconstruction. The composite polymer scaffold was then fabricated using layer by layer deposition with the 3D printing system Bioplotter. These constructs were seeded with osteogenically primed MSCs. An overlaying layer of PEG hydrogel (containing chondrogenically primed MSCs) was moulded into anatomic shape and attached to the PCL/HA osseous base to form an osteochondral construct.

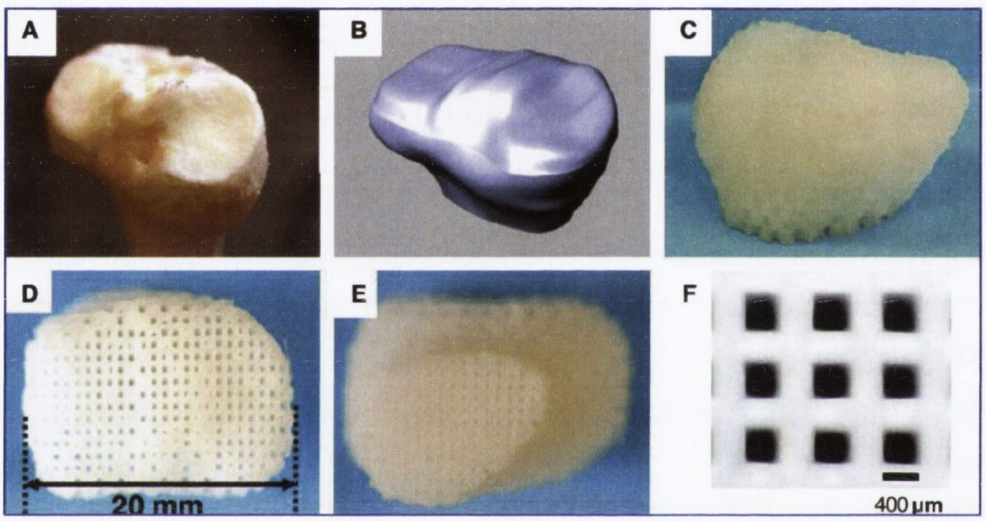

Figure 2-24: Bioengineering design of synovial joint condyle. The anatomical shape of a human proximal tibial condyle (A) was captured using computed tomography scanning and manipulated using computer-aided design (B). (C-F) A composite of PCL and hydroxyapatite was fabricated into anatomical shape using layer deposition of 3D interlaid strands (Lee et al., 2009).

A follow-up study involved forming anatomically accurate PCL/HA constructs mimicking the shape of the articular surface of unilateral proximal humeral joint condyles of rabbits (Lee et al., 2010). These bioscaffolds were infused with TGF-β3-adsorbed collagen hydrogel. After 4 months *in vivo*, it was found that the entire articular surface of the synovial joint could be regenerated. The regenerated cartilage was also integrated with regenerated subchondral bone that

had well defined blood vessels. Similar attempts to regenerate the femoral condyle using osteochondral strategies have also occurred. One such study combined an osteogenically primed MSC seeded PCL/HA base with a CC seeded PGA/PLA chondral layer when trying to regenerate a goat femoral head (Ding et al., 2013). The surface morphology of the goat femoral head was obtained by laser scanning. CAD software was used to design a mould from 3D rendered images, and an anatomically accurate mould was then fabricated by 3D printing (fused deposition modelling). After 10 weeks of implantation, successful generation of smooth, continuous homogeneous cartilage and stiff-bone like tissue was observed in the two engineered layers of the osteochondral constructs. These studies demonstrate the potential of anatomically accurate engineered grafts in regenerating whole joints.

An interesting study by Woodfield *et al.* compared anatomical femoral and tibial cartilage constructs fabricated through either three-dimensional fibre deposition (3DF) (fused deposition modelling technique) or compression moulding/particulate leaching (CM) (Woodfield et al., 2009). The following figure illustrates their manufacturing process.

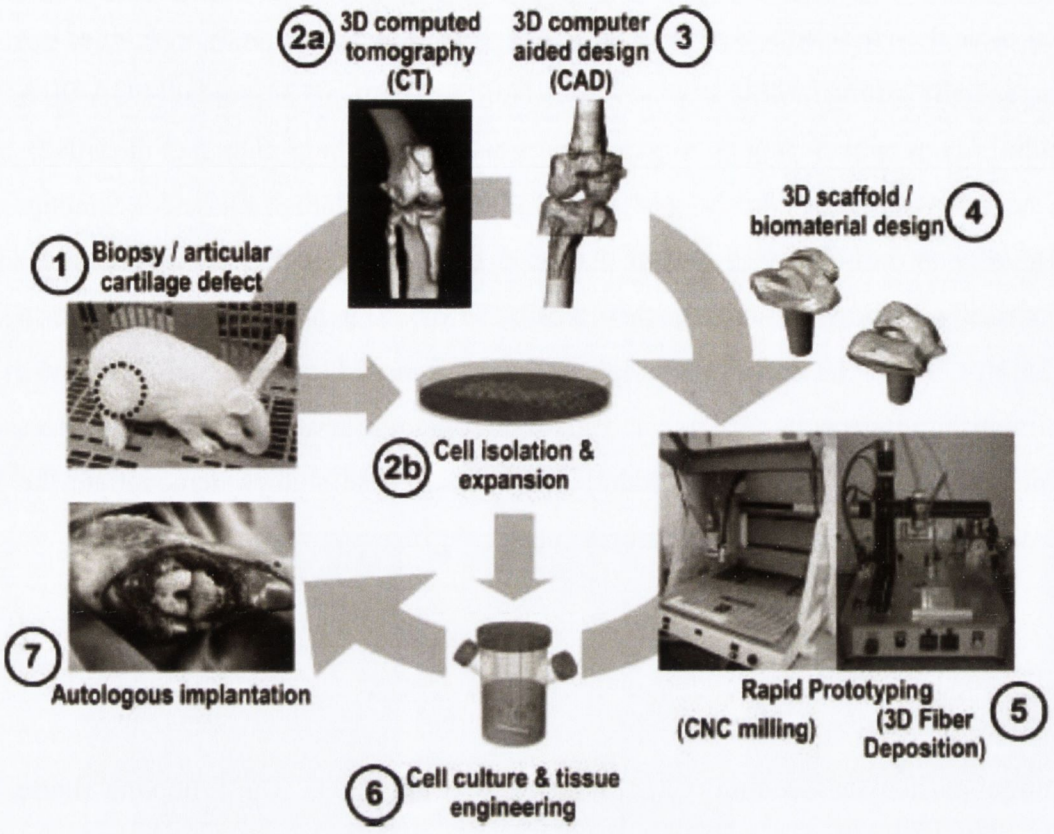

Figure 2-25: Process for developing anatomically shaped, tissue-engineered constructs with congruent articulating surfaces. (1) Harvest of cartilage biopsy; (2a) development of three-dimensional (3D) model by computed tomography (CT) scans; (2b) cell isolation and expansion to obtain sufficient cell numbers; (3) 3D computer-aided design of desired anatomical shape from CT scan; (4) manipulation and rendering of 3D scaffold model in suitable format ready for rapid prototyping (RP); (5) processing of scaffold by RP, using computer numerical-controlled (CNC) milling of PEGT/PBT foam or 3D fibre deposition (3DF) of molten PEGT/PBT; (6) seeding and dynamic culture of expanded cells from (2a) in anatomically shaped RP scaffolds; and (7) autologous implantation of the anatomically shaped, tissue-engineered construct *in vivo* (Woodfield et al., 2009).

Differences between the two manufacturing processes can be seen in

Figure 2-26 below. 3DF scaffolds contained a simple, highly accessible pore volume due to large interconnecting pores, whereas CM scaffolds contained a less accessible pore volume due to smaller interconnecting pores. At the end of *in vitro* culture, it was observed that rapid prototyping of 3DF architectures promoted

homogeneous distribution of viable cells, sGAG and collagen type II, with superior levels of sGAG produced when compared to CM architectures. Constructs were subsequently implanted in rabbits, with satisfactory integration with rabbit bone observed 6 weeks post-surgery. However, repair tissue post-implantation appeared fibrocartilage-like, and did not resemble cartilage pre-implantation.

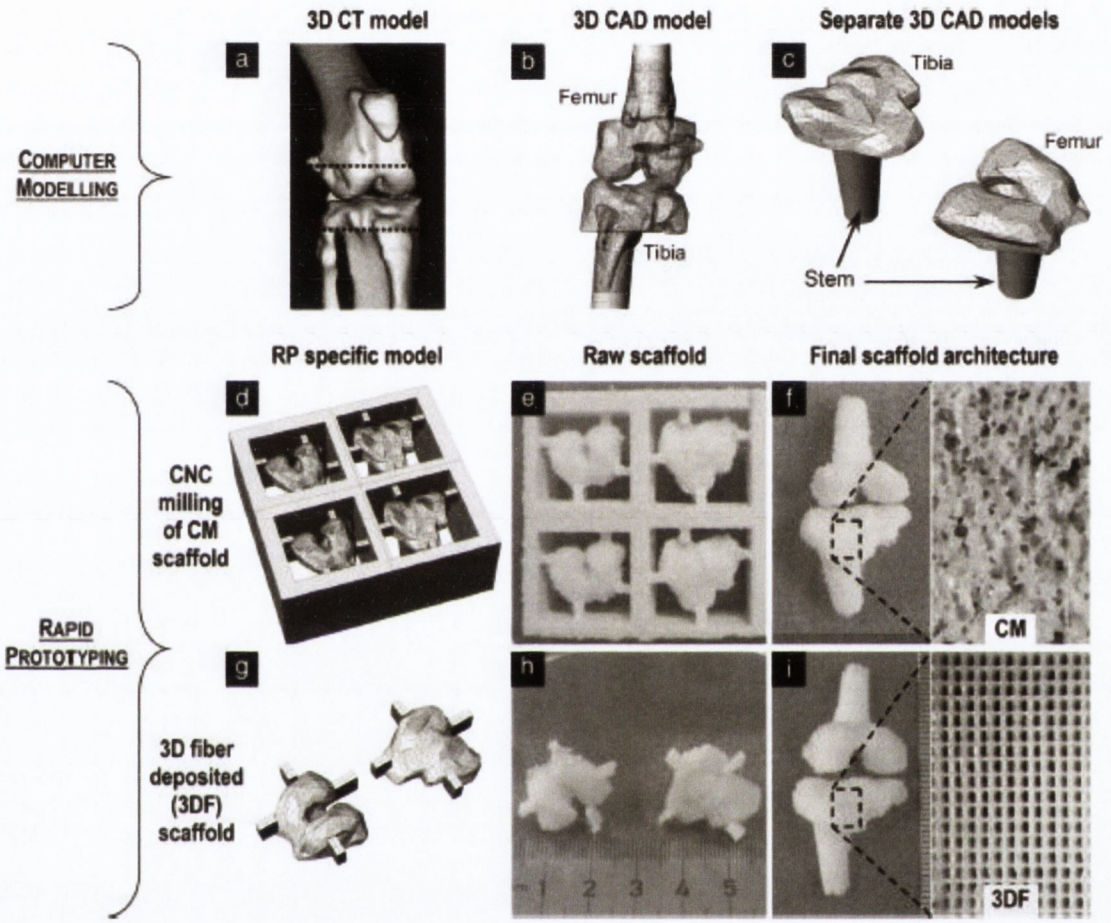

Figure 2-26: Computer modelling and rapid prototyping (RP) of porous, anatomically shaped femoral and tibial scaffolds. (a) 3D CT surface model of rabbit knee; (b) solid 3D CAD model redesigned to isolate articulating surfaces and integrate anatomical positioning of stem for medullary fixation; (c) solid 3D femoral and tibial models; (d-f) rapid prototyping of porous scaffolds using computer numerical-controlled (CNC) milling of compression moulded (CM) block of PEGT/PBT foam; and (g-i) 3D fibre deposition (3DF) of molten PEGT/PBT. Separate RP-specific models (d, g) were generated from which the raw scaffold could be manufactured (e, h). After removal of support structures, identical anatomically shaped CM (f) and 3DF (i) scaffolds were produced but with distinctly different internal pore architectures (Woodfield et al., 2009).

Fedorovich *et al.* also investigated the 3DF technique, characterising its use for the fabrication of cell-laden, heterogeneous hydrogel constructs for potential use as osteochondral grafts (Fedorovich et al., 2012). It was first shown that changing fibre spacing or angle of fibre deposition yielded scaffolds of varying porosity and elastic modulus. CCs and osteogenic progenitors were then printed in alginate hydrogels using the rapid prototyping technique. Distinctive tissue formation was observed in each component of the osteochondral construct (1 x 2 cm) *in vitro* and *in vivo*, with high cell viability. As the authors state, the results demonstrate the possibility of manufacturing large viable structured tissues through rapid prototyping, which could potentially be used for the repair of osteochondral defects.

Hung *et al.* investigated the feasibility of generating anatomically shaped osteochondral constructs in a very relevant study aimed at replacing the entire articular surface of a diarthrodial joint (Hung et al., 2003). Bovine chondrocytes were seeded in anatomically shaped agarose constructs reproducing the human patellar articular layer (diameter of approximately 4 cm), with subsequent integration into a corresponding anatomically shaped (devitalised) trabecular bone substrate (Figure 2-27). Human cadaver joints were used to acquire the geometry of the articular cartilage layer; this was then used in combination with CAD and CNC machining to create the anatomically accurate moulds. CCs were shown to be viable over the entire culture period, while the agarose they were encapsulated in maintained its shape in culture and remained firmly attached to the underlying osseous substrate. It was observed, however, that peak material properties of the constructs remained well below that of native tissue (one-eighth).

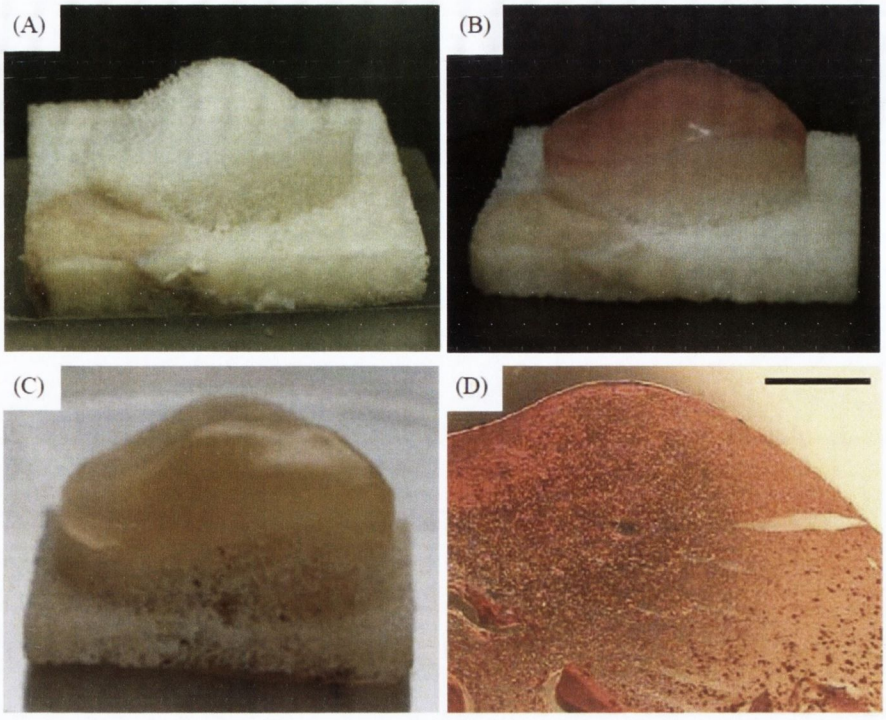

Figure 2-27: (A) Bony substrate of osteochondral construct having the subchondral shape of the patella machined from devitalised bovine trabecular bone. (B) CC seeded osteochondral patella construct with gel penetration. (C) Patellar osteochondral construct 14 days later. (D) Magnified region from chondral layer stained with Safranin O (Hung et al., 2003).

Generating large homogeneous constructs such as these (Hung et al., 2003) is an essential pre-requisite to treating large defects in the body. A more recent study attempting to generate scaled-up constructs reported the use of a perfusion bioreactor system (Santoro et al., 2010). This perfusion bioreactor system was developed in order to engineer human cartilage grafts of a clinically relevant size, which could potentially be used for unicompartmental resurfacing of human knee joints. It was found that human chondrocytes could be seeded throughout the large scaffold (50 mm diameter x 3 mm thick) with a uniform distribution. After 2 weeks *in vitro* culture, tissues were viable and homogeneously cartilaginous, with biomechanical properties approaching those of native cartilage. However, the fact that this study (and many of the previously cited papers) utilised chondrocytes for forming cartilaginous tissue is a major limiting factor when considering clinical

translation of such an approach to treat elderly patients and/or patients suffering from OA.

Studies from our own lab have investigated the potential of scaling-up tissue engineered constructs. These studies involved incorporating microchannels throughout the scaffolds, in the hope that they would lead to a more homogenous construct (Buckley et al., 2009b, Sheehy et al., 2011). Another study (from a different lab) showed that large partial thickness cartilage defects could be resurfaced effectively using hyaline-like cartilage, with the cartilage formed using transgene activated periosteal cells (Gelse et al., 2008).

These "scaling-up" studies show promise for the clinical treatment of large chondral defects, but they must be combined with an appropriate cell source, and also with an osteochondral model to repair damaged bone. As alluded to previously, in a clinical setting it is also highly desirable to engineer the geometry of the construct to match that of the joint it is replacing, in order to maintain proper joint mechanics during articulation with adjacent surfaces (Grayson et al., 2008). Looking to the future, these are the challenges which must be met when attempting to generate constructs suitable for partial or total joint resurfacing

2.10 Summary

There have clearly been dramatic advances in the fields of cartilage and bone tissue engineering in recent years. This literature review has discussed, for example, the potential of using self-assembly to generate cartilaginous constructs, as well as the potential of recapitulating the process of endochondral ossification when attempting to generate bone tissue. Current tissue engineering treatments, however, are generally concerned with testing and optimising techniques used in treating small chondral and osteochondral defects in the body. Significant engineering and scientific challenges must be overcome before tissue engineering approaches can be used in the treatment of much larger defects affecting damaged joints. This would involve the generation of large homogenous constructs using suitable cell sources,

engineering well-structured osteochondral constructs and generating anatomically shaped grafts mimicking the articulating surface of damaged joints. This leads directly to the objective of this thesis, namely to tissue engineer a scaled-up, anatomically shaped osteochondral construct suitable for partial or total synovial joint resurfacing.

It is first hypothesised in this thesis that dynamic compression in combination with modified scaffold architecture can result in enhanced, homogeneous cartilage formation, as a means of scaling-up to engineer functional cartilaginous constructs of clinically relevant dimensions. It is next hypothesised that self-assembly of chondrocytes can be a more effective method for forming cartilaginous tissues as opposed to the traditional method of hydrogel encapsulation. Self-assembly of fat pad derived stem cells will also be investigated for the first time, as an alternative to using chondrocytes for cartilage tissue engineering purposes. Using different cell sources (than chondrocytes) is particularly pertinent to the goal of scaling-up cartilaginous constructs for the treatment of diseased joints. Co-culture of chondrocytes and mesenchymal stem cells will also be investigated for generating cartilage tissue *in vitro*. In the final part of the thesis it is hypothesised that chondrogenically primed bone marrow derived MSC seeded alginate hydrogels can support endochondral bone formation within an osteochondral construct *in vivo*, and furthermore, that a phenotypically stable layer of articular cartilage can be engineered over this bony tissue using a self-assembled co-culture of chondrocytes and MSCs. These tissue engineering strategies will then be scaled-up and combined with rapid prototyping techniques to create anatomically shaped tissue engineered osteochondral grafts of a clinically relevant size (formed from moulds mimicking the geometry of medial femorotibial joint replacement prostheses).

3 Scaffold Architecture Determines Chondrocyte Response to Externally Applied Dynamic Compression

[A modified version of this chapter has been published in Biomechanics and Modeling in Mechanobiology (BMMB), 12, 889-899 (2013) (10.1007/s10237-012-0451-2)]

3.1 Introduction

Tissue engineering strategies aim to repair cartilaginous defects through the use of porous scaffolds or hydrogels which provide an appropriate environment to allow chondrocytes to maintain their differentiated phenotype and deposit extracellular matrix (ECM). Agarose hydrogels are commonly used for cartilage tissue engineering applications as they have been found to support the chondrogenic phenotype and the synthesis of cartilaginous ECM (Benya and Shaffer, 1982, Sun et al., 1986, Buschmann et al., 1992a). In addition they provide a well characterized, homogeneous mechanical environment (Buckley et al., 2009c) suitable for investigating cellular responses to biophysical stimuli (Buschmann et al., 1995b, Grodzinsky et al., 2000). The application of appropriate levels of dynamic compressive loading to chondrocyte-seeded agarose hydrogels has been shown to enhance cartilage specific matrix synthesis (Lee and Bader, 1997, Lee et al., 1998, Lee et al., 2000, Mauck et al., 2000a, Chowdhury et al., 2001, Mauck et al., 2002a, Mauck et al., 2003b, Kelly et al., 2004, Ng et al., 2006). The use of applied dynamic compression as a means to stimulate chondrocytes has also been extended to other scaffolds and hydrogels, with the response to this stimulus shown to depend on the material within which the cells are encapsulated (Bryant et al., 2004b, Hunter et al., 2004, Villanueva et al., 2008, Bryant et al., 2008, Appelman et al., 2009, Villanueva et al., 2010, Appelman et al., 2011).

Despite the extensive body of research in this area, it remains unclear how specific mechanical signals generated by dynamic compression regulate chondrocyte biosynthetic activity. This task is complicated by the fact that dynamic compression has been shown to enhance solute transport within hydrogels (Mauck et al., 2003a, Albro et al., 2010b). Finite element (FE) models have been used to demonstrate that the mechanical environment varies spatially throughout dynamically compressed cartilage explants and cell seeded hydrogels (Kim et al., 1994, Buschmann et al., 1999, Mauck et al., 2007), with higher levels of fluid flow predicted in the periphery of compressed tissues compared to the core. Increased protein and aggrecan synthesis has been observed around the periphery of dynamically compressed cartilage explants and chondrocyte seeded hydrogels (Kim et al., 1994, Buschmann et al., 1999), leading to the hypothesis that load-induced interstitial fluid flow positively impacts cartilage specific matrix production. Fluid flow is also known to be an important stimulus to cells in numerous other tissues, such as bone (Cowin, 2002, Cowin, 2007).

Modifying the levels of fluid flow within dynamically compressed scaffolds or hydrogels would therefore appear to represent a promising approach to controlling chondrocyte behavior. This can potentially be achieved by changing the architecture of a scaffold or hydrogel. Previous studies have incorporated channels throughout cell seeded constructs for the specific purpose of increasing nutrient transport to the core, and achieving a more homogeneous engineered tissue (Silva et al., 2006, Bian et al., 2009a, Buckley et al., 2009b, Sheehy et al., 2011).

The objective of this study was to determine the influence of both construct architecture and dynamic compressive loading on the resulting mechanical environment within chondrocyte seeded agarose hydrogels using FE modeling and experimental techniques, and to further explore how chondrocytes would respond to this altered mechanical environment. I hypothesized that introducing channels into dynamically compressed agarose hydrogels would increase the levels of fluid flow throughout the construct, and not just in the periphery of the engineered tissue, leading to significantly greater elaboration of cartilaginous matrix throughout the hydrogel. If such an approach is successful, it could potentially be used in the generation of scaled-up cartilaginous tissues of a clinically relevant size.

3.2 Materials and Methods

3.2.1 Cell isolation and expansion

Articular cartilage was aseptically harvested from porcine femoral condyles (4 month old, ~50kg, one donor). Cartilage slices were removed from the articular surfaces of the joint and rinsed thoroughly with Dulbecco's phosphate buffered saline (Sigma-Aldrich, Dublin, Ireland; PBS) containing penicillin (200 U/ml)-streptomycin (100μg/ml) (GIBCO, Invitrogen, Dublin, Ireland) and amphotericin B (2.5μg/ml) (Sigma-Aldrich, Dublin, Ireland). Chondrocytes were isolated from cartilage slices *via* digestion with high-glucose Dulbecco's modified Eagle's medium GlutaMAX (4.5 mg/ml D-Glucose, 200mM L-Glutamine; hgDMEM) (GIBCO, Invitrogen, Dublin, Ireland) containing collagenase type II (315 U/mg) (Worthington, Langanbach Services, Ireland) for 12-14 hours under constant rotation at 37°C. The resulting cell suspension was passed through a 40μm pore-size cell sieve (Fisher Scientific, Ireland), the filtrate centrifuged and rinsed twice with PBS. Cell number and viability were determined using a haemocytometer and 0.4% trypan blue staining (Sigma-Aldrich, Dublin, Ireland). Chondrocytes were then frozen in hgDMEM supplemented with 10% v/v foetal bovine serum (GIBCO, Invitrogen, Dublin, Ireland; FBS) and 10% dimethyl sulphoxide (Sigma-Aldrich, Dublin, Ireland; DMSO) in a liquid nitrogen tank. Before experiments were initiated cells were thawed and counted, with viability observed to be greater than 75%. Chondrocytes were plated at a seeding density of 5×10^3 cells/cm^2 in 500 cm^2 triple flasks (Thermo Fisher Scientific, Ireland) and expanded to passage one (P1) in a humidified atmosphere at 37°C and 5% CO_2. Chondrocytes were maintained in DMEM GlutaMAX supplemented with 10% v/v FBS, penicillin (100 U/ml)-streptomycin (100μg/ml) and 5ng/ml human fibroblast growth factor-2 (FGF-2; Prospec, Israel) during the expansion phase.

3.2.2 Cell encapsulation in solid and channeled hydrogel constructs

At P1 cells were trypsinized, counted and suspended in basic chondrogenic medium (basic CDM) consisting of hgDMEM supplemented with penicillin (100 U/ml)-streptomycin (100μg/ml) (both from GIBCO, Invitrogen, Dublin, Ireland), 100

μg/ml sodium pyruvate, 40 μg/ml L-proline, and 1.5 mg/ml bovine serum albumin (all Sigma-Aldrich, Arklow, Ireland). This cell suspension was mixed with 4% agarose (Type VII, Sigma-Aldrich, Arklow, Ireland) in PBS at a ratio of 1:1 at ~40°C, to yield a final gel concentration of 2% and a cell density of 15×10^6 cells/ml. The agarose/cell suspension was cast in a polytetrafluoroethylene (PTFE) mould (Figure 3-1a), allowed to cool for 30 min, and solid construct cylinders (Ø6mm x 4mm thickness) were removed using a biopsy punch (with PTFE moulds described previously (Buckley et al., 2009b)).

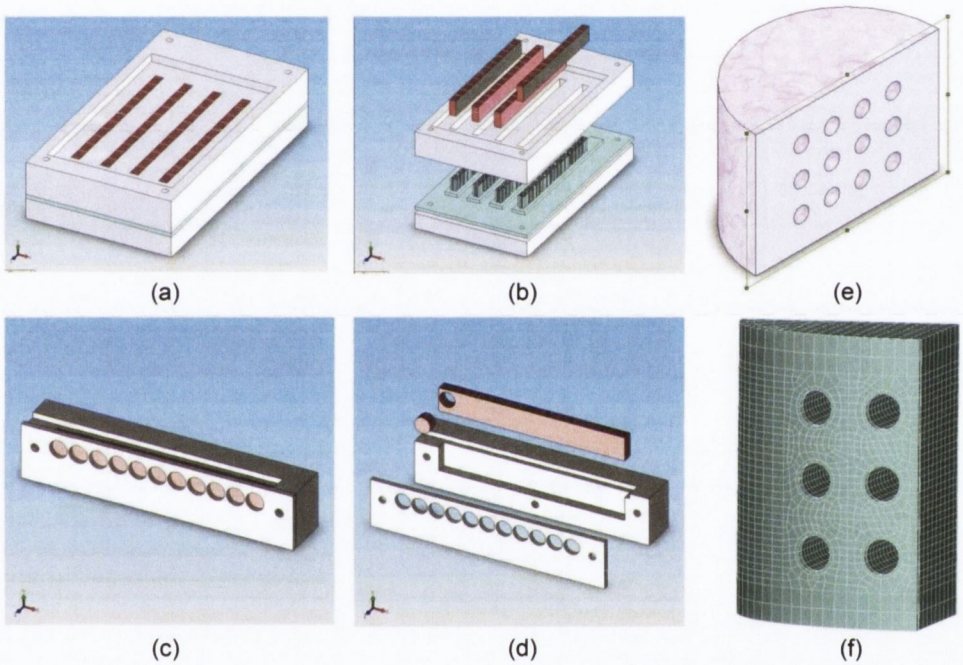

Figure 3-1: (a) Mould system for creating rectangular channeled agarose blocks. (b) After the chondrocyte cell laden agarose is cast and allowed to gel, the PDMS structure is removed to produce channeled agarose blocks. (c) - (d) A punch guide unit is placed over the agarose blocks to facilitate coring with a 6mm biopsy punch. (e) Channeled construct cut longitudinally. (f) Finite element mesh of channeled construct. Both architecture types were modelled in unconfined compression between impermeable platens. Boundary conditions are free draining and stress free on free surfaces, with sealed contact where platens are positioned. Moulds were fabricated as described previously (Buckley et al., 2009b).

An equal number of channeled construct cylinders (Figure 3-1e) were fabricated *via* a moulding process (Figure 3-1a-d) as previously described (Buckley

et al., 2009b). Briefly, the moulding process utilised a pillared array polydimethylsiloxane (PDMS) structure (fabricated through indirect casting of a computer numerical controlled (CNC) machined mould) to create the architecture. Extraction of the mould from the cast agarose-cell suspension produced a unidirectional channeled array in the transverse direction with diameters of 500μm and a centre-centre spacing of 1mm.

All constructs were maintained in defined CDM, consisting of basic CDM supplemented with 0.25 μg/ml amphotericin B, 1x insulin-transferrin-selenium, 4.7 μg/ml linoleic acid, 50μg/ml L-ascorbic acid-2-phosphate, 100nM dexamethasone (all Sigma-Aldrich, Arklow, Ireland) and 10 ng/ml transforming growth factor-beta 3 (TGF-β3) (ProSpec-Tany TechnoGene Ltd., Israel). After cell encapsulation, constructs were left in free swelling conditions for 48 hours before the addition of TGF-β3, and the initiation of dynamic loading (Day 0). Constructs were maintained in 3.5ml fully supplemented CDM per gel, and cultured in 6 well plates (Fisher Scientific, Ireland). Medium was fully exchanged every 3-4 days, with 500μl samples taken from wells for each group (n=3) at each medium exchange for biochemical analysis.

3.2.3 Dynamic compression application

Intermittent dynamic compression (DC) was carried out using a custom-built DC bioreactor, housed within an incubator as previously described (Thorpe et al., 2010b). The lower chamber of the bioreactor contained the constructs within a 35mm petri dish submerged in culture medium with a thin (1.5 mm) PTFE base holder to prevent lateral movement of constructs during loading, and a 1mm polystyrene cover disk to ensure direct contact with the actuator during the loading regime. The petri dish was positioned on a 316L stainless steel base platen connected to a 1000g load cell (RDP Electronics Ltd, Wolverhampton, UK) to measure the applied force. Axial compression was applied *via* impermeable platens using an electric linear actuator with 0.05 μm resolution (Zaber Technologies Inc., Vancouver, Canada). The system was controlled and data logged using LabVIEW 7 control and data acquisition software (National Instruments Corp., Newbury, UK). The DC protocol consisted of an initial pre-load of 0.01N/construct. Platen to platen

distance was measured, and a 1% pre-strain applied. A strain amplitude of 10% was subsequently applied to the constructs at a frequency of 1Hz. Constructs were loaded each day for 2 consecutive hours, 5 days per week over 21 days, in a humidified atmosphere at 37°C and 5% CO_2. Free swelling (FS) controls were maintained adjacent to the bioreactor during loading periods, in the same volume of medium. Solid and channeled constructs were subjected to both culturing regimes (DC and FS). Constructs were assessed at days 0 and 21.

3.2.4 Biochemical analysis

The biochemical content of constructs (n = 3-4) was assessed at both time points (days 0 and 21). To gain an appreciation of the spatial accumulation of sulphated glycosaminoglycan (sGAG) and collagen, the core of constructs was removed using a 3mm biopsy punch and analysed separately from the annulus. On removal from culture, construct diameter was measured, the wet mass of both the core and annulus recorded and samples were frozen at -85°C for subsequent analyses. Samples were digested with papain (125μg/ml) in 0.1M sodium acetate, 5mM L-cysteine-HCL, 0.05 M EDTA, pH 6 (all Sigma-Aldrich, Ireland) under constant rotation at 60°C for 18 hours. DNA content was quantified using the Hoechst Bisbenzimide 33258 dye assay as previously described (Kim et al., 1988). Proteoglycan content was estimated by quantifying the amount of sGAG in each hydrogel core/annulus using the dimethylmethylene blue dye binding assay (Blyscan, Biocolor Ltd., Carrickfergus, UK), with a shark chondroitin sulphate standard. sGAG secreted to culture media at each media exchange was also analysed for each group (n=3). Total collagen content was determined by measuring the hydroxyproline content (Kafienah and Sims, 2004), using a hydroxyproline to collagen ratio of 1:7.69 (Ignat'eva et al., 2007).

3.2.5 Histology and immunohistochemistry

At each time point, two or more samples per group were fixed in 4% paraformaldehyde (Sigma-Aldrich, Arklow, Ireland), dehydrated through a graded series of alcohol and embedded in paraffin. Samples were sectioned (5μm) to produce a cross section perpendicular to the disc face as illustrated in Figure 3-1e.

Sections were stained with 1% alcian blue 8GX (Sigma-Aldrich, Arklow, Ireland) in 0.1M HCL for sGAG accumulation. Collagen type I and II deposition were identified by immunohistochemical analysis. Briefly, sections were treated with peroxidase, and then rinsed with PBS before treatment with chondroitinase ABC (Sigma-Aldrich, Arklow, Ireland) in a humidified environment at 37°C to enhance the permeability of the ECM. The sections were rinsed in PBS and then incubated with goat serum to block non-specific sites, before the primary antibody was applied to the sections for 1 hour. A mouse monoclonal collagen type I antibody (1:400; 1.4 mg/ml; Abcam, Cambridge, UK) and mouse monoclonal anti-collagen type II antibody (1:100; 1mg/ml; Abcam, Cambridge, UK) were used as primary antibodies for collagen types I and II respectively. Next, an anti-mouse IgG biotin conjugate secondary antibody (1:133; 2mg/ml; Sigma-Aldrich, Arklow, Ireland) was applied for 1 hour, followed by incubation with ABC reagent (Vectastain PK-4000, Vector Labs, Petersbough, UK) for 45 mins. Finally, the samples were developed with DAB peroxidase (Vector Labs, Petersbough, UK) for 5 minutes. Positive and negative controls (either porcine cartilage or ligament) were included for each batch.

3.2.6 Finite element analysis

Finite element analysis was carried out by Dr. Thomas Nagel in the Trinity Centre for Bioengineering. The methodology for this is included in Appendix II.

3.2.7 Statistical Analysis

Statistical analyses were performed using the software package MINITAB 15.1 (Minitab Ltd., Coventry, UK). Groups were analysed for significant differences using a general linear model for analysis of variance with factors of group, construct region, architecture, DC condition, and interactions between these factors examined. Tukey's test for multiple comparisons was used to compare conditions. Significance was accepted at a level of $p<0.05$. Numerical and graphical results are presented as mean ± standard deviation (n=3-4 for each group at each time point), with graphical results produced using GraphPad Prism (San Diego, USA; Version 4.03).

3.3 Results

3.3.1 Predicted mechanical environment within dynamically compressed channeled hydrogels

The finite element models predicted minimal spatial variation in the magnitudes of pore pressure and strain in dynamically compressed solid hydrogels, with highest levels of fluid flow observed at the periphery of the construct (Figures 3-2a, d, and g). In comparison, a highly heterogeneous distribution of pore pressure, fluid flow and strain was predicted in the dynamically loaded channeled constructs (Figures 3-2b, e, and h). The highest levels of strain and fluid flow were predicted at the edges of channels, with pore pressure greatest in the (radial) spaces separating the channels. The mean and maximum magnitudes of pore pressure were predicted to be similar in the core and annulus of compressed channeled constructs. While fluid flow was predicted to be negligible in the core of solid constructs, it was found to increase in the periphery of such constructs (Figure 3-2f). In channeled constructs, it was found to fluctuate between approximately 0-8μm/s. The magnitudes of equivalent strain fluctuated in a similar manner (Figure 3-2i). Comparing the levels of the predicted biophysical stimuli, it would appear that the introduction of channels has the largest effect on fluid flux (Figures 3-2c, f, and i).

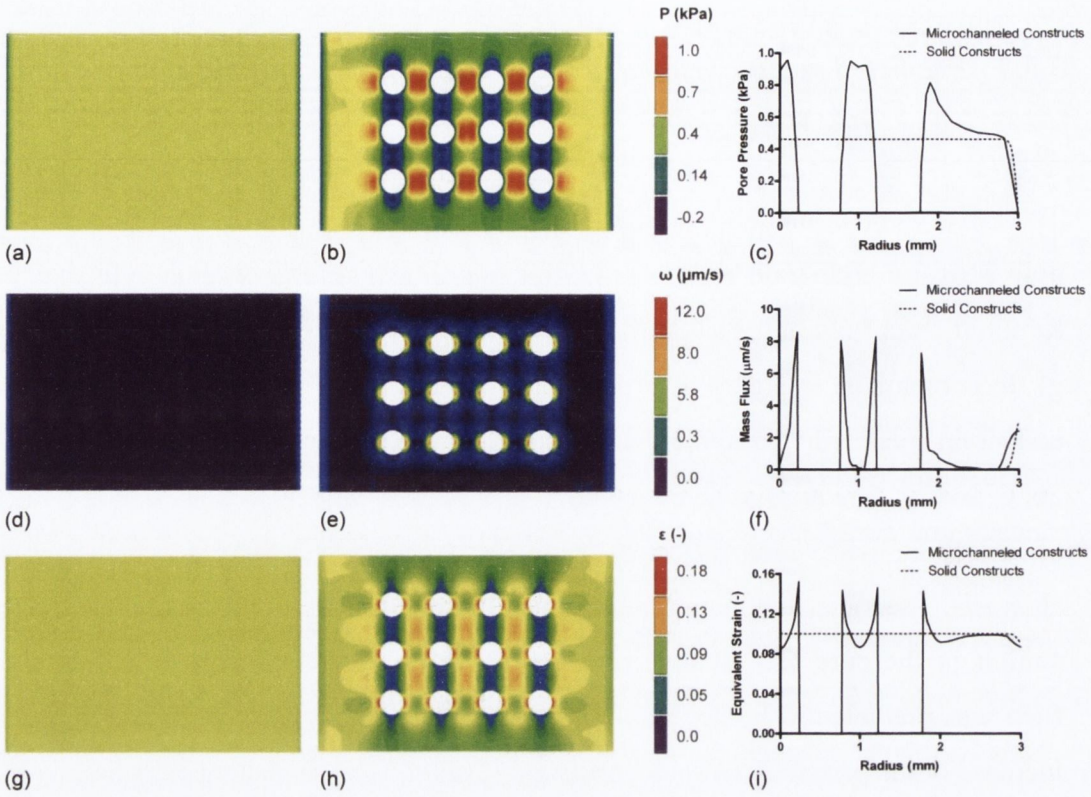

Figure 3-2: Spatial patterns of biophysical stimuli predicted by the FE models for solid (a, d, g) and channeled (b, e, h) constructs, and graphical representation of same along a radial line in the centre of the constructs (c, f, i). (a-c) Fluid pressure, P (kPa); (d-f) Fluid flux, ω (μm/s); (g-i) Equivalent strain. Material properties used to define the model are provided in Table S1 in Appendix II. Predictions are for the end of the ramp loading phase at peak load.

3.3.2 Influence of dynamic compression on total levels of matrix accumulation and release

Neither dynamic compression (DC) nor hydrogel architecture had a significant effect on construct wet weight, diameter, or thickness (data not shown). DC was found to significantly increase DNA content in solid constructs (Figure 3-3a). To compare DNA content between solid and microchanneled constructs, measurements were normalized to construct wet weight. DC led to an increase in DNA content in

solid constructs, but had no significant effect on microchanneled constructs (Figure 3-3b). By day 21 dynamically compressed solid (DCS) constructs were found to have significantly greater sGAG content (721.1±21.1 μg) compared to all other groups (Figure 3-3c). In microchanneled constructs, DC was found to result in a small but significant decrease in sGAG accumulation (346.1±26.8 μg in dynamically compressed microchannel (DCM) constructs compared to 393.8±23.5 μg in free swelling microchannel (FSM) constructs), although no differences were observed if sGAG levels were normalized to DNA content (Figure 3-3g).

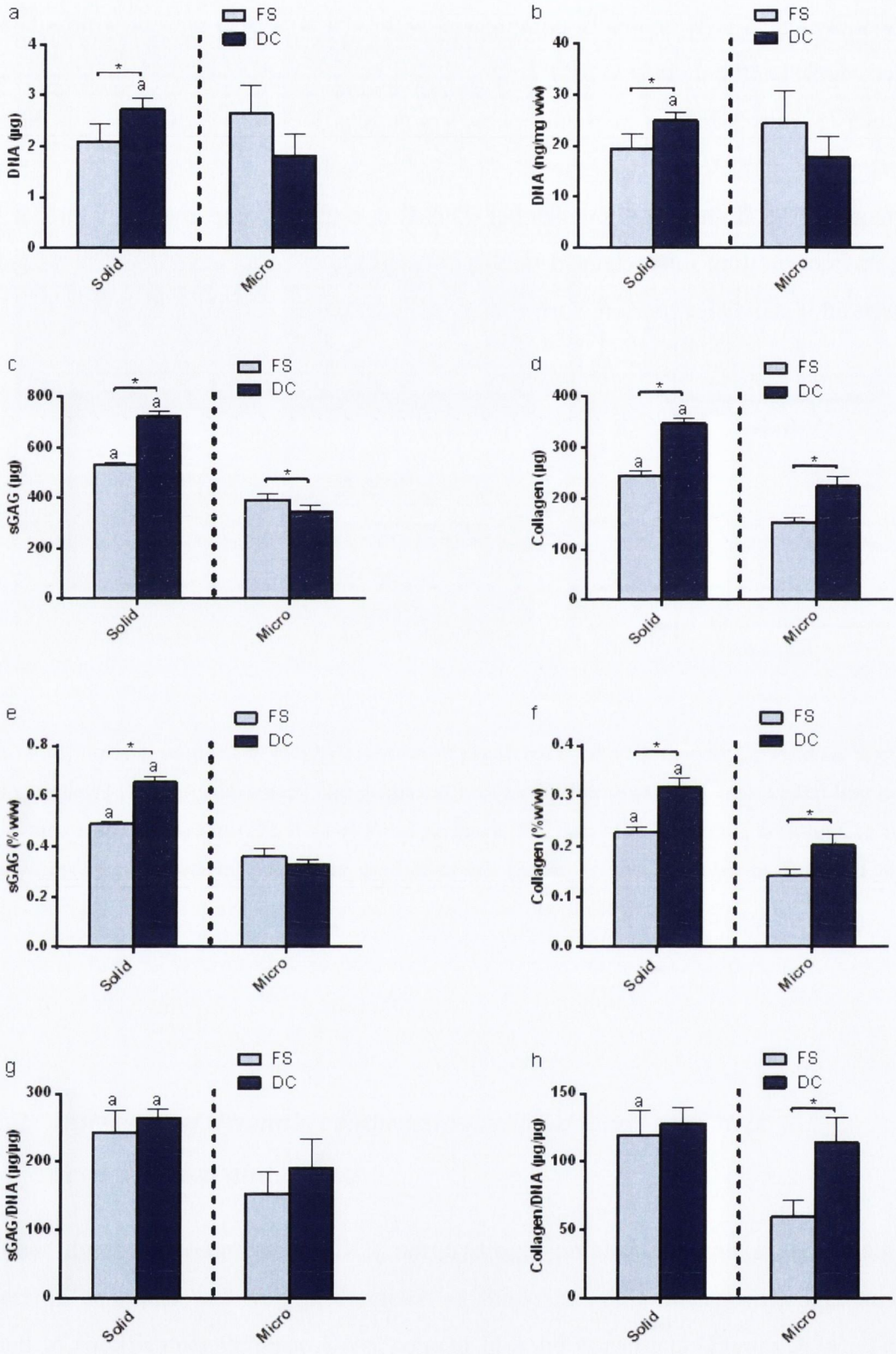
a
FS
DC
DNA (µg)
Solid
Micro
b
DNA (ng/mg ww)
c
sGAG (µg)
d
Collagen (µg)
e
sGAG (% ww)
f
Collagen (% ww)
g
sGAG/DNA (µg/µg)
h
Collagen/DNA (µg/µg)

Figure 3-3: Biochemical composition of constructs for free swelling (FS) and dynamically compressed (DC) solid and microchanneled constructs at day 21. (a) DNA content (μg); (b) DNA content (ng/mg w/w); (c) sGAG content (μg); (d) Collagen content (μg); (e) sGAG content (%w/w); (f) Collagen content (%w/w); (g) sGAG/DNA (μg/μg); (h) Collagen/DNA (μg/μg). a: $p<0.05$ vs. microchannel with same loading conditions. * denotes significant difference with $p<0.05$.

DC significantly increased collagen accumulation in both solid and microchanneled constructs (Figure 3-3d), with DCS constructs accumulating the greatest levels of collagen (347.5±9.4 μg) by day 21 ($p<0.05$). Almost identical results were obtained when collagen accumulation was normalized to wet weight (Figure 3-3f). Free swelling solid (FSS) gels accumulated more collagen than FSM gels, although there was no significant difference between DCS and DCM constructs when collagen content was normalized to DNA content (Figure 3-3h).

DCM constructs were found to release the greatest amount of sGAG (571.5±15.6 μg) to the media ($p<0.05$) over the 21 day culture period (Figure 3-4a). DC was also found to increase sGAG secretion in solid constructs, with DCS gels (454.1±19.3 μg) releasing significantly more than FSS gels (245.6±4.5 μg). Taking into account sGAG both accumulated and released per construct over the 21 day culture period, total sGAG synthesis was greatest in DCS constructs (1175.2±28.6 μg). When normalized to DNA there was a trend towards greatest sGAG synthesis in DCM gels but this was not statistically significant (Figure 3-4b). DCM gels did, however, synthesize significantly more sGAG than their free swelling counterparts on a per cell basis ($p<0.05$).

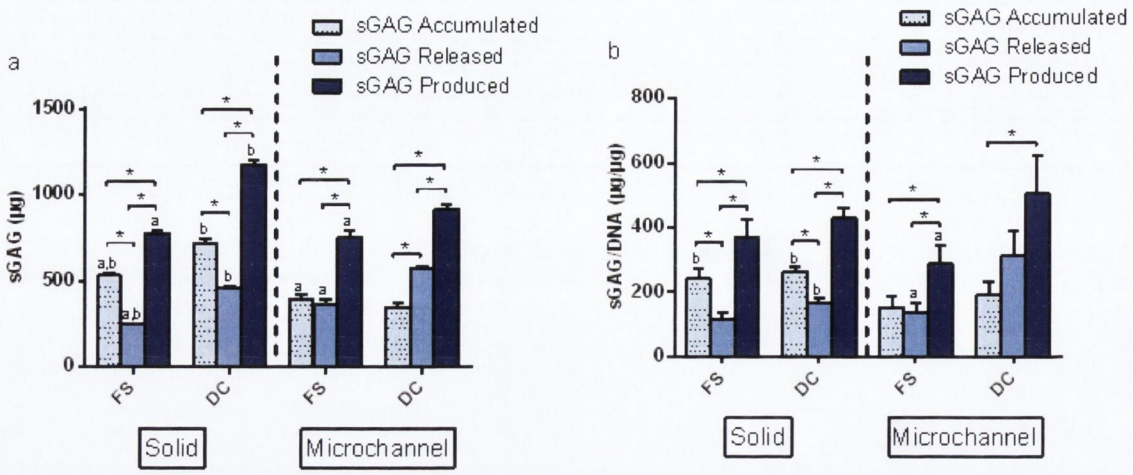

Figure 3-4: Total sGAG accumulated, released, and produced for free swelling (FS) and dynamically compressed (DC) solid and microchanneled constructs at day 21. (a) sGAG (µg); (b) sGAG/DNA (µg/µg). a: $p<0.05$ vs. DC conditions with same architecture in same sGAG category; b: $p<0.05$ vs. microchannel with same loading conditions in same sGAG category. * denotes significant difference with $p<0.05$.

3.3.3 The influence of dynamic compression on the spatial accumulation of matrix components in solid and channeled constructs

To gain an appreciation of spatial variations in matrix accumulation, I next compared sGAG and collagen accumulation in the core and annular regions of the constructs (Figure 3-5). All groups were found to have significantly greater sGAG levels in the annulus compared to their corresponding core (measured in total µg of sGAG accumulated) (data not shown). This is to be expected, as the annulus represents a volume three times that of the core. When normalized to tissue wet weight (Figure 3-5a), sGAG accumulation was found to be significantly higher in the core compared to the annulus. DC was found to enhance sGAG accumulation within all regions of solid constructs, but had no significant effect on sGAG accumulation in either region of microchanneled constructs. Significantly greater collagen accumulation was observed in the periphery of compressed solid constructs (Figure 3-5b), with DC having no effect on collagen accumulation in the core

region. In contrast, DC led to significant increases in collagen accumulation in both the core and annulus of microchannel constructs.

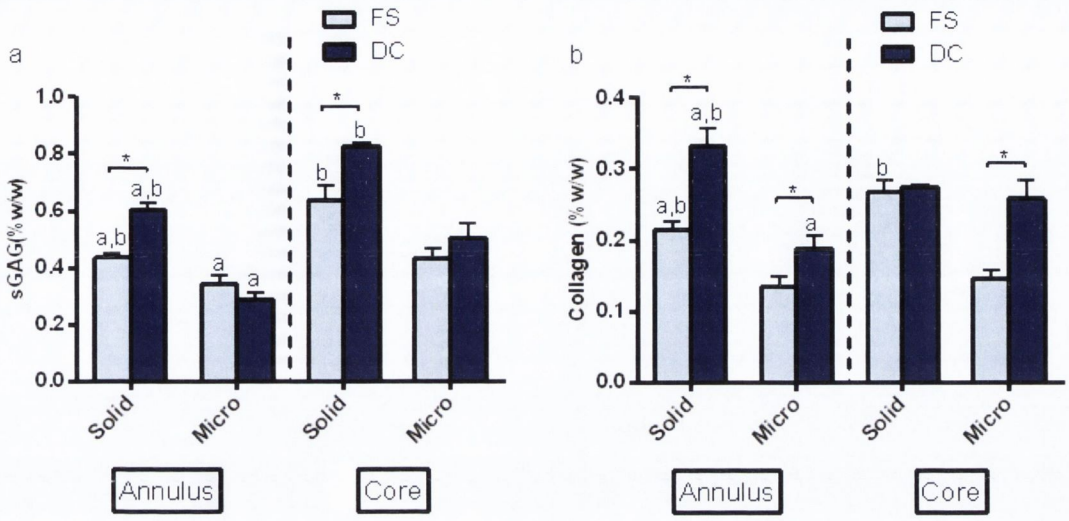

Figure 3-5: Biochemical composition of core and annular regions for free swelling (FS) and dynamically compressed (DC) solid and microchanneled constructs at day 21. (a) sGAG content (%w/w); (b) Collagen content (%w/w). a: $p<0.05$ vs. core of same group; b: $p<0.05$ vs. microchannel with same loading conditions in same region. * denotes significant difference with $p<0.05$.

A replicate of this study was undertaken, where chondrocytes were not expanded in the presence of FGF-2, and the gels were maintained for 42 days instead of 21 days of culture. The results of this replicate study are presented in Appendix I. In this replicate study similar results with regards to spatial sGAG and collagen accumulation were observed by day 42 (see Figure S4 in Appendix III).

Construct sections from all experimental groups stained positively with Alcian Blue (Figure 3-6). DCS constructs exhibited slightly more intense staining for sGAG than FSS constructs, while staining was comparable between the DCM and FSM groups. Less intense staining was observed around the very periphery of constructs. Homogeneous staining for Alcian Blue was observed in microchannel constructs. Immunohistochemistry demonstrated positive staining for collagen type II (Figures 3-6, 7) and negligible staining for collagen type I (data not shown).

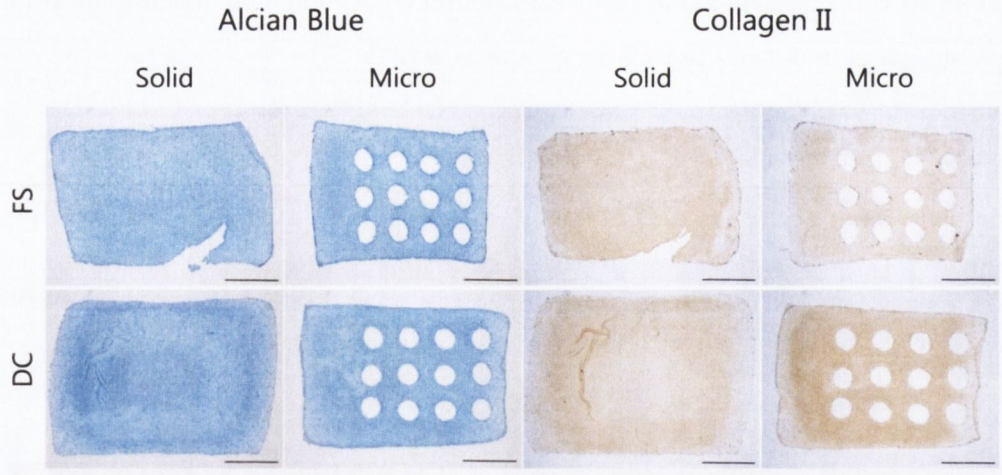

Figure 3-6: Alcian Blue staining and type II collagen immunohistochemistry staining of solid and microchanneled constructs subjected to free swelling (FS) and dynamic compression (DC) conditions. Scale bar 1mm.

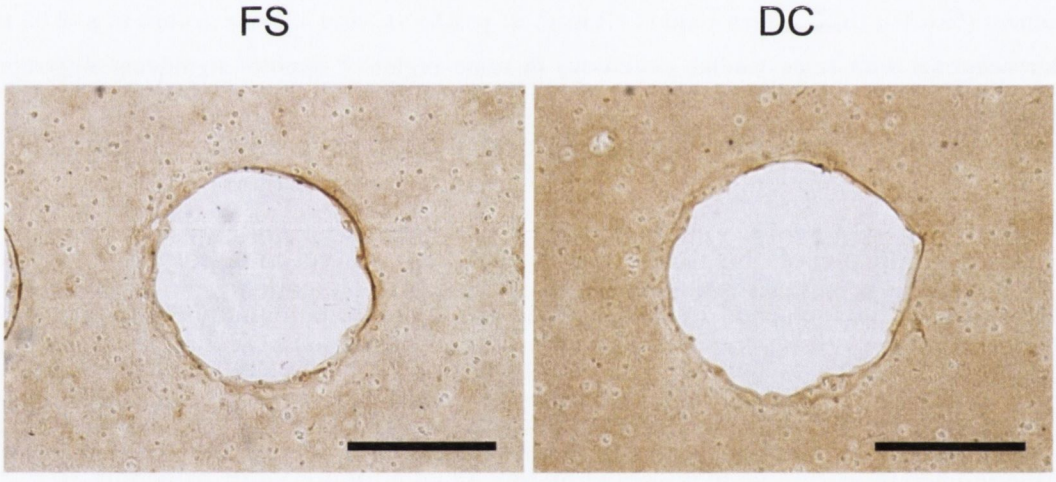

Figure 3-7: High magnification images of type II collagen immunohistochemistry staining of microchanneled constructs subjected to free swelling (FS) and dynamic compression (DC) conditions. Scale bar 250µm.

3.4 Discussion

The objective of this study was to determine the influence of both construct architecture and dynamic compressive loading on the resulting mechanical environment within chondrocyte seeded agarose hydrogels using FE modeling, and to further investigate how chondrocytes respond to this altered mechanical environment using experimental techniques. Dynamic compression was found to significantly increase sGAG accumulation and overall levels of sGAG synthesis in solid constructs, although it only led to increased sGAG release to the media in channeled constructs. Dynamic compression was also found to increase collagen accumulation in tissue engineered constructs, but preferentially in regions of the construct where FE modeling predicted fluid flow to be higher. In solid constructs, this is confined to the periphery of the construct, but increased collagen accumulation was observed in both the core and annulus of dynamically compressed channeled constructs. These results provide further support for the hypothesis that fluid flow stimulation is key to promoting collagen synthesis by chondrocytes encapsulated in agarose hydrogels.

It is well established that dynamic compression can enhance cartilage specific ECM accumulation in chondrocyte seeded scaffolds (Buschmann et al., 1995b, Mauck et al., 2000a, Mauck et al., 2002a, Waldman et al., 2006, Villanueva et al., 2010). It has previously been reported that proteoglycan and protein synthesis is preferentially enhanced in the annular regions of chondrocyte seeded agarose constructs subjected to dynamic compression, correlating with regions of increased fluid flow (Buschmann et al., 1995b). In contrast, other studies have reported that dynamic loading enhances the material properties and GAG content of cores, annuli, and whole constructs relative to free-swelling controls, but does not alter the radial variations compared to free swelling conditions (Kelly et al., 2009). In agreement with this latter study, I observed that sGAG accumulation was higher in both the core and annular regions of loaded solid constructs, which suggests that stimuli other than fluid flow, such as dynamic compression induced cell deformation may be driving this response. For example, it has been demonstrated that dynamic compression of a single chondron (chondrocyte and its pericellular matrix) up-

regulates aggrecan and type II collagen gene expression (Wang et al., 2009). The finite element model predicts a reasonably homogenous strain distribution within compressed solid constructs, which correlates with increases in sGAG accumulation in both the core and annulus of this construct. It should be noted, however, that dynamic compression also acted to increase the DNA content in solid constructs, and when sGAG levels were normalized to DNA content, no significant increase in matrix synthesis was observed. This suggests that enhanced matrix accumulation in dynamically compressed solid constructs can be attributed primarily to greater cell viability/proliferation.

In microchannel constructs, no significant increase in sGAG accumulation was found in either the core or annulus of loaded constructs; however there was a dramatic increase in sGAG released to the media. This suggests that the channels provide a conduit for the diffusion or convection of synthesized macromolecules into the surrounding culture media. Taking into account sGAG both accumulated and released per construct over the 21 day culture period (Figure 3-4b), we observe a trend towards greater sGAG synthesis in microchanneled constructs on a per cell basis. This indicates that while the introduction of channels may lead to greater ECM synthesis in constructs, the additional ECM components appear to diffuse into the surrounding media and are not retained within the engineered tissue. Overall, total sGAG accumulation is reduced by the introduction of channels into the hydrogel, which represents a potential obstacle with the use of such constructs for tissue engineering applications.

In contrast to the sGAG accumulation data, all regions of either the solid or channeled constructs which were predicted to experience high levels of fluid flow in response to dynamic compression demonstrated increases in collagen accumulation. One interpretation of this result is that distinct biophysical signals generated by dynamic compression (e.g. tissue strain, fluid flow) are differentially regulating sGAG and collagen synthesis. Flow-generated shear stresses have previously been suggested as key regulators of chondrocyte activity (Buschmann et al., 1999), with other studies suggesting that fluid shear stress can help promote collagen synthesis (Martin et al., 2000, Gemmiti and Guldberg, 2006). On the other hand, theoretical models of tissue differentiation suggest that high magnitudes of fluid flow can lead

to fibrous tissue formation (Prendergast et al., 1997, Kelly and Prendergast, 2005), although all constructs in this study stained positively for type II collagen. Alternatively it may be that certain levels of nutrient availability are required for increases in either sGAG or collagen synthesis in response to biophysical cues. In this context, interpreting the results of such spatial analysis of matrix accumulation is further complicated by the fact that dynamic compression can also enhance nutrient transport in cell seeded hydrogels (Mauck et al., 2003a, Albro et al., 2010b). Further work is required to decouple the relative roles of these various potential mechanisms in determining chondrocyte activity in mechanically loaded constructs.

3.5 Concluding Remarks

It is well established that dynamic compression can enhance sGAG accumulation (Lee and Bader, 1997, Mauck et al., 2000a, Mauck et al., 2002a), and that fluid induced shear stress can promote collagen synthesis (Martin et al., 2000, Gemmiti and Guldberg, 2006). The results of this study demonstrate that the architecture of cell seeded scaffolds or hydrogels can be modified to alter the spatial levels of fluid flow throughout the constructs, which is hypothesized to lead to greater collagen accumulation throughout the tissue rather than preferentially in the construct periphery. Whether such modifications are ultimately incorporated into engineered tissues for clinical application is an open question; however such systems as described in this study may help to better understand basic chondrocyte mechanobiology.

Overall, dynamic compression was found to significantly increase sGAG synthesis in solid CC seeded agarose hydrogels, and preferentially increase collagen accumulation in regions of constructs where FE modelling predicted highest levels of fluid flow. The introduction of nutrient channels, however, was found to have a detrimental effect on cartilage formation within constructs. Overall, it was observed that cartilage extracellular matrix (ECM) accumulation was quite low in agarose hydrogels (maximum sGAG levels of approximately 0.7 %w/w; maximum collagen levels of approximately 0.3 %w/w), at least when compared to typical native

articular cartilage values (4-7 %w/w sGAG; 15-22 %w/w collagen (Mow et al., 1992)). Therefore, this thesis next compared a self-assembly (or scaffold-free) approach to agarose hydrogel encapsulation as a means to engineer functional cartilaginous grafts using culture expanded CCs (chapter 4).

4 A comparison of self-assembly and hydrogel encapsulation as a means to engineer functional cartilaginous grafts using culture expanded chondrocytes

[A modified version of this chapter has been published in Tissue Engineering Part C, Methods, 20, 52-63 (2014) (10.1089/ten.TEC.2013.0118)]

4.1 Introduction

Cartilage damage can arise from degenerative diseases such as osteoarthritis or due to physical trauma to the articular surface. A large number of tissue engineering strategies have been proposed to repair such cartilaginous defects. Typical approaches involve the use of a scaffold or hydrogel for supporting and organizing the cells in a three dimensional (3D) environment. Agarose hydrogels are commonly used for cartilage tissue engineering applications as they have been found to support the chondrogenic phenotype and the synthesis of cartilaginous extracellular matrix (ECM) (Benya and Shaffer, 1982, Sun et al., 1986, Buschmann et al., 1992a, Mauck et al., 2000a, Mauck et al., 2002a, Mauck et al., 2003d, Mauck et al., 2006, Erickson et al., 2009, Huang et al., 2009, Buckley et al., 2009a, Buckley et al., 2010b, Vinardell et al., 2010, Meyer et al., 2011, Buckley et al., 2012, Liu et al., 2012, Vinardell et al., 2012a). When seeded with primary chondrocytes, such hydrogels can be used to engineer tissues attaining native levels of compressive moduli and sGAG content (Byers et al., 2008). However, as with many scaffolds or hydrogels, such an approach raises the issues of scaffold degradation products, inflammatory responses to the implanted materials, stress shielding of cells, and a reduction in cell to cell communication (Hu and Athanasiou, 2006b, Elder et al., 2009). This has

motivated research into scaffold-free techniques as a potential method for generating functional cartilage tissue.

One of the first reported uses of a scaffold-free or self-assembly (SA) (or self-aggregating) approach for engineering cartilage-like tissue involved directly seeding chondrocytes onto plastic dishes pre-coated with poly(2-hydroxyethyl methacrylate) (Reginato et al., 1994, Estrada et al., 2001, Novotny et al., 2006, Kim et al., 2011, Kraft et al., 2011), which leads to the development of a graft with a hyaline cartilage phenotype in terms of the expression of collagen type II and aggrecan (Novotny et al., 2006). Alternative SA approaches involve aliquoting chondrocytes into an agarose mould or similar, and allowing these cells to self-assemble over time (Hu and Athanasiou, 2006b). After 12 weeks of culture, this SA approach has been shown to support the generation of a hyaline-like cartilaginous tissue with biochemical and mechanical properties approaching those of native articular cartilage. Numerous other studies have investigated the SA of chondrocytes (Yu et al., 1997, Naumann et al., 2004, Hoben et al., 2007, Elder and Athanasiou, 2008b, Elder and Athanasiou, 2008c, Ofek et al., 2008, Revell et al., 2008, Elder and Athanasiou, 2009a, Elder and Athanasiou, 2009c), with determination of the initial cell seeding number identified as a key parameter to successfully engineer a cartilaginous graft using the SA approach. Researchers have also investigated the potential of generating cartilage grafts through self-assembly of mesenchymal stem cells (MSCs) (Murdoch et al., 2007, Elder et al., 2009), with some success reported in repairing chondral defects *in vivo* using this approach (Ando et al., 2007, Ando et al., 2008). Furthermore, in terms of chondrogenic differentiation of human bone marrow derived MSCs, the SA method has demonstrated benefits over traditional pellet culture system (Zhang et al., 2010).

Despite the extensive research into scaffold-free cartilage tissue engineering, particularly in the area of chondrocyte SA, to the best of our knowledge no study to date has been undertaken to directly compare the SA approach to hydrogel encapsulation for engineering functional cartilaginous grafts. The objective of this study was to directly compare SA to agarose hydrogel encapsulation (AE) as a means to engineer such grafts. Passaged chondrocytes were encapsulated into agarose hydrogels at different cell seeding densities and maintained in a chemically

defined media. The properties of these engineered tissues were then compared to those generated using a SA approach. As it is known that articular chondrocytes dedifferentiate after they attach to cell culture plastic (Benya and Shaffer, 1982), the cells were allowed to self-assemble on an agarose bed that prevents cell attachment. Previous studies have shown that the SA of chondrocytes on a nonadhesive agarose coating leads to the development of a more smooth, flat, and hyaline-like construct, when compared to those assembled on culture treated plastic (Hu and Athanasiou, 2006b). Constructs were seeded at two seeding densities; first a typical AE seeding density (approx. 900,000 cells per construct or 30 million cells/ml for 5mm diameter x 1.5mm thick construct), and secondly a typical SA seeding density (4 million cells per construct). Finally, as transient TGF-β3 stimulation has been shown to enhance chondrogenesis in chondrocyte seeded agarose hydrogels (Byers et al., 2008), I compared the effect of such media supplementation conditions on the development of cartilaginous grafts engineered using both SA and AE.

4.2 Materials and Methods

4.2.1 Cell isolation and expansion

Articular cartilage was aseptically harvested from porcine femoral condyles (4 months old), and the cartilage slices were rinsed thoroughly with Dulbecco's phosphate buffered saline (Sigma-Aldrich, Dublin, Ireland; PBS) containing penicillin (200 U/ml)-streptomycin (100μg/ml) (GIBCO, Invitrogen, Dublin, Ireland), and amphotericin B (2.5μg/ml) (Sigma-Aldrich, Dublin, Ireland). Chondrocytes were isolated from cartilage slices via digestion with high-glucose Dulbecco's modified Eagle's medium GlutaMAX (4.5 mg/ml D-Glucose, 200mM L-Glutamine; hgDMEM) (GIBCO, Invitrogen, Dublin, Ireland) containing collagenase type II (315 U/mg) (Worthington, Langanbach Services, Ireland) for 12-14 h under constant rotation at 37°C. The resulting cell suspension was passed through a 40μm pore-size cell sieve (Fisher Scientific, Ireland) and the filtrate centrifuged and rinsed with PBS twice. Cell number and viability were determined using a haemocytometer and 0.4% trypan blue staining (Sigma-Aldrich, Dublin,

Ireland), and the chondrocytes were then frozen in hgDMEM supplemented with 10% v/v foetal bovine serum (GIBCO, Invitrogen, Dublin, Ireland; FBS) and 10% dimethyl sulphoxide (Sigma-Aldrich, Dublin, Ireland; DMSO) and stored in liquid nitrogen. Before experiments were initiated cells were thawed and counted. Chondrocytes were plated at a seeding density of 5×10^3 cells/cm^2 in 500 cm^2 triple flasks (Thermo Fisher Scientific, Ireland) and expanded to passage two (P2) in a humidified atmosphere at 37°C and 5% CO_2. Chondrocytes were maintained in DMEM GlutaMAX supplemented with 10% v/v FBS, penicillin (100 U/ml)-streptomycin (100µg/ml) and 5ng/ml human fibroblast growth factor-2 (FGF-2; Prospec, Israel) during the expansion phase.

4.2.2 Formation and culture of self-assembled and agarose hydrogel constructs

At P2 cells were trypsinized, counted and suspended in basic chondrogenic medium (basic CDM) consisting of hgDMEM supplemented with penicillin (100 U/ml)-streptomycin (100µg/ml) (both from GIBCO, Invitrogen, Dublin, Ireland), 100 µg/ml sodium pyruvate, 40 µg/ml L-proline, and 1.5 mg/ml bovine serum albumin (all Sigma-Aldrich, Arklow, Ireland). A custom built polydimethylsiloxane (PDMS) mould was used to create sterile, 3% agarose wells (Type VII, Sigma-Aldrich, Arklow, Ireland) of 5mm diameter and 3mm thickness. Self-assembled constructs were formed by adding either 900,000 cells (low seeding density; 46,000 cells/mm^2) or 4 million cells (high seeding density; 204,000 cells/mm^2) in 40 µl aliquots of defined CDM to the 5mm diameter agarose wells, seated in either 12 well plates (low seeding density constructs), or 6 well plates (high seeding density constructs) (Fisher Scientific, Ireland). Defined CDM consisted of basic CDM supplemented with 0.25 µg/ml amphotericin B, 1x insulin-transferrin-selenium, 4.7 µg/ml linoleic acid, 50µg/ml L-ascorbic acid-2-phosphate and 100nM dexamethasone (all Sigma-Aldrich, Arklow, Ireland). Self-assembled constructs were initially not supplemented with TGF-β3 to minimize cell contraction. Cells self-assembled within 12 h, upon which defined CDM supplemented with 10 ng/ml of transforming growth factor-beta 3 (TGF-β3) (ProSpec-Tany TechnoGene Ltd., Israel) was added to each well; t = 0 was defined at this time point.

Chondrocyte encapsulated agarose hydrogel constructs were formed by mixing the chondrocyte cell suspension in basic CDM with 4% agarose in sterile PBS. This solution was mixed at a ratio of 1:1 at ~40°C, to yield a final gel concentration of 2% and a cell density of either 30×10^6 cells/ml or 136×10^6 cells/ml. The agarose/cell suspensions were cast in a stainless steel mould, allowed to cool for 30 min, and solid construct cylinders (5mm diameter x 1.5mm thick) were removed using a biopsy punch. Constructs were then placed in 6 or 12 well plates corresponding to their cell number, and immersed in defined CDM supplemented with 10 ng/ml of transforming growth factor-beta 3 (TGF-β3). The low and high agarose cell seeding densities correspond to the self-assembly (SA) seeding density of 900,000 and 4 million cells respectively. The high seeding density of 4 million cells was chosen as this has been previously shown to be the optimal initial seeding number for chondrocyte self-assembled constructs (Revell et al., 2008). The low seeding density of 900,000 cells (30×10^6 cells/ml) was chosen to enable comparisons to be made with other chondrocyte agarose hydrogel studies previously undertaken in our laboratory. Typical values for SA thickness range from 0.8mm (Hu and Athanasiou, 2006b) to 1.4 mm (Elder et al., 2009); therefore I chose a thickness value of 1.5mm for the agarose constructs in order to generate similarly sized constructs to the SA approach at the end of the experiment.

Constructs at low seeding density were maintained in 2.5ml fully supplemented CDM, with high seeding density constructs maintained in 11 ml (hence maintaining the ratio of media to cells constant). Medium was fully exchanged every 3 or 4 days, with 500μl samples taken from wells for each group (n=3) at each medium exchange for biochemical analysis (as described below). All agarose and self-assembled constructs were maintained for 2 weeks in fully supplemented CDM, upon which TGF-β3 was withdrawn from half the samples of all experimental groups for the remaining 4 weeks. In addition, all self-assembled constructs were removed from their agarose moulds after 2 weeks of *in vitro* culture, as this has been shown to enhance aggregate moduli and collagen organization in self-assembled constructs (Elder and Athanasiou, 2008b).

4.2.3 Biochemical analysis

The biochemical content of constructs (n = 3-4) was assessed at each time point (0, 21 and 42 days). To gain an appreciation of the spatial accumulation of sulphated glycosaminoglycan (sGAG) and collagen, the core of high seeding density constructs was removed using a 3mm biopsy punch and analyzed separately from the annulus. On removal from culture, construct diameter was measured, the wet mass of both the core and annulus was recorded and all samples were subsequently frozen at -85°C for later analyses. Samples were digested with papain (125μg/ml) in 0.1M sodium acetate, 5mM L-cysteine-HCL, 0.05 M EDTA, pH 6 (all Sigma-Aldrich, Ireland) under constant rotation at 60°C for 18 h. DNA content was quantified using the Hoechst Bisbenzimide 33258 dye assay as previously described (Kim et al., 1988). Proteoglycan content was estimated by quantifying the amount of sGAG in each hydrogel core/annulus using the dimethylmethylene blue dye binding assay (Blyscan, Biocolor Ltd., Carrickfergus, UK), with a shark chondroitin sulphate standard. sGAG secreted to culture media at each media exchange was also analysed for each group (n=3). Total collagen content was determined by measuring the hydroxyproline content (Kafienah and Sims, 2004), using a hydroxyproline to collagen ratio of 1:7.69 (Ignat'eva et al., 2007).

4.2.4 Histology and immunohistochemistry

At each time point, two or more samples per group were fixed in 4% paraformaldehyde (Sigma-Aldrich, Arklow, Ireland), dehydrated with a graded series of alcohol and embedded in paraffin. 5μm sections were produced of the cross section perpendicular to the construct face. Sections were stained with 1% alcian blue 8GX (Sigma-Aldrich, Arklow, Ireland) in 0.1M HCL for sGAG accumulation. Collagen type II deposition was identified by immunohistochemical analysis. Briefly, sections were treated with peroxidase, and then rinsed with PBS before treatment with chondroitinase ABC (Sigma-Aldrich, Arklow, Ireland) in a humidified environment at 37°C to enhance permeability of the ECM. The sections were rinsed in PBS, and then incubated with goat serum to block non-specific sites, before the primary antibody was applied to the sections for 1 h. A mouse monoclonal anti-collagen type II antibody (1:100; 1mg/ml; Abcam, Cambridge,

UK) was used as the primary antibody for collagen type II. Next, an anti-mouse IgG biotin conjugate secondary antibody (1:133; 2mg/ml; Sigma-Aldrich, Arklow, Ireland) was applied for 1 h, followed by incubation with ABC reagent (Vectastain PK-4000, Vector Labs, Petersbough, UK) for 45 mins. Finally, the samples were developed with DAB peroxidase (Vector Labs, Petersbough, UK) for 5 min. Positive and negative controls (porcine cartilage and ligament respectively) were included.

4.2.5 Statistical Analysis

Statistical analyses were performed using the software package MINITAB 15.1 (Minitab Ltd., Coventry, UK). Groups were analysed for significant differences using a general linear model for analysis of variance with factors of time point, scaffold type, culturing conditions, construct region, and interactions between these factors examined. Tukey's test for multiple comparisons was used to compare conditions. Significance was accepted at a level of $p<0.05$. Numerical and graphical results are presented as mean ± standard deviation (n=3-4 for each group at each time point), with graphical results produced using GraphPad Prism (San Diego, USA; Version 4.03).

4.3 Results

4.3.1 Self-assembly (SA) using large numbers of chondrocytes leads to the development of a tissue with a more articular cartilage-like composition compared to hydrogel encapsulation

The morphology of self-assembled constructs seeded at low and high seeding densities varied dramatically (Figure 4-1). By week 6, constructs formed with 4 million cells were firm, smooth and flat with a hyaline-like appearance. This was in stark contrast to SA constructs engineered at the lower seeding density (900,000 cells), which were uneven in their appearance, with a significantly reduced diameter (Table 4-1). Hence it would appear that 900,000 cells is too low a cell number to generate a satisfactory self-assembled construct. Agarose constructs seeded with 4

million cells were found to significantly increase in thickness over 42 days, with evidence of bulging at the top and bottom surfaces. These constructs were found to weigh substantially more than self-assembled constructs (Figures 4-2A, B).

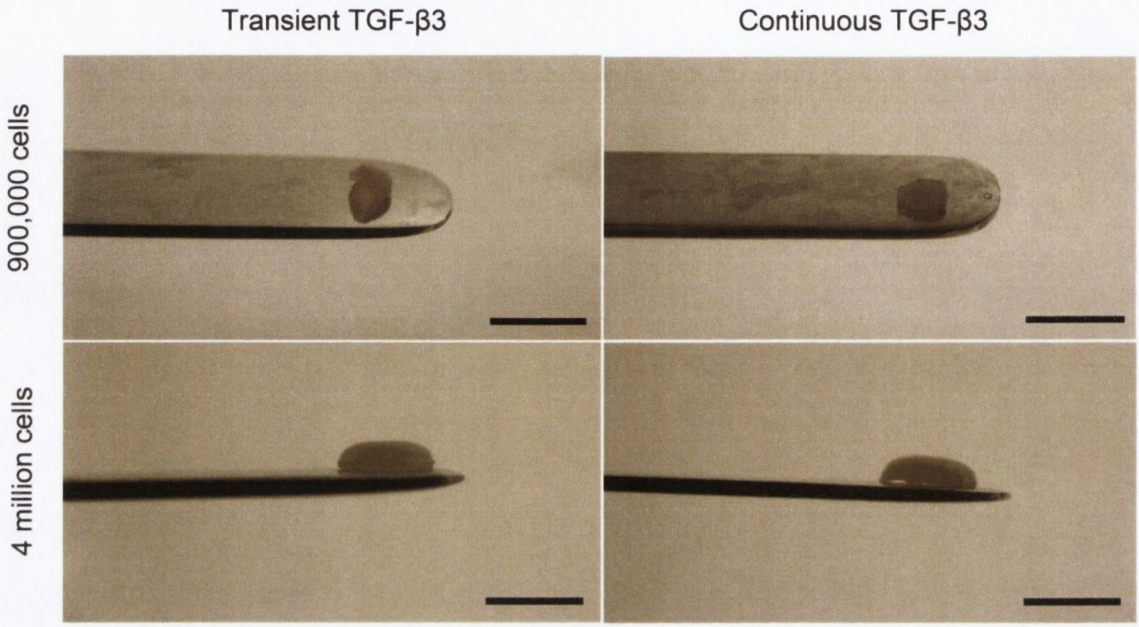

Figure 4-1: Self-assembled constructs at day 42. Scale bar = 5mm.

Table 4-1: Construct physical parameters of diameter (mm) and thickness (mm) for chondrocyte encapsulated agarose and self-assembled constructs for low seeding densities. a: $p<0.05$ vs. day 0; b: $p<0.05$ vs. day 21 with same culturing conditions; c: $p<0.05$ vs. continuous TGF-β3 (same time point); e: $p<0.05$ vs. corresponding agarose group.

Construct Type	Parameter	Low Seeding Density				
		D0	D21		D42	
			Transient TGF-β3	Continuous TGF-β3	Transient TGF-β3	Continuous TGF-β3
Agarose	Diameter (mm)	4.97±0.08	5.04±0.1	5.08±0.04	5.08±0.03	5.05±0.08
	Thickness (mm)	1.56±0.02	1.57±0.06	1.64±0.01	1.62±0.05	1.69±0.06[a]
Self-Assembly	Diameter (mm)	3.62±0.1[e]	3.03±0.39[e]	2.31±0.75[a,e]	3.24±0.3[e]	3.1±0.18[e]
	Thickness (mm)	0.13±0.01[e]	0.99±0.27[a,e]	0.69±0.59[a,e]	1.1±0.13[a,e]	1.11±0.2[a,e]

Table 4-2: Construct physical parameters of diameter (mm) and thickness (mm) for chondrocyte encapsulated agarose and self-assembled constructs for high seeding densities. a: $p<0.05$ vs. day 0; b: $p<0.05$ vs. day 21 with same culturing conditions; c: $p<0.05$ vs. continuous TGF-β3 (same time point); d: $p<0.05$ vs. corresponding group in low seeding density (in Table 4-1); e: $p<0.05$ vs. corresponding agarose group.

Construct Type	Parameter	High Seeding Density				
		D0	D21		D42	
			Transient TGF-β3	Continuous TGF-β3	Transient TGF-β3	Continuous TGF-β3
Agarose	Diameter (mm)	5.06±0.18	5.53±0.05[a,d]	5.39±0.19[a]	5.52±0.06[a,d]	5.54±0.1[a,d]
	Thickness (mm)	1.61±0.01[d]	2.86±0.23[a,c,d]	2.32±0.16[a,d]	3.86±0.47[a,b,c,d]	3.08±0.03[a,b,d]
Self-Assembly	Diameter (mm)	4.67±0.29[d]	5.13±0.04[a,d,e]	5.04±0.05[a,d,e]	5.1±0.36[d,e]	5.18±0.14[a,d,e]
	Thickness (mm)	0.23±0.02[d,e]	1.47±0.38[a,e]	1.31±0.06[a,e]	1.35±0.14[a,e]	1.38±0.1[a,e]

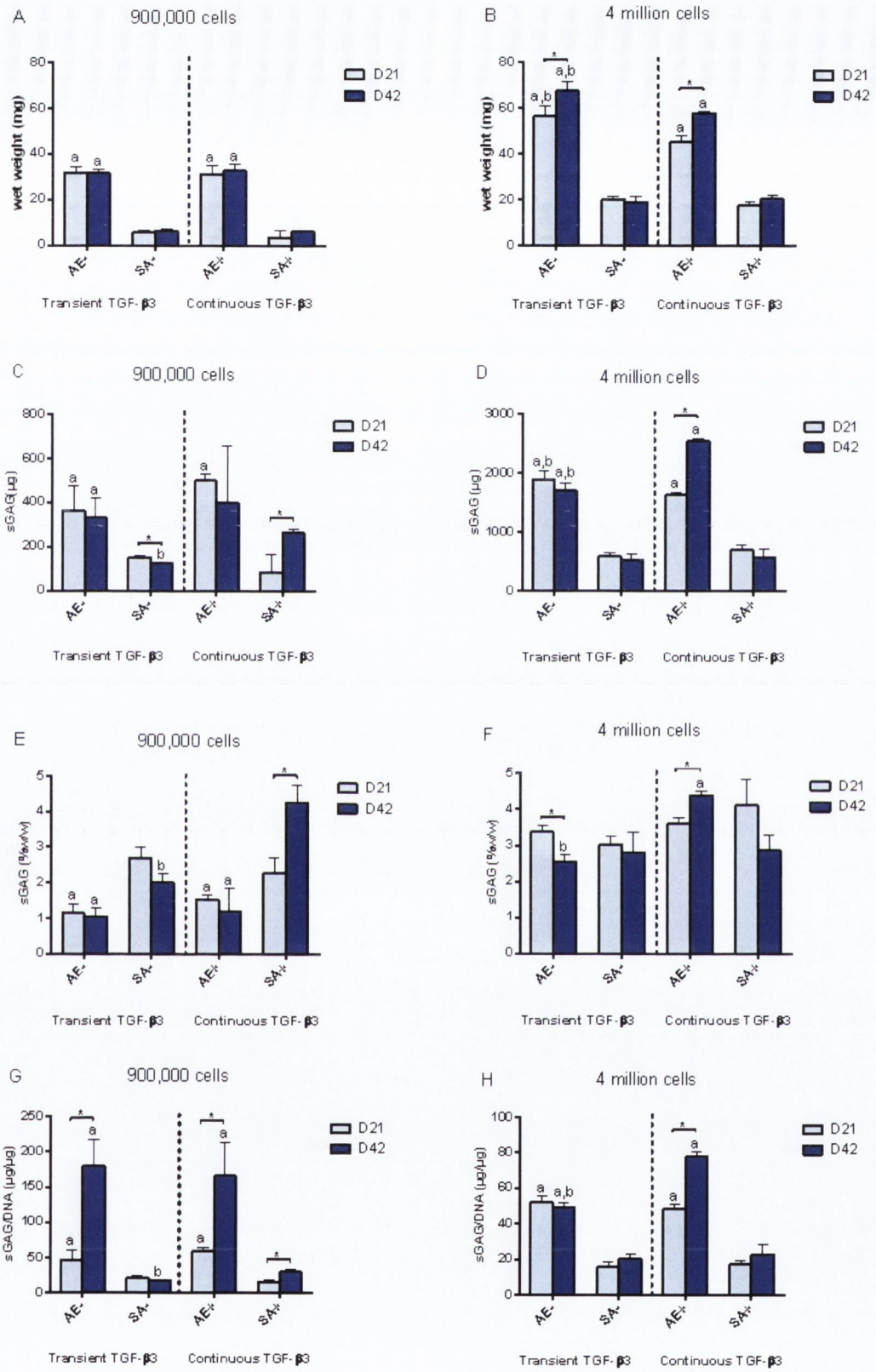
A
900,000 cells
wet weight (mg)
D21
D42
AE-
SA-
AE+
SA+
Transient TGF-β3
Continuous TGF-β3
B
4 million cells
C
900,000 cells
sGAG(µg)
D
4 million cells
sGAG (µg)
E
900,000 cells
sGAG (%w/w)
F
4 million cells
G
900,000 cells
sGAG/DNA (µg/µg)
H
4 million cells

Figure 4-2: Wet weight and sGAG content of agarose (AE) and self-assembled (SA) constructs for both transient (AE-, SA-) and continuous (AE+, SA+) TGF-β3 supplementation. (A) wet weight for low seeding density constructs (mg); (B) wet weight for high seeding density constructs (mg); (C) sGAG content for low seeding density constructs (μg); (D) sGAG content for high seeding density constructs (μg); (E) sGAG content normalized to wet weight for low seeding density constructs (%w/w); (F) sGAG content normalized to wet weight for high seeding density constructs (%w/w); (G) sGAG content normalized to DNA content for low seeding density constructs (μg/μg); (H) sGAG content normalized to DNA content for high seeding density constructs (μg/μg). a: $p<0.05$ vs. self-assembly with same culturing conditions at same time point; b: $p<0.05$ vs. continuous TGF-β3 with same scaffold at same time point. * denotes significant difference with $p<0.05$.

By day 42 in culture, agarose constructs seeded with 4 million chondrocytes accumulated higher levels of sGAG (2555.21±46.05 μg) compared to any other group (Figures 4-2C, D). For both transient and continuous TGF-β3 supplementation, AE led to greater amounts of absolute sGAG accumulation (measured in μg) compared to SA. However when normalized to wet weight, SA constructs were found to accumulate comparable levels of sGAG to agarose hydrogels (Figures 4-2E, F). Finally, when normalized to DNA content (Figures 4-2G, H), sGAG accumulation was found to be significantly greater in agarose gels compared to self-assembled constructs for both seeding densities. In addition, a lower seeding density was more conducive to matrix synthesis (on a per cell basis) in agarose constructs.

Similar trends were observed in collagen accumulated per construct (Figure 4-3), with continuously supplemented agarose hydrogels accumulating significantly more collagen than other constructs by day 42 (Figure 4-3B). When normalized to wet weight however, the SA constructs accumulated more collagen than corresponding AE constructs, for both low and high seeding densities (Figures 4-3C, D). When normalized to DNA content (Figures 4-3E, F), collagen accumulation was observed to follow similar trends to sGAG/DNA. Collagen synthesis (Collagen/DNA) did not appear to be dramatically affected by transient TGF-β3 supplementation for either SA or AE.

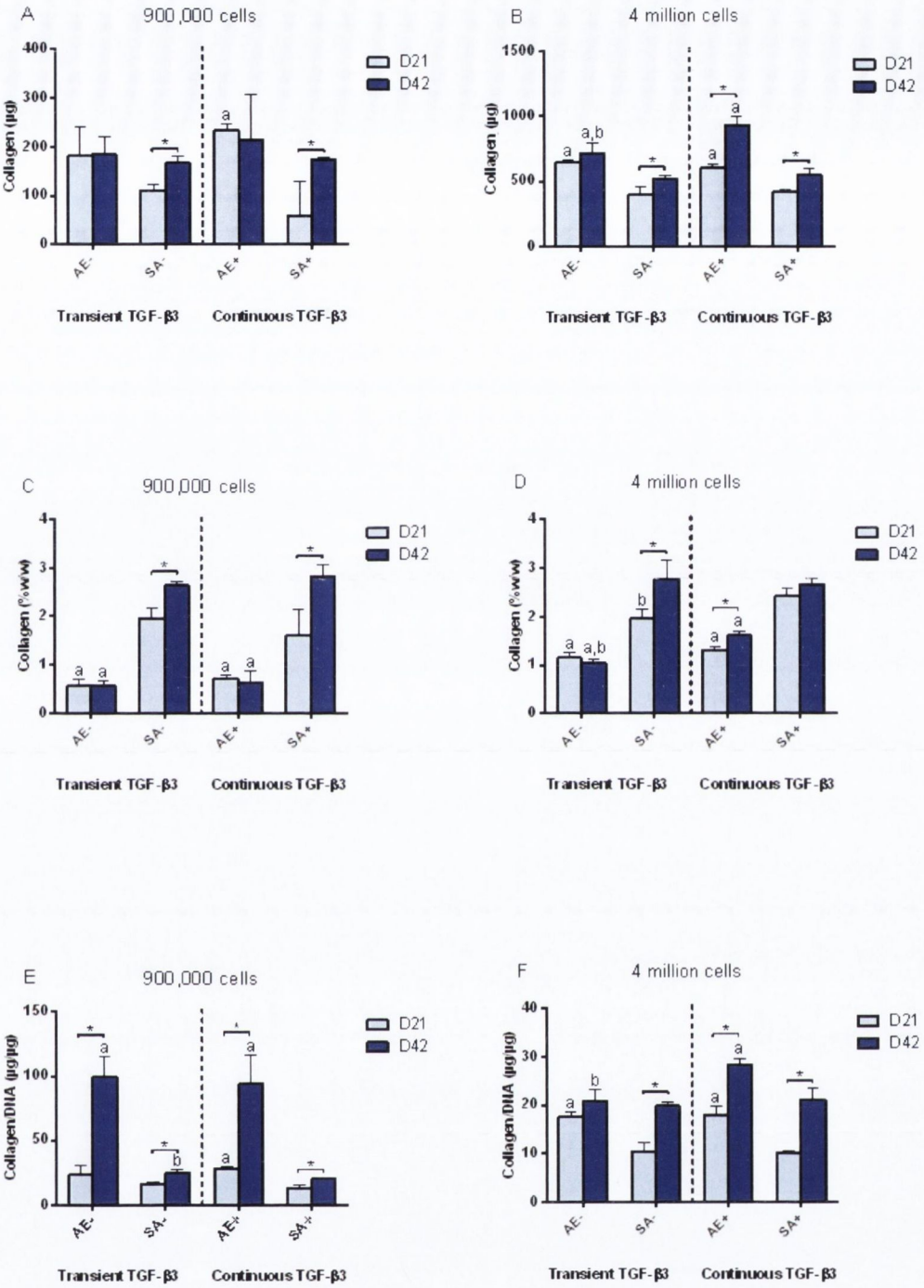
A
900,000 cells
Collagen (µg)
D21
D42
AE-
SA-
AE+
SA+
Transient TGF-β3
Continuous TGF-β3
B
4 million cells
C
900,000 cells
Collagen (%w/w)
D
4 million cells
E
900,000 cells
Collagen/DNA (µg/µg)
F
4 million cells

Figure 4-3: Collagen content of agarose (AE) and self-assembled (SA) constructs for both transient (AE-, SA-) and continuous (AE+, SA+) TGF-β3 supplementation. (A) collagen content for low seeding density constructs (μg); (B) collagen content for high seeding density constructs (μg); (C) collagen content normalized to wet weight for low seeding density constructs (%w/w); (D) collagen content normalized to wet weight for high seeding density constructs (%w/w); (E) collagen content normalized to DNA content for low seeding density constructs (μg/μg); (F) collagen content normalized to DNA content for high seeding density constructs (μg/μg). a: $p<0.05$ vs. self-assembly with same culturing conditions at same time point; b: $p<0.05$ vs. continuous TGF-β3 with same scaffold at same time point. * denotes significant difference with $p<0.05$.

The temporal development of grafts engineered using hydrogel encapsulation and SA was also different. At high seeding densities, sGAG and collagen accumulation in AE constructs continued to increase from days 21 to 42 in continuously supplemented conditions (Figures 4-2F, 4-3D). In contrast, ECM accumulation in SA constructs appeared to peak by day 21 (Figures 4-2F, 4-3D), with smaller changes over the subsequent 21 days of culture. There were comparable levels of sGAG and greater levels of collagen accumulation (measured as %w/w) in day 21 SA grafts compared to day 42 agarose constructs (Figures 4-2E, F; 4-3C, D).

In normal articular cartilage, the tissue contains approximately 3 times more collagen than sGAG as a percentage of wet weight (Mow et al., 1992). To enable the comparison between the relative compositions of our engineered tissue with normal articular cartilage, I normalized collagen accumulation within all constructs to corresponding sGAG accumulation (Figure 4-4). At higher seeding densities (Figure 4-4B), SA constructs at day 42 displayed a ratio of approximately 1, significantly greater than that of agarose constructs (less than 0.5). This would suggest SA using a sufficient number of chondrocytes leads to the development of a tissue with a more cartilage-like composition compared to hydrogel encapsulation.

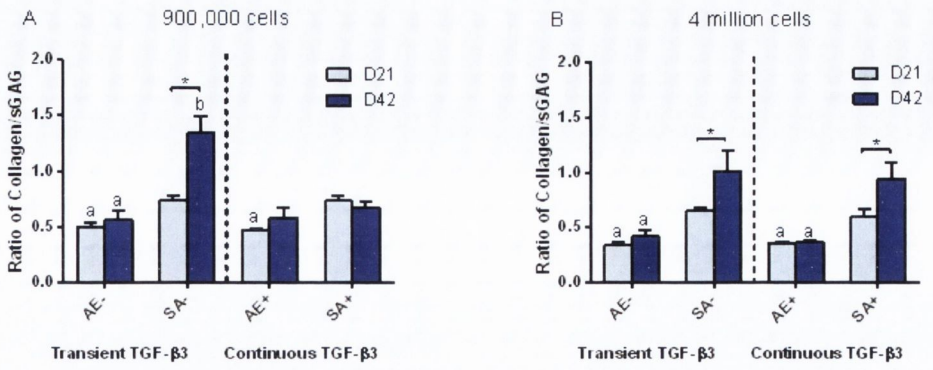

Figure 4-4: Ratio of collagen to sGAG content of agarose (AE) and self-assembled (SA) constructs for both transient (AE-, SA-) and continuous (AE+, SA+) TGF-β3 supplementation at days 21 and 42. (A) low seeding density; (B) high seeding density. a: $p<0.05$ vs. self-assembly with same culturing conditions at same time point; b: $p<0.05$ vs. continuous TGF-β3 with same scaffold at same time point. * denotes significant difference with $p<0.05$.

4.3.2 The spatial accumulation of matrix components in tissues engineered using self-assembly and hydrogel encapsulation

All constructs stained positively for sGAG and collagen type II (Figure 4-5), with evidence of increased staining of collagen type II in constructs continuously supplemented with TGF-β3. SA at a higher seeding density resulted in the development of a more uniform tissue, with contraction and distortion of SA constructs witnessed at low seeding densities. High seeding density SA constructs exhibited a peripheral region with weak sGAG staining and strong collagen type II staining. At higher magnification it was observed that the structure and organization of self-assembled constructs mimics certain aspects of native articular cartilage (Figure 4-6). Clustering of chondrocytes was observed in the deeper zones of the tissue. The superficial regions of the tissue stained intensely for type II collagen. Transiently supplemented SA constructs appeared more homogeneous than continuously supplemented constructs.

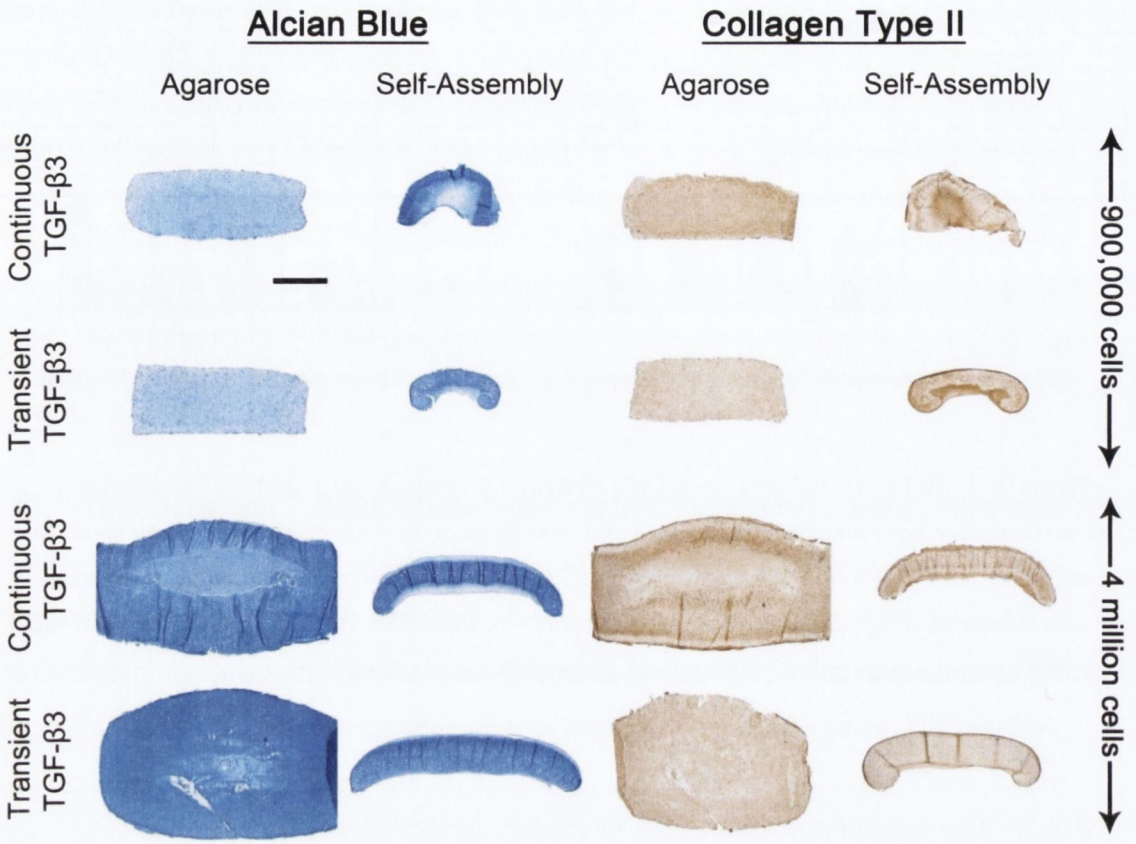

Figure 4-5: Alcian Blue staining for sGAG production, and type II collagen immunohistochemistry staining of agarose and self-assembled constructs for both transient and continuous TGF-β3 supplementation at day 42. Scale bar = 1mm.

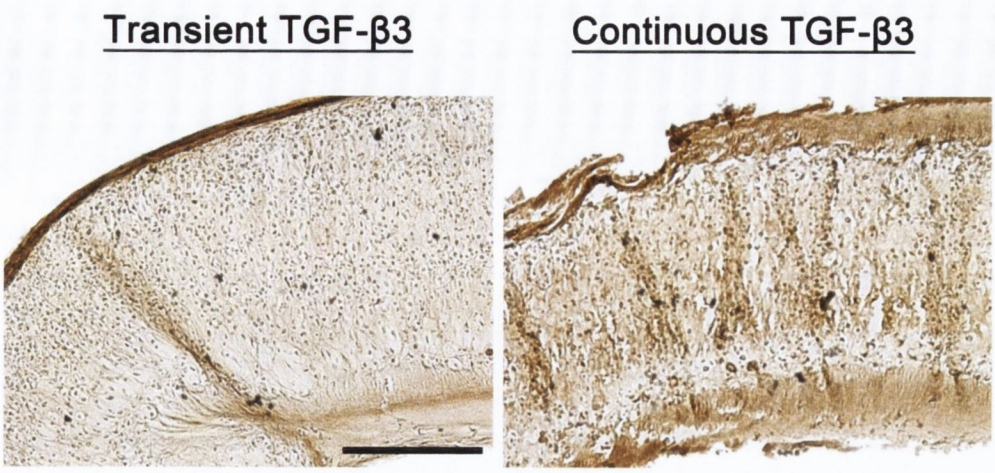

Figure 4-6: High magnification images of type II collagen immunohistochemistry staining of self-assembled constructs for both transient and continuous TGF-β3 supplementation at day 42 (high seeding density constructs). Scale bar = 250μm

It was decided to only investigate high seeding density constructs from this point forward in the experiment, as it was clear from the analysis that the low seeding density generated an inadequate SA construct.

Prevention of core degradation is an important challenge when scaling up engineered grafts. To gain an appreciation of spatial variations in matrix synthesis within constructs engineered using AE and SA, I next compared sGAG and collagen accumulation in the core and annular regions of these constructs (Figure 4-7). In each region of the constructs, similar trends were seen between groups in terms of respective sGAG and collagen accumulation. Continuously supplemented AE constructs accumulated significantly more sGAG than other constructs in both the core (4.87±0.14 %w/w) and annulus (4.24±0.04 %w/w). AE constructs accumulated significantly more sGAG in their core compared to their annuli, as did transiently supplemented SA constructs. In contrast to this, a more homogeneous sGAG distribution was observed in continuously supplemented SA constructs, with no significant difference found between core and annulus. As noted before, SA constructs accumulated significantly more collagen (measured as %w/w) than their corresponding AE constructs. Greater collagen accumulation was observed in the annular regions of all groups compared to their respective cores (although this was not significant in transiently supplemented SA constructs).

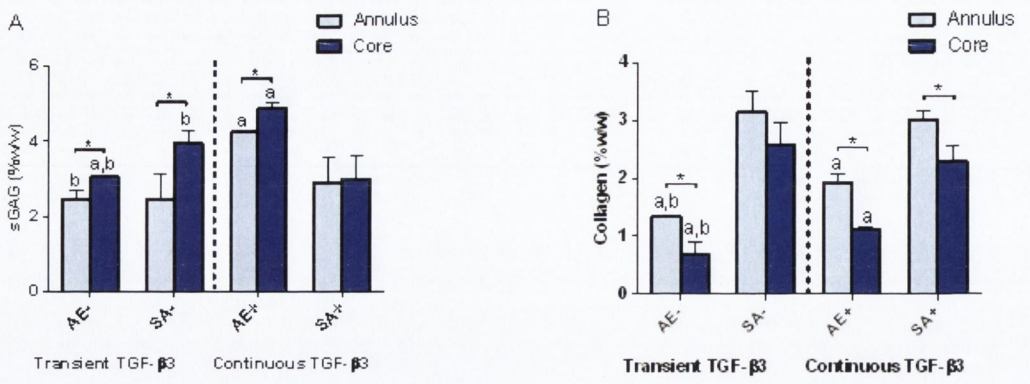

Figure 4-7: Biochemical composition of core and annular regions of agarose (AE) and self-assembled (SA) constructs for both transient (AE-, SA-) and continuous (AE+, SA+) TGF-β3 supplementation at day 42. (A) sGAG content normalized to wet weight for high seeding density constructs (%w/w); (B) collagen content normalized to wet weight for high seeding density constructs (%w/w). a: $p<0.05$ vs. self-assembly with same culturing conditions at same time point; b: $p<0.05$ vs. continuous TGF-β3 with same scaffold at same time point. * denotes significant difference with $p<0.05$.

4.3.3 Total matrix synthesis is greater in hydrogels than self-assembly

I next wished to determine if the greater levels of sGAG accumulation within the agarose hydrogels (measured in μg) were due to greater total sGAG synthesis or enhanced retention of sGAG within the construct (Figures 4-8, 9). Agarose constructs were found to accumulate significantly more sGAG than corresponding SA constructs, but they also released more sGAG to the culture media, with the highest levels of sGAG release observed in transiently supplemented agarose constructs (1447.56±61.88 μg) (Figure 4-8A). Continuously supplemented agarose constructs synthesized the greatest overall levels of sGAG (3809.72±48.58 μg). The total amount of sGAG synthesis in these AE constructs was approximately double that of SA constructs. To ascertain whether this increased level of sGAG production was due to changes in cell number, I normalized the results to DNA content (Figure 4-8B). I found almost identical trends, indicating that the greater sGAG production within AE constructs was mainly due to an enhanced matrix synthesizing capacity of the encapsulated cells. Agarose hydrogels were also more efficient at retaining

sGAG within the construct (Figure 4-9), with continuously supplemented constructs retaining approximately 67% of synthesized sGAG (day 42 samples). All constructs were found to retain a lower % of sGAG at day 42 compared to day 21.

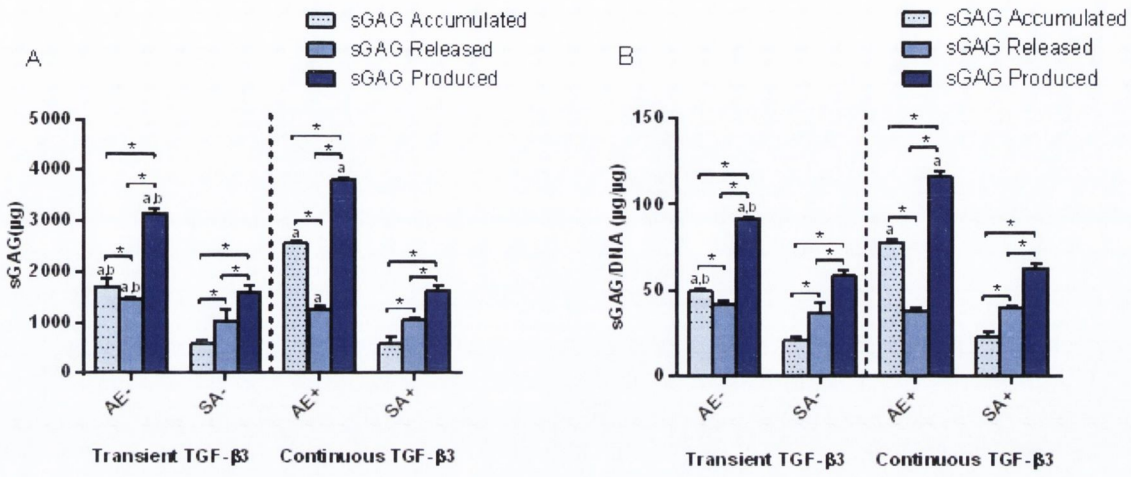

Figure 4-8: Total sGAG accumulated, released, and produced for agarose (AE) and self-assembled (SA) constructs for both transient (AE-, SA-) and continuous (AE+, SA+) TGF-β3 supplementation over 42 days. (A) sGAG for high seeding density constructs (µg); (B) sGAG normalized to DNA content for high seeding density constructs (µg/µg). a: $p<0.05$ vs. self-assembly with same culturing conditions at same time point; b: $p<0.05$ vs. continuous TGF-β3 with same scaffold at same time point. * denotes significant difference with $p<0.05$.

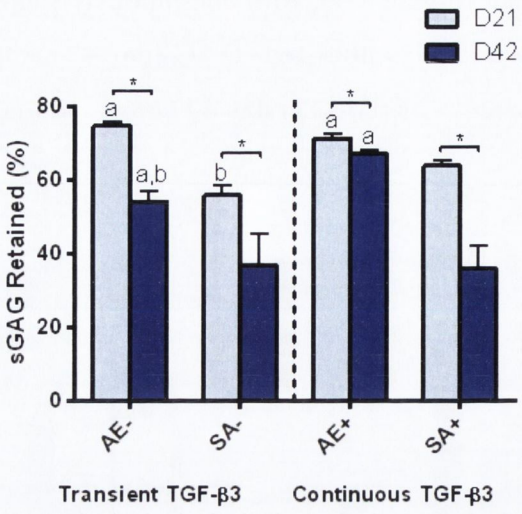

Figure 4-9: Percentage of sGAG retained in agarose (AE) and self-assembled (SA) constructs for both transient (AE-, SA-) and continuous (AE+, SA+) TGF-β3 supplementation. a: $p<0.05$ vs. self-assembly with same culturing conditions at same time point; b: $p<0.05$ vs. continuous TGF-β3 with same scaffold at same time point. * denotes significant difference with $p<0.05$.

4.4 Discussion

The objective of this study was to directly compare the self-assembly (SA) method to agarose encapsulation (AE) for engineering cartilaginous grafts using passaged chondrocytes. Two seeding densities were chosen as it is known that a minimum number of cells are required to form stable self-assembled constructs (Revell et al., 2008). It was found that at a low seeding density of 900,000 cells (46,000 cells/mm^2), generating a uniform 5mm diameter SA construct proved difficult. Previous studies have shown that the minimum number of cells needed to generate a uniform 5mm diameter chondrocyte SA construct is 2 million cells (102,000 cells/mm^2) (Revell et al., 2008). At the high seeding density (4 million cells total or 204,000 cells/mm^2) I observed that sGAG and collagen synthesis was greater using AE compared to SA. When normalized to wet weight however, SA constructs accumulated significantly greater levels of collagen compared to agarose gels. Consequently, SA led to the formation of an engineered cartilaginous tissue with a ratio of collagen to sGAG more comparable to native articular cartilage. A further benefit of SA is that such grafts can be generated within a relatively short time

frame (approximately 3 weeks), with comparable sGAG levels and higher collagen levels to AE constructs. Shortened culture times are important for clinical translation of tissue engineered products.

An inherent advantage to using agarose hydrogels is the ability to easily control the height and width of the engineered tissue. However depending on the cell seeding density, the construct can experience bulging at the top and bottom surfaces, as was observed in the high seeding density AE constructs. Self-assembled constructs reached a maximum thickness of approximately 1.4mm. This is similar to previous studies (Hu and Athanasiou, 2006b) where a SA thickness of approximately 1mm was reached. Articular cartilage thickness is on average 2.4 ± 0.5 mm in human medial femoral condyles (Hunziker et al., 2002a, Klein et al., 2009), demonstrating that further optimization is required if SA constructs are to be used to treat full thickness cartilage defects.

sGAG accumulation was greater in agarose constructs compared to SA. To assess if this was simply due to greater retention of sGAG within hydrogels, or due to overall higher levels of sGAG synthesis, I evaluated sGAG release to the media. Both the amount of sGAG released and total sGAG retained was higher in the agarose hydrogels, clearly demonstrating that total sGAG synthesis was higher in this system. To determine if this greater sGAG synthesis was due to greater cell proliferation in the hydrogel environment, I normalized the sGAG data to DNA content. Even by this measure, sGAG synthesis was higher in agarose hydrogels, indicating that altered ECM synthesis and not simply greater proliferation in the hydrogel environment was responsible for this different level of sGAG accumulation. This may be considered an advantage to using agarose, with more sGAG synthesis on a per cell basis, and also a greater percentage of sGAG retained within the constructs. This occurs despite higher levels of collagen accumulation (%w/w) in the SA constructs, which presumably play an important role in proteoglycan retention in engineered tissues, highlighting the benefit of agarose for maintaining synthesized matrix components. The higher levels of cartilage specific ECM synthesis in the AE constructs may be due to the agarose promoting a more spherical chondrocyte morphology, which previously has been shown to support the re-establishment of a chondrogenic phenotype in passaged chondrocytes (Benya and

Shaffer, 1982). It could also be due to the physical separation of cells within the agarose hydrogel, whereas in SA constructs significant cell to cell contact occurs.

While chondrocytes appear more synthetically active in hydrogels, the composition of the engineered tissue (as a % of wet weight), as well as the relative amounts of collagen to proteoglycans, are more like native articular cartilage in the SA constructs. It has been well documented that achieving native levels of collagen accumulation is more challenging than reaching native levels of proteoglycan accumulation in tissue engineered cartilage (Freed et al., 1998, Waldman et al., 2003b, Hung et al., 2004, Gemmiti and Guldberg, 2006). Indeed, rapid GAG synthesis has been hypothesized to be an impediment to collagen synthesis in chondrocyte seeded agarose hydrogels, with recent studies demonstrating that inducing enzymatic GAG loss during the early phase of culture can increase the ultimate collagen concentration and tensile properties of the engineered tissue (Bian et al., 2009c). The local environment within SA constructs would appear to suppress sGAG synthesis while maintaining collagen synthesis at levels approaching that found in the agarose hydrogels. Therefore, in spite of the fact that both sGAG synthesis and retention were lower in SA constructs compared to AE constructs, it would appear that the SA process generates a tissue with a composition more akin to that of native articular cartilage.

By spatially analysing the biochemical composition of the engineered tissues, I observed greater collagen accumulation in the annulus of constructs compared to their corresponding cores (Figure 4-7). This could be due to gradients in nutrients and other regulatory molecules developing within the constructs. It should be noted that sGAG levels were comparable between the core and annuli of continuously supplemented SA constructs. This would suggest that collagen synthesis may be more sensitive to nutrient availability than sGAG synthesis.

It was noted that collagen type II staining was more intense in superficial regions of self-assembled constructs, which is similar to native articular cartilage where staining is generally highest in the superficial tangential zone. Clustering of chondrocytes was also observed in the deeper zones of the SA tissues. Previous studies have demonstrated that organization of cartilaginous tissues generated by

self-assembly of MSCs mimic certain aspects of the native articular cartilage architecture. Specifically these tissues stained intensely for collagen type II, and weakly for proteoglycans, in the superficial region of the engineered tissue (Elder et al., 2009). It may be that surface tension developing at the surface of self-assembled constructs is contributing to the higher level of collagen type II production in the superficial region of the developing tissue. Greater nutrient/growth factor availability in this region of the engineered tissue could also play a role.

As transient TGF-β3 stimulation has been shown to enhance chondrogenesis in bovine chondrocyte seeded agarose hydrogels (Byers et al., 2008), I compared the effect of such media supplementation conditions on the development of cartilaginous grafts engineered using both the SA and AE approaches. I found no clear benefit to transient TGF- β3 supplementation for either SA or AE, apart from the fact that the financial cost of this approach is lower than continuous growth factor supplementation. The differences between our findings and that of previous studies (Byers et al., 2008) may possibly be due to our use of expanded chondrocytes or species differences.

The lack of mechanical property data is a limitation of this study. The non-uniform shape of the self-assembled tissue (and indeed agarose constructs at high seeding densities, see Figure 4-5) led to varying and possibly unreliable mechanical testing results in pilot studies and such tests not undertaken as part of the main study. The fact that chondrocytes were obtained from the femoral condyles of a 4 month old pig might also be considered a limitation of the study. At this age such animals have not reached skeletal maturity. Chondrocytes from such tissue would probably be more adept at producing cartilage-specific ECM than chondrocytes obtained from an older donor, as seen in bovine (Tran-Khanh et al., 2005, Erickson et al., 2011) and human donors (Barbero et al., 2004). As with many tissue engineering studies, cells were expanded and differentiated in high glucose (25mM) culture medium. One possible implication of this could be hyperglycaemic conditions leading to the copious production of hyaluronic acid (HA) (Wang et al., 2011). As rapid GAG synthesis has been hypothesized to be an impediment to collagen production (Bian et al., 2009c), this additionally produced HA could inhibit

collagen production of our tissue engineered constructs. Future studies will explore the influence of altered glucose conditions on tissue engineered cartilage.

4.5 Concluding Remarks

The objective of chapter 4 was to directly compare the SA approach to agarose hydrogel encapsulation (AE) as a means to engineer functional cartilaginous grafts using chondrocytes (CCs). No other studies to date have been undertaken to achieve this. In conclusion, a higher seeding density was required to develop robust cartilaginous grafts using a self-assembly approach. If achieving such high numbers of chondrocytes is clinically feasible, the SA approach has many attractive attributes, including the generation of grafts with a high collagen content, and the development of a tissue with an architecture and a ratio of collagen to sGAG content more closely resembling native articular cartilage. The SA process also generated tissues with such high levels of ECM within a relatively short time-frame. Coupled with the inherent advantages of a scaffold-free approach, the results of this study provide strong support for the use of the SA approach for engineering functional cartilaginous grafts for clinical applications.

In theory, the SA approach is simple to scale-up; simply seeding larger number of cells over a wider area enables the engineering of scaled-up tissues. However, there are many inherent limitations associated with the use of CCs for cartilage tissue engineering, such as the lack of available healthy donor cartilage for harvesting cells in older or diseased patients and dedifferentiation of CCs during culture expansion. Therefore, the objective of chapter 5 was to attempt to engineer cartilage-like grafts through self-assembly of infrapatellar fat pad-derived mesenchymal stem cells (FPSCs).

5 Engineering articular cartilage-like grafts by self-assembly of infrapatellar fat pad-derived stem cells

[A modified version of this chapter has been published in Biotechnology and Bioengineering, 111, 1686-1698 (2014) (10.1002/bit.25213)]

5.1 Introduction

Due in part to its avascular nature, articular cartilage has a very poor intrinsic capacity for repair. Damage to cartilage can occur due to physical trauma or because of degenerative diseases such as osteoarthritis. Many tissue engineering strategies have been proposed to repair damaged cartilage, with typical approaches involving the use of a scaffold or hydrogel for supporting and organizing the cells in a three dimensional (3D) environment (Roy et al., 2008, Van Vlierberghe et al., 2011, Thorpe et al., 2013, Kharkar et al., 2013, Sheehy et al., 2013). Hydrogels such as agarose are commonly used for such applications, as they have been shown to support the chondrogenic phenotype and the synthesis of cartilaginous extracellular matrix (ECM) (Benya and Shaffer, 1982, Sun et al., 1986, Buschmann et al., 1992a, Mauck et al., 2000a, Mauck et al., 2002a, Mauck et al., 2003c, Huang et al., 2009, Mesallati et al., 2013). However, there are limitations associated with the use of scaffolds or hydrogels for cartilage tissue engineering, including stress shielding of cells from biophysical stimulation, poor cell attachment, toxic scaffold degradation products, inflammatory response to the implanted material, poorly controlled biodegradability and a reduction in cell to cell communication, amongst others (Temenoff and Mikos, 2000a, Hutmacher, 2000, Bryant et al., 2004a, Liu and Ma, 2004, Hu and Athanasiou, 2006b, Elder et al., 2009, Athanasiou et al., 2013, Kharkar et al., 2013). This has motivated increased interest into scaffold-free or self-

assembly techniques as an alternative approach to generating functional cartilaginous grafts.

The self-assembly (SA) process typically involves the aggregation of cells within transwell inserts (Yu et al., 1997, Naumann et al., 2004, Murdoch et al., 2007, Hayes et al., 2007) or custom made agarose moulds (Hu and Athanasiou, 2006a, Elder and Athanasiou, 2008b), allowing the cells to secrete their own ECM which collectively acts as a scaffold forming a cohesive construct. I have previously compared this SA process to agarose encapsulation as a means to generate functional cartilaginous grafts using passaged chondrocytes, demonstrating that SA constructs more closely resemble native articular cartilage in their tissue architecture and in the ratio of collagen to sGAG within the construct (Mesallati et al., 2014a).

Early SA studies mainly focused on the use of chondrocytes for engineering cartilaginous grafts (Reginato et al., 1994, Dodge et al., 1998, Estrada et al., 2001, Novotny et al., 2006, Hu and Athanasiou, 2006b, Hoben et al., 2007, Elder and Athanasiou, 2008b, Ofek et al., 2008, Elder and Athanasiou, 2009b, Tran et al., 2011, Kraft et al., 2011, Kim et al., 2011). The potential use of chondrocytes for cartilage tissue engineering applications is however severely limited due to the lack of available healthy donor cartilage for harvesting cells, especially in older or diseased patients. In addition, chondrocytes have been shown to dedifferentiate towards a fibroblastic phenotype when expanded *in vitro* (Temenoff and Mikos, 2000b). The difficulty in obtaining large numbers of healthy chondrocytes in a clinical setting has motivated research into alternative cell types, particularly mesenchymal stem cells or multi-potent stromal cells (MSCs), for cartilage tissue engineering applications.

Bone marrow-derived MSCs (BMSCs) have been utilised in the SA model to generate cartilage grafts (Zhang et al., 2011), often with the use of transwell inserts (Elder et al., 2009, Lee et al., 2011) or by allowing cells to self-assemble on the surface of tissue culture plastic (Zhang et al., 2010). Indeed, the benefits of SA over the traditional pellet culture system have been demonstrated with BMSCs in both the transwell model (Murdoch et al., 2007) and the plastic tissue culture model (Zhang et al., 2010), with SA constructs synthesizing and depositing more cartilage-

like matrix than corresponding pellet cultures. Self-assembled cartilaginous tissues have also been generated using alternative cell sources such as synovial tissue-derived stem cells (SDSCs) (Ando et al., 2007, Ando et al., 2008). Joint tissue-derived stem cells such as SDSCs are a particularly promising cell source for cartilage tissue engineering due to their strong chondrogenic potential (Nishimura et al., 1999, Mochizuki et al., 2006, Shirasawa et al., 2006, Marsano et al., 2007, Pei et al., 2008, Pei et al., 2009, Sampat et al., 2011). The infrapatellar fat pad (IFP) is another joint tissue which has also been shown to possess progenitor cells with a strong chondrogenic capacity (Wickham et al., 2003a, Khan et al., 2007, Lee et al., 2008, Jurgens et al., 2009, Buckley et al., 2010a, Buckley et al., 2010c, Buckley and Kelly, 2012). Furthermore, it may represent a more clinically appealing cell source as large biopsies of tissue can be isolated with relative ease (Dragoo et al., 2003), which facilitates the procurement of large numbers of cells required for SA strategies. Several studies have demonstrated that infrapatellar fat pad-derived stem cells (FPSCs) possess at least a comparable chondrogenic capacity to BMSCs (English et al., 2007, Vinardell et al., 2011, Vinardell et al., 2012a), however no study has been performed to determine if functional cartilage-like grafts can be engineered through SA of FPSCs.

The first objective of this study was to investigate if cartilage-like grafts could be engineered by SA of FPSCs, and if so, to determine what effect two different cell seeding density and growth factor supplementation conditions would have on cartilage tissue formation. Specifically, SA constructs were formed by adding either 900,000 or 4 million porcine FPSCs within 5mm diameter silicone rings (PDMS, Polydimethylsiloxane) seated on tissue culture plastic or onto polyethylene terephthalate (PET) transwell membranes. Motivated by previous studies (Byers et al., 2008, Huang et al., 2009, Buxton et al., 2011, Sampat et al., 2011), I also compared the development of self-assembled tissues following either transient or continuous exposure to transforming growth factor (TGF)-β3. The second objective of the study was to compare the biochemical properties of self-assembled tissues to those generated by agarose hydrogel encapsulation (AE) of FPSCs.

5.2 Materials and Methods

5.2.1 Cell isolation and expansion

IFPs were harvested from 4 month old porcine femoropatellar joints and rinsed thoroughly with Dulbecco's phosphate-buffered saline (Sigma-Aldrich, Dublin, Ireland; PBS) containing penicillin (100 U/mL)-streptomycin (100 µg/mL) (GIBCO, Invitrogen, Dublin, Ireland), and amphotericin B (0.25 µg/mL) (Sigma-Aldrich). IFPs were diced followed by 3-4 h incubation under constant rotation at 37°C with high-glucose Dulbecco's Modified Eagle Medium GlutaMAX (4.5 mg/mL D-Glucose, 200mM L-Glutamine; hgDMEM) (GIBCO, Invitrogen) containing collagenase type II (750 U/mL) (Worthington Biochemical, LanganBach Services, Ireland) as previously described (Buckley and Kelly, 2012). After tissue digestion, the resulting cell suspension was passed through a 40 µm pore-size cell sieve (Fisher Scientific, Dublin, Ireland), and the filtrate centrifuged and rinsed twice with PBS. Cell number and viability were determined using a haemocytometer and 0.4% trypan blue staining (Sigma-Aldrich). Mononucleated cells were plated at a seeding density of 500 cells/cm^2 in T-75 cm^2 flasks (Sarstedt, Wexford, Ireland) and expanded in a humidified atmosphere at 37°C and 5% CO_2. Non-adherent cells were removed from flasks during the first medium change after 3 days. All cells were maintained in hgDMEM GlutaMAX supplemented with 10% v/v fetal bovine serum (GIBCO, Invitrogen; FBS), penicillin (100 U/mL)-streptomycin (100 µg/mL) and 5 ng/mL human fibroblast growth factor-2 (FGF-2; ProSpec-Tany TechnoGene Ltd., Israel) during all expansion phases.

At the first passage (~10 days), all FPSCs were frozen in hgDMEM GlutaMAX supplemented with 10% v/v FBS and 10% dimethyl sulphoxide (Sigma-Aldrich; DMSO), and stored in liquid nitrogen. When needed, frozen FPSCs were thawed and expanded to passage 2 at a seeding density of 5 x 10^3 cells/cm^2 in 500 cm^2 triple flasks (Thermo Fisher Scientific, Dublin, Ireland).

5.2.2 Formation and differentiation of self-assembled and agarose hydrogel constructs

At P2, cells were trypsinized, counted, and suspended in basic chondrogenic medium (basic CDM) consisting of hgDMEM GlutaMAX supplemented with penicillin (100 U/mL)-streptomycin (100 μg/mL) (both from GIBCO, Invitrogen), 100 μg/mL sodium pyruvate, 40 μg/mL L-proline, and 1.5 mg/mL bovine serum albumin (all Sigma-Aldrich). SA constructs were formed by adding either 900,000 cells (low seeding density; 46,000 cells/mm^2) or 4 million cells (high seeding density; 204,000 cells/mm^2) in 40 μL aliquots of defined CDM to 5mm diameter, 3mm thick PDMS O-rings, seated in either 12-well plates (low seeding density constructs) or 6-well plates (high seeding density constructs) (Fisher Scientific); see Appendix Figure S5. Defined CDM consisted of basic CDM supplemented with 0.25 μg/mL amphotericin B, 1x insulin-transferrin-selenium, 4.7 μg/mL linoleic acid, 50μg/ml L-ascorbic acid-2-phosphate and 100nM dexamethasone (all Sigma-Aldrich). After 3 h, a further 60 μL of defined CDM was added to each O-ring. Cells were left to self-assemble in this state for a further 9 hours before additional defined CDM was added to each well; t = 0 was defined at this time point. Pilot studies showed that immediate TGF-β3 supplementation resulted in construct contraction. Therefore, SA constructs were not supplemented with TGF-β3 for the initial 24 h (from t = 0). After 24 h, medium in each well was replaced with fresh defined CDM supplemented with 10 ng/mL TGF-β3 (ProSpec-Tany TechnoGene Ltd.).

FPSC encapsulated agarose hydrogel constructs were formed by mixing a FPSC cell suspension with 4% agarose (Type VII) at a ratio of 1:1 at ~40°C, yielding a final gel concentration of 2% and a cell density of either 30 million cells/mL or 136 million cells/mL. Agarose-cell suspensions were cast in a stainless steel mould and cored using a 5mm diameter biopsy punch, thus creating solid construct cylinders of 5mm diameter, 1.5mm thickness. Agarose constructs were cultured in defined CDM supplemented with 10ng/mL of TGF-β3 (fully supplemented CDM). The low and high agarose seeding densities of 30 million cells/mL and 136 million cells/mL correspond to the SA seeding densities of

900,000 and 4 million cells, respectively. The low seeding density of 900,000 cells (30 million cells/mL) was chosen to allow construct comparisons with other FPSC agarose hydrogel studies previously undertaken in the laboratory (Buckley et al., 2010a, Buckley et al., 2010c, Buckley and Kelly, 2012). The high seeding density of 4 million cells was chosen as this has previously been shown to be the optimal seeding number for chondrocyte SA constructs (Revell et al., 2008), and also gave satisfactory results in our previous SA study (Mesallati et al., 2014a). Previous BMSC work has found the final volume of tissue engineered SA constructs to be proportional to the initial cell seeding density when seeded up to a density of 4 million cells per construct (Ando et al., 2008). Further increases in cell seeding density led to a plateau in the resultant construct volume.

BMSC SA constructs have been reported in the thickness range of ~ 0.8 - 1.5 mm (Murdoch et al., 2007, Elder et al., 2009), with my previous work with chondrocyte SA generating constructs ~ 1.4 mm thick. Therefore, I chose a thickness value of 1.5 mm for the agarose constructs in order to generate similarly sized constructs to those likely formed through the SA approach.

Low seeding density constructs were maintained in 2.3 mL fully supplemented CDM, with high seeding density constructs maintained in 10 mL (maintaining a constant ratio of media to cells), with medium changes every 3 days. All SA and agarose tissue engineered constructs were maintained in fully supplemented CDM for the first 3 weeks of culture, after which TGF-β3 was withdrawn from half the samples of all experimental groups for the final 3 weeks. In addition, all SA constructs were removed from their PDMS ring moulds after 4-5 days of *in vitro* culture, in order to improve homogeneous nutrient transfer to the engineered tissues.

Finally, the study was repeated by forming SA constructs in cell culture transwell inserts. It has previously been reported that SA using BMSCs on PET transwell membrane inserts leads to the generation of morphologically uniform tissues (Elder et al., 2009). Frozen FPSCs were expanded to P2 as before, trypsinized, and suspended in basic expansion medium consisting of hgDMEM GlutaMAX supplemented with 10% v/v FBS and penicillin (100 U/mL)-

streptomycin (100 μg/mL). SA constructs were formed by adding 4 million cells (~1.2 x 10^5 cells/mm^2) in 250 μL aliquots of basic expansion medium to 6.5mm diameter transwell cell culture inserts (Corning Transwell®, VWR, Dublin, Ireland), seated in 6-well plates (see Appendix Figure S5). Each transwell insert consisted of a PET membrane containing 3μm pores. Cells were left to settle for 12-14 h, upon which the wells were filled with basic expansion medium, completely submerging the inserts. Medium was changed to defined CDM after 24 h, supplemented with 10 ng/mL TGF-β3. In conjunction with these SA constructs, identically seeded FPSC encapsulated agarose hydrogel constructs (6mm diameter; 1.5 mm thickness) were formed using the same method as before (seeding density of 94 million cells/mL corresponding to 4 million total cells, as used previously). Constructs were maintained in 10 mL fully supplemented CDM. Half of all samples were transiently supplemented with TGF-β3 as before.

5.2.3 Biochemical analysis

The biochemical content of engineered constructs (n=3 for high seeding density constructs, n=4 for low seeding density) was assessed at each time point (21 and 42 days). On removal from culture, construct diameter was measured, the wet mass of samples was recorded, and all samples were subsequently frozen at -85 °C for later analyses. Samples were digested with papain (125 μg/mL) in 0.1 M sodium acetate, 5 mM L-cysteine-HCL, 0.05 M EDTA, pH 6 (all Sigma-Aldrich) under constant rotation at 60°C for 18 h. DNA content of constructs was quantified using the Hoechst Bisbenzimide 33258 dye assay (Kim et al., 1988). Proteoglycan content was estimated by quantifying the amount of sulphated glycosaminoglycans (sGAG) in each construct using the dimethylmethylene blue dye binding assay (Blyscan, Biocolor Ltd., Carrickfergus, UK), with a shark chondroitin sulphate standard. Total collagen content of constructs was determined by measuring the hydroxyproline content via the dimethylaminobenzaldehyde and chloramine T assay (Kafienah and Sims, 2004), using a hydroxyproline to collagen ratio of 1:7.69 (Ignat'eva et al., 2007).

5.2.4 Histology and immunohistochemistry

At each time point, 2-3 samples per group were fixed in 4% paraformaldehyde (Sigma-Aldrich), dehydrated with a graded series of alcohol and embedded in paraffin. 5μm sections were produced of the cross section perpendicular to the construct face. Sections were stained with 1% alcian blue 8GX (Sigma-Aldrich) in 0.1M HCL for sGAG accumulation. Collagen type II deposition was identified by immunohistochemical analysis, as described previously (Mesallati et al., 2014a). A mouse monoclonal anti-collagen type II antibody was used as the primary antibody, followed by an anti-mouse IgG biotin conjugate secondary antibody. Positive and negative controls (porcine cartilage and ligament respectively) were included in the immunohistochemistry staining process.

5.2.5 Statistical analysis

Statistical analyses were performed using the software package MINITAB 15.1 (Minitab Ltd., Coventry, UK). Groups were analyzed for significant differences using a general linear model for analysis of variance with factors of scaffold type, culturing conditions, time point, and interactions between these factors examined. Tukey's test for multiple comparisons was used to compare conditions. A Box-Cox transformation was used to normalize data sets where necessary. Significance was accepted at a level of $p \leq 0.05$. Numerical and graphical results are presented as mean ± standard deviation (n=3 for high seeding density constructs at each time point, n=4 for low seeding density constructs at each time point), with graphical results produced using GraphPad Prism (Version 6.02).

5.3 Results

5.3.1 Tissues with a cartilage-like biochemical composition can be engineered by self-assembly of FPSCs

I first investigated if it was possible to engineer cartilaginous tissues using FPSCs through a self-assembly (SA) process. By day 42 in culture, transiently supplemented SA constructs generated using 4 million cells had accumulated over twice the amount of sGAG (1070.8±215.8 μg) than those supplemented with TGF-

β3 for the full 6 weeks of culture (495.8±29.5 μg) (Figure 5-1B). There was no such beneficial effect to TGF-β3 withdrawal at the lower seeding density of 900,000 cells (Figure 5-1A). An approximately 5 fold higher level of sGAG accumulation was observed in transiently supplemented SA constructs at the high seeding density when compared with the low seeding density, with a 2 fold increase observed in continuously supplemented SA constructs (Figure 5-1A, B). Similar results were found for collagen accumulation (Figure 5-1C, D), with transient TGF-β3 supplementation enhancing collagen accumulation at a high seeding density by day 42. When measured as a percentage of tissue wet weight, SA constructs were found to accumulate relatively high levels of sGAG (Figure 5-1E, F) and collagen (Figure 5-1G, H). The highest levels of matrix accumulation was observed in transiently supplemented SA constructs at the high seeding density (8.4±1.5 %w/w sGAG; 4.7±1.2 %w/w collagen).

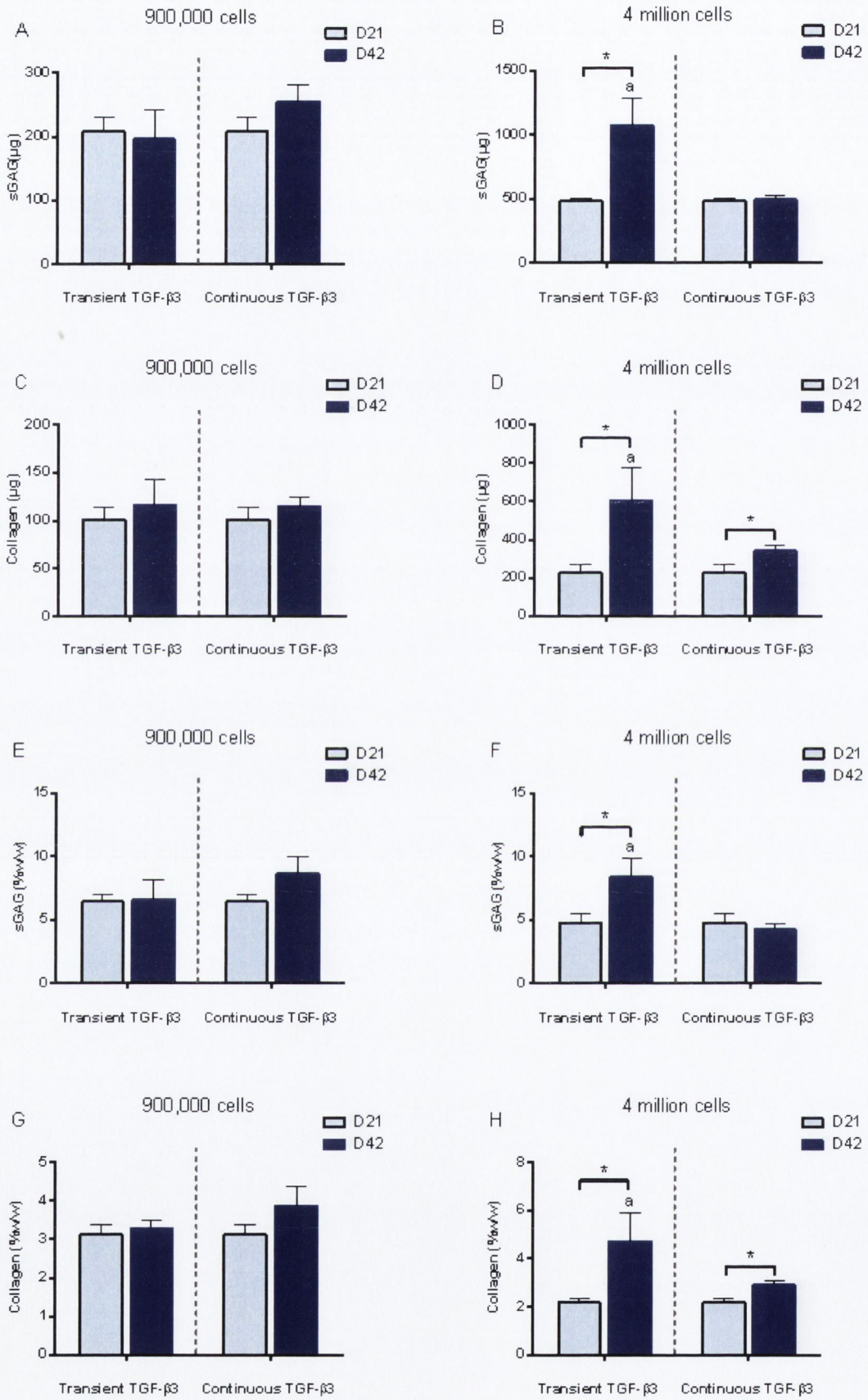
A
900,000 cells
D21
D42
sGAG(µg)
300
200
100
0
Transient TGF-β3
Continuous TGF-β3
B
4 million cells
D21
D42
*
a
sGAG(µg)
1500
1000
500
0
Transient TGF-β3
Continuous TGF-β3
C
900,000 cells
D21
D42
Collagen (µg)
200
150
100
50
0
Transient TGF-β3
Continuous TGF-β3
D
4 million cells
D21
D42
*
a
*
Collagen (µg)
1000
800
600
400
200
0
Transient TGF-β3
Continuous TGF-β3
E
900,000 cells
D21
D42
sGAG (%w/w)
15
10
5
0
Transient TGF-β3
Continuous TGF-β3
F
4 million cells
D21
D42
*
a
sGAG (%w/w)
15
10
5
0
Transient TGF-β3
Continuous TGF-β3
G
900,000 cells
D21
D42
Collagen (%w/w)
5
4
3
2
1
0
Transient TGF-β3
Continuous TGF-β3
H
4 million cells
D21
D42
*
a
*
Collagen (%w/w)
8
6
4
2
0
Transient TGF-β3
Continuous TGF-β3

Figure 5-1: sGAG and collagen content of self-assembled constructs formed on plastic for both transient and continuous TGF-β3 supplementation. sGAG content for (A) low seeding (B) high seeding density constructs (μg); collagen content for (C) low seeding (D) high seeding density constructs (μg); sGAG content normalized to wet weight for (E) low seeding (F) high seeding density constructs (%w/w); collagen content normalized to wet weight for (G) low seeding (H) high seeding density constructs (%w/w). [a] $p<0.05$ versus continuous TGF-β3 at same time point. *Denotes significant difference with $p<0.05$ (n=4 for low seeding density constructs; n=3 for high seeding density constructs).

All SA constructs stained positively for sGAG and collagen type II (Figure 5-2), with the latter mainly localized to the top and bottom surfaces in high seeding density constructs. SA constructs formed at the high seeding density were larger than those formed at the lower seeding density (for example, continuously supplemented SA constructs reached a diameter of 3.9±0.5 mm at the high seeding density, significantly greater than corresponding low seeding density SA measurements of 2.1±0.3 mm; p=0.012 (see Table 5-1)). Macroscopically, low seeding density SA constructs formed a pellet-like structure. Even at high seeding densities some contraction of self-assembled tissues on the underlying plastic still occurred (see Table 5-1), resulting in the majority of SA constructs forming generally uneven, inhomogeneous constructs (Appendix Figure S6), particularly with transient TGF-β3 supplementation.

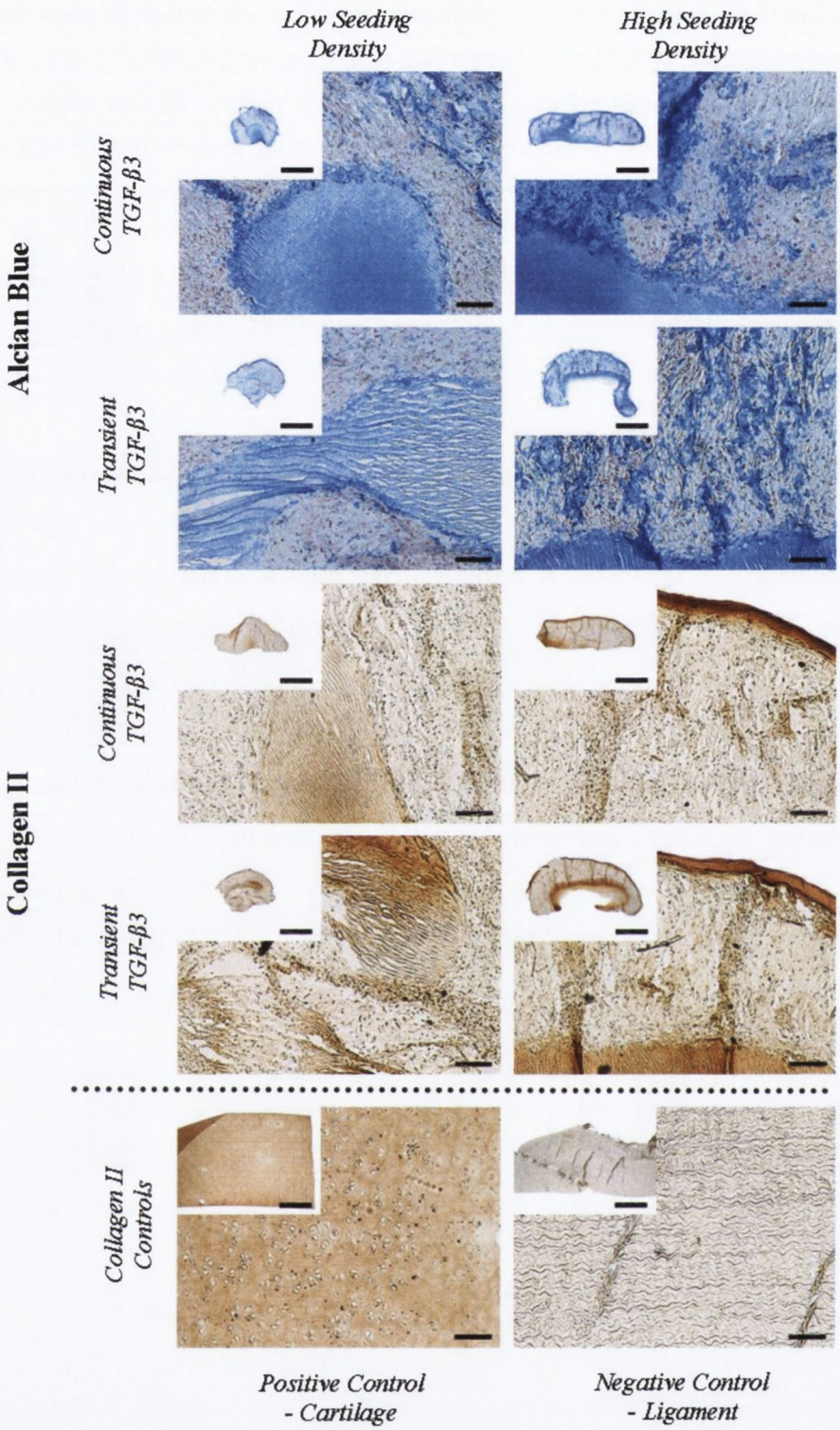

Figure 5-2: Alcian Blue staining for sGAG production, and type II collagen immunohistochemistry staining of low and high seeding density self-assembled constructs formed on plastic for both transient and continuous TGF-β3 supplementation at day 42. Main image is high magnification shot of inset construct. Scale bar in main images = 100 µm. Scale bar in insets = 1 mm.

Table 5-1: Physical parameters of wet weight, thickness and diameter for FPSC encapsulated agarose and self-assembled constructs formed on plastic for both low and high seeding densities at week 6. * signifies that parameters not measured due to construct contraction. a: $p<0.05$ vs. continuous TGF-β3 supplementation; b: $p<0.05$ vs. corresponding self-assembly group; c: $p<0.05$ vs. corresponding group in high seeding density.

			Low Seeding Density	High Seeding Density
Agarose	*Transient TGF-β3 supplementation*	Wet weight (mg)	$31.98\pm2.66^{b,c}$	$39.48\pm1.75^{a,b}$
		Thickness (mm)	1.78 ± 0.06	1.71 ± 0.01^{b}
		Diameter (mm)	$4.99\pm0.04^{b,c}$	$5.18\pm0.02^{a,b}$
	Continuous TGF-β3 supplementation	Wet weight (mg)	$33.55\pm1.53^{b,c}$	45.5 ± 0.59^{b}
		Thickness (mm)	1.6 ± 0.16	1.79 ± 0.09^{b}
		Diameter (mm)	$5.01\pm0.02^{b,c}$	5.37 ± 0.04^{b}
Self-Assembly	*Transient TGF-β3 supplementation*	Wet weight (mg)	2.99 ± 0.34^{c}	12.58 ± 1.4
		Thickness (mm)	*	0.95 ± 0.17
		Diameter (mm)	2.02 ± 0.14^{c}	3.5 ± 0.13
	Continuous TGF-β3 supplementation	Wet weight (mg)	3.02 ± 0.47^{c}	11.68 ± 0.76
		Thickness (mm)	*	1.1 ± 0.25
		Diameter (mm)	2.06 ± 0.3^{c}	3.87 ± 0.49

5.3.2 FPSCs synthesize higher levels of ECM components following hydrogel encapsulation, but generate a more cartilage-like tissue through self-assembly

I next sought to compare SA to AE for engineering functional cartilaginous grafts. At the high seeding density, under continuous TGF-β3 supplementation conditions (Figure 5-3A, B), I found that total sGAG and collagen accumulation (in μg) by day 42 was higher using AE (1149.9±195.1 μg sGAG; 1100.3±34.7 μg collagen) when compared to the SA approach (495.8±29.5 μg sGAG; 340.7±28 μg collagen). Transient TGF-β3 culture conditions were found to significantly benefit the development of cartilage grafts engineered using the SA approach at this high seeding density, but to have a detrimental effect on grafts generated using AE, consistent with previous findings (Buckley et al., 2010c). Greatest overall levels of sGAG (measured in μg) were found in continuously supplemented agarose constructs and transiently supplemented SA constructs when seeded with 4 million cells (Figure 5-3A). Continuously supplemented AE constructs accumulated the greatest levels of collagen (measured in μg) (Figure 5-3B). Continuously supplemented AE constructs also accumulated the greatest levels of sGAG (432.7±31.6 μg) and collagen (516.4±28.2 μg) at the lower seeding density of 900,000 cells (Appendix Figure S7A, B).

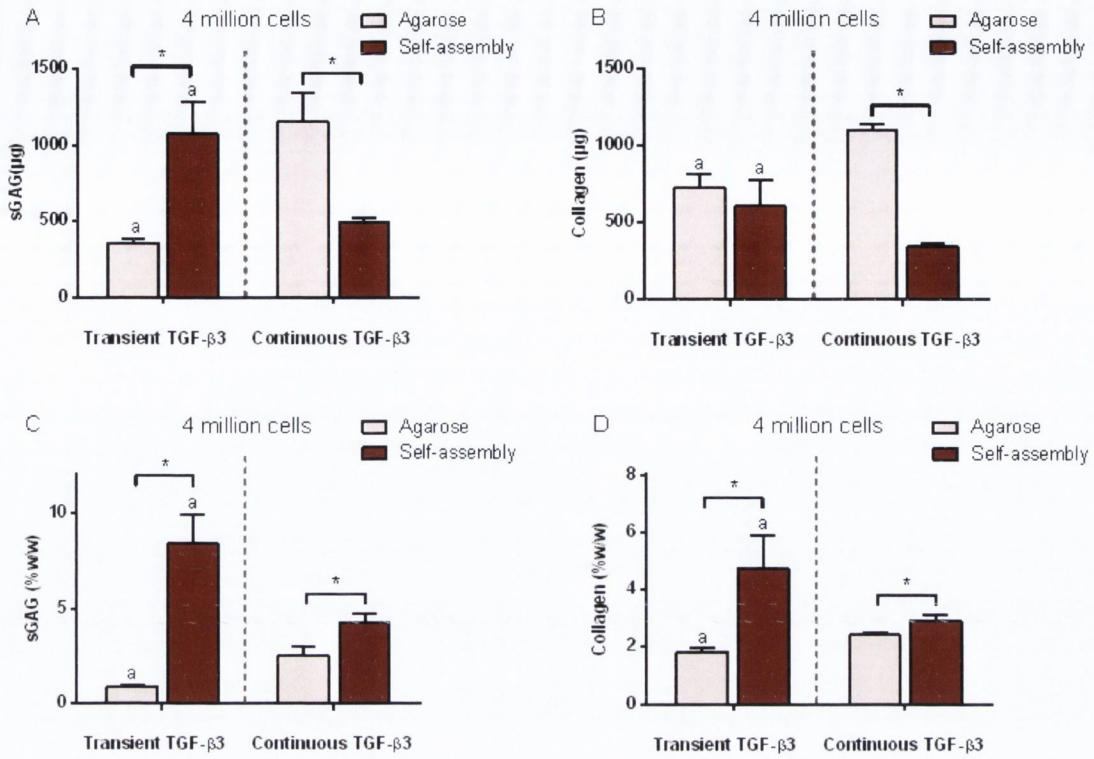

Figure 5-3: sGAG and collagen content of agarose and self-assembled constructs formed on plastic at day 42 at high seeding density for both transient and continuous TGF-β3 supplementation. (A) sGAG content (µg); (B) collagen content (µg) (C) sGAG content normalized to wet weight (%w/w); (D) collagen content normalized to wet weight (%w/w). [a] $p<0.05$ versus continuous TGF-β3 with same scaffold. *Denotes significant difference with $p<0.05$ (n=3).

In general, total sGAG and collagen accumulation (measured in µg) was found to be highest following agarose encapsulation. However, SA constructs were considerably lighter than corresponding agarose constructs (Table 5-1), and as a result were found to accumulate significantly greater levels of both sGAG and collagen (for both supplementation conditions) when normalized to tissue wet weight (Figure 5-3C, D). The same result was seen at low seeding densities (Appendix Figure S7C, D). All constructs stained positively for sGAG and collagen type II (Figure 5-4).

Figure 5-4: Alcian Blue staining for sGAG production, and type II collagen immunohistochemistry staining of agarose and self-assembly constructs formed on plastic for both transient and continuous TGF-β3 supplementation at day 42. Scale bar = 1 mm.

5.3.3 Self-assembly of FPSCs on transwell inserts leads to the development of geometrically uniform grafts

Having demonstrated that self-assembled FPSC constructs are compositionally attractive, but morphologically fail to form implantable grafts (Appendix Figure S6), the final phase of the study explored if more geometrically stable and

homogenous constructs could be engineered by SA of FPSCs on polyethylene terephthalate (PET) transwell membranes. SA constructs formed on transwells with 4 million cells were smooth, firm, and flat with a hyaline-like appearance by day 42. Unlike before, there was no benefit to transient TGF-β3 supplementation in terms of sGAG (Figure 5-5A) or collagen accumulation (Figure 5-5B). FPSCs embedded into agarose hydrogels synthesized significantly more sGAG (Figure 5-5A) and collagen (Figure 5-5B) than cells self-assembled onto transwell inserts. When normalized to wet weight, SA led to greater sGAG accumulation (Figure 5-5C) than AE for both TGF-β3 conditions. In contrast, there was no significant difference in collagen accumulation normalized to wet weight between AE and SA (Figure 5-5D).

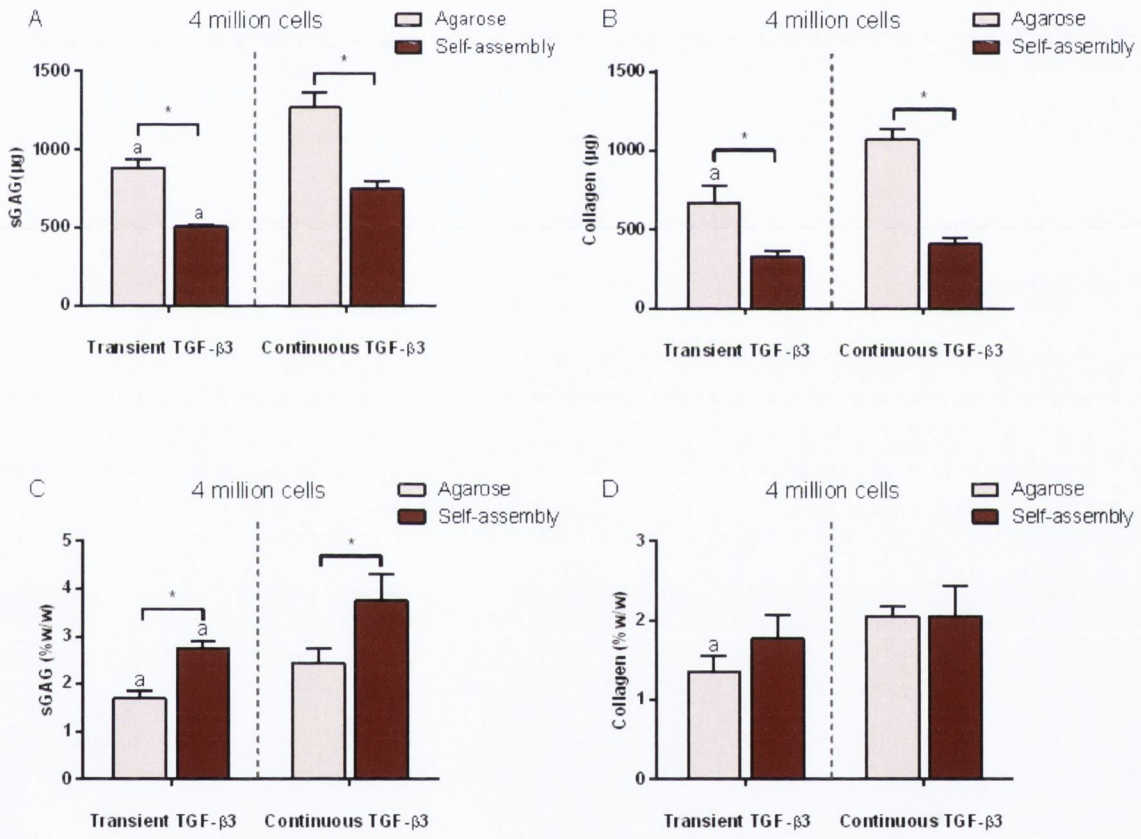

Figure 5-5: sGAG and collagen content of agarose and self-assembled constructs formed on transwells at day 42 at high seeding density for both transient and continuous TGF-β3 supplementation. (A) sGAG content (µg); (B) collagen content (µg) (C) sGAG content normalized to wet weight (%w/w); (D) collagen content normalized to wet weight (%w/w). [a] $p<0.05$ versus continuous TGF-β3 with same scaffold. *Denotes significant difference with $p<0.05$ (n=3).

High seeding density SA constructs formed on transwells formed more geometrically uniform constructs than those formed on plastic, with all constructs consistent in their shape (Appendix Figure S6). Transwell constructs were also considerably larger in diameter (for example, continuously supplemented transwell SA constructs reached a diameter of 6.4±0.2 mm, significantly greater than corresponding plastic SA measurements of 3.9±0.5 mm; p=0.014 (see Tables 5-1 and 5-2)), with little contraction observed during culture. SA constructs formed on transwells were generally thinner than those formed on plastic (for example, continuously supplemented transwell SA constructs reached a thickness of 0.61±0.04 mm, compared to 1.1±0.25 mm on plastic; p=0.078 (see Tables 5-1 and 5-2)).

Table 5-2: Physical parameters of wet weight, thickness and diameter for FPSC encapsulated agarose and self-assembled constructs formed on transwells at a high seeding density at week 6. a: $p<0.05$ vs. corresponding self-assembly group.

			High Seeding Density
Agarose	*Transient TGF-β3 supplementation*	Wet weight (mg)	49.57±2.77[a]
		Thickness (mm)	3.75±0.1[a]
		Diameter (mm)	6.22±0.12
	Continuous TGF-β3 supplementation	Wet weight (mg)	52.34±3.2[a]
		Thickness (mm)	3.84±0.07[a]
		Diameter (mm)	6.27±0.06
Self-Assembly	*Transient TGF-β3 supplementation*	Wet weight (mg)	18.66±1
		Thickness (mm)	0.73±0.1
		Diameter (mm)	6.57±0.42
	Continuous TGF-β3 supplementation	Wet weight (mg)	20.16±1.8
		Thickness (mm)	0.61±0.04
		Diameter (mm)	6.42±0.2

All tissue engineered constructs again stained positively for sGAG and collagen type II (Figure 5-6). SA constructs exhibited a superficial region with weak sGAG staining and strong collagen type II staining, as seen in previous chondrocyte SA work (Mesallati et al., 2014a). There was also evidence of clustering of cells and the appearance of a column-like organization in the deeper regions of continuously supplemented SA constructs.

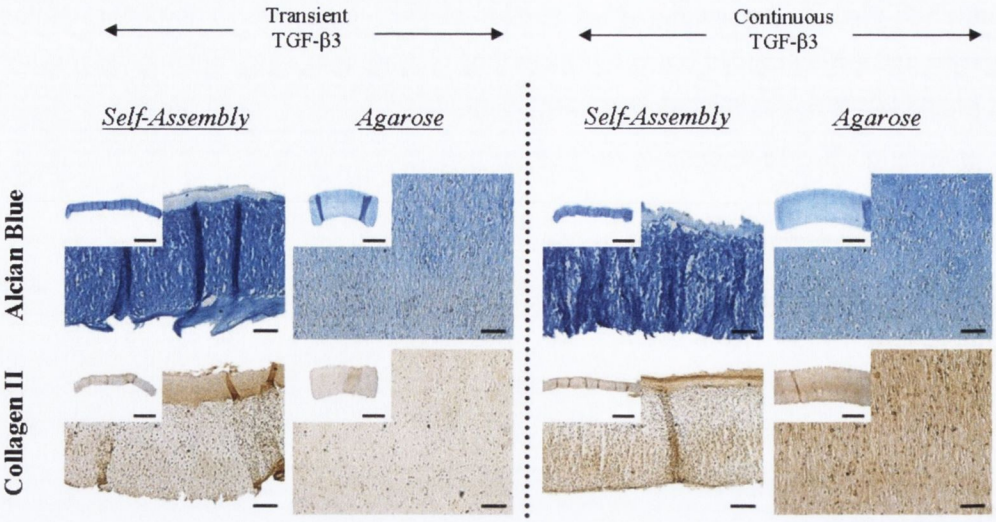

Figure 5-6: Alcian Blue staining for sGAG production, and type II collagen immunohistochemistry staining of agarose and SA constructs formed on transwells for both transient and continuous TGF-β3 supplementation at day 42. Main image is high magnification shot of inset construct. Scale bar in main images = 100 μm. Scale bar in insets = 1 mm.

5.4 Discussion

The objective of this study was to investigate if FPSCs could be used to engineer cartilage-like tissues through a self-assembly (SA) process, and if successful, to compare the properties of such grafts to those generated by agarose hydrogel encapsulation (AE). When normalized to tissue wet weight, I found high levels of matrix accumulation (approximately 8 %w/w sGAG; 5 %w/w collagen) in self-assembled tissues. This compares to reported values of 4-7 %w/w sGAG and 15-22 %w/w collagen for normal articular cartilage (Mow et al., 1992). Engineering of such SA constructs on plastic, however, led to the development of contracted, geometrically inconsistent tissues. At low FPSC seeding densities, SA constructs formed a pellet-like structure. Even at high seeding densities some contraction of self-assembled tissues on the underlying plastic still occurred, resulting in the majority of such constructs forming uneven, inhomogeneous grafts. I also compared the SA method to AE, demonstrating that SA appears to result in the development of more cartilage-like grafts with higher levels of sGAG and collagen accumulation when normalized to tissue wet weight. In an attempt to engineer more geometrically

stable and homogeneous SA constructs, I repeated the study using cell culture inserts with PET transwell membranes (Elder et al., 2009). SA constructs formed on transwells formed more geometrically stable constructs than those formed on plastic. Transwell constructs were also considerably larger in diameter, with little tissue contraction observed during culture. These findings strongly suggest that SA of FPSCs on PET transwell membranes represents a novel approach to tissue engineering scalable articular cartilage-like grafts.

Motivated by previous studies that pointed to the importance of transient growth factor stimulation for engineering functional cartilage grafts (Byers et al., 2008, Huang et al., 2009, Sampat et al., 2011, Buxton et al., 2011), I first sought to determine the appropriate TGF-β3 supplementation conditions for SA of cartilage tissues using FPSCs. Transient exposure to TGF-β3 was found to enhance the development of SA constructs formed by seeding high numbers of FPSCs onto plastic. This result was not seen for FPSCs embedded in agarose hydrogels at either seeding density. It has previously been shown that transient exposure to TGF-β3 enhances matrix production for chondrocytes, perhaps because continuous TGF-β treatment may drive an aggressive turnover of matrix by triggering catabolic pathways (Byers et al., 2008, Ng et al., 2011). The same effect has been observed in agarose hydrogels seeded with large numbers (60 million cells/mL) of synovium-derived MSCs (Sampat et al., 2011) (for comparative purposes, the low and high agarose cell seeding densities used in this study correspond to 30 million cells/mL and 136 million cells/mL respectively). The differential response of FPSCs to transient TGF-β3 supplementation conditions observed in this study following AE and SA may potentially be explained by the differential levels of ECM accumulation at the time of TGF-β3 withdrawal. High seeding density SA constructs engineered on plastic achieved the highest levels of ECM maturation (when normalized to wet weight) by week 3 (4.8±0.7 %w/w sGAG; 2.2±0.2 %w/w collagen), the time-point at which TGF-β3 supplementation was withdrawn. This group was the only one in which transient TGF-β3 supplementation led to greater matrix production. The fact that such levels of matrix maturity were not reached in agarose hydrogels (average 2.2±0.3 %w/w sGAG; 1.4±0.1 %w/w collagen), or in self-assembled tissues engineered on transwell inserts (3.3±0.3 %w/w sGAG;

1.2±0.1 %w/w collagen) by week 3, might suggest that transient exposure is only beneficial once a certain threshold level of ECM accumulation is reached. It has been previously shown that agarose hydrogels seeded with large numbers (60 million cells/mL) of BM-MSCs accumulate significantly more sGAG and collagen when subjected to transient TGF-β3 supplementation (Huang et al., 2009). In the same study, however, agarose hydrogels seeded with 20 million cells/mL did not benefit from the same growth factor regime, indicating that higher levels of ECM accumulation may result in a more positive effect to transient TGF-β3 supplementation. It should be noted that it may not be that explicit levels of matrix accumulation must be reached before temporal withdrawal of TGF-β3 becomes beneficial, but rather that such levels of ECM accumulation are a surrogate marker for a more general change in FPSC phenotype, leading to cells which are more responsive to TGF-β3 withdrawal. Previously published work investigating transient TGF-β supplementation of chondrocyte SA constructs found no difference in sGAG or collagen accumulation (normalized to wet weight) between transiently supplemented SA constructs (10 ng/mL TGF-β1) and constructs with no growth factor supplementation (Elder and Athanasiou, 2009b). As continuous TGF-β exposure has been shown to benefit matrix accumulation of chondrocyte SA constructs (compared to no growth factor supplementation) (Elder and Athanasiou, 2008c), together these results would suggest that continuous TGF-β exposure is more beneficial for chondrocyte SA than transient supplementation, similar to our results for transwell FPSC self-assembled tissues.

With high seeding density SA constructs formed on tissue culture plastic, collagen type II accumulation was mainly localized to the top and bottom surfaces of the graft (Figure 5-4). Corresponding agarose hydrogels stained more homogeneously for collagen type II. This localization of such high levels of collagen in SA constructs may be due in part to the development of surface tension at the top and bottom of the engineered tissue. Tensile strain has been shown to increase collagen accumulation in MSC seeded constructs (Connelly et al., 2010, Baker et al., 2011), and to increase the expression of collagen type II in chondrocytes (Thomas et al., 2011) and other chondrocytic cells (Furumatsu et al., 2013). Differences in nutrient and growth factor transport between the SA and

hydrogel system may also help explain the specific spatial collagen type II deposition patterns in SA and AE constructs. The superficial region of SA constructs formed on transwells stained weakly for sGAG deposition, whilst strong staining was observed for collagen type II. There was also evidence of clustering of cells and the appearance of a column-like organization in the deeper regions of some transwell SA constructs. Future studies will investigate the presence of lubricin in the superficial zone of SA constructs. Also, scanning electron microscopy (SEM) will be performed to investigate the matrix organization of self-assembled tissues, and compare to native articular cartilage.

Total collagen accumulation (μg), and in some cases total sGAG accumulation (μg), was higher following AE compared to SA. This agrees with our previous study comparing chondrocyte SA to agarose encapsulation (Mesallati et al., 2014a). Higher levels of sGAG accumulation in AE constructs could be due to agarose promoting a more spherical cell morphology, which has been shown to support a chondrogenic phenotype (Benya and Shaffer, 1982). However, as a % of wet weight, ECM levels in SA were much greater than AE, as the self-assembled tissues were lighter with a lower water content.

A limiting factor with SA of FPSCs on tissue culture plastic was tissue contraction, particularly at low seeding densities where constructs formed an almost pellet-like construct (see Figure 5-2 and diameter measurements in Table 5-1). Even at high seeding densities, contraction was an issue (see Appendix Figure S6 and diameter measurements in Table 5-1). Contraction of SA constructs engineered using bone marrow-derived MSCs on plastic has been previously reported (Zhang et al., 2010), where low seeding density constructs (250,000 cells) contracted over the initial 24 hours of culture. It has been suggested that contractile forces generated within the actin-cytoskeleton may be partially responsible for contraction of tissue engineered SA constructs (Ando et al., 2008). Contraction of self-assembled tissues has also been observed on other substrates, where SA of MSCs led to constructs contracting over 4 days (Zhang et al., 2011). No contraction of SA constructs engineered on transwell cell culture inserts was observed in this study. This could be due to stronger adherence of cells and their ECM to the transwell. The differential adhesion hypothesis states that a tissue will tend to minimize the adhesive free

energy of its cell populations via cell-to-cell binding (Steinberg, 1970, Foty and Steinberg, 2005, Athanasiou et al., 2013). If cells are allowed to self-assemble on a non-adhesive surface/substrate, cell attachment is prevented; this forces the cells in the developing self-assembled tissue to spontaneously adhere and bind to one another in order to minimize free energy (Athanasiou et al., 2013). Thus, when a self-assembled tissue has no substrate to attach to, or where adherence to the substrate is relatively weak, these cell-to-cell interactions could lead to greater contraction of the tissue.

sGAG accumulation (% w/w) within SA constructs engineered on transwell inserts did not increase from week 4 to week 6, but collagen accumulation continued to increase during this time period (data not shown). In contrast, we have previously shown that collagen accumulation (% w/w) peaks in chondrocyte SA constructs by week 3, with no increase from week 4-6 (Mesallati et al., 2014a). This indicates that longer culture times may be required for MSCs to produce cartilage-like tissue compared to primary chondrocytes. Other studies comparing BM-MSCs and chondrocytes have shown that cartilage-specific ECM accumulation in MSC seeded constructs lags that observed in chondrocyte seeded constructs (Mauck et al., 2006, Huang et al., 2009, Huang et al., 2010b).

Self-assembled tissues generated by FPSCs on transwells reached a maximum thickness of ~ 0.7mm (Table 5-2), while SA constructs formed with chondrocytes have been found to reach a thickness of ~ 1.4mm over the same length of culture (Mesallati et al., 2014a). Articular cartilage thickness has been reported in the range of 2.4 ± 0.5mm in human medial femoral condyles (Hunziker et al., 2002b). To address these SA construct thickness limitations, future studies will explore alternative tissue engineering strategies, such as the co-culture of chondrocytes and MSCs, which have been shown to enhance overall levels of chondrogenesis (Bian et al., 2011, Meretoja et al., 2012, Dahlin et al., 2014b). Such strategies could potentially lead to increased SA construct thickness and could also reduce the *in vitro* culture time required to engineer articular cartilage-like grafts.

5.5 Concluding Remarks

The objective of chapter 5 was to attempt to engineer cartilage-like grafts through self-assembly of infrapatellar fat pad-derived mesenchymal stem cells (FPSCs). This was the first reported work in the literature investigating if FPSCs could be used to engineer cartilage-like tissues through a SA process. In this chapter, I successfully used the SA process to engineer cartilage-like tissues using FPSCs, an easily accessible and clinically relevant cell source. SA resulted in the formation of a denser tissue than AE, with cartilage ECM accumulation approaching values previously reported for articular cartilage (Mow et al., 1992, Gannon et al., 2012). Future work will investigate the potential of scaling-up such an approach as a means to treat large chondral defects. However, as an alternative strategy to using CCs or mesenchymal stems cells (MSCs) alone, the next chapter, chapter 6, will investigate if a co-culture of CCs and MSCs can be used to generate a more cartilaginous graft *in vitro*.

6 Engineering functional cartilaginous grafts using chondrocyte-agarose constructs supported by a superficial layer of stem cells

6.1 Introduction

A number of methodologies have been proposed to engineer functional cartilage tissue. Two methods that would appear to have significant promise are hydrogel encapsulation (Buschmann et al., 1992a, Buschmann et al., 1995b, Mauck et al., 2000a, Mauck et al., 2002a) and self-assembly (SA) (Hu and Athanasiou, 2006b, Athanasiou et al., 2013). Traditionally both methodologies make use of chondrocytes (CCs) for engineering cartilage (Mauck et al., 2000a, Mauck et al., 2002a, Hu and Athanasiou, 2006b, Elder and Athanasiou, 2008a, Mesallati et al., 2013, Mesallati et al., 2014a). However, the difficulty in obtaining large numbers of healthy chondrocytes in a clinical setting has motivated research into mesenchymal stem cells or multi-potent stromal cells (MSCs). Bone marrow-derived MSCs (BMSCs) are commonly used for cartilage tissue engineering, either by encapsulating the cells into a hydrogel (Mauck et al., 2006, Mauck et al., 2007, Thorpe et al., 2008), or using self-assembly or scaffold-free approaches (Murdoch et al., 2007, Elder et al., 2009, Zhang et al., 2011, Lee et al., 2011). More recently, infrapatellar fat pad-derived stem cells (FPSCs) have been shown to possess a strong chondrogenic capacity when encapsulated in agarose hydrogels (Buckley et al., 2010a, Buckley et al., 2010c, Buckley and Kelly, 2012). I have shown in the previous chapter that FPSCs can be used to engineer cartilage-like tissues through the SA process, with sGAG accumulation (%w/w) reaching native like levels after 6 weeks of culture.

Recently, there has been increased interest in the co-culturing of CCs and MSCs for cartilage repair strategies (Hendriks et al., 2007, Giovannini et al., 2010, Wu et al., 2011, Acharya et al., 2012, Wu et al., 2012, Wu et al., 2013b, Leijten et

al., 2013). Co-culture of expanded articular CCs with BMSCs has been shown to promote chondrocyte proliferation, cartilaginous extracellular matrix (ECM) production and type II collagen gene expression in mixed pellet cultures compared to monoculture controls (Tsuchiya et al., 2004). From a clinical perspective, studies have shown that a co-culture of BMSCs and CCs not only leads to increased cartilage matrix formation, but furthermore, can provide better macroscopic cartilage regeneration within focal cartilage lesions, when compared with microfracture (Bekkers et al., 2013a, Bekkers et al., 2013b). Increased cartilage matrix production has also been reported in the co-culture of adipose-derived stem cells (ASCs) and CCs (Hildner et al., 2009, Lee and Im, 2010, Acharya et al., 2012). Evidence has recently emerged to suggest that the spatial positioning of different cell populations in such co-cultures may be critical for driving chondrogenesis. So called 'structured co-cultures', where the different cell types are initially separated in distinct layers, have been shown to outperform mixed co-cultures (Allon et al., 2010), and lead to the development of cartilaginous tissues more resistant to the hypoxic and inflammatory conditions expected at the site of injury (Cooke et al., 2011). To date, such structured co-cultures have only been performed in pellet cultures. What remains unclear is how CCs and MSCs should be structured in 3D engineered tissues to optimise the functional development of such constructs prior to implantation.

To date, attempts to engineer 3D grafts using a mixed co-culture of BMSCs and CCs have generally simply mixed the two cell populations within a hydrogel or 3D scaffold (Mo et al., 2009, Yang et al., 2009, Miao et al., 2009, Liu et al., 2010, Meretoja et al., 2012, Sabatino et al., 2012, Meretoja et al., 2013, Dahlin et al., 2014b). For example, a mixed co-culture of MSCs and CCs (4:1 ratio) in hyaluronic acid hydrogels has been found to lead to significantly higher Young's modulus, glycosaminoglycan levels, and collagen content than single cell only controls (Bian et al., 2011). The synergistic cartilage forming effect of co-culture has also been shown *in vivo*, with collagen scaffolds seeded with BMSCs and CCs accumulating higher amounts of GAG than corresponding single cell only controls following subcutaneous implantation into nude mice (Sabatino et al., 2012).

During early postnatal development, a slowly proliferating, self-renewing population of progenitor cells residing in the superficial zone of articular cartilage drive a lateral expansion of the articular cartilage layer, which in turn causes rapid expansion and elongation of the epiphyseal bone (Hunziker et al., 2007, Hunziker, 2009). This surface layer of stem cells plays a further role later on in directing the formation of mature hyaline cartilage beneath it (Archer et al., 2003). These developmental processes may provide directions for the optimal structuring of co-cultured CCs and stem cells required for engineering 3D cartilaginous grafts. Consequently, the objective of this study was to attempt to engineer functional cartilaginous grafts using CC seeded agarose constructs combined with a supporting layer of surface MSCs. It was hypothesised that recapitulating aspects of normal articular cartilage growth, where a pool of superficial stem cells drives the development of the tissue, would lead to the development of a more functional cartilaginous graft compared to the more traditional model of mixed co-culture.

6.2 Materials and Methods

6.2.1 Experimental Design

The study comprised of two main experiments (Figure 6-1). In experiment 1, either fat pad-derived MSCs (FPSCs) or bone marrow-derived MSCs (BMSCs) were mixed with chondrocytes (CCs) to form a homogeneous cell suspension (termed a 'mixed co-culture'); these cell suspensions were then encapsulated into agarose hydrogels (2mm thick). To determine any benefit of mixed co-culture, single-cell type control gels (CC, FPSC and BMSC) were cultured independently using the same respective cell numbers as those used in the mixed co-culture constructs. Further details are provided below.

Experiment 2 investigated structured co-cultures where either FPSCs or BMSCs were self-assembled on top of CC laden hydrogels (1.5 mm thick). The cell numbers chosen for this study were identical to those used in the mixed co-culture study, so direct comparisons could be made between the two co-culture configurations. Also, agarose gels were designed so that the overall thickness of co-culture constructs would be similar between the two configurations. In order to

determine the effect of structured co-culture on the different cell types, CC laden hydrogels, and in some cases MSC self-assembled constructs were cultured independently using the same cell numbers as those used in the structured co-culture constructs.

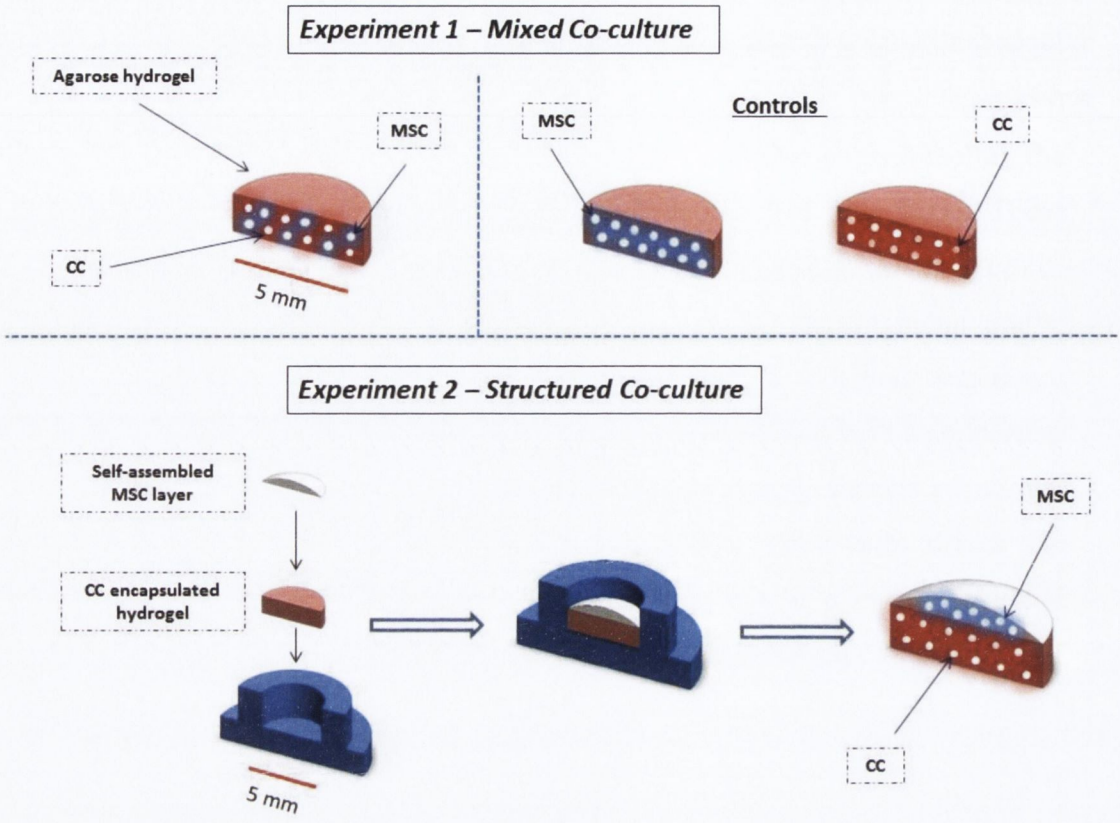

Figure 6-1: Schematic of experimental design. MSC, mesenchymal stem cell; CC, chondrocyte.

6.2.2 Cell isolation and expansion

Articular cartilage was aseptically harvested from porcine femoral condyles (4 months old, 1 donor), and the cartilage slices were rinsed thoroughly with Dulbecco's phosphate buffered saline (Sigma-Aldrich, Dublin, Ireland; PBS) containing penicillin (100 U/ml)-streptomycin (100 µg/ml) (GIBCO, Invitrogen, Dublin, Ireland), and amphotericin B (2.5µg/ml) (Sigma-Aldrich, Dublin, Ireland). Chondrocytes (CCs) were isolated from cartilage slices via digestion with high-glucose Dulbecco's modified Eagle's medium GlutaMAX (4.5 mg/ml D-Glucose, 200mM L-Glutamine; hgDMEM) (GIBCO, Invitrogen, Dublin, Ireland) containing collagenase type II (350 U/ml) (Worthington, Langanbach Services, Ireland) for 12-14 h under constant rotation at 37°C. The resulting cell suspension was passed

through a 40μm pore-size cell sieve (Fisher Scientific, Ireland) and the filtrate centrifuged and rinsed with PBS twice. Cell number and viability were determined using a haemocytometer and 0.4% trypan blue staining (Sigma-Aldrich, Dublin, Ireland); the CCs were then frozen in fetal bovine serum (GIBCO, Invitrogen, Dublin, Ireland; FBS) supplemented with 10% v/v dimethyl sulphoxide (Sigma-Aldrich, Dublin, Ireland; DMSO) and stored in liquid nitrogen.

Infrapatellar fat pads (IFPs) were harvested from 4 month old porcine femoropatellar joints (1 donor) and rinsed thoroughly with PBS containing penicillin-streptomycin. IFPs were diced followed by 3-4 h incubation under constant rotation at 37°C with hgDMEM GlutaMAX containing collagenase type II (750 U/mL) as previously described (Buckley and Kelly, 2012). Mononucleated cells were plated at a seeding density of 5×10^3 cells/cm^2 in T-75 cm^2 flasks (Sarstedt, Wexford, Ireland). At the first passage (~10 days), all FPSCs were frozen in FBS supplemented with 10% v/v DMSO, and stored in liquid nitrogen.

Finally, bone marrow-derived MSCs (BMSCs) were isolated from the femora of one porcine donor (4 months old). BMSCs were isolated and expanded based on a modified protocol developed for human MSCs (Lennon and Caplan, 2006). All BMSCs were frozen at the first passage (~10 days).

Before experiments were initiated cells were thawed and counted. CCs, FPSCs and BMSCs were plated at a seeding density of 5×10^3 cells/cm^2 in 500 cm^2 triple flasks (Thermo Fisher Scientific, Ireland) and expanded to passage two (P2) in a humidified atmosphere at 37°C and 5% CO_2. All cells were maintained in hgDMEM GlutaMAX supplemented with 10% v/v FBS, penicillin (100 U/mL)-streptomycin (100 μg/mL) and 5 ng/mL human fibroblast growth factor-2 (FGF-2; ProSpec-Tany TechnoGene Ltd., Israel) during all expansion phases.

6.2.3 Experiment 1 - Formation and differentiation of mixed co-culture constructs

At the end of passage 2 (P2), CCs, FPSCs and BMSCs were trypsinised and counted. Cells were suspended in basic chondrogenic medium (basic CDM) consisting of hgDMEM GlutaMAX supplemented with penicillin (100 U/mL)-

streptomycin (100 μg/mL), 100 μg/mL sodium pyruvate, 40 μg/mL L-proline, and 1.5 mg/mL bovine serum albumin (all Sigma-Aldrich). Both FPSCs and BMSCs were mixed together with CCs to form two homogeneous cell suspensions. These mixed cell suspensions were combined with 4% agarose (Type VII) at a ratio of 1:1 at ~40°C, yielding a final gel concentration of 2% and a cell seeding density of ~30 million cells/mL. Agarose-cell suspensions were cast in a stainless steel mold and cored using a 5mm diameter biopsy punch, thus creating solid construct cylinders of 5mm diameter, 2mm thickness. MSCs (either FPSCs or BMSCs) were mixed with CCs in a 0.3:1 ratio so that the final agarose constructs contained 250,000 MSCs and 900,000 CCs. These numbers were chosen to correspond to the structured co-culture study, as explained below. This mixed co-culture agarose formation process was repeated using a higher number of MSCs and the same number of CCs (2.2:1 ratio) resulting in agarose constructs containing 2 million MSCs and 900,000 CCs (seeding density of ~75 million cells/mL). Control agarose constructs were also fabricated using the same dimensions as mixed co-culture constructs. These single-cell type constructs were seeded with either 250,000 MSCs (FPSCs or BMSCs), 2 million MSCs or 900,000 CCs (seeding densities of ~6 million cells/mL, ~50 million cells/mL or ~22 million cells/mL respectively).

All constructs from Experiment 1 were cultured in defined CDM consisting of basic CDM supplemented with 0.25 μg/mL amphotericin B, 1x insulin-transferrin-selenium, 4.7 μg/mL linoleic acid, 50μg/ml L-ascorbic acid-2-phosphate, 100nM dexamethasone (all Sigma-Aldrich), and 10 ng/mL TGF-β3 (ProSpec-Tany TechnoGene Ltd.). Mixed co-culture constructs at the low seeding density (250,000 MSCs & 900,000 CCs) were maintained in 3 mL of defined CDM, with high seeding density mixed constructs (2 million MSCs & 900,000 CCs) maintained in 8 mL. Control constructs (5mm diameter, 2 mm thickness) encapsulated with 250,000 MSCs, 2 million MSCs or 900,000 CCs were maintained in 0.7 mL, 5.5 mL or 2.5 mL of defined CDM respectively. These media volumes were chosen to maintain a constant ratio of media to cells. All constructs from Experiment 1 were cultured for 5 weeks with medium changes every 3 days.

6.2.4 Experiment 2 - Formation and differentiation of structured co-culture constructs

CCs were trypsinised and counted at P2. These cells were suspended in basic CDM and combined with agarose, yielding a final gel concentration of 2% and a cell seeding density of 30 million cells/mL. CC encapsulated agarose hydrogels were then fabricated (5mm diameter, 1.5 mm thickness) with each hydrogel containing 900,000 cells. These constructs were cultured in CDM (2.5 mL) for a week, before being placed and constrained in custom made agarose moulds (5mm diameter) (Figure 6-1), seated in 6-well plates (Fisher Scientific).

Next, 'structured co-cultures' were formed by adding either 250,000, 1 million, or 2 million FPSCs (P2) in 30 μL aliquots of basic expansion medium (hgDMEM GlutaMAX supplemented with 10% v/v FBS and penicillin-streptomycin) to the agarose moulds. FPSCs were left for 12 h to attach to the top surface of CC seeded agarose hydrogels contained within the moulds, after which the wells were filled with additional expansion medium. These structured co-cultures were then maintained in basic expansion medium for 24 h (not supplemented with TGF-β3). After 24 h, medium in each well was replaced with fresh defined CDM supplemented with 10 ng/mL TGF-β3.

Structured co-culture constructs consisting of a self-assembled FPSC layer and underlying CC encapsulated agarose layer, were cultured in defined CDM for 4 weeks. In order to increase nutrient transfer to the tissues, structured co-culture constructs were removed from the confining agarose wells after 7 days. Medium volumes used corresponded to those previously provided for mixed co-cultures in Experiment 1: constructs consisting of 250,000, 1 million, or 2 million FPSCs self-assembled on CC hydrogels were maintained in 3 mL, 5 mL and 8 mL of defined CDM respectively. Control agarose hydrogels (5mm diameter, 1.5 mm thickness) encapsulated with 900,000 CCs were maintained in 2.5 mL of defined CDM.

To determine any differences associated with the source of MSCs, the study was repeated using either 250,000 or 2 million BMSCs (P2) self-assembled on CC agarose hydrogels.

A structured co-culture experiment also took place involving the SA of 4 million FPSCs on top of CC encapsulated hydrogels (maintained in 11 mL media). To determine any effect of the co-culture on the FPSCs, these cells (4 million) were seeded onto transwell cell culture inserts and cultured independently (maintained in 9 mL media). CC control gels (900,000 cells) were also maintained in independent culture (maintained in 2 mL media).

An additional control involved culturing FPSCs and CCs in the same well but with indirect contact between the two types of cells. 2 million FPSCs were seeded onto transwell cell culture inserts. These transwell inserts were then placed in the same well as CC encapsulated agarose constructs (same hydrogels as those used previously, differentiated for 1 week in chondrogenic conditions) and both constructs were left in this physically separated co-culture for 4 further weeks (maintained in 8 mL media).

6.2.5 Fluorescent labelling of cells

For the structured co-culture experiment involving the SA of 2 million FPSCs on top of CC encapsulated agarose hydrogels, additional constructs were formed using fluorescently labelled cells. PKH67 (Green) and PKH26 (Red) fluorescent cell linker kits (Sigma-Aldrich, Dublin, Ireland) were used to label the cell membranes of FPSCs and CCs respectively to allow for subsequent analysis of the spatial distribution of cells within the constructs. Cells were labelled separately according to the manufacturer's protocol. Briefly, expanded cells were detached from culture plastic at P2, washed in serum-free medium and resuspended at the desired concentration in 1 mL of dilution buffer from the manufacturer's labelling kit. The respective cell suspensions were mixed with an equal volume of dilution buffer containing either PKH67 or PKH26 (final concentration $2x10^{-6}$ M) and incubated for 5 min at room temperature. The reaction was terminated by adding 2 mL of FBS, and cells were washed and counted. Structured co-culture constructs were formed as before using the fluorescently labelled FPSCs and CCs. CC encapsulated agarose constructs were cultured for one week before structured co-culture constructs were formed. After 3 weeks of co-culture, constructs were imaged using an Olympus FV-1000 Point-Scanning Confocal Microscope (Southend-on-Sea, UK) at 488 and 546

nm channels. Subsequent analysis involved the use of FV10-ASW 2.0 Viewer software.

6.2.6 Biochemical analysis

The biochemical content of engineered constructs (n=4) was assessed at the beginning and end of experiments. On removal from culture, construct diameter was measured, the wet mass of samples was recorded, and all samples were subsequently frozen at -85 °C for later analyses. Samples were digested with papain (125 μg/mL) in 0.1 M sodium acetate, 5 mM L-cysteine-HCL, 0.05 M EDTA, pH 6 (all Sigma-Aldrich) under constant rotation at 60°C for 18 h. DNA content of constructs was quantified using the Hoechst Bisbenzimide 33258 dye assay (Kim et al., 1988). Proteoglycan content was estimated by quantifying the amount of sulphated glycosaminoglycans (sGAG) in each construct using the dimethylmethylene blue dye binding assay (Blyscan, Biocolor Ltd., Carrickfergus, UK), with a shark chondroitin sulphate standard. Total collagen content of constructs was determined by measuring the hydroxyproline content via the dimethylaminobenzaldehyde and chloramine T assay (Kafienah and Sims, 2004), using a hydroxyproline to collagen ratio of 1:7.69 (Ignat'eva et al., 2007).

6.2.7 Histology and immunohistochemistry

At the end of each experiment, 2 samples per group were fixed in 4% paraformaldehyde (Sigma-Aldrich), dehydrated with a graded series of alcohol and embedded in paraffin. 10μm sections were produced of the cross section perpendicular to the construct face. Sections were stained with 1% alcian blue 8GX (Sigma-Aldrich) in 0.1M HCL for sGAG accumulation, and picrosirius red (Sigma-Aldrich) for collagen accumulation. Collagen type II deposition was identified by immunohistochemical analysis, as described previously (Mesallati et al., 2014a). A mouse monoclonal anti-collagen type II antibody was used as the primary antibody, followed by an anti-mouse IgG biotin conjugate secondary antibody. Positive and negative controls (porcine cartilage and ligament respectively) were included in the immunohistochemistry staining process.

6.2.8 Statistical analysis

Statistical analyses were performed using the software package MINITAB 15.1 (Minitab Ltd., Coventry, UK). Groups were analyzed for significant differences using a general linear model for analysis of variance. Where appropriate, 2 sample t-tests were used. Tukey's test for multiple comparisons was used to compare conditions. A Box-Cox transformation was used to normalize data sets where necessary. Significance was accepted at a level of $p \leq 0.05$. Numerical and graphical results are presented as mean ± standard deviation, with graphical results produced using GraphPad Prism (Version 6.02).

6.3 Results

6.3.1 The impact of a mixed co-culture depends on the source of the MSCs

I first investigated the effects of a mixed co-culture on overall levels of cellular proliferation and matrix accumulation within agarose hydrogels (Figure 6-2). Biochemical results for mixed co-culture agarose groups were compared to monoculture controls for FPSC and BMSC groups at both low (250,000 MSCs) and high (2 million MSCs) seeding densities at week 5. The DNA (μg), sGAG (μg), and collagen (μg) content of CC control and MSC control constructs were summed together to give a cumulative value termed "controls combined", allowing a direct comparison to corresponding "mixed co-culture" constructs (Figures 6-2A-H, M-P),. For sGAG/DNA values (Figures 6-2I-L), "controls combined" was calculated by first summing the sGAG content (μg) of CC control and MSC control constructs, and dividing this by the corresponding total DNA content (μg) of both constructs. This was repeated for collagen/DNA (Figures 6-2Q-T).

For a mixed co-culture of BMSCs and CCs, the total DNA content of the construct was higher than the sum of independent monocultures for both BMSC seeding densities (Figures 6-2C, D). In contrast, the DNA content of the FPSC and CC mixed co-culture was lower than independent controls combined (Figures 6-2A, B). Similar results were found for sGAG accumulation (Figures 6-2E-H), with co-

culture beneficial for BMSCs, but detrimental in the case of FPSCs. It should be noted however, that absolute levels of sGAG accumulation were similar between FPSC-CC and BMSC-CC co-culture groups at both the low MSC seeding density (923.1±57.9 μg vs. 1028.2±42.1 μg respectively) and the high seeding density (2016.8±109.7 μg vs. 1986.5±261 μg respectively). Agarose hydrogels seeded with 2 million FPSCs only accumulated greatest levels of sGAG (2271±175.6 μg), significantly higher ($p<0.0001$) than corresponding BMSC only constructs (724.3±57.6 μg). Absolute levels of sGAG accumulation were also higher with FPSC monoculture constructs at the low seeding density compared to BMSC alone (410.3±16.5 μg vs. 45.3±5.3 μg respectively; $p<0.0001$ significant difference). No major differences were found in sGAG/DNA levels between mixed constructs or controls combined (Figures 6-2I-L).

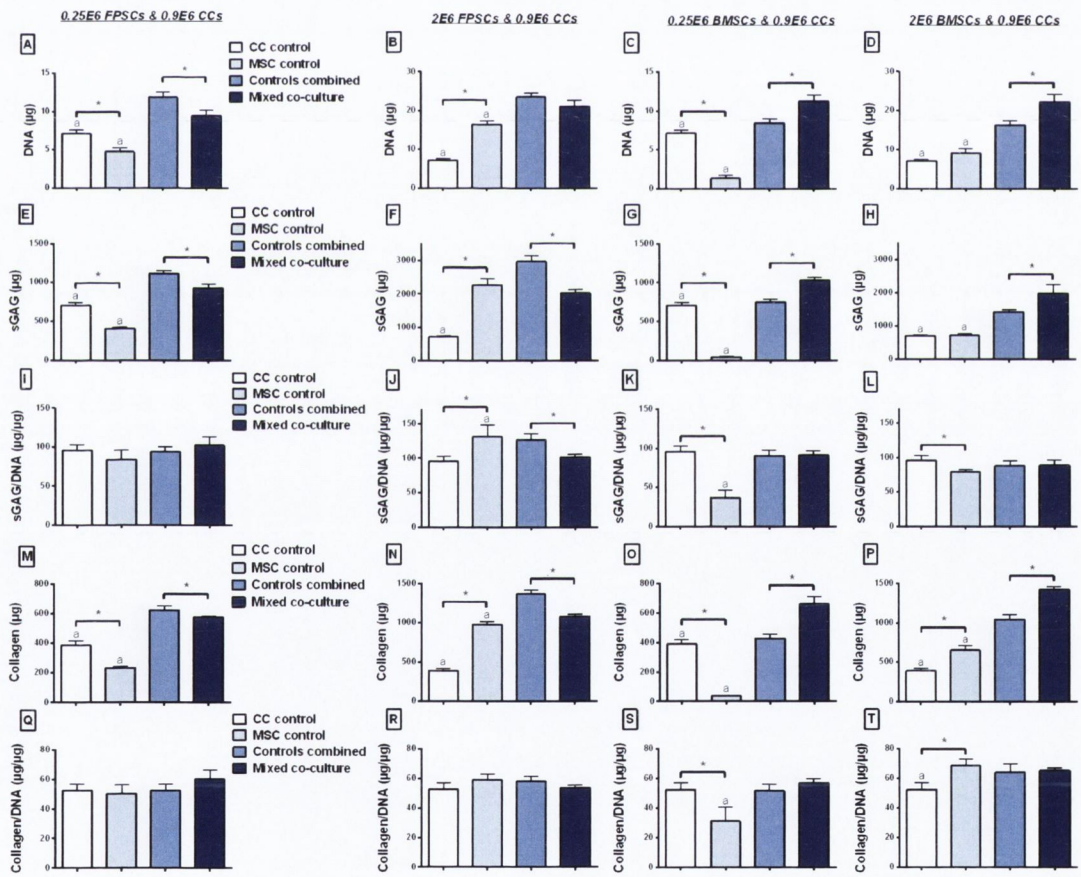

Figure 6-2: (A-D) DNA (μg) accumulated by mixed co-culture constructs and appropriate controls at week 5. (E-H) sGAG (μg). (I-L) sGAG/DNA (μg/μg). (M-P) Collagen (μg). (Q-T) Collagen/DNA (μg/μg). FPSCs, fat pad-derived MSCs; BMSCs, bone marrow-derived MSCs; CCs, chondrocytes. [a] $p<0.05$ versus mixed co-culture. * denotes significant difference with $p < 0.05$.

Results for collagen accumulation (Figures 6-2M-P) were similar to those found for sGAG accumulation, with co-culture beneficial with BMSCs, and detrimental using FPSCs. For both seeding densities, collagen accumulation in BMSC co-culture constructs was significantly greater ($p<0.05$) than corresponding FPSC co-culture constructs (1421.3±39.1 μg and 663.1±48.1 μg for collagen accumulation of BMSC co-culture constructs at high and low MSC seeding densities respectively; 1081.8±29 μg and 578.6±6.2 μg for collagen accumulation of FPSC co-culture constructs at high and low MSC seeding densities respectively). It should be noted that absolute levels of collagen accumulation were higher in FPSC monoculture constructs compared to BMSC monoculture constructs at both the low MSC seeding density (235.9±7.9 μg vs. 38.1±2.9 μg respectively; $p<0.0001$ significant difference) and the high seeding density (979.2±36.3 μg vs. 652.5±55.4 μg respectively; $p<0.0001$ significant difference). No major differences were found in collagen/DNA between mixed constructs or controls combined (Figures 6-2Q-T).

All mixed co-culture and monoculture constructs stained positively for sGAG, and collagen type II (Figure 6-3), apart from constructs seeded with BMSCs at the low MSC seeding density (250,000 BMSCs). FPSC monoculture constructs at the high seeding density (Figure 6-3D) stained most intensely for alcian blue, in agreement with earlier biochemical data.

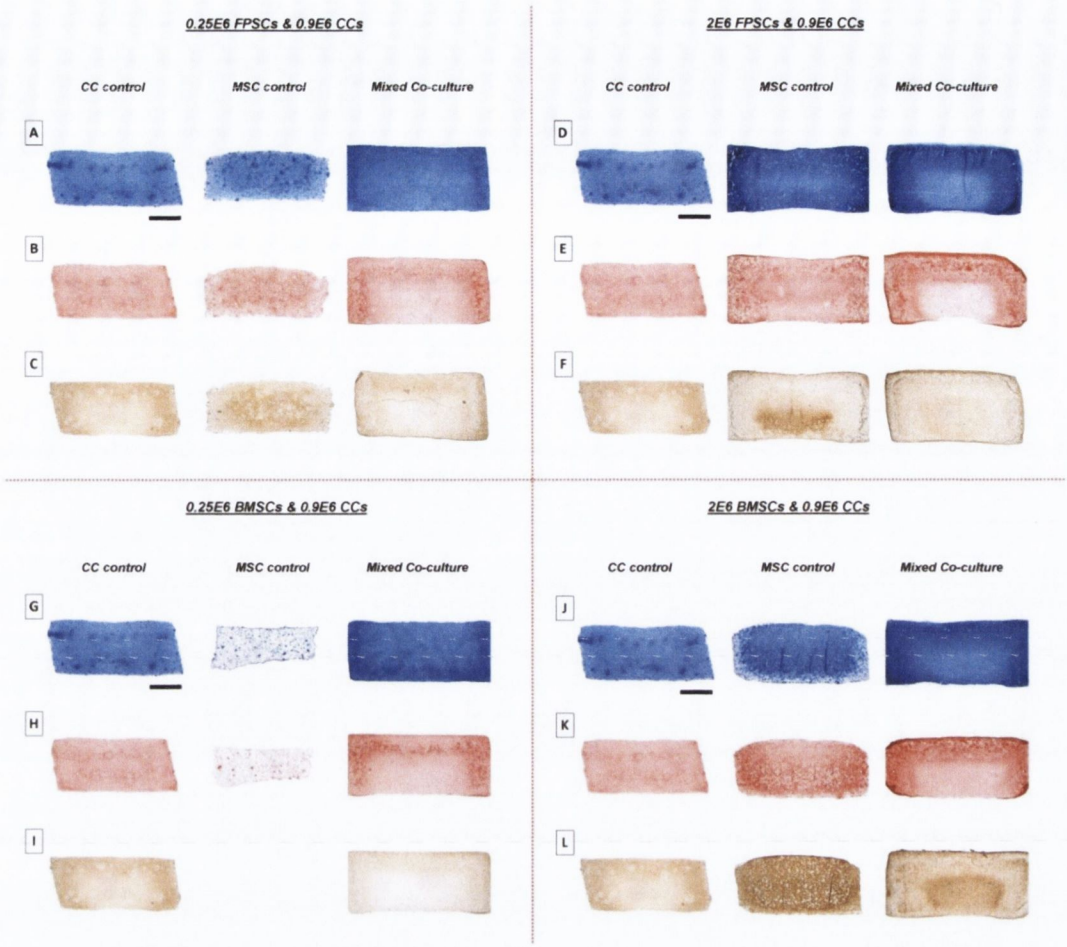

Figure 6-3: Alcian Blue staining for sGAG production, picrosirius red staining for collagen production, and type II collagen immunohistochemistry staining of mixed co-culture constructs and monoculture controls at week 5. (A-C) Low MSC seeding density using FPSCs. (D-F) High MSC seeding density with same. (G-I) Low MSC seeding density using BMSCs. (J-L) High MSC seeding density with same. Scale bar = 1 mm.

6.3.2 A structured co-culture promotes more robust chondrogenesis than a mixed co-culture

The superficial region of articular cartilage contains a slowly proliferating, self-renewing population of progenitor cells. With this in mind, I next sought to compare the effect of randomly mixing cells, as in mixed co-culture, to a structured co-culture, where a hydrogel containing CCs is supported by a superficial layer of 250,000 MSCs (Figure 6-4).

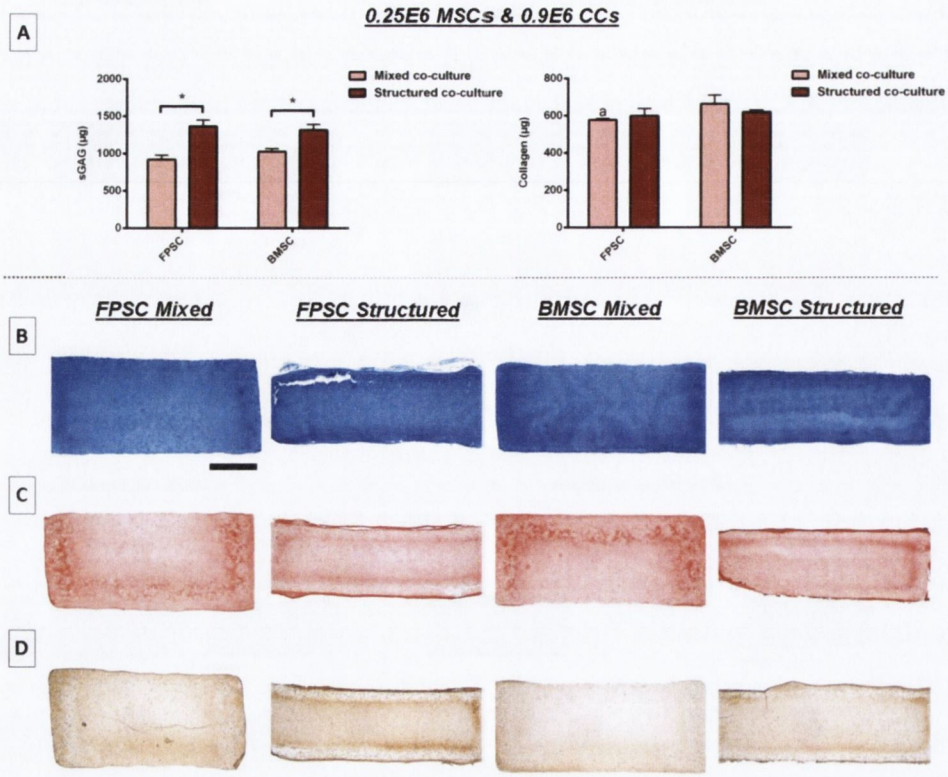

Figure 6-4: Comparison of mixed to structured co-culture for FPSCs and BMSCs at the 0.25E6 MSC seeding density at week 5. (A) sGAG and collagen accumulation (µg). (B) Alcian Blue staining for sGAG production. (C) Picrosirius red staining for collagen production. (D) Type II collagen immunohistochemistry staining. [a] $p<0.05$ versus corresponding BMSC group. * denotes significant difference with $p < 0.05$. Scale bar = 1 mm.

Total sGAG accumulation was higher for structured co-culture constructs compared to corresponding mixed co-culture constructs for both FPSCs and BMSCs (Figure 6-4A). No difference in sGAG accumulation was found between the two stem cell types in either mixed or structured co-culture. No significant differences in collagen accumulation were found between the mixed and structured co-culture (Figure 6-4A). Structured co-culture constructs stained positively for sGAG, collagen, and collagen type II (Figures 6-4B-D).

6.3.3 A superficial layer of MSCs drives proliferation and chondrogenesis of underlying chondrocytes (CCs) in structured co-culture constructs

To confirm that FPSCs were not infiltrating the underlying CC laden agarose hydrogel during structured co-culture, additional structured co-culture constructs were formed using fluorescently labelled FPSCs and CCs. After 3 weeks of co-culture (Figure 6-5), it is clear that the PKH67 (green) stained FPSCs did not significantly infiltrate the underlying agarose hydrogel containing PKH26 (red) stained CCs; a clear boundary was observed between the supporting layer of FPSCs and CC laden agarose construct.

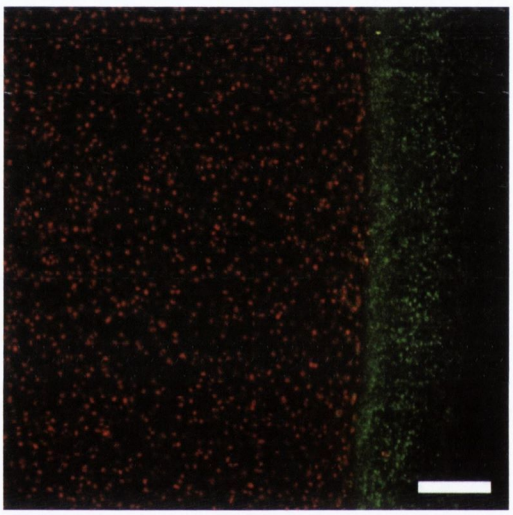

Figure 6-5: Structured co-culture construct with PKH67 (green) stained FPSCs self-assembled on agarose hydrogel containing PKH26 (red) stained chondrocytes at 3 weeks. Scale bar = 100 µm.

I next compared the underlying CC encapsulated agarose layer of structured co-culture constructs (at the low MSC seeding density) to CC only controls by carefully removing the MSCs and the tissue they had laid from the agarose hydrogels at the end of the culture period. CC only controls involved agarose gels seeded with the same number of CCs and cultured in isolation for an identical length of time. A superficial layer of 250,000 FPSCs was found to significantly increase DNA (Figure 6-6A), sGAG (Figure 6-6B), and collagen (Figure 6-6C) accumulation in the underlying layer of CCs compared to CC monoculture controls. The

chondrogenic capacity of CC cells was also improved with structured co-culture as shown by increased sGAG/DNA (Figure 6-6D) and collagen/DNA (Figure 6-6E).

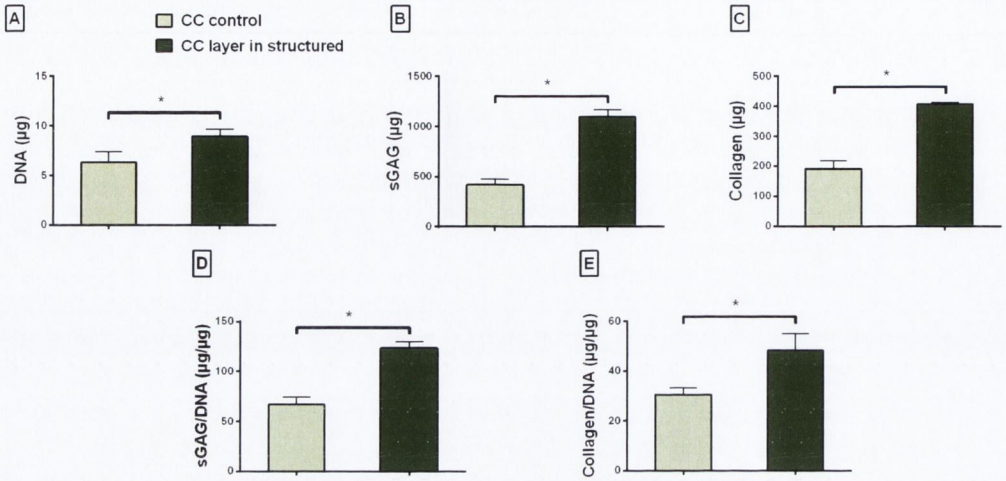

Figure 6-6: Comparison of structured co-culture chondrocyte (CC) layers (0.25E6 FPSC seeding density) to CC only controls at week 5. (A) DNA accumulation (µg). (B) sGAG accumulation (µg). (C) Collagen accumulation (µg). (D) sGAG/DNA (µg/µg). (E) Collagen/DNA (µg/µg). * denotes significant difference with $p < 0.05$. Note: DNA content of CC gels at day 0 was 5.3±0.8 µg.

Similar results were observed for structured co-culture CC layers where the superficial layer contained 250,000 BMSCs (Figure 6-7). As before, progenitor cells were found to drive overall matrix accumulation in the underlying layer of CCs, and improve chondrogenesis on a per cell basis.

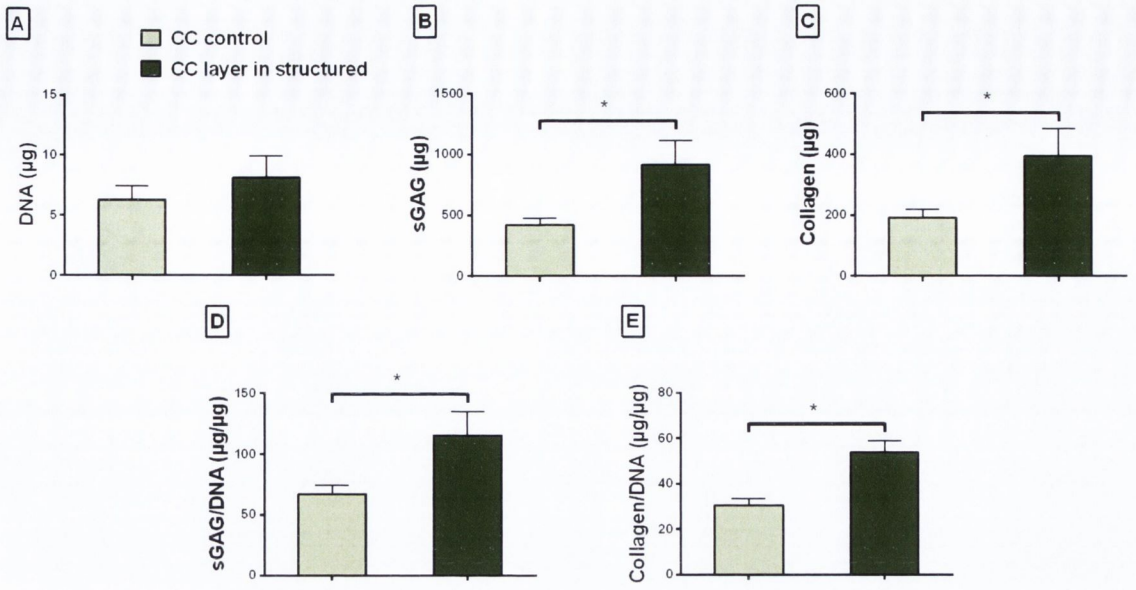

Figure 6-7: Comparison of structured co-culture chondrocyte (CC) layers (0.25E6 BMSC seeding density) to CC only controls at week 5. (A) DNA accumulation (µg). (B) sGAG accumulation (µg). (C) Collagen accumulation (µg). (D) sGAG/DNA (µg/µg). (E) Collagen/DNA (µg/µg). * denotes significant difference with $p < 0.05$. Note: DNA content of CC gels at day 0 was 5.3±0.8 µg.

6.3.4 The beneficial effects of a structured co-culture are not accentuated with increases in the number of MSCs

Having determined that a relatively low number of MSCs can approximately double the levels of matrix accumulated in the underlying CC gel in a structured co-culture, I next sought to investigate the effect of increasing MSC number (in the superficial layer) on the underlying CCs (Figures 6-8:6-11). Increasing the number of FPSCs in a structured co-culture increased proliferation of the underlying CCs, as evident by increases in the DNA content of the hydrogel (Figure 6-8A). No increase in CC proliferation was observed for FPSC seeding densities exceeding 1 million cells. Collagen accumulation also increased (Figure 6-8C) as the number of supporting FPSCs increased from 250,000 to 1 million cells. Total sGAG accumulation within CC seeded agarose hydrogels was not significantly affected by the number of overlying FPSCs (Figure 6-8B), although sGAG/DNA levels were found to drop in

the CC layer for increasing numbers of supporting FPSCs (Figure 6-8D). Indeed, for high MSC seeding densities, no benefit was observed for a structured co-culture compared to a mixed co-culture (see Appendix Figure S8). There were no dramatic differences in the staining of sGAG or collagen between the different FPSC structured co-culture groups (Figure 6-9).

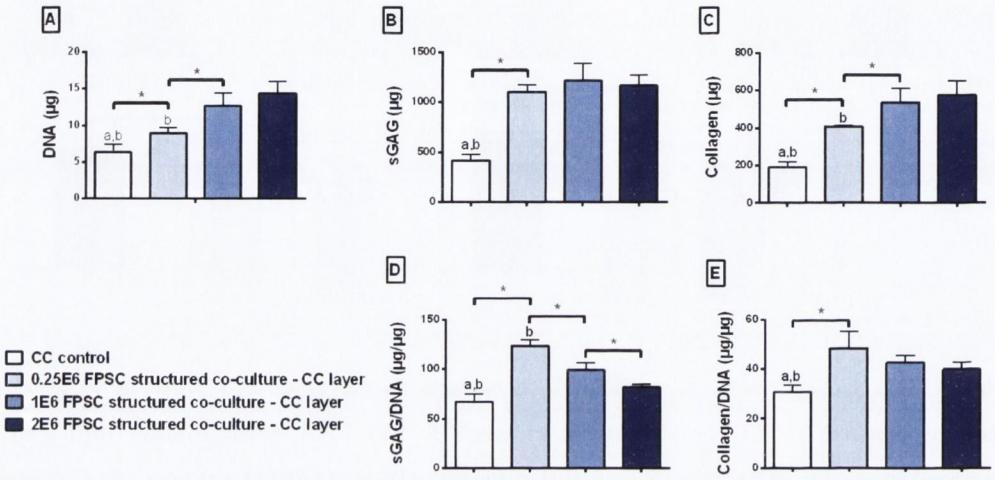

Figure 6-8: Comparison of structured co-culture chondrocyte (CC) layers (0.25E6, 1E6 or 2E6 FPSC seeding density) to CC only controls at week 5. (A) DNA accumulation (µg). (B) sGAG accumulation (µg). (C) Collagen accumulation (µg). (D) sGAG/DNA (µg/µg). (E) Collagen/DNA (µg/µg). [a] $p<0.05$ versus 1E6 group. [b] $p<0.05$ versus 2E6 group. * denotes significant difference with $p < 0.05$.

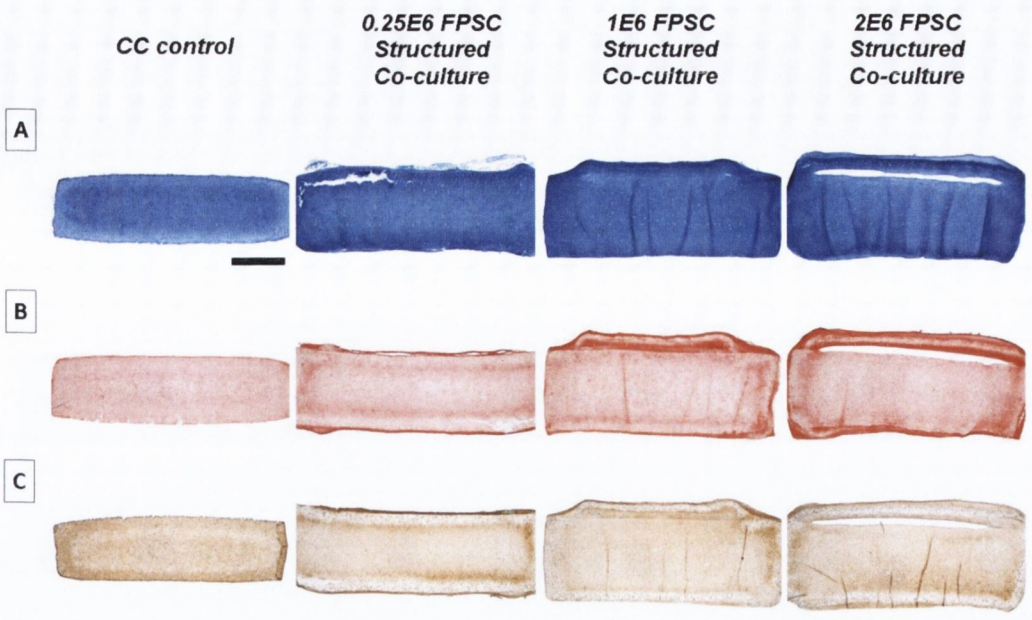

Figure 6-9: Comparison of structured co-culture constructs (0.25E6, 1E6 or 2E6 FPSC seeding density) to chondrocyte (CC) only controls at week 5. (A) Alcian Blue staining. (B) Picrosirius red staining. (C) Type II collagen immunohistochemistry staining. Scale bar = 1 mm.

Increasing the number of BMSCs in the superficial layer of the structured CC-BMSC co-culture constructs had no significant effect on either DNA, sGAG or collagen accumulation (Figures 6-10, 6-11).

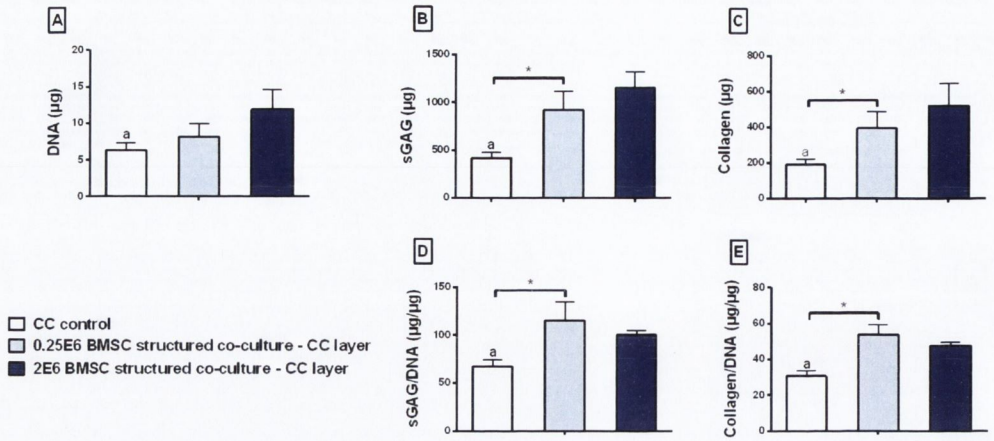

Figure 6-10: Comparison of structured co-culture chondrocyte (CC) layers (0.25E6 or 2E6 BMSC seeding density) to CC only controls at week 5. (A) DNA accumulation (µg). (B) sGAG accumulation (µg). (C) Collagen accumulation (µg). (D) sGAG/DNA (µg/µg). (E) Collagen/DNA (µg/µg). ^{a} $p<0.05$ versus 2E6 group. * denotes significant difference with $p < 0.05$.

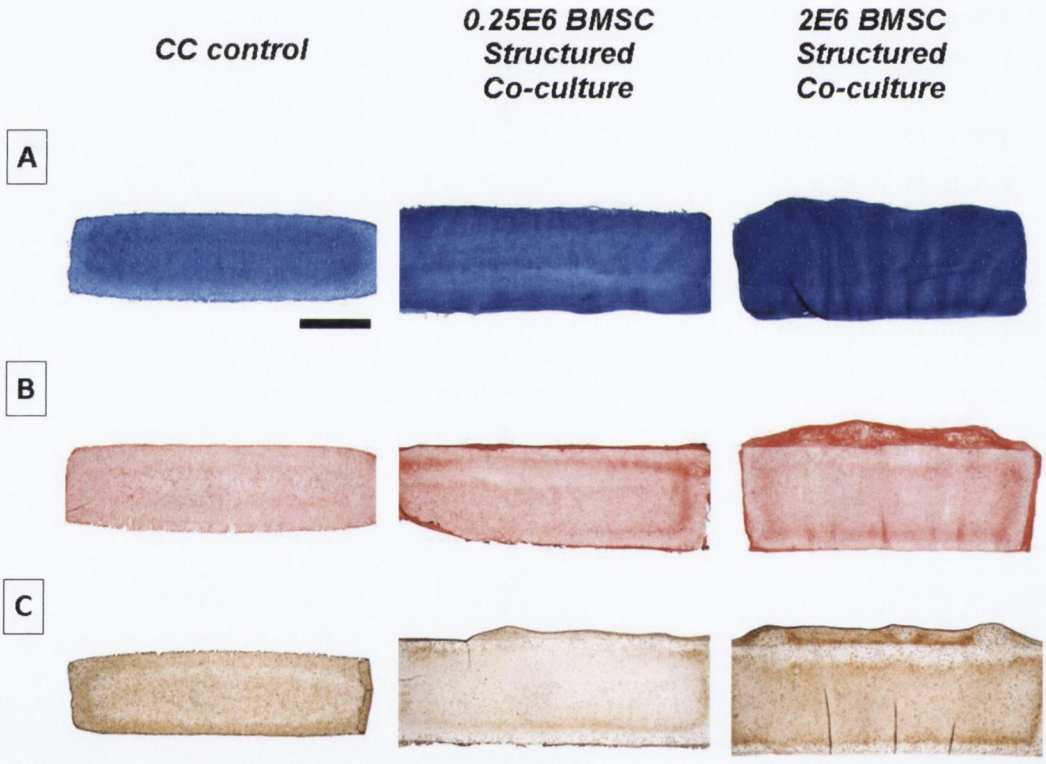

Figure 6-11: Comparison of structured co-culture constructs (0.25E6 or 2E6 BMSC seeding density) to chondrocyte (CC) only controls at week 5. (A) Alcian Blue staining. (B) Picrosirius red staining. (C) Type II collagen immunohistochemistry staining. Scale bar = 1 mm.

6.3.5 Close proximity between chondrocytes and MSCs is not a key component of a structured co-culture

Having established that structured co-culture of FPSCs and CCs leads to an increase in CC proliferation and matrix synthesis (Figure 6-8), I next sought to determine if close physical proximity between the two cell types was needed for this to occur. 2 million FPSCs were consequently seeded onto transwell cell culture inserts and placed in the same culture dish well as CC encapsulated agarose constructs. The two constructs were placed on opposite sides of the well and separated by culture medium.

After 4 weeks of culture, it was found that FPSCs were driving CC proliferation even without close proximity of constructs (Figure 6-12A), with separated co-culture CC gels accumulating significantly more DNA than CC controls cultured in isolation. However, greater proliferation of CCs was observed in physically close structured co-cultures compared to physically separate co-cultures. A physically separated co-culture also led to increased sGAG and collagen accumulation in CC hydrogels compared to CC controls cultured in isolation (Figures 6-12B, C). There was no significant difference in total matrix accumulation between structured and separated co-culture CC gels, although matrix synthesis on a per cell basis (sGAG/DNA and collagen/DNA) was higher in the separated CC gels (Figures 6-12D, E). In agreement with these biochemical assays, co-culture CC gels stained more intensely for sGAG and collagen than isolated CC controls (Figure 6-13).

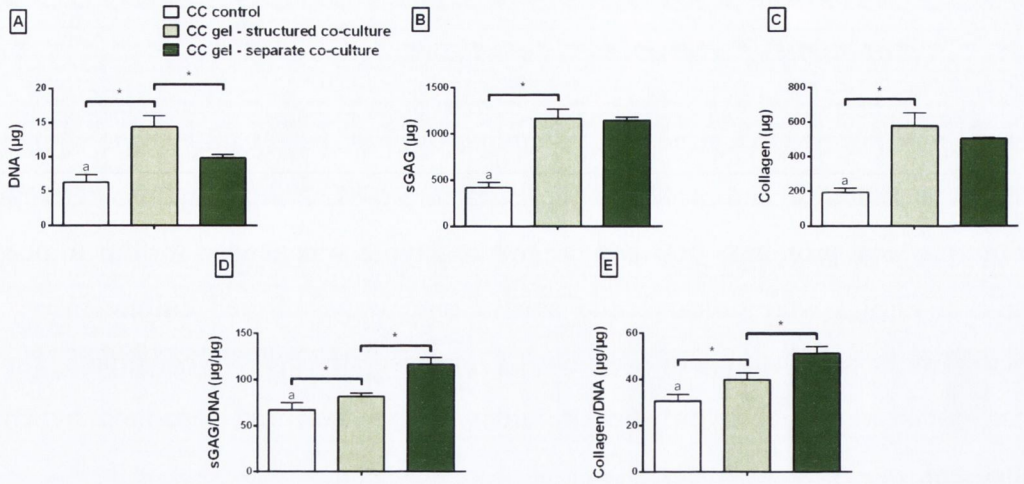

Figure 6-12: Chondrocyte (CC) only controls, structured co-culture CC layers and separated co-culture CC gels at week 5. (A) DNA accumulation (µg). (B) sGAG accumulation (µg). (C) Collagen accumulation (µg). (D) sGAG/DNA (µg/µg). (E) Collagen/DNA (µg/µg). [a] $p<0.05$ versus separated co-culture CC gel. * denotes significant difference with $p < 0.05$.

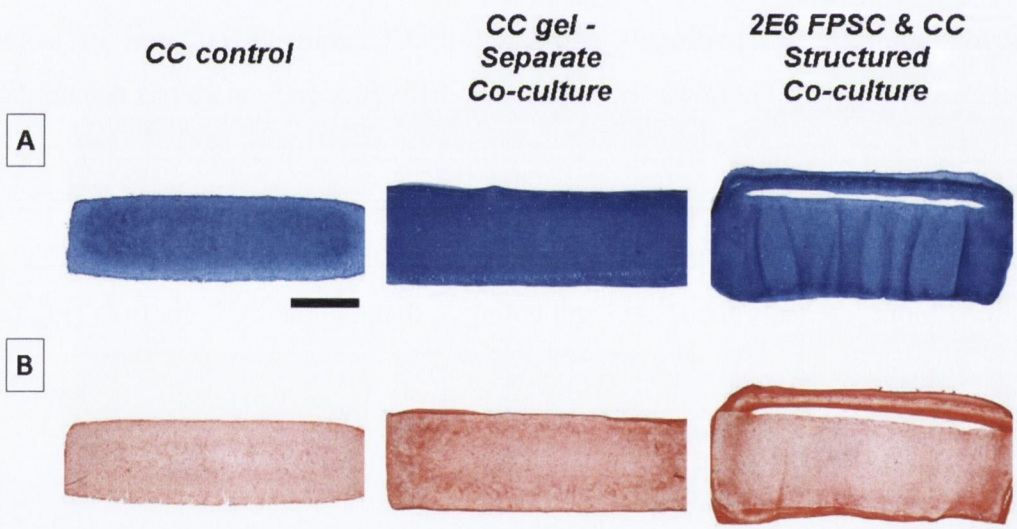

Figure 6-13: Chondrocyte (CC) only controls, separated co-culture CC gels and structured co-culture constructs (2E6 FPSC seeding density) at week 5. (A) Alcian Blue staining. (B) Picrosirius red staining. Scale bar = 1 mm.

6.3.6 A structured co-culture has little effect on the population of MSCs

The final arm of the experiment involved analysis of the MSC self-assembled layer in structured co-culture constructs. 4 million FPSCs were self-assembled on CC laden hydrogels and cultured for 4 weeks (Figure 6-14). As a control, FPSCs were self-assembled in individual transwell cell culture inserts and cultured in isolation. Structured co-culture was found to have very little effect on the FPSC self-assembled layer. DNA, sGAG and collagen accumulation within the self-assembled layer were all similar to independently cultured controls (Figures 6-14A-C). There was a trend towards increased sGAG synthesis, and significantly greater collagen synthesis in the structured FPSCs compared to controls (Figures 6-14D, E). Results in the structured CC layer (Figures 6-14F-H) were similar to before with increased CC proliferation, sGAG and collagen accumulation compared to CC only controls.

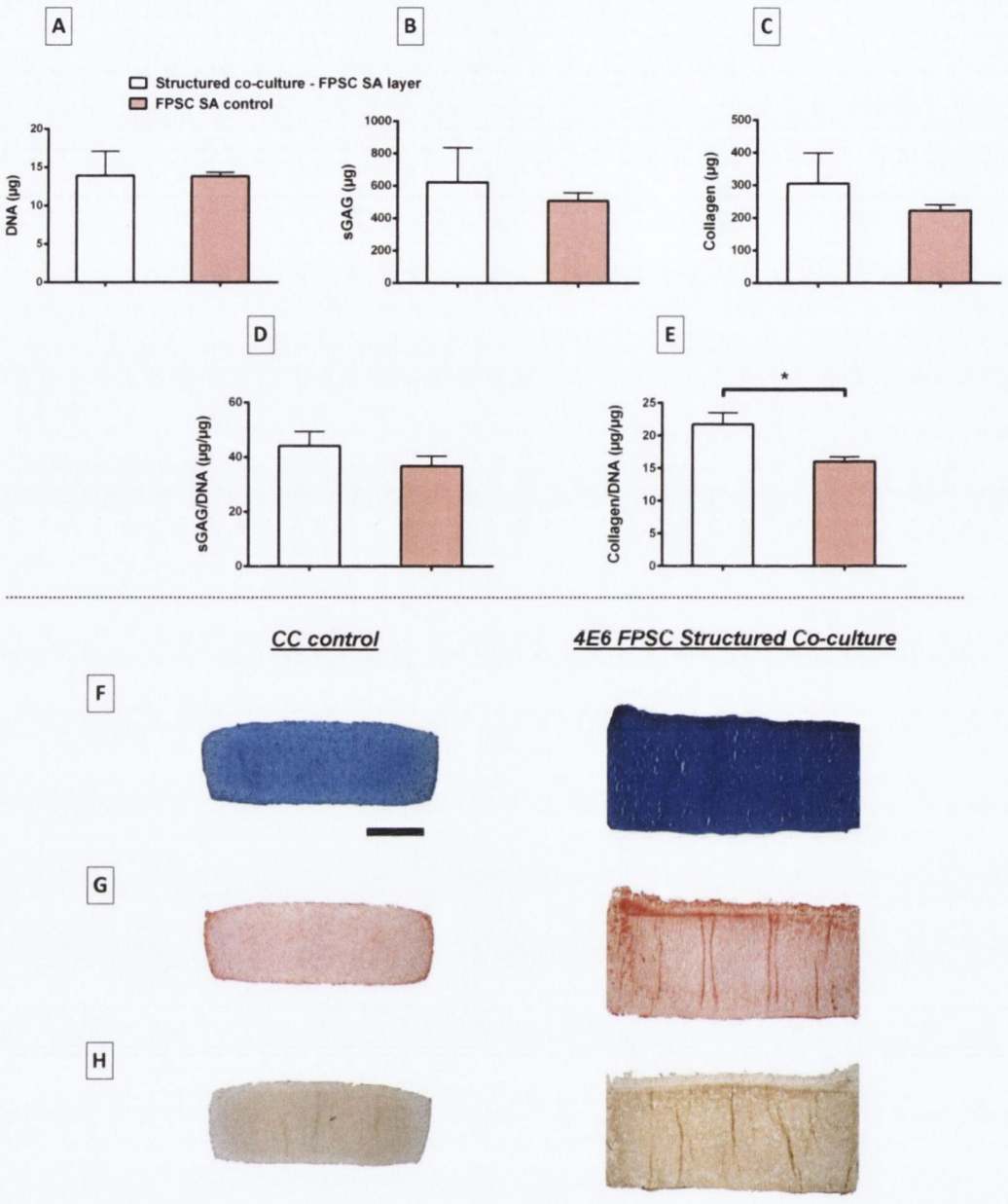

Figure 6-14: Comparison of structured co-culture self-assembly (SA) layers (4E6 FPSCs) to transwell SA controls at week 5. (A) DNA accumulation (µg). (B) sGAG accumulation (µg). (C) Collagen accumulation (µg). (D) sGAG/DNA (µg/µg). (E) Collagen/DNA (µg/µg). (F) Alcian Blue staining of CC control and structured co-culture construct at week 5. (G) Picrosirius red staining. (H) Type II collagen immunohistochemistry staining. * denotes significant difference with $p < 0.05$. Scale bar = 1 mm.

6.4 Discussion

The objective of this study was to engineer more articular-like cartilaginous grafts by recapitulating aspects of normal articular cartilage growth where a pool of superficial cells drives the development of the tissue. This involved self-assembling a layer of supporting MSCs (either fat pad-derived or bone marrow-derived stem cells) on top of chondrocyte (CC) laden agarose hydrogels. These structured co-cultures were compared to mixed co-cultures, where MSCs and CCs were combined, mixed and then seeded into a single agarose construct. A mixed co-culture of FPSCs and CCs was found to decrease proliferation and accumulation of sGAG and collagen when compared to appropriate single cell only controls. In contrast, a mixed co-culture of BMSCs and CCs led to increased proliferation and sGAG and collagen accumulation compared to controls. A structured co-culture of MSCs (250,000 cells) and CCs (900,000 cells) led to greater sGAG accumulation than a mixed co-culture for both FPSCs and BMSCs. The superficial layer of stem cells in structured co-culture constructs was found to drive proliferation of underlying CCs and enhance the biochemical development of the engineered tissue. Increasing the number of MSCs in the superficial layer of structured co-culture constructs did not have a dramatic effect on the underlying CCs in terms of overall sGAG and collagen accumulation. Interestingly, even if MSCs and CC were physically separated in the same culture well, increased proliferation and chondrogenic differentiation was still observed in the CC laden agarose hydrogels compared to monoculture controls.

As has previously been shown in agarose monoculture, FPSCs were found to synthesize higher amounts of sGAG and collagen compared to BMSCs alone (Vinardell et al., 2011, Vinardell et al., 2012b). In a mixed co-culture with CCs, FPSCs and BMSCs also appeared to respond differently. A mixed co-culture of BMSCs and CCs was found to drive proliferation, whilst reduced proliferation was observed with FPSCs in co-culture compared to monoculture. The concept of MSCs secreting a variety of cytokines and growth factors that have both paracrine and autocrine activities is well established (Caplan and Dennis, 2006) (Wu et al., 2012, Wu et al., 2013a). It has been demonstrated that BMSCs secrete factors such as

fibroblast growth factor-1 (FGF-1) which can lead to increased proliferation of co-cultured CCs (Wu et al., 2013b), potentially explaining the results observed in this study. The finding that a mixed culture of FPSCs and CCs was not beneficial to construct development might suggest that FPSCs do not secrete factors that drive proliferation of CCs, however in a structured co-culture FPSCs were found to drive proliferation of underlying CCs (PKH26/67 fluorescent labelling of cells also confirmed that the increase in DNA accumulation within the underlying CC seeded agarose hydrogels was not due to FPSCs infiltrating the CC layer). Furthermore, both FPSCs and BMSCs enhanced matrix synthesis of CCs (on a per cell basis) in a structured co-culture, demonstrating that both MSC types can release factors to drive both CC proliferation and increased sGAG and collagen synthesis. Previous studies have also shown that both adipose-derived stem cells and BMSCs have a similar trophic effect on CCs resulting in significant proliferation of the latter in pellet co-culture (Wu et al., 2012, Acharya et al., 2012). Another explanation for these results may be differences in nutrient availability in the two mixed co-cultures that are leading to alterations in CC proliferation and matrix synthesis. Given that FPSCs are more biosynthetically active than BMSCs, as evident by generally higher levels of matrix accumulation in monoculture, it could be that too many cells are competing for limited nutrient resources in FPSC mixed co-culture groups, thereby lowering cell viability and/or proliferation. The fact that this does not happen in FPCS-CC structured co-culture constructs could be due to the phenotype of FPSCs being different when self-assembled on the surface of gels as opposed to when encapsulated within the body of gels. This would likely alter the FPSC metabolic phenotype, potentially altering nutrient availability to the underlying CC cells of structured co-culture constructs.

Structured co-cultures, at the appropriate cell density, led to greater sGAG accumulation than a mixed co-culture for both sources of MSCs. This could be due to an altered MSC phenotype in self-assembly increasing nutrient availability to the underlying CCs of structured co-culture constructs. Greater MSC-MSC communication in structured co-culture due to their close physical proximity may be important for maximizing the trophic effect they exert. Also, CC-MSC signalling is likely affected by the physical location of both cell populations. Perhaps localising

the MSCs to the surface of the graft provides them with cues that again maximise their trophic effect. Future studies should try to unravel this.

Interestingly, direct contact between CCs and MSCs was not integral to a structured co-culture, as separating the two cell types in the same 6 well plate led to similar (although not comparable) results, with increased CC proliferation and matrix synthesis compared to monoculture controls. Previous studies have shown separated co-culture of MSCs and CCs to have no effect on CC proliferation or matrix synthesis (Bian et al., 2011, Acharya et al., 2012). In fact, one study has even shown that a noncontact co-culture of MSCs and CCs can lead to significantly less deposition of cartilaginous ECM, including sGAG and collagen type II by 3D cultured CCs compared to controls (Xu et al., 2013). It may be that our transwell self-assembly constructs are releasing higher concentrations of soluble factors in separated co-culture than MSCs in other studies. The structured co-culture setup led to greater proliferation of CCs than separated co-culture; possibly due to the shorter distance soluble factors had to travel between cells. However, structured co-culture resulted in lower sGAG and collagen synthesis on a per cell basis compared to separated co-culture, with no significant differences observed between the two methods in terms of overall sGAG and collagen accumulation. The fact that structured co-culture CC gels were confined in agarose moulds and also covered with a layer of MSCs could have contributed to lower matrix synthesis levels in the constructs, as this experimental set-up would be more likely to lead to nutrient transport limitations.

An implication of this finding is that perhaps the optimal route to engineering functional cartilage is to use MSCs as a feeder layer to secrete factors which drive proliferation and chondrogenesis in CCs physically separated from MSCs. An advantage of this approach would be optimal nutrient transport to CCs. Further work is required to identify which exact factors MSCs are secreting to drive this increase in CC proliferation and chondrogenic differentiation. Microarray analysis could be used to identify genes regulated by co-culture of CCs and MSCs (Wu et al., 2013b). As mentioned previously, MSCs have been shown to increase FGF-1 secretion in co-culture with CCs, which leads to enhanced CC proliferation (Wu et al., 2013b). Other soluble factors detected in the supernatant of MSC-CC co-

culture constructs include TGF-β1, IGF-1 and BMP-2 (Liu et al., 2010) which have been shown to affect cell proliferation (Richter, 2009, Shu et al., 2011, Li et al., 2011). Indeed, BMP-2 has been shown to promote chondrocyte proliferation *via* the Wnt/β-catenin signalling pathway (Li et al., 2011).

Increasing the number of MSCs in the superficial self-assembled layer of structured co-culture constructs was found to increase proliferation in the underlying CC layer. This was likely due to increasing MSC numbers releasing greater levels of certain soluble factors driving CC proliferation. However, a consequence of increasing the number of supporting MSCs and the associated increase in CC proliferation was a decrease in matrix synthesis on a per cell basis. This resulted in only small differences in the overall levels of sGAG and collagen accumulation in the CC layers of the structured co-culture constructs supported by different numbers of MSCs. Diminished biosynthetic activity in high density agarose cultures may again be due to mass transport limitations.

6.5 Concluding Remarks

In conclusion, assembling MSCs onto CC laden hydrogels dramatically enhances the biochemical development of the engineered tissue, with the superficial layer of stem cells driving both chondrocyte proliferation and cartilage tissue development. The results of this study point to the benefit of looking to developmental processes for inspiration when developing tissue engineering strategies.

In addition, a mixed co-culture of BMSCs and CCs led to increased proliferation and sGAG and collagen accumulation within tissue engineered constructs. The next and final chapter aims to bring all the previous work of the thesis together, in order to tissue engineer a scaled-up, anatomically shaped osteochondral construct suitable for partial or total joint resurfacing (using as few chondrocytes as possible, due to clinical restrictions associated with this cell type). As mentioned previously, a well-documented limitation associated with the use of MSCs for cartilage tissue engineering is their failure to form phenotypically stable cartilage tissue *in vivo* (Pelttari et al., 2006, Pelttari et al., 2008b, Farrell et al., 2009, Farrell et al., 2011, Vinardell et al., 2012b). As part of the next chapter, two

strategies will be explored to engineer phenotypically stable cartilage tissue *in vivo* using stem cells. First, it will be investigated whether cartilage engineered *in vitro* using a scaffold-free or self-assembly approach can lead to the development of more phenotypically stable cartilage *in vivo*. Secondly, it will be investigated whether a co-culture of CCs and either BMSCs or FPSCs can engineer a layer of phenotypically stable articular cartilage as part of an osteochondral construct *in vivo*.

7 Tissue engineering scaled-up, anatomically shaped osteochondral constructs for joint resurfacing

7.1 Introduction

Approximately 714,000 people in Ireland currently suffer from the degenerative disease osteoarthritis (OA), with 18% of patients less than 55 years old (Source: Arthritis Ireland). Treatment options for OA are limited to surgical replacement of the diseased joint with a metal and polyethylene prosthesis (Guilak, 2010). While this procedure is well established, it is not without its limitations and failures are not uncommon (Pavone et al., 2001, Ma et al., 2005, Browne et al., 2010, Kerin et al., 2011, Seil and Pape, 2011). Joint replacement prostheses also have a finite lifespan, making them unsuitable for the growing population of younger and more active patients requiring treatment for OA (Kurtz et al., 2009, Guilak, 2010, Keeney et al., 2011). In recent years there has been increased interest in the use of cell and tissue engineering based therapies for the treatment of focal cartilage defects (Brittberg et al., 1994, Temenoff and Mikos, 2000b). While significant progress has been made in this field, realizing an efficacious therapeutic option for the treatment of OA remains elusive and is considered to be one of the greatest challenges in the field of orthopaedic medicine. The overall aim of this study was to tissue engineer a scaled-up, anatomically shaped osteochondral construct suitable for partial or total joint resurfacing. Given that OA affects multiple tissues in the diseased joint, including the articular cartilage and underlying subchondral bone, the first objective of this study was to develop a scalable approach to simultaneously engineer both of these tissue types within an osteochondral construct.

A number of different strategies have been developed to engineer osteochondral constructs. These include the development of bi-phasic or multi-layered scaffolds (Gao et al., 2001, Oliveira et al., 2006, Mano and Reis, 2007,

Martin et al., 2007, Theodoropoulos et al., 2011, St-Pierre et al., 2012, Rodrigues et al., 2012, Sheehy et al., 2013), physical conditioning of tissues through the use of novel bioreactors (Wang et al., 2004, Wendt et al., 2005, Mahmoudifar and Doran, 2005, Grayson et al., 2010, Rodrigues et al., 2011) and spatial growth factor or gene delivery systems (Mason et al., 1998, Guo et al., 2009, Guo et al., 2010, Chen et al., 2011, Re'Em et al., 2012, Santo et al., 2013a, Santo et al., 2013b). It has also been possible to engineer scaffolds and grafts mimicking the geometrical form of articular surfaces (Hung et al., 2003, Alhadlaq et al., 2004, Alhadlaq and Mao, 2005, Lee et al., 2009, Lee et al., 2010, Ding et al., 2013), however tissue engineering anatomically accurate osteochondral constructs of scale remains a significant challenge in the field.

It is well documented that chondrogenically primed bone marrow-derived mesenchymal stem cells (BMSCs) have an inherent tendency to become hypertrophic and undergo endochondral ossification *in vivo* (Pelttari et al., 2006, Farrell et al., 2009, Scotti et al., 2010, Janicki et al., 2010, Farrell et al., 2011, Scotti et al., 2013). This is a major limitation for cartilage tissue engineering, but this property of MSCs can be leveraged for large bone defect regeneration (Harada et al., 2014, van der Stok et al., 2014). Previous studies have demonstrated that cartilaginous constructs engineered using BMSCs embedded in a hydrogel will proceed along an endochondral pathway following subcutaneous implantation (Dickhut et al., 2008, Vinardell et al., 2012b). Indeed, previous work in our lab has shown that it is possible to engineer osteochondral constructs by spatially regulating endochondral ossification within bi-layered agarose cartilaginous grafts (Sheehy et al., 2013). However, BMSC seeded agarose constructs were found to not degrade *in vivo*, thereby limiting the utility of this hydrogel for endochondral bone tissue engineering applications. It was hypothesised in this work that a BMSC seeded alginate hydrogel could support endochondral bone formation within an osteochondral construct. This was motivated by the fact that alginate hydrogels are commonly used for *in vitro* cartilage tissue engineering purposes (Ma et al., 2003, Mehlhorn et al., 2006, Shen et al., 2009, Igarashi et al., 2010, Lee and Mooney, 2012, de Vries-van Melle et al., 2014), and furthermore, have been combined with

MSCs and/or different growth factors for use in bone regeneration (Simmons et al., 2004, Weng et al., 2006, Kolambkar et al., 2011a, Kolambkar et al., 2011b).

Another key challenge in developing a biological implant for the treatment of degenerative joint diseases is engineering phenotypically stable cartilaginous tissues of sufficient scale to resurface the entire joint. This is particularly challenging in the context of OA, as only a limited number of therapeutically useful chondrocytes (CCs) can be isolated from diseased joints (Kock et al., 2012), and because CCs in OA cartilage produce cartilage-degrading enzymes, such as MMP13 and aggrecanases (Van der Kraan and Van den Berg, 2012). Furthermore, the expansion of CCs *in vitro* to obtain sufficient numbers of cells can lead to de-differentiation of cells towards a more fibroblast-like phenotype (Benya and Shaffer, 1982, Diaz-Romero et al., 2005). Also, there is evidence suggesting an age-related loss in the chondrogenic capacity of culture expanded CCs (Barbero et al., 2004). As shown in previous chapters of this thesis, mesenchymal stem cells (MSCs) can be used as an alternative to CCs for cartilage tissue engineering (Mesallati et al., 2014b). MSCs possess the ability to proliferate extensively *in vitro* while maintaining their multipotent differentiation potential (Pittenger et al., 1999), making them an almost ideal cell type for engineering scaled-up cartilaginous constructs large enough to resurface an entire joint. However, as outlined previously, cartilage tissue engineered using MSCs has been shown to become hypertrophic and undergo endochondral ossification *in vivo* (Farrell et al., 2009, Scotti et al., 2010, Janicki et al., 2010, Farrell et al., 2011, Scotti et al., 2013, Yang et al., 2013). As part of this study, two strategies were explored to engineer phenotypically stable cartilage tissue *in vivo* using stem cells. I first asked whether cartilage engineered *in vitro* using a scaffold-free or self-assembly approach (which has previously been shown to lead to the development of more hyaline cartilage-like tissue *in vitro* compared to hydrogel encapsulation) could lead to the development of more phenotypically stable cartilage *in vivo*. Secondly, based on previous studies that demonstrate that co-culture of CCs and MSCs enhances cartilage matrix synthesis (Tsuchiya et al., 2004, Bian et al., 2011, Wu et al., 2011, Acharya et al., 2012, Wu et al., 2012, Meretoja et al., 2012) and suppresses markers of MSC hypertrophy (such as type X collagen expression) *in vitro* (Fischer et al., 2010,

Cooke et al., 2011, Bian et al., 2011, Aung et al., 2011, Acharya et al., 2012, Kang et al., 2012), I asked whether a co-culture of CCs and either BMSCs or infrapatellar fat pad-derived stem cells (FPSCs) could be used to engineer a layer of phenotypically stable articular cartilage as part of an osteochondral construct *in vivo*.

The final objective of the study was to scale-up the proposed approach in order to tissue engineer an anatomically shaped osteochondral construct which could potentially replace an entire diseased joint. I hypothesised that this would be possible by combining scaled-up, anatomically shaped BMSC seeded alginate tissues (formed from moulds fabricated by rapid prototyping) with self-assembled cartilage tissue (formed through a co-culture of CCs and BMSCs).

7.2 Materials and Methods

7.2.1 Experimental Design

The first objective of the study was to determine the combination of cell and scaffold type that could be used to tissue engineer phenotypically stable cartilage overlaying functional bone. Bilayered constructs were formed as shown in Figure 7-1 (further details provided below). The bottom layer of bilayered constructs, termed the endochondral or osseous layer, consisted of bone marrow derived mesenchymal stem cells (BMSCs) seeded within an alginate hydrogel. The top layer, termed the chondral layer, consisted of either an agarose hydrogel seeded with cells or a layer of 'self-assembled' or 'scaffold-free' tissue (formed from a high density layer of cells). To determine the effect of cell source on formation and development of cartilage within the top chondral layer of the osteochondral construct, these layers were formed using either chondrocytes (CCs) alone, BMSCs alone, infrapatellar fat pad-derived stem cells (FPSCs) alone, a BMSC & CC co-culture (4:1 ratio) or a FPSC & CC co-culture (4:1 ratio) using either a self-assembly approach or agarose hydrogel encapsulation. Bi-layered constructs were maintained *in vitro* for 6 weeks in a chemically defined chondrogenic medium containing 10ng/mL TGF-β3.

Constructs were subsequently implanted subcutaneously into the back of nude mice for a further 6 weeks.

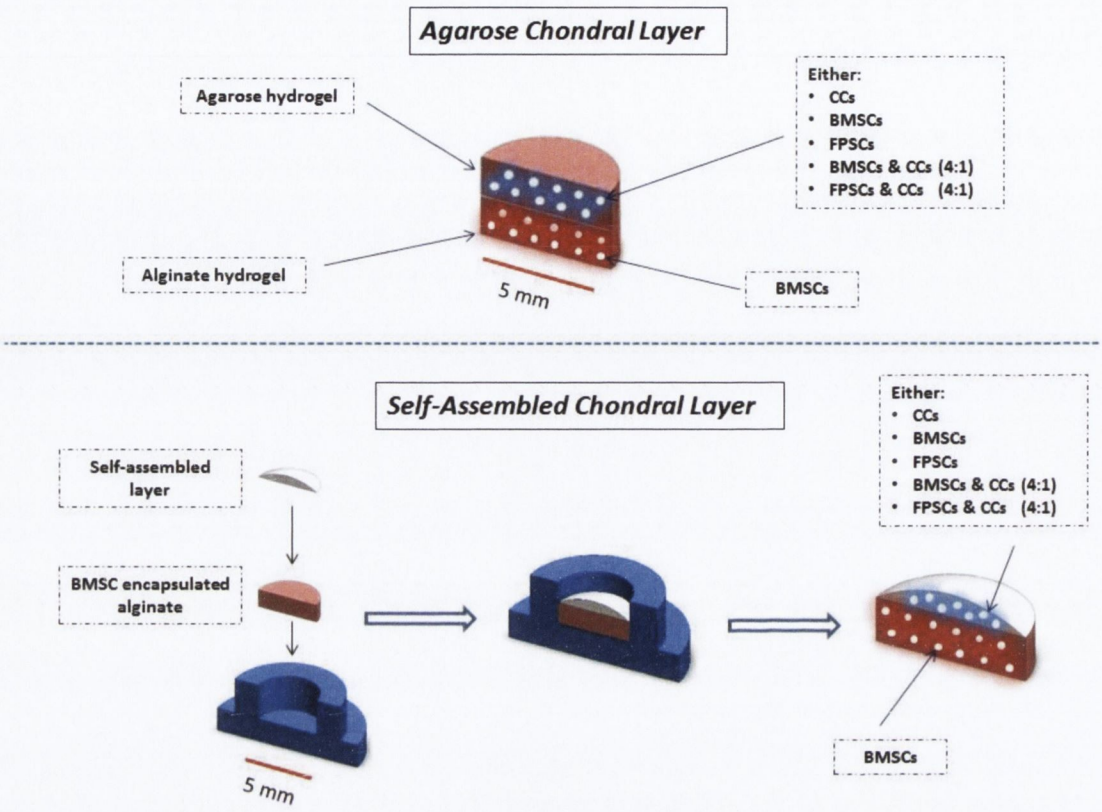

Figure 7-1: Schematic of experimental design. Agarose or self-assembled chondral layers were combined with alginate hydrogels in custom built agarose moulds (blue moulds in figure) to form osteochondral constructs. CC, chondrocyte; BMSC, bone marrow-derived mesenchymal stem cell; FPSC, infrapatellar fat pad-derived stem cell.

In the second phase of the study, scaled-up BMSC-seeded alginate constructs (~2 cm diameter) mimicking the geometry of femorotibial joint replacement prostheses were generated from moulds fabricated by rapid prototyping (Figure 7-2). Briefly, this involved firstly scanning unicondylar knee replacement prostheses in a 3D laser scanner. The files were manipulated in SolidWorks, and imported into a stratasys dimension FDM (fused deposition modelling) machine. This allowed for the creation of acrylonitrile butadiene styrene (ABS) moulds, from which large MSC-seeded alginate constructs were fabricated. These scaled-up

constructs were covered by a self-assembled layer (~2 cm diameter) of engineered cartilaginous tissue (formed through BMSC & CC co-culture). After 6 weeks of *in vitro* culture, the scaled-up constructs were implanted subcutaneously into nude mice for a further 8 weeks.

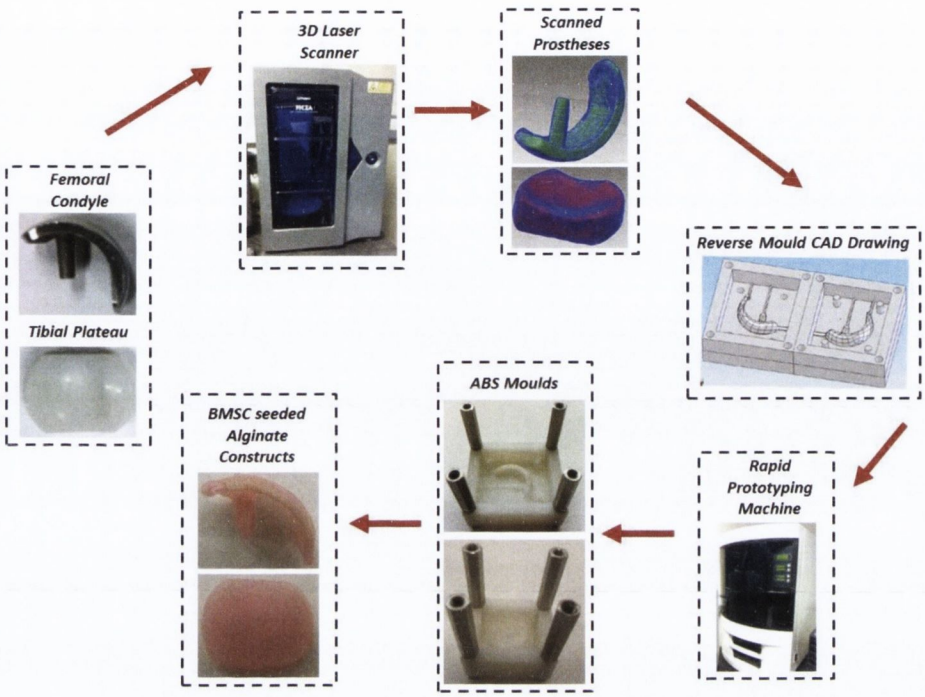

Figure 7-2: Fabrication of scaled-up, anatomically shaped BMSC seeded alginate constructs in the shape of the femoral condyle and the tibial plateau.

7.2.2 Cell Isolation and Expansion

CCs, BMSCs and FPSCs were isolated from porcine femoropatellar joints (4 month donor) as described in the previous chapter. All cells were expanded to passage 1 (P1) at a seeding density of 5×10^3 cells/cm^2, after which they were frozen in fetal bovine serum (GIBCO, Invitrogen, Dublin, Ireland; FBS) supplemented with 10% v/v dimethyl sulphoxide (Sigma-Aldrich, Dublin, Ireland; DMSO) and stored in liquid nitrogen. Before experiments were initiated cells were thawed and counted. CCs, FPSCs and BMSCs were plated at a seeding density of 5×10^3 cells/cm^2 in 500 cm^2 triple flasks (Thermo Fisher Scientific, Ireland) and expanded to passage two (P2) in a humidified atmosphere at 37°C and 5% CO_2. All cells were maintained in

hgDMEM GlutaMAX supplemented with 10% v/v FBS, penicillin (100 U/mL)-streptomycin (100 μg/mL) and 5 ng/mL human fibroblast growth factor-2 (FGF-2; ProSpec-Tany TechnoGene Ltd., Israel) during all expansion phases.

7.2.3 Formation of the Osseous and Chondral Layer of the Bi-layered Constructs

The first objective of the study was to determine the combination of cell and scaffold type that could be used to tissue engineer phenotypically stable cartilage overlaying functional bone *in vivo* (Figure 7-1). The *in vitro* development of these bi-layered constructs consisted of two phases. In the first phase, each individual layer was cultured separately for 2 weeks. In the second phase, the two layers were then stacked and maintained in culture for a further 4 weeks prior to implantation. The osseous (bottom) layers of all bilayered/osteochondral constructs consisted of a cylindrical alginate hydrogel seeded with BMSCs. To create these cylindrical alginate constructs, an agarose/calcium chloride solution was first created by mixing 6% molten agarose (routine agarose; Sigma Aldrich) with 100 mM $CaCl_2$ (Sigma-Aldrich) in a 1:1 ratio. This solution was poured into a custom-built tufset mould to create an agarose/$CaCl_2$ mould (Figure 7-3) consisting of multiple wells of diameter 5 mm and thickness 2 mm. The final concentration of this mould was 3% agarose/50 mM $CaCl_2$. Next, 2% w/v alginate (Pronova UP LVG, FMC BioPolymer, Norway) was dissolved overnight in Dulbecco's phosphate buffered saline (Sigma-Aldrich; PBS), sterile filtered and encapsulated with P2 BMSCs (20 million cells per mL). This alginate is a low viscosity (20-200 mPas) sodium alginate where minimum 60% of the monomer units are guluronate. The cell encapsulated alginate solution was pipetted into the wells of the agarose/$CaCl_2$ mould, and allowed to ionically cross-link with the $CaCl_2$ (i.e., with the Ca^{2+} divalent cations) contained within the mould for 30 mins. After this time, stable and solid BMSC seeded alginate hydrogels (5mm diameter, 2mm thick; 800,000 cells per construct) were removed from the wells and washed twice with basic chemically defined medium (basic CDM). Basic CDM consisted of hgDMEM GlutaMAX supplemented with penicillin (100 U/mL)-streptomycin (100 μg/mL), 100 μg/mL sodium pyruvate, 40 μg/mL L-proline, and 1.5 mg/mL bovine serum albumin (all Sigma-Aldrich).

BMSC seeded alginate constructs were then cultured for 2 weeks in chondrogenic media, consisting of basic CDM supplemented with 0.25 μg/mL amphotericin B, 1x insulin-transferrin-selenium, 4.7 μg/mL linoleic acid, 50μg/ml L-ascorbic acid-2-phosphate, 100nM dexamethasone (all Sigma-Aldrich), and 10 ng/mL TGF-β3 (ProSpec-Tany TechnoGene Ltd.).

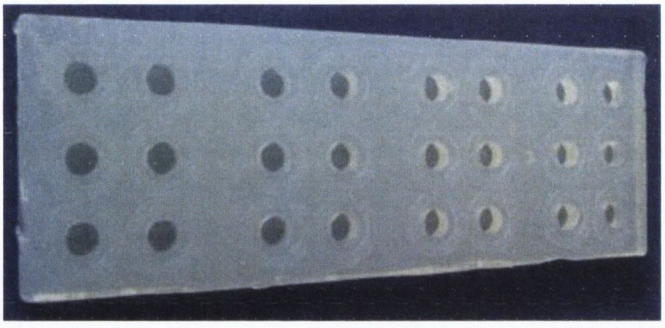

Figure 7-3: The agarose/calcium chloride mould used to create cylindrical alginate hydrogels.

The top layer of the bilayered constructs (termed the chondral layer) was formed next. This layer consisted of either a cell seeded agarose hydrogel or a layer of scaffold-free cartilage generated using self-assembly of cells. Cylindrical 2% agarose hydrogels (5 mm diameter, 1.5 mm thickness) were formed as previously described (Mesallati et al., 2011, Mesallati et al., 2013, Mesallati et al., 2014a, Mesallati et al., 2014b) with a cell seeding density of 20 million cells/mL (600,000 cells per construct). Agarose constructs were formed using chondrocytes (CCs) alone, BMSCs alone, infrapatellar fat pad-derived stem cells (FPSCs) alone, a BMSC & CC co-culture (4:1 ratio) and a FPSC & CC co-culture (4:1 ratio). All cells had been expanded to P2. These constructs were cultured for 2 weeks in chondrogenic media.

Self-assembled constructs were formed as previously described (Mesallati et al., 2014b). Briefly, 4 million cells in 250 μL aliquots of expansion medium (hgDMEM GlutaMAX supplemented with 10% v/v FBS and penicillin-streptomycin) were added to 6.5 mm diameter transwell cell culture inserts (Corning Transwell®, VWR, Dublin, Ireland). These cell seeding numbers equated to approximately 1.2 x 10^5 cells/mm^2 of transwell membrane. Each transwell insert

consisted of a polyethylene terephthalate (PET) membrane containing 3 μm pores. Cells were left in expansion medium for 24 h, after which medium was switched to chondrogenic media for a further 2 weeks of culture. Self-assembled constructs were formed using CCs alone, BMSCs alone, FPSCs alone, a BMSC & CC co-culture (4:1 ratio) and a FPSC & CC co-culture (4:1 ratio). All cells had been expanded to P2.

7.2.4 In Vitro Development of Osteochondral Constructs

After 2 weeks in chondrogenic media, self-assembled constructs were carefully removed from their transwells; 5 mm diameter samples were then cored from the 6.5 mm diameter transwell self-assembled constructs (each new 5mm construct was equivalent to ~ 2.4 million cells). Agarose and alginate gels were also removed from isolated culture at this point. Bilayered constructs were then formed by first confining the osseous layer (BMSC seeded alginate gels cultured as described above) within 5 mm diameter custom made agarose moulds (Figure 7-1), and placing the chondral layer (either 5 mm diameter agarose gels or self-assembled constructs cultured as described above) on top of the osseous layer. These confined osteochondral constructs were cultured in defined CDM for 2 weeks *in vitro*, before being removed from confinement and cultured for 2 additional weeks (total of 6 weeks *in vitro* culture in chondrogenic medium at 20% pO_2). To prevent alginate gels from dissolving in the culture medium (due to release of divalent ions from the gels), the chondrogenic medium was supplemented with 0.25 mM $CaCl_2$ for the final 2 weeks of the *in vitro* culture period. Constructs were subsequently implanted subcutaneously into the back of nude mice.

7.2.5 Subcutaneous Implantation in Nude Mice

Following 6 weeks *in vitro* priming, 5 mm diameter bilayered constructs (n=9 per group) were implanted subcutaneously into the back of nude mice (Balb/c; Harlan, UK). This involved making two subcutaneous pockets along the central line of the spine (at shoulders and hips), and inserting three constructs into each pocket. Nine constructs were implanted per experimental group. Mice were sacrificed 6 weeks

post-implantation by CO_2 inhalation. The animal protocol was reviewed and approved by the ethics committee of Trinity College Dublin.

7.2.6 Generating Scaled-up Geometrically Accurate Osteochondral Constructs

In order to generate scaled-up tissue engineered osteochondral constructs mimicking the geometry of knee implants (Figure 7-2), scans were taken of prostheses of both the femoral condyle and tibial plateau using a PICZA 3D laser scanner (model LPX-250). The program Pixform was used to render and mesh the scans taken from the laser scanner and consequently assemble 3D images of the constructs. Next, these files were imported into SolidWorks. The femoral condyle construct was split in half and used to design a two-part reverse mould drawing of the original, while the tibial plateau construct was used to design a single reverse mould drawing of itself. A rapid prototyping machine (stratasys dimension FDM) was then used to create acrylonitrile butadiene styrene (ABS) moulds of the SolidWorks designs through fused deposition modelling (this work was carried out by Simon McCoy in the Trinity Centre for Bioengineering).

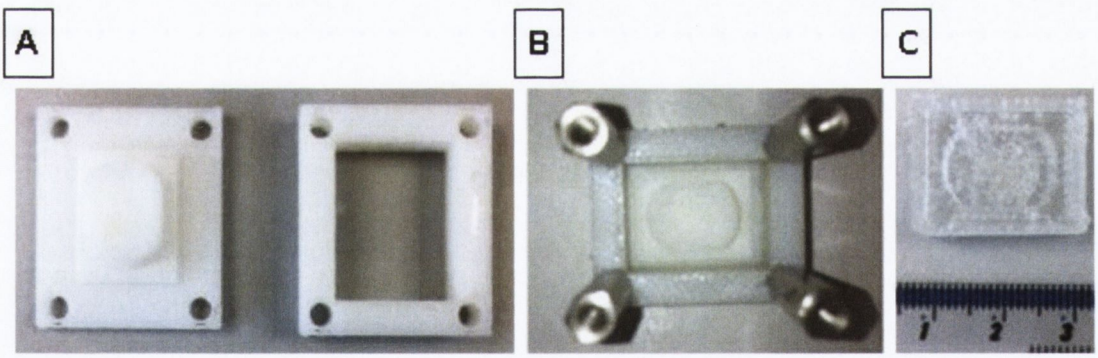

Figure 7-4: (A-B) Acrylonitrile butadiene styrene (ABS) reverse mould of tibial plateau construct. (C) Agarose/calcium chloride mould used to create scaled-up alginate construct in the shape of the tibial plateau.

A solution of 8% molten agarose (routine agarose) mixed with 100 mM $CaCl_2$ (1:1 ratio) was then then used to fill the ABS moulds, thus creating a two-part agarose/$CaCl_2$ mould for the femoral condyle, and a single agarose/$CaCl_2$ mould for the tibial plateau (final concentration of 4% agarose and 50 mM $CaCl_2$). For the

femoral condyle, the two-part agarose/$CaCl_2$ moulds were fitted together and filled with a mixture of BMSCs (P2) and uncrosslinked alginate (2% w/v). By using these moulds, $CaCl_2$ is allowed to diffuse through the agarose and crosslink the alginate to form scaled-up, anatomically shaped constructs in the shape of the femoral condyle (2 cm diameter). The alginate was injected using a hypodermic needle and syringe, through an infiltration extrusion included in the original mould design. A similar process was used to form scaled-up BMSC seeded alginate constructs in the shape of the tibial plateau (dimensions 18 mm x 12 mm x 6 mm). These alginate constructs were seeded at 20 million cells/mL (equating to ~ 15 million cells per femoral construct, and ~ 20 million cells per tibial construct). These scaled-up alginate constructs, which ultimately formed the osseous region of scaled-up osteochondral constructs, were cultured for 2 weeks in chondrogenic medium supplemented with 1 mM $CaCl_2$.

The articular or chondral layers of the scaled-up osteochondral constructs were formed using a scaffold-free or self-assembly approach similar to that described previously. BMSCs and CCs were expanded to P2, trypsinised, and mixed together to form a homogenous cell suspension (BMSC to CC ratio of 4:1). This cell suspension was then used to form self-assembled constructs on PET transwell membranes confined within custom made PDMS moulds. Self-assembled layers for the femoral condyle were 20 mm x 6 mm, whilst those for the tibial plateau were 18 mm x 12 mm; they were formed using the same cell/mm^2 value as used in the first self-assembly (SA) phase of the study (1.2 x 10^5 cells/mm^2). This equated to ~ 15 million cells per femoral SA layer, and ~ 25 million cells per tibial SA layer. SA constructs were cultured for 2 weeks in defined CDM. After this time, they were combined with their corresponding scaled-up BMSC-alginate bases described above to create scaled-up, geometrically accurate osteochondral constructs. The osseous region and self-assembled chondral layer was initially attached using a small amount of fibrin gel (to act like glue). Osteochondral constructs were cultured for 4 additional weeks *in vitro* in defined CDM supplemented with 1 mM $CaCl_2$ (6 weeks total culture pre-implantation at 20% pO_2). In addition, the engineered tibial implant was implanted subcutaneously into the back of nude mice (Balb/c, Harlan). A subcutaneous pocket was made to the side of the central line of the spine, and one

construct was implanted per animal (n = 2). Mice were sacrificed 8 weeks post-implantation.

7.2.7 Biochemical Analysis

The biochemical content of 5 mm diameter osteochondral constructs (n=5) was assessed at the beginning of the experiment (day 0), pre-implantation (day 42) and post-implantation (day 84). Prior to biochemical analysis, osteochondral constructs were sliced at the interface to separate the top chondral layer and bottom osseous layer. These separated layers were then sliced in half, washed in DI water, weighed and frozen for subsequent analysis. The first half of each layer was digested in papain (125 μg/mL) in 0.1 M sodium acetate, 5 mM L-cysteine-HCL, 0.05 M EDTA, pH 6 (all Sigma-Aldrich) under constant rotation at 60°C for 18 h. After this time samples were rotated in 55 mM sodium citrate at 37°C for 40 mins to allow all alginate to dissolve. DNA content of constructs was quantified using the Hoechst Bisbenzimide 33258 dye assay (Kim et al., 1988). Proteoglycan content was estimated by quantifying the amount of sulphated glycosaminoglycans (sGAG) in each construct using the dimethylmethylene blue (DMMB) dye binding assay (Blyscan, Biocolor Ltd., Carrickfergus, UK), with a shark chondroitin sulphate standard. Using DMMB for measuring sGAG in constructs containing alginate is complicated by the fact that the carboxyl groups of alginate bind with DMMB which can interfere with the spectrophotometric detection of sulphated sGAG-DMMB (Enobakhare et al., 1996). The pH of the DMMB dye was therefore adjusted to 1.5 to remove any detection of carboxylated alginate during the sGAG assay. Total collagen content of constructs was determined by measuring the hydroxyproline content via the dimethylaminobenzaldehyde and chloramine T assay (Kafienah and Sims, 2004), using a hydroxyproline to collagen ratio of 1:7.69 (Ignat'eva et al., 2007). The second half of each layer was digested in 1 M hydrochloric acid at 60°C and 10 rpm for 18 h. The calcium content was then determined using a Sentinel Calcium kit (Alpha Laboratories Ltd., UK). Scaled-up anatomically shaped osteochondral constructs were assessed pre- and post-implantation, using the same techniques as described above.

7.2.8 Histology and Immunohistochemistry

At the end of each experiment, at least 2 samples per experimental group were fixed overnight in 4% paraformaldehyde (Sigma-Aldrich) supplemented with barium chloride (in order to permanently crosslink the alginate matrix and constructs). Post-implantation osteochondral constructs (5 mm diameter) were decalcified in EDTA for 7 days prior to wax embedding. Likewise, scaled-up anatomically shaped constructs were decalcified for 14 days. Samples were dehydrated with a graded series of alcohol and embedded in paraffin. 10μm sections were produced of the cross section perpendicular to the construct face. Sections were first stained with haematoxylin and eosin (H and E) and 1% alcian blue 8GX (Sigma-Aldrich) in 0.1M HCL for sGAG accumulation, with a counter stain of nuclear fast red to assess cellular distribution. Sections were next stained with aldehyde fuchsin to differentiate between cartilage sGAG deposition and residual alginate. The final stains involved 1% alizarin red to assess mineral accumulation and picro-sirius red (Sigma-Aldrich) to visualise collagen accumulation.

Collagen types 1, II and X deposition were identified by immunohistochemical analysis. Briefly, sections were treated with peroxidase, followed by treatment with chondroitinase ABC (Sigma-Aldrich) in a humidified environment at 37°C to enhance permeability of the extracellular matrix. Sections were then incubated with goat serum to block non-specific sites, before the primary antibody was applied to the sections. Collagen type I (ab90395, 1:400, 1 mg/mL), collagen type II (ab3092, 1:100, 1 mg/mL) or collagen type X (ab49945, 1:100, 1.4 mg/mL) primary antibodies (mouse monoclonal, Abcam, Cambridge, UK) were applied for 1 hour at room temperature. Next, the secondary antibody (for collagen types I and II, Anti-Mouse IgG biotin conjugate, 1:200, 2.1 mg/mL, Sigma-Aldrich; for collagen type X, ab49760 Anti-Mouse IgM mu chain (Biotin), 1:100, 0.1 mg/mL, Abcam) was added for 1 hour followed by incubation with ABC reagent (Vectastain PK-400, Vector Labs, Peterborough, UK) for 45 min. Finally sections were developed with DAB peroxidase (Vector Labs) for 5 min. Positive and negative controls were included in the immunohistochemistry staining protocol for each batch.

7.2.9 Micro-Computed Tomography

Micro-computed tomography (μCT) scans were carried out using a Scanco Medical 40 μCT system (Scanco Medical, Bassersdorf, Switzerland) in order to quantify mineral content and to assess mineral distribution in all osteochondral constructs post implantation. For all 5 mm diameter osteochondral constructs, samples were scanned at the end of the 6 week *in vivo* time period. Constructs were scanned in DI water, at a voxel resolution of 16 μm, a voltage of 70 kVp, and a current of 114 μA. Circular contours were drawn in an anti-clockwise direction around the periphery of the constructs. A Gaussian filter (sigma=0.8, support=1) was used to suppress noise and a global threshold of 210, corresponding to a density of 399.5 mg hydroxyapatite/cm^3, was applied. This threshold was chosen through visual inspection of individual scan slices so as to include mineralise tissue and exclude non-mineralised tissue. 3D evaluation was carried out on the segmented images in order to reconstruct a 3D image. 3 constructs were analysed per experimental group. For scaled-up, anatomically shaped osteochondral constructs, samples were scanned at the end of the 8 week *in vivo* time period.

7.2.10 Statistical Analysis

Statistical analyses were performed using the software package MINITAB 15.1 (Minitab Ltd., Coventry, UK). Groups were analyzed for significant differences using a general linear model for analysis of variance. Tukey's test for multiple comparisons was used to compare conditions. A Box-Cox transformation was used to normalize data sets where necessary. Significance was accepted at a level of $p \leq 0.05$. Numerical and graphical results are presented as mean ± standard deviation (n=5), with graphical results produced using GraphPad Prism (Version 6.02).

7.3 Results

7.3.1 The osseous region of an osteochondral construct can be engineered using a chondrogenically primed MSC laden alginate hydrogel that undergoes endochondral ossification in vivo

We have previously shown that it is possible to engineer stable cartilaginous tissue on top of a layer of mineralised hypertrophic cartilage by seeding chondrocytes (CCs) into the top 'chondral' layer of bilayered agarose hydrogels, and BMSCs into the bottom 'osseous' layer of these bilayered agarose hydrogels (Sheehy et al., 2013). The main drawback to this method was that the agarose did not degrade *in vivo* and hence prevented vascularisation and any subsequent endochondral ossification of the mineralised cartilaginous tissue in the bottom 'osseous' layer from occurring. Alginate has been shown to facilitate vascularisation and bone formation *in vivo* (Simmons et al., 2004, Weng et al., 2006, Kolambkar et al., 2011a, Kolambkar et al., 2011b). Hence, alginate gels were seeded with BMCSs and used to form the 'osseous' or 'endochondral' layer of bilayered constructs, where the overlaying articular cartilage or 'chondral' layer was formed using either an agarose hydrogel seeded with chondrocytes (CCs) or a layer of scaffold-free cartilage engineered through self-assembly of CCs (Figures 7-5A, B). After 6 weeks in chondrogenic media, a cartilaginous layer staining positively for sGAG (alcian blue staining) and type II collagen was generated on top of alginate hydrogels using both the agarose encapsulation and the self-assembly (SA) approach (Figure 7-5D). The SA approach generated a cartilage layer with significantly higher levels of sGAG and collagen (as a % of tissue wet weight) compared to agarose encapsulation (Figure 7-5C) (SA constructs reached levels of 6.9±1.0 %w/w sGAG, 2.5±0.6 %w/w collagen; agarose constructs reached levels of 2.6±0.1 %w/w sGAG, 1.3±0.1 %w/w collagen). The underlying alginate layer, which was seeded with BMSCs, also stained positively for sGAG (aldehyde fuchsin staining) and type II collagen (Figure 7-5E) prior to implantation.

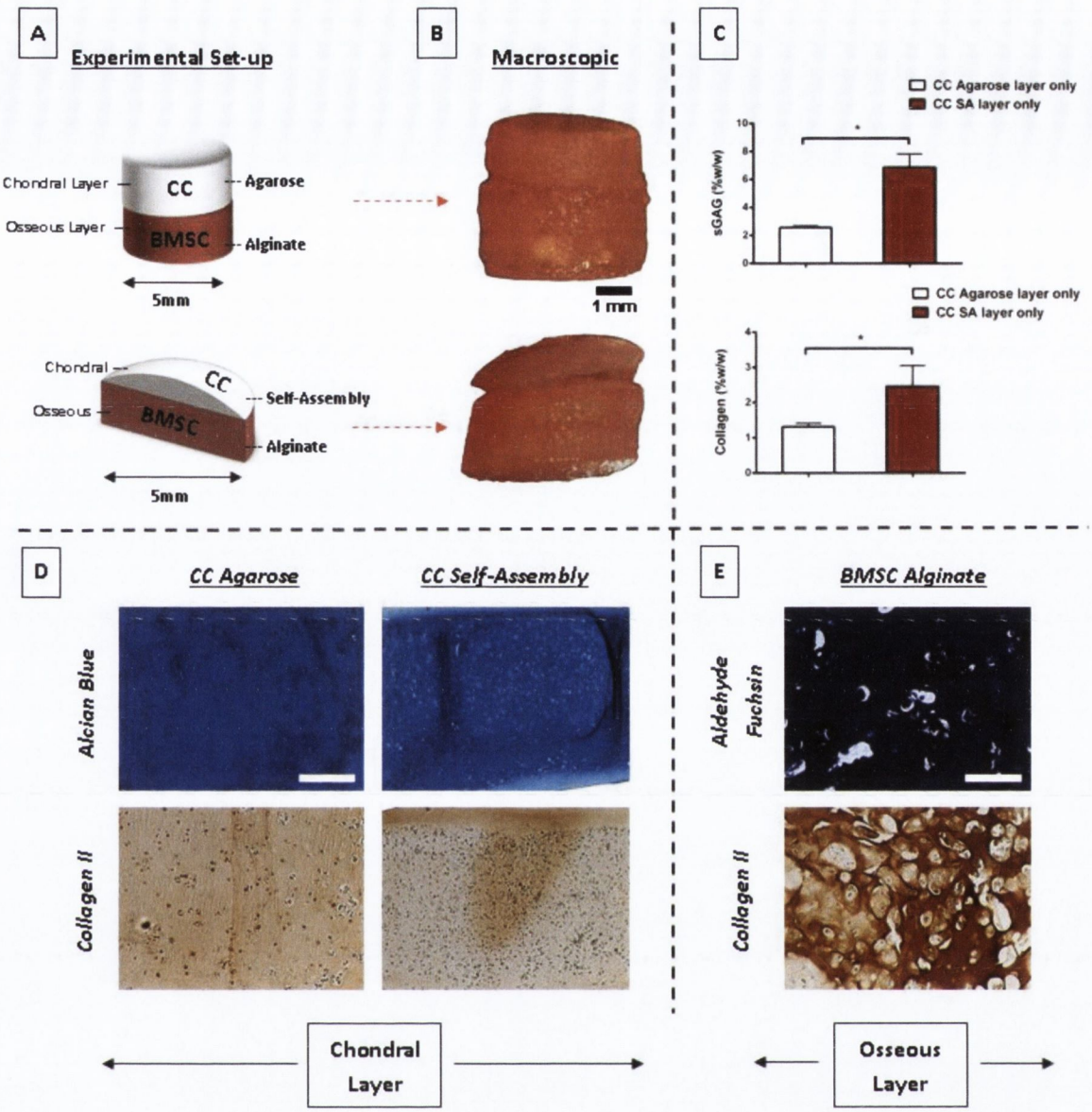

Figure 7-5: Bilayered constructs pre-implantation, formed using chondrocytes (CCs) in the chondral layer and bone marrow-derived MSCs (BMSCs) in the bottom osseous alginate layer. (A) Schematic of bilayered constructs, with chondral layers formed through agarose or self-assembly (SA). (B) Macroscopic images after 6 weeks *in vitro* culture. (C) sGAG and collagen accumulation (%w/w) within the chondral layer of these osteochondral constructs. (D) Alcian blue staining for sGAG production and type II collagen immunohistochemistry of chondral layers. (E) Histological staining of osseous alginate layers. * denotes significant difference with $p < 0.05$. Scale bar = 200 μm.

Following subcutaneous implantation into nude mice, the osseous region (MSC laden alginate hydrogels) of the bi-layered constructs appeared hard and calcified (Figure 7-6A). Indeed, μCT analysis demonstrated extensive mineralisation in the alginate layers (Figure 7-6A). The calcium content of the underlying osseous region of the osteochondral constructs was not affected by the approach (agarose encapsulation or self-assembly) used to engineer the overlaying chondral layer (data not shown). H&E staining of the osseous region of the constructs revealed the formation of bony-like tissue (Figure 7-6B). Collagens type I and X were also detected in this osseous layer (Figure 7-6B), suggesting the formation of bone through the process of endochondral ossification. A phenotypically stable cartilage tissue was generated in the top layer of the osteochondral construct *in vivo* (Figure 7-6C), with positive staining for sGAG and type II collagen, irrespective of whether this tissue was engineered using agarose encapsulation or SA. There was some staining of collagen type I in the cartilage generated by these expanded chondrocytes, with no evidence of collagen type X deposition observed (Figure 7-6C). No mineralisation was detected in the chondral layers (Figure 7-6A).

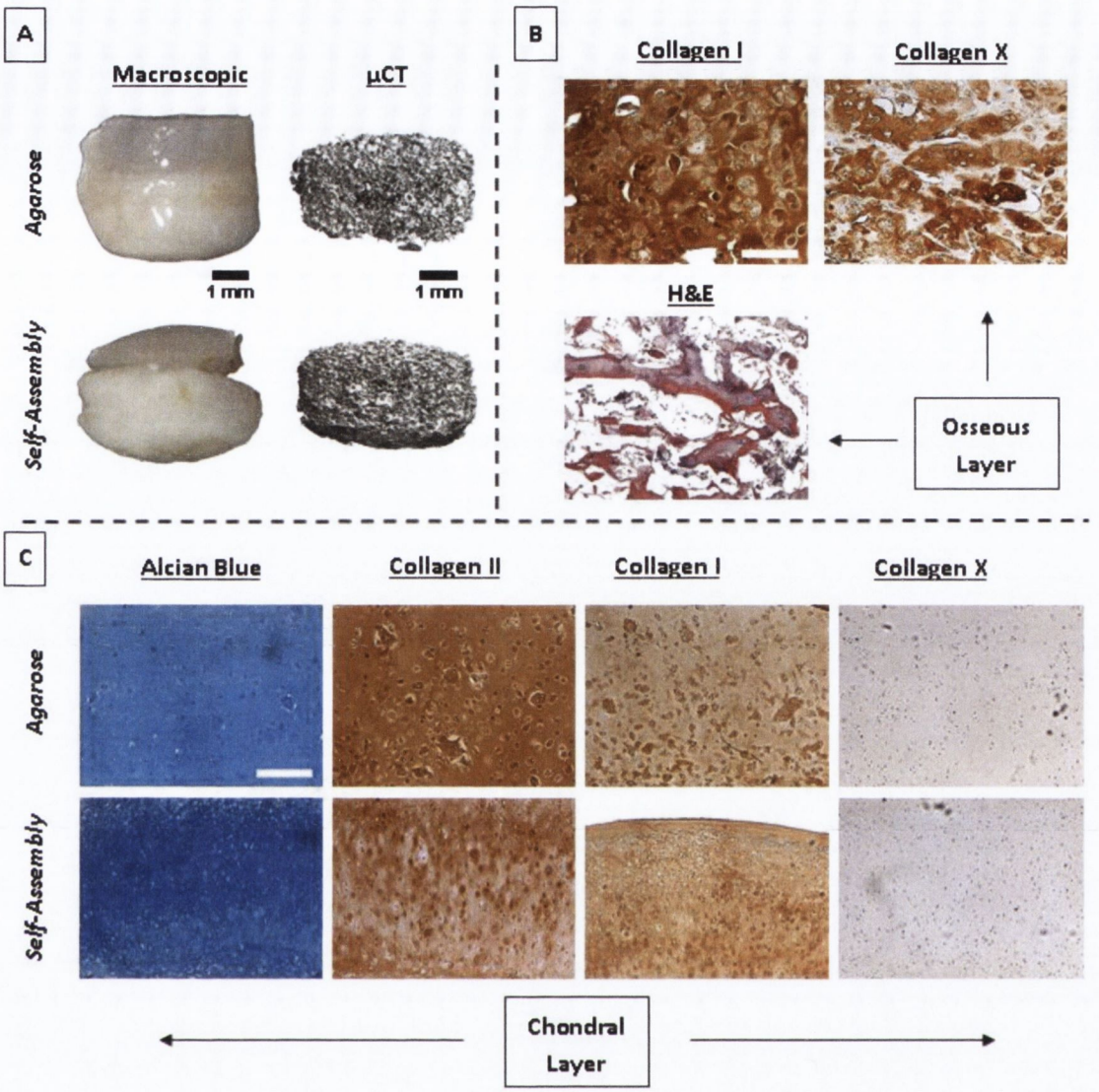

Figure 7-6: Osteochondral constructs post-implantation, with chondral layers formed using only chondrocytes (CCs). (A) Macroscopic images and μCT scans of bilayered constructs, with chondral layers formed through agarose or self-assembly. (B) Collagen types I and X immunohistochemistry and H&E staining of osseous alginate layers of osteochondral constructs (representative of all alginate samples). (C) Alcian blue staining and collagen immunohistochemistry of chondral layers. Scale bar = 200 μm.

7.3.2 Self-assembled cartilaginous grafts engineered using either bone marrow (BM) or infrapatellar fat pad-derived MSCs (FPSCs) fail to form phenotypically stable tissue in vivo

While a phenotypically stable layer of articular cartilage can be engineered on an osteochondral construct using primary CCs alone, from a clinical perspective it may not be feasible to obtain the large number of CCs required to engineer a graft capable of resurfacing an entire joint. While an abundant number of MSCs can be obtained theoretically for such purposes, we have shown that both BMSCs and FPSCs encapsulated within agarose fail to form phenotypically stable cartilage *in vivo* (Vinardell et al., 2012b). Given that SA using FPSCs has been shown to lead to the generation of a more cartilage-like graft *in vitro* compared to agarose hydrogel encapsulation (chapter 5), I next sought to determine if this would translate into the development of a more phenotypically stable tissue *in vivo*. To this end, the previous study was repeated, using MSCs isolated from different tissues in place of CCs to engineer the chondral layer of the osteochondral constructs, again using either agarose encapsulation or a self-assembly approach (Figure 7-7A).

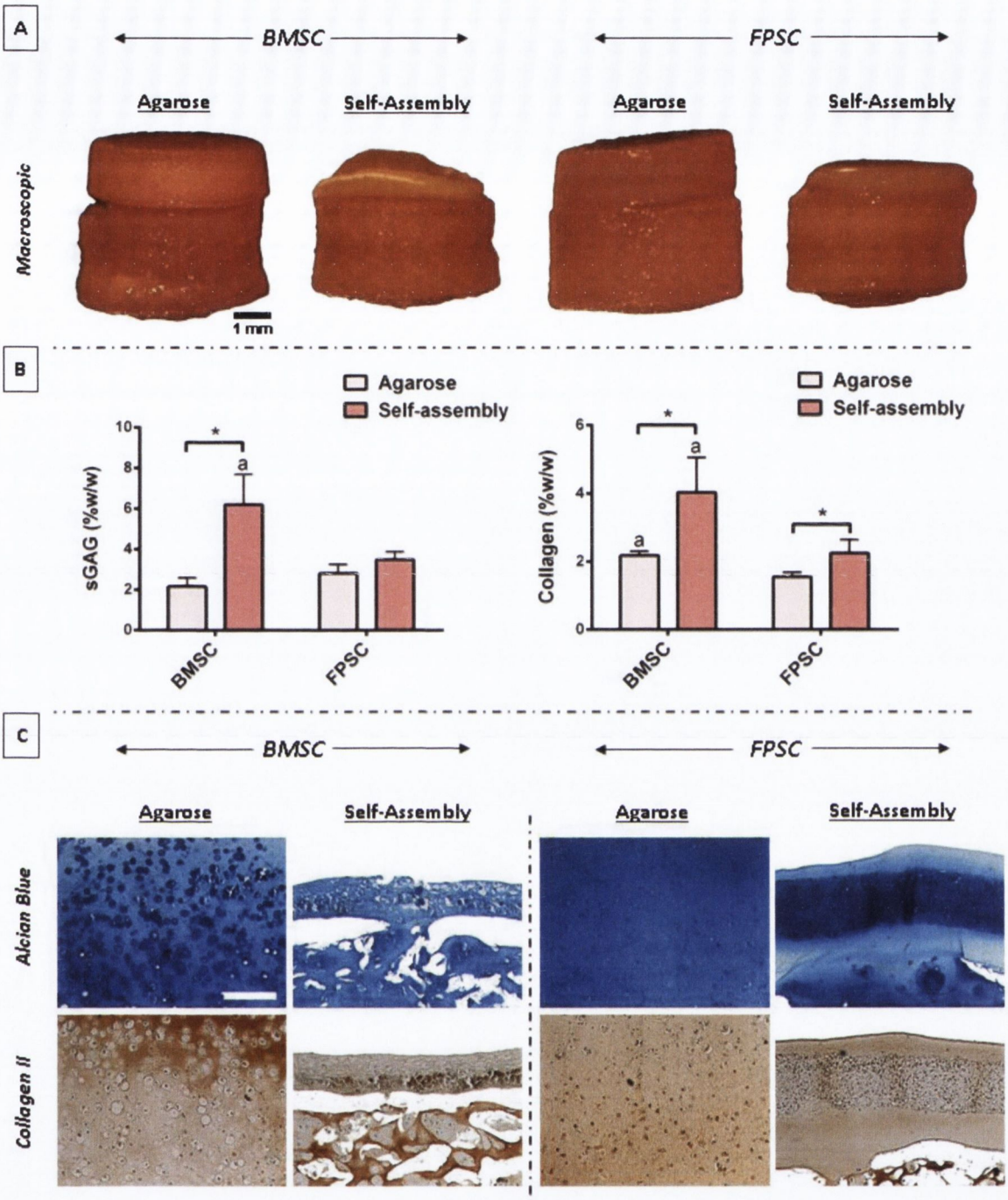
A
BMSC
FPSC
Agarose
Self-Assembly
Agarose
Self-Assembly
Macroscopic
1 mm
B
Agarose
Self-assembly
sGAG (%w/w)
10
8
6
4
2
0
*
a
BMSC
FPSC
Agarose
Self-assembly
Collagen (%w/w)
6
4
2
0
*
a
a
*
BMSC
FPSC
C
BMSC
FPSC
Agarose
Self-Assembly
Agarose
Self-Assembly
Alcian Blue
Collagen II

Figure 7-7: Osteochondral constructs pre-implantation, with chondral layers formed using either bone marrow-derived MSCs (BMSCs) or infrapatellar fat pad-derived stem cells (FPSCs). (A) Macroscopic images of bilayered constructs after 6 weeks *in vitro* culture, with chondral layers formed through agarose or self-assembly. (B) sGAG and collagen accumulation (%w/w) within the chondral layers of these osteochondral constructs. (C) Alcian blue staining and type II collagen immunohistochemistry of chondral layers. [a] $p<0.05$ versus corresponding FPSC group in same scaffold. * denotes significant difference with $p < 0.05$. Scale bar = 200 μm.

Pre-implantation, both BMSCs and FPSCs could be used (using either agarose encapsulation or SA) to generate a chondral layer rich in proteoglycans and type II collagen (Figure 7-7C). The highest levels of sGAG and collagen accumulation (%w/w) were observed in the chondral layers generated using SA with BMSCs (Figure 7-7B) (6.2±1.5 %w/w sGAG; 4±1 %w/w collagen).

Post-implantation, both the chondral and osseous layers of constructs engineered using BMSCs appeared hard and calcified (Figure 7-8A). The chondral layers of osteochondral constructs generated using FPSCs were macroscopically different, with a more fibrous or fibrocartilaginous appearance (Figure 7-8A). μCT analysis demonstrated that mineralisation occurred in the osseous (MSC seeded alginate) layer of all bilayered constructs, and furthermore, that the chondral layer of constructs engineered using BMSCs (agarose and SA) also mineralized (Figure 7-8A). The chondral layer of constructs engineered using BMSCs accumulated the highest levels of calcium (highest levels of 11.4±1.3 %/w/w in BMSC SA), with significantly lower levels of calcium observed in the FPSC seeded chondral layers (Figure 7-8C).

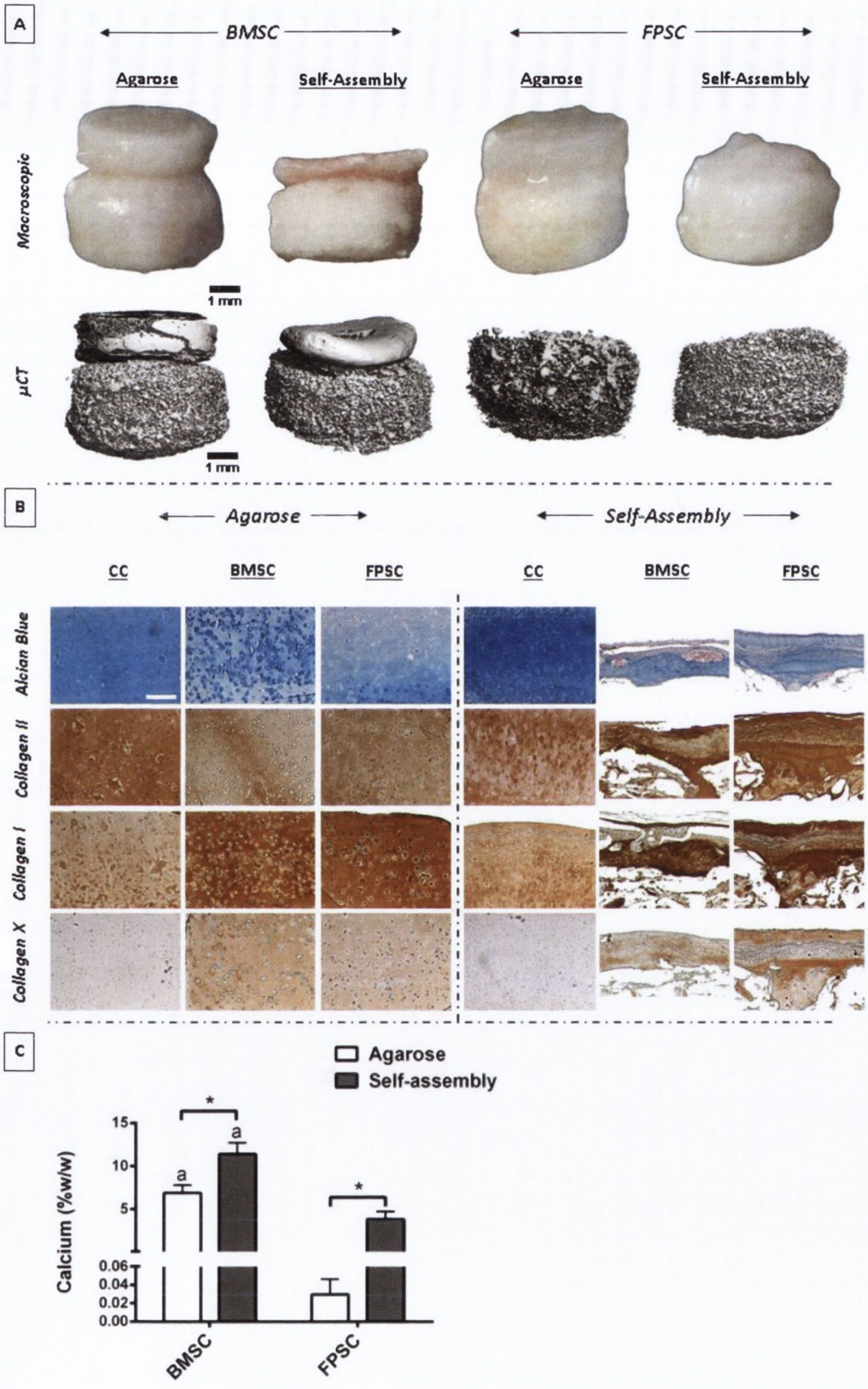
A
BMSC
FPSC
Agarose
Self-Assembly
Agarose
Self-Assembly
Macroscopic
1 mm
µCT
1 mm
B
Agarose
Self-Assembly
CC
BMSC
FPSC
CC
BMSC
FPSC
Alcian Blue
Collagen II
Collagen I
Collagen X
C
Agarose
Self-assembly
Calcium (%w/w)
15
10
5
0.06
0.04
0.02
0.00
a
a
*
*
BMSC
FPSC

Figure 7-8: Osteochondral constructs post-implantation, with chondral layers formed using either bone marrow-derived MSCs (BMSCs) or infrapatellar fat pad-derived stem cells (FPSCs). (A) Macroscopic images and μCT scans of bilayered constructs. (B) Alcian blue staining and collagen immunohistochemistry of chondral layers (chondrocyte (CC) chondral layers included for comparison purposes). (C) Calcium accumulation (%w/w) within the chondral layers of osteochondral constructs. [a] $p<0.05$ versus corresponding FPSC group in same scaffold. * denotes significant difference with $p < 0.05$. Scale bar = 200 μm.

Post-implantation, the chondral layers of all constructs engineered using BMSCs or FPSCs stained positively for sGAG and collagen type II, although staining was generally weaker than that found in the chondral layers generated using CCs (Figure 7-8B), with particularly weak staining for sGAG. Conversely, staining of collagen types I and X was much stronger in the chondral layers engineered using MSCs compared to respective CC chondral layers (for both agarose and SA) (Figure 7-8B). In addition, chondral layers engineered using self-assembly of MSCs were considerably thinner than those generated using CCs.

7.3.3 A co-culture of chondrocytes (CCs) and either BMSCs or FPSCs enhances the in vitro development of engineered cartilage and in vivo leads to the development of a more phenotypically stable tissue

I next sought to determine if phenotypically stable cartilage could be generated *in vivo* using a co-culture of CCs and either BMSCs or FPSCs. The chondral layers of bilayered constructs were created by self-assembly of co-cultured MSCs and CCs in a 4:1 ratio (Figure 7-9A). Self-assembled cartilaginous tissues engineered using such a co-culture of CCs and either BMSCs or FPSCs were found to be considerably thicker pre-implantation than their respective stem cell only controls (Figure 7-9A). For BMSC & CC co-cultures, these tissues also stained more intensely *in vitro* for sGAG and type II collagen than BMSC only controls. A cartilage tissue engineered using a co-culture of CCs and either BMSCs or FPSCs contained significantly higher levels of both sGAG and collagen pre-implantation compared to those engineered using either stem cell type alone (Figure 7-9B). There was no significant difference in the collagen content of chondral layers engineered using a co-culture or CCs only, although the sGAG of CC only chondral layers was significantly higher than all other groups. Only chondral layers engineered using self-assembled BMSCs stained positive for mineral (alizarin red staining) pre-implantation (Figure 7-9A). No evidence of mineral accumulation was observed in chondral layers engineered using a co-culture of BMSCs and CCs. These results were confirmed by biochemical assays to determine the calcium content of the chondral layer of each construct (Figure 7-9B), where a co-culture of BMSCs & CCs was found to dramatically reduce calcium accumulation compared to BMSC only controls. Chondral layers engineered using FPSCs accumulated negligible calcium *in vitro*.

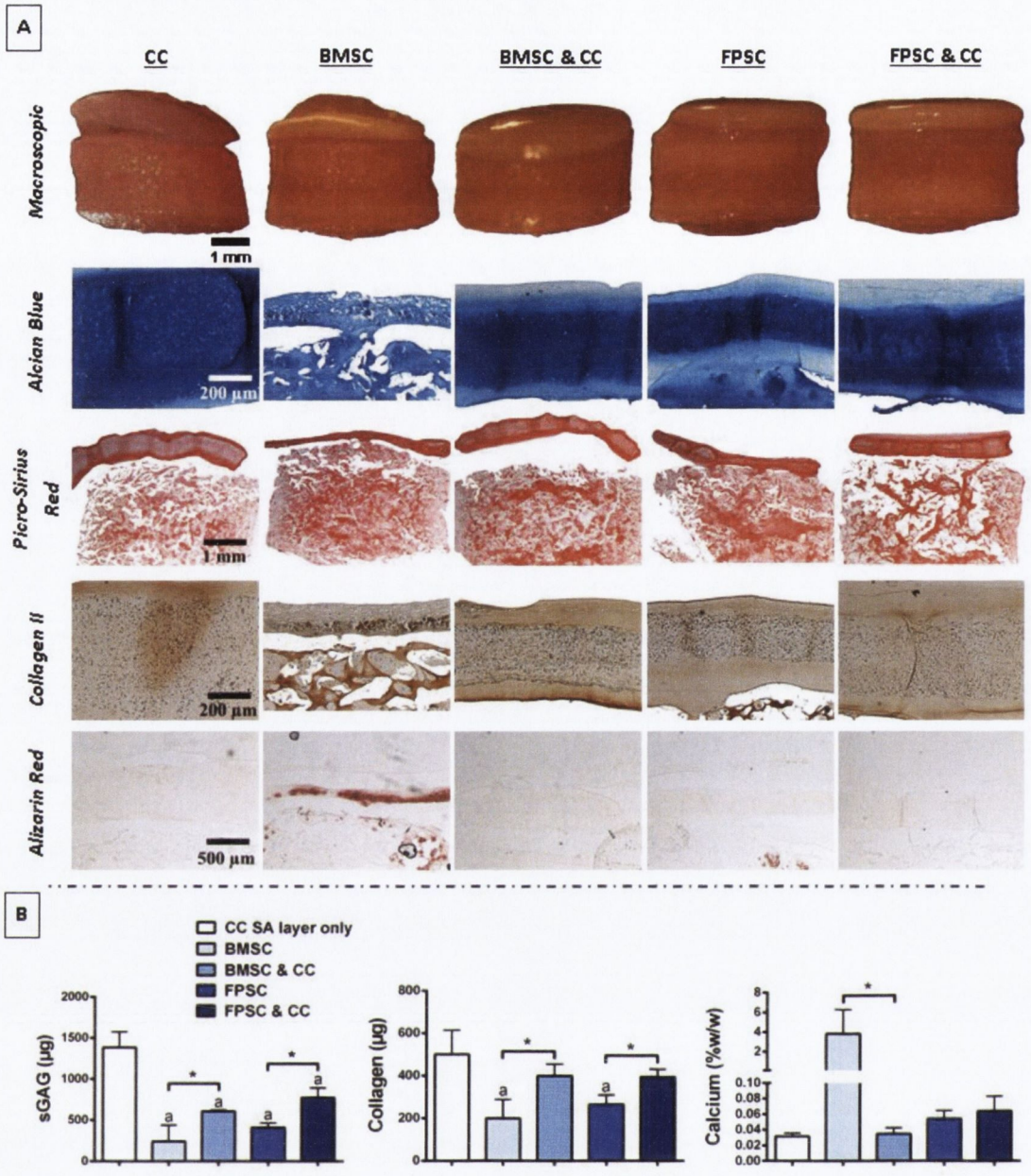

Figure 7-9: Osteochondral constructs pre-implantation, with chondral layers formed through self-assembly (SA) of either chondrocytes (CCs), bone marrow-derived MSCs (BMSCs), BMSCs & CCs, fat pad-derived stem cells (FPSCs) or FPSCs & CCs. (A) Macroscopic images of bilayered constructs followed by chondral layer staining of alcian blue for sGAG, picro-sirius red for collagen (both chondral and osseous layer), type II collagen immunohistochemistry and alizarin red for mineralisation. (B) sGAG (µg), collagen (µg) and calcium (%w/w) accumulation within SA chondral layers of osteochondral constructs. [a] $p<0.05$ versus CC SA layer. * denotes significant difference with $p < 0.05$.

Post-implantation it appeared that the chondral and osseous layers of osteochondral constructs were better integrated when the chondral layer was engineered using co-cultured cells, as opposed to MSC only groups (Figure 7-10A). Macroscopically, very little calcification of the chondral layer engineered using a co-culture was observed post-implantation. μCT analysis confirmed this, showing that the high level of mineral deposition observed in the chondral layer engineered using BMSCs only was almost completely absent in the BMSC & CC co-cultured layers (Figure 7-10A). A near 7-fold reduction in calcium accumulation was observed in BMSC & CC SA layers (1.7±0.3 %w/w) compared to BMSC only controls (11.4±1.3 %w/w). Furthermore, co-culture of FPSCs & CCs also significantly reduced calcium accumulation compared to FPSC only SA controls (reduction from 3.8±0.9 %w/w in FPSC only to 1.0±0.5 %w/w in co-culture). Histologically, the SA chondral layer engineered using a co-culture of stem cells and CCs appeared thicker, more homogeneous, more morphologically stable and more cartilage-like compared to stem cell only groups (Figure 7-10A). sGAG and type II collagen staining of the chondral layers of co-culture groups was comparable to chondral layers engineered using CCs only.

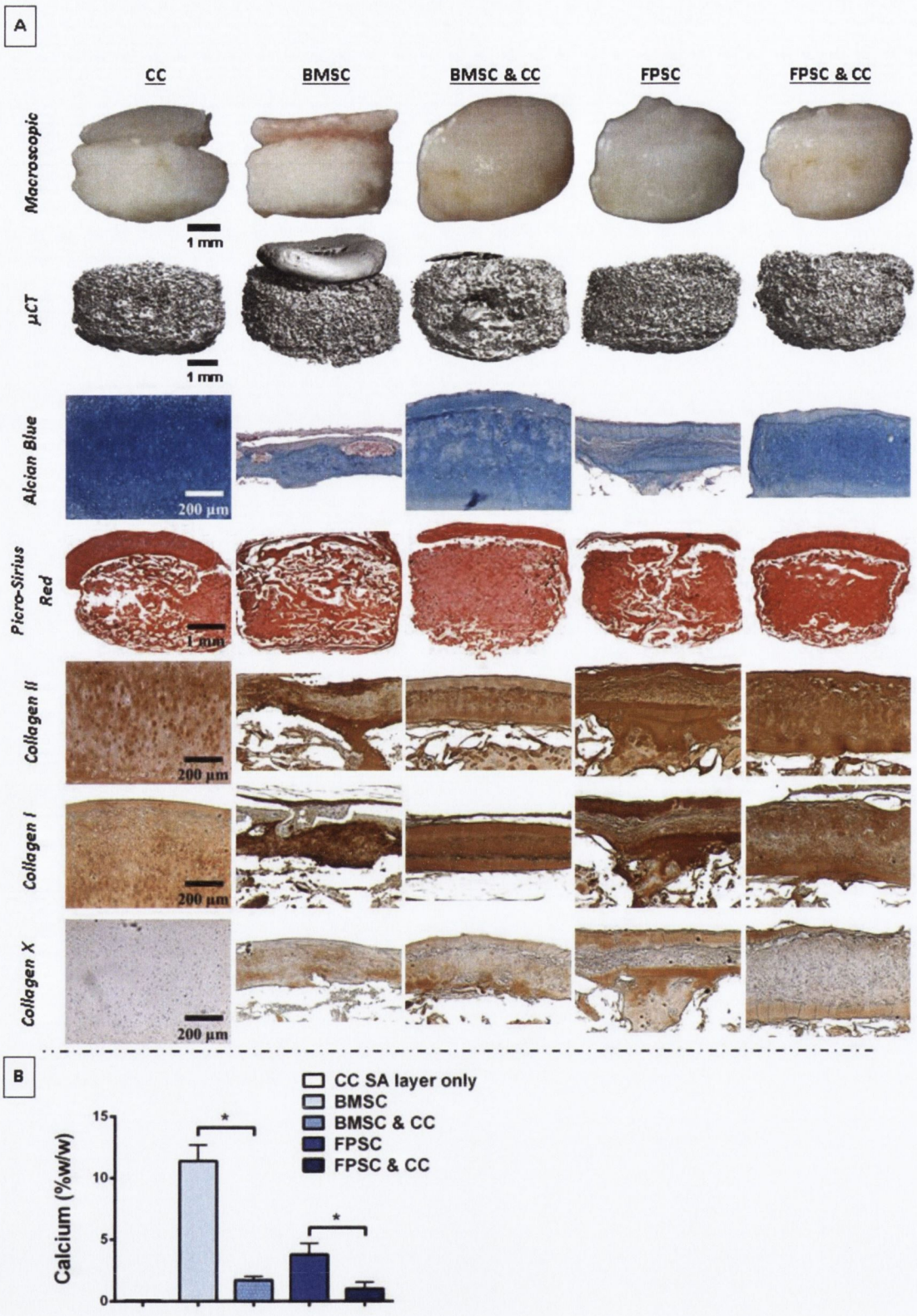
A
CC
BMSC
BMSC & CC
FPSC
FPSC & CC
Macroscopic
µCT
Alcian Blue
Picro-Sirius Red
Collagen II
Collagen I
Collagen X
1 mm
200 µm
B
CC SA layer only
BMSC
BMSC & CC
FPSC
FPSC & CC
Calcium (%w/w)
15
10
5
0
*
*

Figure 7-10: Osteochondral constructs post-implantation, with chondral layers formed through self-assembly (SA) of either chondrocytes (CCs), bone marrow-derived MSCs (BMSCs), BMSCs & CCs, fat pad-derived stem cells (FPSCs) or FPSCs & CCs. (A) Macroscopic images of bilayered constructs followed by μCT scans, chondral layer alcian blue staining, picro-sirius red staining (whole osteochondral construct) and collagen immunohistochemistry of chondral layers. (B) Calcium accumulation (%w/w) within SA chondral layers of osteochondral constructs. * denotes significant difference with $p < 0.05$.

This study to determine if phenotypically stable cartilage could be generated *in vivo* using a co-culture of CCs and either BMSCs or FPSCs was repeated using agarose encapsulation as opposed to SA to engineer the chondral layer (Figure 7-11A). The chondral layers of these bilayered constructs were created by encapsulating MSCs and CCs in a 4:1 ratio within the agarose hydrogels. Co-culture of MSCs and CCs in agarose led to stronger staining of sGAG and type II collagen within cartilaginous tissues *in vitro* compared to stem cell only chondral layers (Figure 7-11A), particularly for the BMSC groups. Co-culture of CCs and either BMSCs or FPSCs also led to higher levels of both sGAG and collagen accumulation pre-implantation compared to cartilage tissue engineered using either stem cell type alone (Figure 7-11B). Co-culture agarose chondral layers accumulated greater levels of sGAG and collagen than CC chondral layers. Co-culture of BMSCs & CCs dramatically reduced calcium accumulation compared to BMSC only chondral layers, as evidenced by alizarin red staining and a biochemical analysis of calcium accumulation (Figure 7-11).

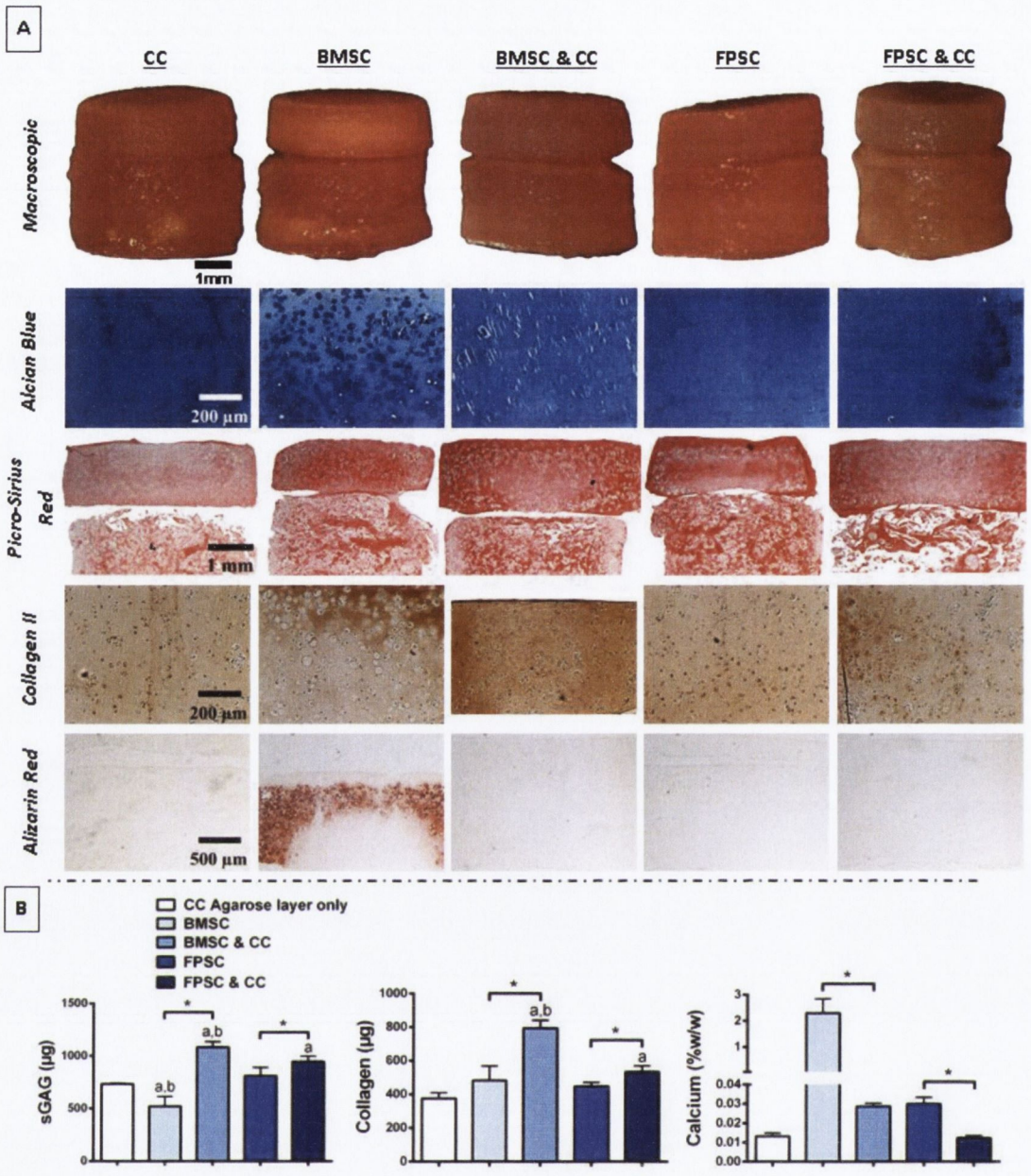

Figure 7-11: Osteochondral constructs pre-implantation, with chondral layers formed through agarose encapsulation of either chondrocytes (CCs), bone marrow-derived MSCs (BMSCs), BMSCs & CCs, fat pad-derived stem cells (FPSCs) or FPSCs & CCs. (A) Macroscopic images of bilayered constructs followed by chondral layer staining of alcian blue for sGAG, picro-sirius red for collagen (both chondral and osseous layer), type II collagen immunohistochemistry and alizarin red for mineralisation. (B) sGAG (µg), collagen (µg) and calcium (%w/w) accumulation within agarose chondral layers of osteochondral constructs. [a] $p<0.05$ versus CC seeded agarose layer. [b] $p<0.05$ versus corresponding group containing FPSCs. * denotes significant difference with $p < 0.05$.

Post-implantation, μCT analysis demonstrated that the high level of mineral deposition observed in the chondral layer engineered using BMSCs only was completely absent in the BMSC & CC co-cultured agarose layers (Figure **7**-12A). Dramatic reductions in calcium accumulation were also observed in BMSC & CC agarose layers (0.05±0.02 %w/w) compared to BMSC only controls (6.9±0.9 %w/w) (Figure 7-12B). Negligible amounts of calcium were detected in agarose chondral layers containing FPSCs *in vivo*. Histologically, the agarose chondral layers engineered using a co-culture of stem cells and CCs appeared more cartilage-like compared to stem cell only groups (Figure **7**-12A), with stronger staining of sGAG and type II collagen in co-culture groups. sGAG and type II collagen staining of the chondral layers of co-culture groups was comparable to agarose chondral layers engineered using CCs only. Finally, co-culture of MSCs and CCs was found to clearly reduce type X collagen expression in agarose chondral layers compared to stem cell only groups *in vivo* (Figure **7**-12A), with comparable staining between CC layers and chondral layers of co-culture groups.

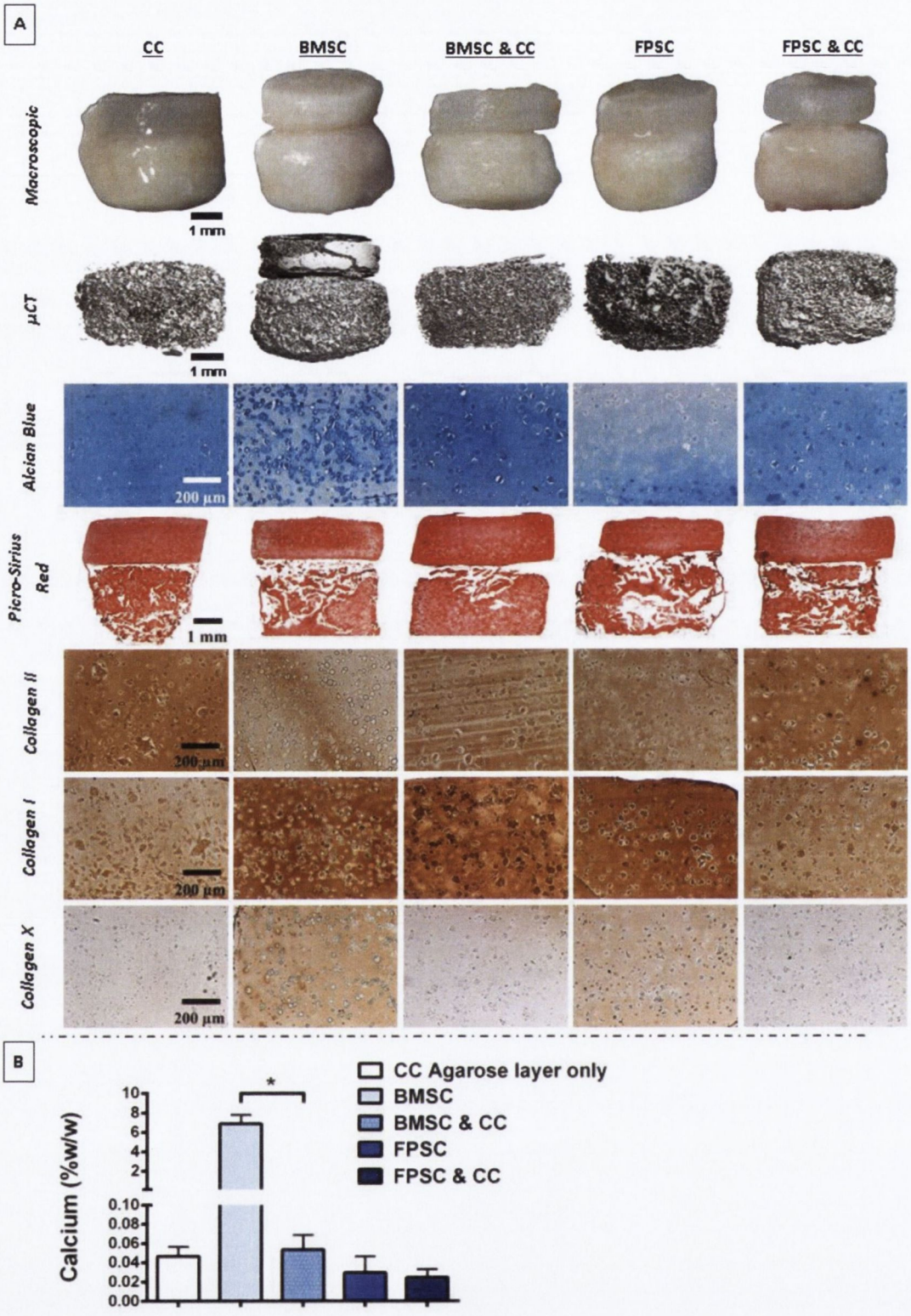
A
CC
BMSC
BMSC & CC
FPSC
FPSC & CC
Macroscopic
µCT
Alcian Blue
Picro-Sirius Red
Collagen II
Collagen I
Collagen X
1 mm
200 µm
B
Calcium (%w/w)
CC Agarose layer only
BMSC
BMSC & CC
FPSC
FPSC & CC
*
10
8
6
4
2
0.10
0.08
0.06
0.04
0.02
0.00

Figure 7-12: Osteochondral constructs post-implantation, with chondral layers formed through agarose encapsulation of either chondrocytes (CCs), bone marrow-derived MSCs (BMSCs), BMSCs & CCs, fat pad-derived stem cells (FPSCs) or FPSCs & CCs. (A) Macroscopic images of bilayered constructs followed by μCT scans, chondral layer alcian blue staining, picro-sirius red staining (whole osteochondral construct) and collagen immunohistochemistry of chondral layers. (B) Calcium accumulation (%w/w) within agarose chondral layers of osteochondral constructs. * denotes significant difference with $p < 0.05$.

7.3.4 Tissue engineering a scaled-up geometrically accurate osteochondral construct for joint re-surfacing

In the final part of the study, scaled up BMSC-seeded alginate constructs (~2 cm diameter) mimicking the geometry of the femoral and tibial components of a partial knee replacement prosthesis were generated from moulds fabricated by rapid prototyping (Figure 7-13A). These scaled-up alginate constructs (in the shape of the femoral condyle and tibial plateau) were cultured in chondrogenic conditions *in vitro*, with the engineered tissues staining positively for sGAG and collagen type II after 6 weeks in culture (Figure 7-13B).

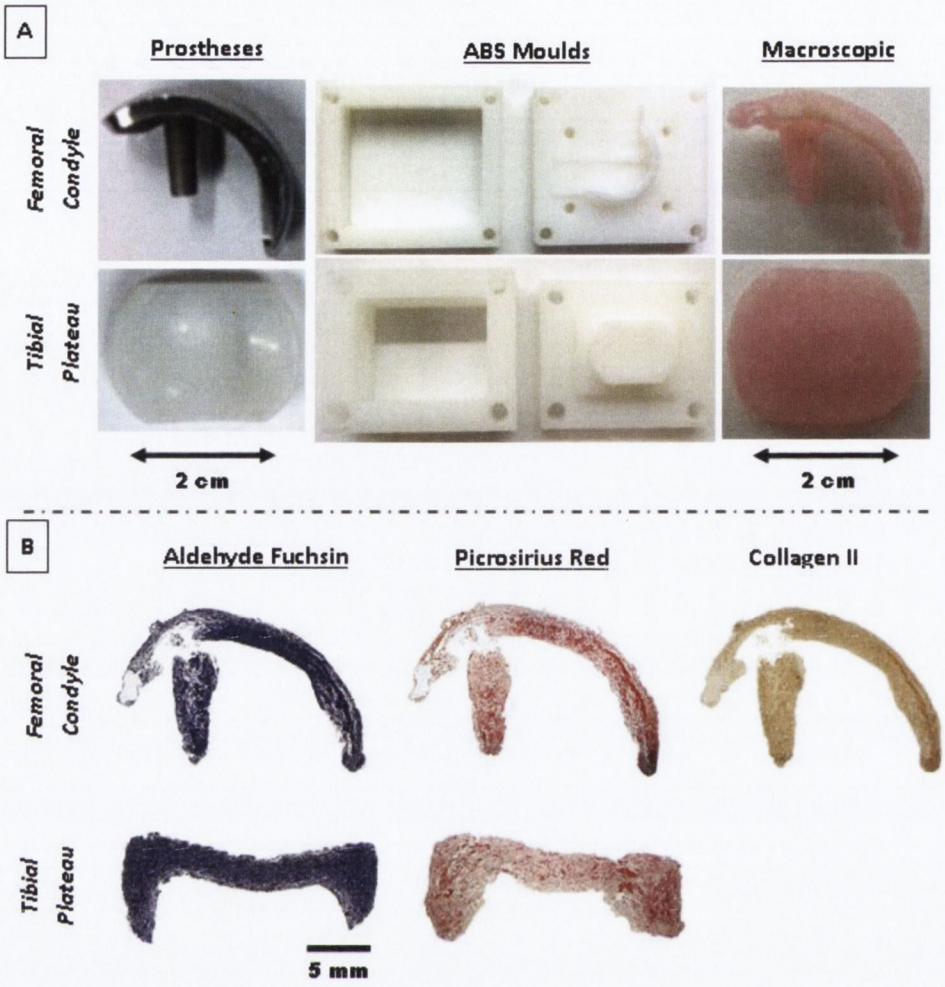

Figure 7-13: Creating scaled-up, anatomically shaped alginate constructs. (A) Prostheses of the femoral condyle and tibial plateau were used to create acrylonitrile butadiene styrene (ABS) reverse moulds, from which scaled-up, anatomically shaped BMSC seeded alginate constructs were created. (B) These constructs stained positively for sGAG (aldehyde fuchsin) and type II collagen.

Scaled-up osteochondral constructs were generated by covering the alginate hydrogel with a self-assembled layer (~2 cm diameter) of engineered cartilaginous tissue (generated using a co-culture of BMSCs & CCs) (Figure 7-14). After 6 weeks *in vitro* culture, the scaled-up osteochondral constructs were implanted subcutaneously into nude mice (Appendix Figure S11).

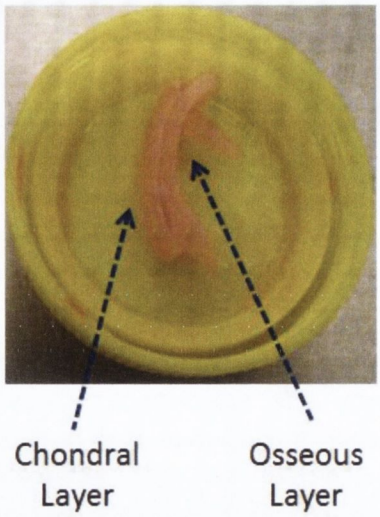

Figure 7-14: Scaled-up osteochondral construct in the shape of the femoral condyle at 6 weeks. These osteochondral constructs consisted of an osseous alginate base, and a self-assembled chondral layer.

After 8 weeks *in vivo* a layer of phenotypically stable cartilage remained on the top surface of the scaled-up anatomically shaped engineered implants (Figures 7-15A-D), bearing a resemblance to native articular cartilage. The chondral layer of these scaled-up constructs stained strongly for sGAG (Figure 7-15B) and type II collagen, with weak staining of collagen types I and X (Figure 7-15D).

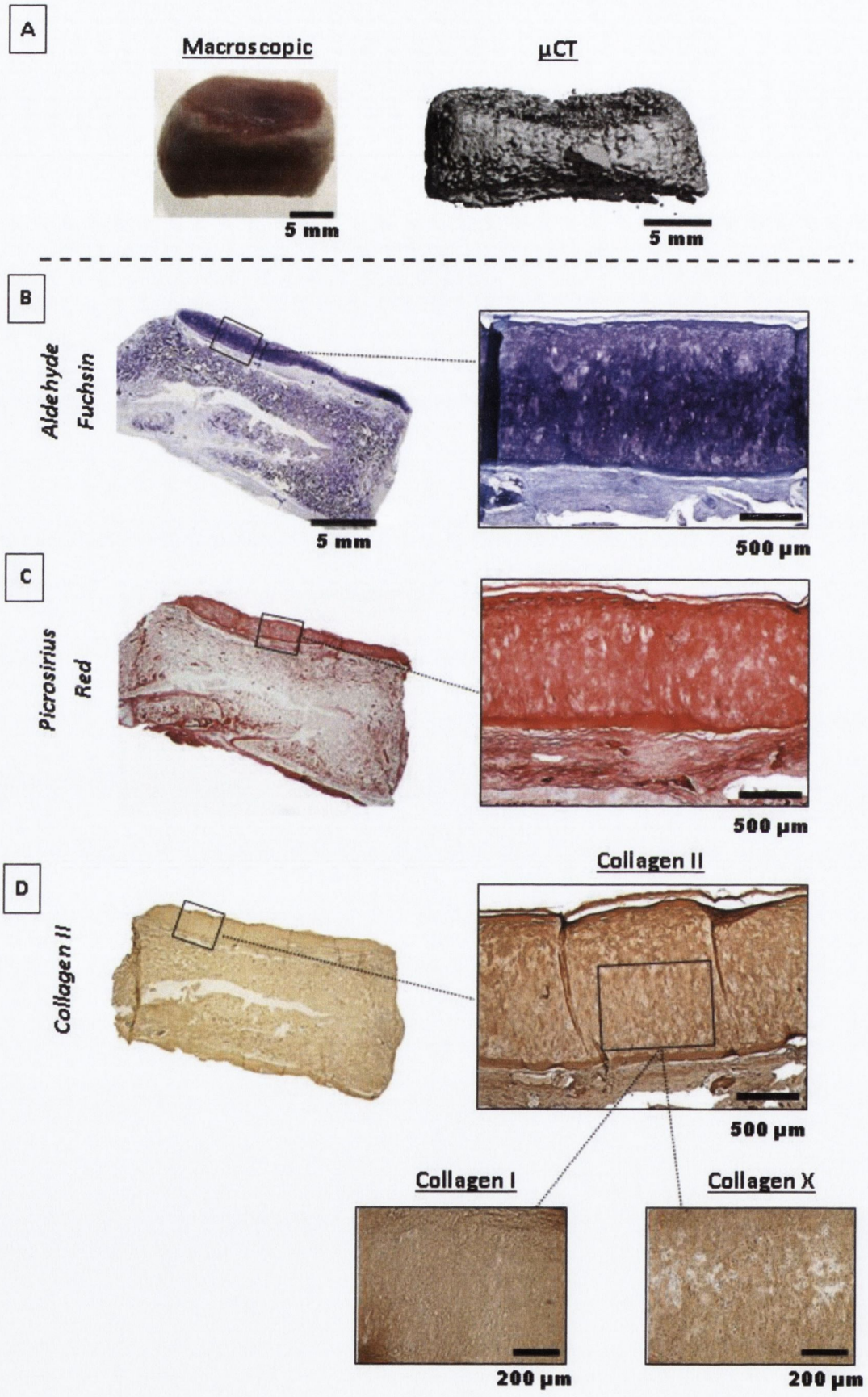
A
Macroscopic
µCT
5 mm
5 mm
B
Aldehyde Fuchsin
5 mm
500 µm
C
Picrosirius Red
500 µm
D
Collagen II
Collagen II
500 µm
Collagen I
Collagen X
200 µm
200 µm

Figure 7-15: Scaled-up osteochondral construct in the shape of the tibial plateau post-implantation. (A) Macroscopic image and μCT scan of construct. (B) Aldehyde Fuchsin staining with strong sGAG production in self-assembled chondral layer. (C) Picro-sirius red staining for collagen. (D) Collagen immunohistochemistry of anatomic osteochondral construct.

μCT analysis confirmed the deposition of mineral within the osseous region of the scaled-up constructs (Figure 7-15A). H&E staining also provided evidence of immature bone formation (Figure 7-16). Blood vessel structures were detected in these H&E stained samples. Finally, there was strong staining of collagen types I and X throughout the scaled-up alginate construct (Figure 7-16), which would suggest that bone was formed through the process of endochondral ossification.

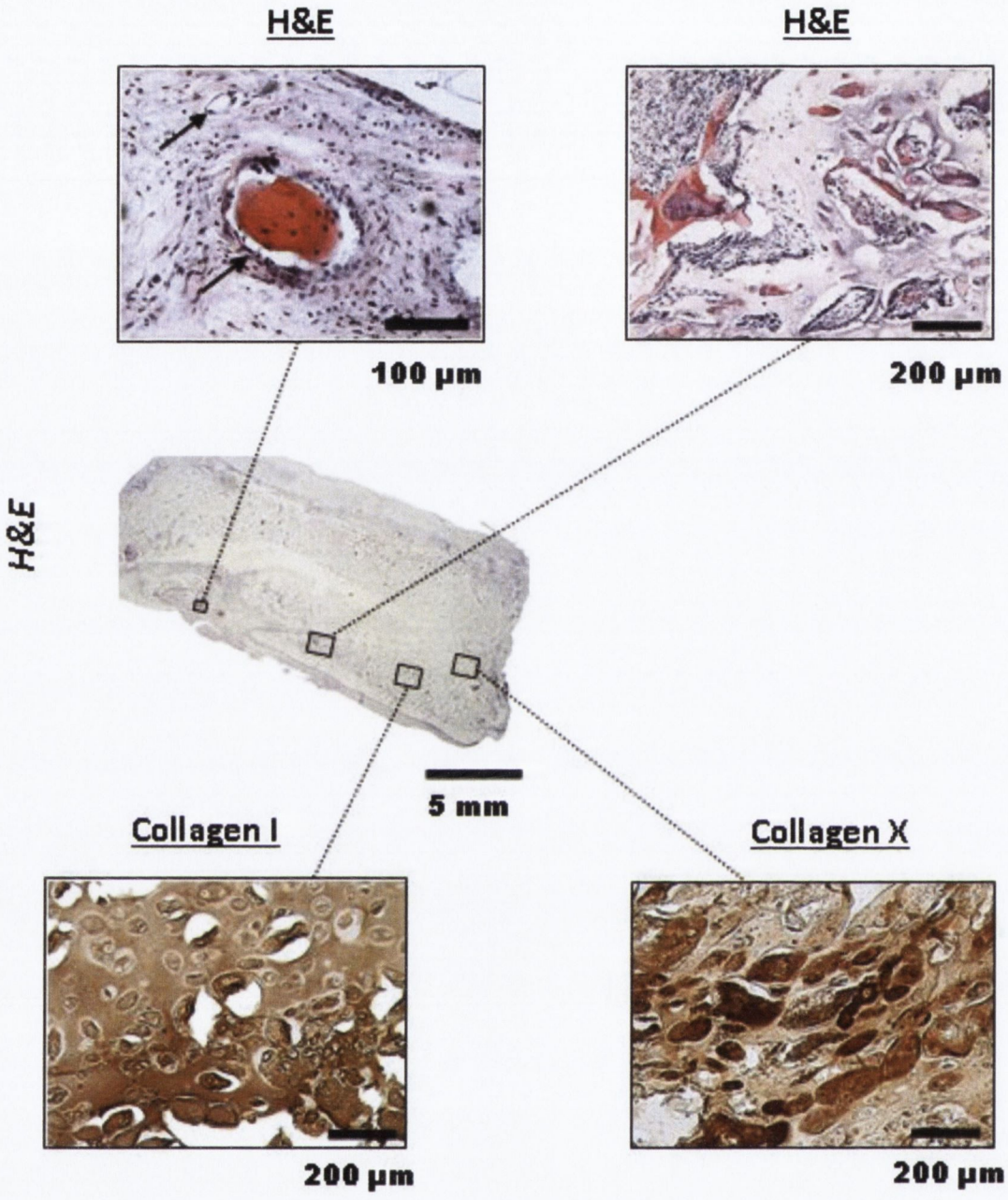

Figure 7-16: Analysis of scaled-up osseous alginate layer of osteochondral construct post-implantation. H&E staining of alginate layer and collagen types I and X immunohistochemistry of same. Arrows indicate blood vessel-like structures.

7.4 Discussion

The overall aim of this study was to tissue engineer scaled-up, geometrically accurate osteochondral constructs that ultimately could be used as an alternative to traditional metal and polymer joint replacement prostheses. To this end, it was first demonstrated that a BMSC seeded alginate hydrogel (5 mm diameter) could support endochondral bone formation *in vivo* to generate the osseous layer of an osteochondral construct. Focusing on the chondral layer next, it was found that unlike chondrocytes, a phenotypically stable layer of cartilage tissue could not be generated *in vivo* using MSCs. This occurred irrespective of whether the chondral layer was engineered using hydrogel encapsulation or using a scaffold-free or self-assembly approach (for both BMSCs and FPSCs). Interestingly, incorporating even a small number of chondrocytes (CCs) with a larger number of MSCs (either BMSCs or FPSCs) was shown to enhance the *in vitro* development of the chondral layer of the constructs, and critically lead to the generation of a phenotypically stable cartilage tissue *in vivo*. Co-culture led to the development of thicker, more homogeneous and more morphologically stable cartilage tissues with dramatically reduced mineralisation/calcification *in vivo*. In the final part of the study, scaled-up BMSC-seeded alginate constructs (~2 cm diameter) mimicking the geometry of the femoral and tibial components of a partial knee replacement prosthesis were generated from ABS moulds fabricated by rapid prototyping. These anatomic alginate constructs were covered by a self-assembled layer (~2 cm diameter) of engineered cartilaginous tissue (generated using a co-culture of BMSCs & CCs) to form scaled-up osteochondral constructs. After 6 weeks of *in vitro* culture, the scaled-up constructs were implanted subcutaneously into nude mice. After 8 weeks *in vivo*, a layer of phenotypically stable cartilage remained on the surface of the scaled-up engineered implant, bearing a resemblance to native articular cartilage. There was also evidence of mineralisation and immature bone development in the underlying osseous alginate layer.

The osseous layer of osteochondral constructs was generated by promoting endochondral ossification within an MSC seeded alginate hydrogel. We have previously shown that chondrogenically primed MSC seeded agarose constructs do

not degrade *in vivo*, thereby limiting the utility of this hydrogel for endochondral bone tissue engineering strategies (Sheehy et al., 2013). In contrast to agarose, the alginate hydrogel began to degrade *in vivo*, thereby facilitating vascularisation and bone formation. Future work will attempt to tailor the degradation kinetics of alginate hydrogels (through gamma-irradiation) to accelerate degradation *in vivo* (Alsberg et al., 2003, Simmons et al., 2004) in the hope that this in turn will facilitate more rapid endochondral bone formation.

Two strategies were used in forming the chondral layers of osteochondral constructs, namely agarose encapsulation and self-assembly (SA). The composition of the chondral layer of osteochondral constructs engineered *in vitro* through SA of BMSCs approached levels seen in immature articular cartilage (Mow et al., 1992, Gannon et al., 2012). Compared to agarose encapsulation, SA using either BMSCs or FPSCs led to the generation of a more cartilage-like articular layer *in vitro*. In spite of this, such chondral layers formed using MSCs alone failed to form phenotypically stable articular cartilage *in vivo*. In agreement to what has been observed previously (Dickhut et al., 2008, Vinardell et al., 2012b, Scotti et al., 2013, Sheehy et al., 2013), cartilage tissues engineered using BMSCs appeared to proceed down the endochondral pathway *in vivo*, with increased type X collagen expression and mineralisation of the engineered tissue. Engineering the chondral layer using FPSCs was also problematic, as it appeared to undergo fibrous dedifferentiation *in vivo*, as evidenced by the *in vivo* development of a tissue staining less intensely for sGAG and strongly for type I collagen, with no evidence of mineralisation.

In an attempt to engineer a more phenotypically stable cartilaginous construct, I next utilised a co-culture of CCs with either BMSCs or FPSCs (MSCs to CCs in 4:1 ratio) to engineer the chondral layer of osteochondral grafts. In agreement with previous studies, a mixed co-culture of CCs and MSCs was found to enhance cartilage specific extracellular matrix (ECM) deposition *in vitro* (Tsuchiya et al., 2004, Bian et al., 2011, Wu et al., 2011, Acharya et al., 2012, Wu et al., 2012, Meretoja et al., 2012). Previous studies have demonstrated that this is due to MSCs secreting factors that drive proliferation of the CC population (Wu et al., 2011, Wu et al., 2012, Acharya et al., 2012, Wu et al., 2013b). Co-culture led to the development of thicker, more homogeneous and more morphologically stable

cartilaginous constructs *in vivo* (compared to corresponding stem cell only groups) that better integrated with the underlying osseous layer. It also led to more robust chondrogenesis (increased sGAG and type II collagen accumulation) in chondral layers *in vivo*, in agreement with other subcutaneous *in vivo* studies (Liu et al., 2010, Sabatino et al., 2012, Dahlin et al., 2014a).

In addition to enhancing the biochemical development of the chondral layer of osteochondral constructs *in vitro*, co-culture also appeared to suppress hypertrophy within BMSC & CC co-cultured cartilaginous constructs, as shown by dramatic reductions in mineralisation (through alizarin red staining) and calcification of the co-cultured tissues compared to BMSC only chondral layers. Co-culture of BMSCs and CCs has been previously shown to suppress markers of BMSC hypertrophy *in vitro* (Fischer et al., 2010, Cooke et al., 2011, Aung et al., 2011, Acharya et al., 2012, Bian et al., 2011). Remarkably, co-culture also almost completely suppressed hypertrophy and mineralisation of the chondral layer *in vivo*. It has previously been speculated in such BMSC & CC co-cultures that the suppression of hypertrophy is mediated, at least in part, by CCs secreting parathyroid hormone-related protein (PTHrP) (Fischer et al., 2010). In addition, a relative increase in the ratio of CCs to MSCs due to the latter cell type releasing factors that increase CC proliferation (Wu et al., 2013b) would also be expected to reduce the over hypertrophic potential of the engineered tissue by increasing the ratio of phenotypically stable CC to hypertrophic BMSCs. In addition, it has been reported that in co-culture of BMSCs and CCs, the former cells die off over time (Wu et al., 2011, Meretoja et al., 2012), further increasing the ratio of CCs to BMSCs in the engineered tissue.

Previous studies have shown that a co-culture of BMSCs and CCs can supress hypertrophy *in vivo*, but this has only been for relatively small tissues engineered using relatively high ratios of CCs to MSCs (Fischer et al., 2010, Kang et al., 2012, Sheehy et al., 2013, Dahlin et al., 2014a). Although these *in vivo* results are important, they are limited in a translational sense due to the relatively small size of the engineered constructs (e.g. 1.5 mm diameter) and due to the fact that equal numbers of CCs to MSCs were required. To the best of my knowledge, my study is the first study demonstrating that co-culture can suppress hypertrophy and

endochondral bone formation *in vivo* using a much lower number of CCs relative to MSCs (4:1 ratio of MSCs to CCs) in a relatively large (5 mm diameter) construct. From a clinical perspective, using a smaller fraction of CC cells (to total cells) is highly desirable, as a limited number of healthy CCs are available in OA diseased joints. In addition, my study also shows that this inhibitory effect of co-culture on hypertrophy translates to much larger cartilaginous constructs of a clinically relevant size (~2 cm diameter).

Apart from the aforementioned clinical advantage of using a small number of CCs in a mixed co-culture set-up, there is also a more subtle advantage in the context of osteochondral tissue engineering. During previous endeavours in our lab to engineer osteochondral constructs, it was discovered that the chondral layer of CCs in structured bilayered co-culture constructs (chondral layer consisting only of CCs at 20 million cells/mL; osseous layer consisting only of BMSCs) suppressed hypertrophy and mineralisation of the BMSCs located adjacent to the interface of the tissue (Sheehy et al., 2013). While this anti-hypertrophic effect of co-culture is advantageous for cartilage tissue engineering, it is obviously detrimental for endochondral bone tissue engineering. However, my study found that using a co-culture of MSCs and CCs in a 4:1 ratio (at a typical seeding density of 20 million total cells/mL for example) is sufficient to drastically reduce hypertrophy within the chondral cartilage layer, whilst not having any noticeable effect on mineralisation or bone formation within the underlying osseous alginate layer. This is probably due to the much lower number of CCs present, and subsequently lower concentration of factors they release. No differences were found in bone formation in the osseous layers of osteochondral constructs (with MSC&CC co-culture chondral layers) compared to single layered MSC alginate control constructs (data not shown).

The final phase of the study demonstrated that it is possible to scale-up tissue engineering approaches to generate biological osteochondral implants of a clinically relevant size. Previous studies have generated scaled-up cartilaginous constructs of clinically relevant dimensions (Hung et al., 2003, Santoro et al., 2010, Ding et al., 2013), but these studies used only chondrocytes to form the cartilage layer. As the availability of healthy CCs is limited in OA sufferers, this study importantly shows that scaled-up, phenotypically stable cartilaginous constructs can be formed using a

small number of CCs mixed with a much larger number of MSCs. In addition, previous attempts to engineer scaled-up endochondral bone using BMSC seeded collagen mesh scaffolds resulted in the development of a core region of constructs devoid of cells and matrix (Scotti et al., 2013), highlighting the importance of utilising a suitable scaffold material when engineering such large constructs.

The osseous region of the scaled-up implants was formed from moulds created using scans taken of existing prostheses. There are a number of different approaches proposed in the literature to form the osseous region of such osteochondral constructs. For example, devitalised trabecular bone disks in the shape of a human patella have been used (Hung et al., 2003). Furthermore, osteogenically primed BMSC-seeded poly-ε-caprolactone/hydroxyapatite composites have been used to form the osseous layer of osteochondral constructs mimicking both the proximal tibial joint condyle (Lee et al., 2009) and the femoral condyle (Ding et al., 2013). Osteogenically primed BMSC-seeded poly (ethylene glycol)-based hydrogels have also been used (Alhadlaq et al., 2004, Alhadlaq and Mao, 2005). In this study, the osseous layer of the scaled-up osteochondral constructs was developed through endochondral ossification of chondrogenically primed MSCs. In theory, the inherent advantage of the endochondral route for engineering such scaled-up grafts is that CCs are inherently capable of surviving the low oxygen, nutrient deprived conditions that would exist in such scaled-up anatomic constructs. Developmentally, all long bones derive from a cartilaginous pre-cursor, making recapitulation of such processes an appealing route to bone regeneration. The moulding technique used in this study is transferable to any geometry, suggesting that this approach could be used in regeneration of any joint.

Overall, this study provides a framework for tissue engineering biological joint replacement prostheses for regenerating damaged/diseased joints. Clearly a number of challenges remain, including confirmation of efficacy of this approach within a load bearing orthotopic environment and implementation of this approach using diseased human MSCs. If these challenges can be overcome, however, it opens up the potential of a therapeutic solution for the millions of people suffering from OA worldwide.

8 Discussion

8.1 Introduction

The objective of this thesis was to tissue engineer a scaled-up anatomically shaped, osteochondral construct that could potentially be used to replace the articulating surface of a synovial joint. This involved developing a scalable approach to simultaneously engineer both articular cartilage and bone using readily available cell sources. Generating anatomically shaped grafts mimicking the articulating surface of damaged joints was also essential. The thesis began by investigating if dynamic compression in combination with modified scaffold architecture could result in enhanced, homogeneous cartilage formation, as a means of engineering scaled-up, functional cartilaginous constructs of a clinically relevant size. Dynamic compression was found to significantly increase sGAG synthesis in solid chondrocyte (CC) seeded agarose hydrogels, but the introduction of nutrient channels was found to have a detrimental effect on cartilage formation within constructs. Cartilage extracellular matrix (ECM) accumulation was generally quite low in agarose hydrogels, at least when compared to typical native articular cartilage values. Therefore, a comparison of self-assembly and agarose encapsulation was next investigated as a means to engineer functional cartilaginous grafts using culture expanded CCs. When normalized to wet weight, self-assembled constructs exhibited significantly higher levels of collagen accumulation, with a tissue architecture and a ratio of collagen to sGAG content more closely resembling native articular cartilage. Only a limited number of therapeutically useful chondrocytes (CCs) can be isolated from diseased joints. The next phase of this thesis therefore investigated whether cartilage-like grafts could be engineered through self-assembly of infrapatellar fat pad-derived mesenchymal stem cells (FPSCs). Self-assembly of FPSCs led to the formation of a dense cartilaginous tissue, with cartilage ECM accumulation approaching native cartilage values. An alternative strategy to using CCs or mesenchymal stems cells (MSCs) alone is to use a co-culture of CCs and MSCs to generate cartilage. This was next examined with the results demonstrating that co-

culture can lead to increased proliferation and cartilage matrix synthesis compared to monoculture controls. In the final part of the thesis, the generation of scaled-up anatomically shaped osteochondral constructs was investigated. Tissue engineered osteochondral grafts (~2 cm diameter) mimicking the geometry of the medial femorotibial joint were generated from moulds fabricated by rapid prototyping. It was found that a chondrogenically primed MSC seeded alginate hydrogel could support endochondral bone formation *in vivo*, and furthermore, that a phenotypically stable layer of articular cartilage could be engineered over this bony tissue using self-assembly of CCs and MSCs.

8.2 Strategies to tissue engineer scaled-up cartilage grafts

The thesis began by investigating if dynamic compression in combination with modified scaffold architecture could result in enhanced, homogeneous cartilage formation, as a means of engineering scaled-up functional cartilaginous constructs of a clinically relevant size (chapter 3). Scaffold architecture of constructs was modified by the introduction of nutrient channels throughout cell seeded hydrogels. Dynamic compression was found to significantly increase sGAG synthesis in solid CC seeded agarose hydrogels, and preferentially increase collagen accumulation in regions of constructs where FE modelling predicted highest levels of fluid flow. The introduction of nutrient channels, however, was found to have a detrimental effect on cartilage formation within constructs. Overall, it was observed that cartilage extracellular matrix (ECM) accumulation was quite low in agarose hydrogels (maximum sGAG levels of approximately 0.7 %w/w; maximum collagen levels of approximately 0.3 %w/w), at least when compared to typical native articular cartilage values (4-7 %w/w sGAG; 15-22 %w/w collagen (Mow et al., 1992)). Therefore, this thesis next compared a self-assembly (or scaffold-free) approach to agarose hydrogel encapsulation as a means to engineer functional cartilaginous grafts using culture expanded CCs (chapter 4).

From a tissue engineering perspective, the self-assembly (SA) method has many advantages compared to cell culturing techniques involving scaffolds such as hydrogels. SA can circumvent many scaffold-related issues, such as stress shielding of cells from biophysical stimulation, poor cell attachment, toxic scaffold

degradation products, inflammatory response to the implanted material, poorly controlled biodegradability and a reduction in cell to cell communication, amongst others (Temenoff and Mikos, 2000a, Hutmacher, 2000, Bryant et al., 2004a, Liu and Ma, 2004, Hu and Athanasiou, 2006b, Elder et al., 2009, Tran et al., 2011, Athanasiou et al., 2013, Kharkar et al., 2013). The SA approach is also simple to scale-up; simply seeding larger number of cells over a wider area enables the engineering of scaled-up tissues. The objective of chapter 4 was to directly compare the SA approach to agarose hydrogel encapsulation (AE) as a means to engineer functional cartilaginous grafts. No other studies to date have been undertaken to achieve this. After forming tissue engineered constructs through either SA or agarose encapsulation of CCs, it was observed (at high seeding densities) that total sGAG and collagen synthesis was greater with agarose encapsulation than SA. When normalized to wet weight however, self-assembled constructs exhibited significantly higher levels of collagen accumulation compared to agarose hydrogels. Furthermore, self-assembly appeared to lead to the faster generation of a more hyaline-like tissue, with a tissue architecture and a ratio of collagen to sGAG content more closely resembling native articular cartilage. It was noted that collagen type II staining was more intense in superficial regions of self-assembled constructs, which is similar to native articular cartilage where staining is generally highest in the superficial tangential zone. Clustering of chondrocytes was also observed in the deeper zones of the SA tissues. The results of this study provided strong support for the use of the SA approach when attempting to engineer functional cartilaginous grafts for clinical applications.

Chapter 4 identified self-assembly of CCs as a means of engineering scalable cartilaginous grafts. However, there are many inherent limitations associated with the use of CCs for cartilage tissue engineering, such as the lack of available healthy donor cartilage for harvesting cells in older or diseased patients and dedifferentiation of CCs during culture expansion. Therefore, the objective of chapter 5 was to attempt to engineer cartilage-like grafts through self-assembly of infrapatellar fat pad-derived mesenchymal stem cells (FPSCs). This is the first reported work in the literature to investigate if FPSCs can be used to engineer cartilage-like tissues through a SA process. Self-assembled cartilaginous tissues

were first engineered by geometrically confining FPSCs on tissue culture plastic, and then either continuously or transiently supplementing these constructs with transforming growth factor-β3 (TGF-β3). Transient supplementation with TGF-β3 (for the first 21 days of culture) enhanced the development of self-assembled grafts, with sGAG accumulation reaching levels of 8.4±1.5 %w/w after 6 weeks of culture. While overall levels of matrix synthesis were higher with AE compared to SA (as seen with chondrocytes in chapter 4), when normalized to tissue wet weight, ECM accumulation was significantly greater in the lighter SA constructs. SA on polyethylene terephthalate (PET) transwell membranes was found to lead to the development of morphologically stable and homogenous tissues. At high seeding densities, SA on such transwell membranes led to the formation of geometrically uniform constructs that underwent minimal contraction during culture. Overall, the results of this chapter demonstrated that a SA process could be used to engineer cartilage-like tissues using FPSCs, an easily accessible and clinically relevant cell source. SA resulted in the formation of a denser cartilaginous tissue than AE, with SA cartilage ECM accumulation approaching values previously reported for native articular cartilage (Gannon et al., 2012, Mow et al., 1992). Since completing this study, further work in our lab has demonstrated that the SA approach can also be used to engineer cartilage grafts using diseased human FPSCs, and furthermore, that cartilage grafts of clinically relevant dimensions can be engineered using such cells (Liu et al., 2014).

8.3 Co-culture as a means to tissue engineer functional, phenotypically stable articular cartilage

As an alternative strategy to using CCs or mesenchymal stems cells (MSCs) alone, chapter 6 investigated if a co-culture of CCs and MSCs could be used to generate a more cartilaginous graft *in vitro*. To this end, MSCs were either self-assembled on top of CC laden agarose gels (termed a *structured* co-culture), or were first mixed with CCs before being embedded in an agarose hydrogel (termed a *mixed* co-culture). Both infrapatellar fat pad-derived stem cells (FPSCs) and bone marrow-derived MSCs (BMSCs) were used as a source of progenitor cells. A mixed co-

culture of FPSCs and CCs was found to reduce construct DNA, sGAG and collagen content when compared to appropriate single cell only controls. In contrast, a mixed co-culture of BMSCs and CCs led to increased proliferation and sGAG and collagen accumulation. Of note was the finding that a structured co-culture, at the appropriate cell density, led to greater sGAG accumulation than a mixed co-culture for both sources of MSCs. CCs in the hydrogel layer of the structured co-culture groups proliferated more and synthesised greater levels of cartilage than monoculture CCs embedded in control hydrogels, leading to significantly greater levels of matrix accumulation. Increasing the number of MSCs in the superficial layer of structured co-culture constructs was found to not have a dramatic effect on the underlying CCs in terms of overall sGAG and collagen accumulation.

A well-documented limitation associated with the use of MSCs for cartilage tissue engineering is their failure to form phenotypically stable cartilage tissue *in vivo* (Pelttari et al., 2006, Pelttari et al., 2008b, Farrell et al., 2009, Farrell et al., 2011, Vinardell et al., 2012b). Therefore, as might be expected, in Chapter 7 it was found that unlike CCs, a phenotypically stable layer of cartilage tissue could not be generated *in vivo* using MSCs. This occurred irrespective of whether the chondral layer was engineered using either hydrogel encapsulation or a scaffold-free or self-assembly approach (or indeed if this chondral layer was engineered using BMSCs or FPSCs). Interestingly, incorporating a small number of chondrocytes (CCs) with a larger number of MSCs (either BMSCs or FPSCs) was shown to not only enhance the *in vitro* development of the chondral layer of the constructs, but critically lead to the generation of a phenotypically stable cartilage tissue *in vivo*. Co-culture led to the development of thicker, more homogeneous and more morphologically stable cartilage tissues with dramatically reduced mineralisation/calcification *in vivo*. From a cartilage tissue engineering perspective, this was a very significant result, namely that co-culture of CCs and MSCs could dramatically reduce mineralisation of the chondral phase of engineered grafts *in vivo*, using a large numbers of MSCs relative to CCs in relatively large constructs.

8.4 Tissue engineering scaled-up, anatomically shaped osteochondral constructs

The aim of chapter 7 was to bring all the previous work together, in order to tissue engineer a scaled-up, anatomically shaped osteochondral construct suitable for partial or total joint resurfacing. As part of the study, two strategies were explored to engineer phenotypically stable cartilage tissue *in vivo* using stem cells. First, it was investigated whether cartilage engineered *in vitro* using a scaffold-free or self-assembly approach could lead to the development of more phenotypically stable cartilage *in vivo*. Secondly, as was already discussed, it was investigated whether a co-culture of CCs and either BMSCs or FPSCs could engineer a layer of phenotypically stable articular cartilage as part of an osteochondral construct *in vivo*. To engineer bone *in vivo*, it was hypothesised that this could be achieved in part by recapitulating key aspects of normal bone and joint development, specifically the process of endochondral ossification where a cartilaginous intermediary is replaced by bone.

The chondral layer of scaled-up osteochondral constructs was formed through the self-assembly (SA) approach, as opposed to agarose encapsulation (AE). This decision was based on data shown in chapter 7 and in previous chapters, demonstrating that SA results in the formation of denser cartilaginous constructs accumulating greater levels of sGAG and collagen than AE tissues, when normalised to wet weight. SA was also shown to lead to the faster generation of a more hyaline-like tissue, with a tissue architecture and a ratio of collagen to sGAG content more closely resembling native articular cartilage in earlier chapters, motivating its use in chapter 7 to generate scaled-up chondral layers.

This scaled-up self-assembled chondral layer was formed using a co-culture of CCs and BMSCs (in a MSC:CC ratio of 4:1). It can be seen from *in vitro* biochemical data (chapter 7) that self-assembled layers (5 mm diameter) formed using a co-culture of BMSCs and CCs accumulated similar levels of sGAG and collagen to self-assembled layers formed using a co-culture of FPSCs and CCs. Therefore, scaled-up self-assembled chondral layers were formed utilising BMSCs (and CCs) instead of FPSCs to minimise the number of cell sources needed in

generating osteochondral constructs. As BMSCs are essential for forming the endochondral bony tissue layer in the osseous component of osteochondral constructs, it makes more sense, from an economic standpoint, to use BMSCs (in co-culture with CCs) to form phenotypically stable cartilage in the chondral layer, rather than FPSCs. From a clinical perspective, isolating only BMSCs and CCs from a patient would be much more appealing than having to isolate FPSCs, BMSCs and CCs.

In the final part of chapter 7, scaled-up BMSC seeded alginate tissues (~2 cm diameter) mimicking the geometry of the femoral and tibial components of a partial knee replacement prosthesis were generated from ABS moulds fabricated by rapid prototyping. These anatomic alginate constructs were covered by a self-assembled layer (~2 cm diameter) of engineered cartilaginous tissue (generated using a co-culture of BMSCs & CCs as discussed) to form scaled-up osteochondral constructs. After 8 weeks *in vivo*, a layer of phenotypically stable self-assembled cartilage remained on the surface of these scaled-up engineered implants, which resembled native articular cartilage. There was also evidence of mineralisation and endochondral bone development in the underlying osseous alginate layer.

In summary, this thesis provides a novel framework for tissue engineering biological joint replacement prostheses that could potentially regenerate damaged/diseased joints. If certain challenges can be overcome, it opens up the potential of a therapeutic solution for the millions of people suffering from OA worldwide.

8.5 Bone marrow or infrapatellar fat pad derived multipotent stem cells for cartilage tissue engineering?

There were some interesting differences found between stem cells from different sources (and differences in how they interacted with chondrocytes and scaffold type) in chapters 6 and 7 of this thesis. As stated earlier, it can be seen from *in vitro* biochemical data in chapter 7 that self-assembled layers (5 mm diameter) formed using a co-culture of BMSCs and CCs accumulated similar levels of sGAG and

collagen to self-assembled layers formed using a co-culture of FPSCs and CCs. This was also true for BMSC only and FPSC only self-assembled layers, with no differences found between the two stem cell layers in terms of sGAG and collagen accumulation. So co-culture was found to have an equally positive effect on both stem cell types in the self-assembly model.

Looking at agarose *in vitro* data (also chapter 7), we can see that for both sGAG and collagen accumulation, the BMSC-CC co-culture group accumulated greatest levels. Greater levels of sGAG accumulation were observed in agarose hydrogels seeded with FPSCs only compared to BMSC only constructs, with no differences in collagen accumulation observed. Overall, in agarose culture, co-culture of BMSCs and CCs had a very positive effect on cartilage ECM accumulation (compared to BMSC only controls), while there were no dramatic differences between FPSC-CC co-culture constructs and FPSC controls (in terms of cartilage ECM accumulation). So co-culture of FPSCs and CCs had much less of an effect on chondrogenesis in agarose constructs than in SA.

If we go back to look at the mixed agarose co-culture of chapter 6, some interesting similarities and differences arise. For a mixed co-culture of BMSCs and CCs in agarose, the total sGAG and collagen content of the construct was higher than the sum of independent monocultures for both BMSC seeding densities. In contrast, sGAG and collagen content of FPSC-CC mixed co-culture constructs was lower than independent controls combined. Agarose hydrogels seeded with 2 million FPSCs accumulated greatest levels of sGAG, significantly higher than corresponding BMSC only constructs. Absolute levels of sGAG accumulation were also higher with FPSC monoculture constructs at the low seeding density compared to BMSC alone.

Taken together, the results of chapters 6 and 7 first indicate that FPSCs synthesise greater amounts of cartilaginous ECM than BMSCs, at least in the agarose model. Indeed, this is in agreement with previous agarose studies (Vinardell et al., 2011, Vinardell et al., 2012b). Mixed co-culture of BMSCs and CCs within agarose (and within SA constructs) was found to dramatically increase cartilage ECM production in both studies, whilst reduced sGAG and collagen accumulation

was observed with mixed co-cultured FPSCs in chapter 6 (in the agarose model), and only small increases were observed with mixed co-cultured FPSC agarose constructs in chapter 7 (*in vitro* arm of *in vivo* study). In both studies it is clear that co-culture has a much more positive effect on BMSCs than FPSCs, in terms of cartilage matrix production (in the agarose model). As mentioned in the discussion of chapter 6, it is likely that the beneficial effects of co-culture in BMSC-CC constructs are due to BMSCs secreting growth factors that lead to increased proliferation and cartilage synthesis of CCs (Wu et al., 2011, Wu et al., 2012, Wu et al., 2013b). Interestingly, in a structured co-culture FPSCs were found to drive proliferation of underlying CCs. Furthermore, both FPSCs and BMSCs enhanced matrix synthesis of CCs (on a per cell basis) in a structured co-culture, demonstrating that both stem cell types can release factors to drive both CC proliferation and increased sGAG and collagen synthesis.

One explanation for all these results could be differences in nutrient availability in the different co-culture configurations that are leading to alterations in CC proliferation and matrix synthesis within these systems. Given that FPSCs are more biosynthetically active than BMSCs in agarose, as evident by generally higher levels of matrix accumulation in monoculture, it could be that too many cells are competing for limited nutrient resources in FPSC mixed co-culture agarose groups, thereby lowering cell viability and/or proliferation. The fact that this does not happen in FPCS-CC structured co-culture constructs (chapter 6) or FPSC-CC mixed self-assembled constructs (chapter 7) could be due to the phenotype of FPSCs being different when self-assembled as opposed to when encapsulated within the body of gels. This would likely alter the FPSC metabolic phenotype, potentially altering nutrient availability to the CC cells of associated co-culture constructs. Greater FPSC-FPSC communication in self-assembled co-culture constructs due to their close physical proximity may be important for maximizing the trophic effect they exert on CCs. Future studies should try to unravel this.

8.6 Limitations of the study

The fact that chondrocytes (CCs), BMSCs and FPSCs used throughout this thesis were obtained from the femoropatellar joints of 4 month old pigs might be considered a limitation of the work. At this age such animals have not reached skeletal maturity. Cells from such tissue would probably be more adept at producing cartilage-specific ECM than cells obtained from an older donor. Indeed, this has been shown to be the case for both bovine CCs and BMSCs, with older cells displaying a diminished capacity to produce functional cartilaginous ECM (Tran-Khanh et al., 2005, Erickson et al., 2011). A diminished capacity of aged cells to form cartilage has also been shown for human CCs (Barbero et al., 2004) and human BMSCs (Payne et al., 2010). In addition, BMSCs isolated from patients suffering from OA have been shown to exhibit a reduced chondrogenic activity compared to healthy cells (Murphy et al., 2002), although results from our lab suggest FPSCs maintain their chondrogenic capacity in disease (Liu et al., 2014). Therefore, the fact that tissue engineered constructs were formed from cells obtained from young porcine donors instead of elderly, diseased human-derived cells (such as those typically derived from sufferers of OA, whom these treatments are primarily aimed at) could be considered a limitation of the thesis.

As with many tissue engineering studies, cells were expanded and differentiated in high glucose (25mM) culture medium. One possible implication of this could be hyperglycaemic conditions leading to the copious production of hyaluronic acid (HA) (Wang et al., 2011). As rapid sGAG synthesis has been hypothesised to be an impediment to collagen production (Bian et al., 2009c), this additionally produced HA could inhibit collagen production of the tissue engineered constructs. This could be a potential limitation of the *in vitro* culturing approach used in this thesis. Future studies could explore the influence of altered glucose conditions on tissue engineered cartilage.

Mechanical testing of engineered tissues was not reported in this thesis, which could be considered a limitation of the work. The non-uniform shape of self-assembled tissue led to varying and possible unreliable mechanical testing results in pilot studies, and such tests were not undertaken as part of the main studies. It was

observed that because of their slightly irregular shape significant variability was obtained between self-assembled constructs tested. Future studies should explore the use of optical techniques to determine strain levels in such tissues and hence their mechanical properties (Wang et al., 2003).

One strategy to successfully engineer endochondral bone *in vivo* is to use BMSC seeded alginate hydrogels incorporated with growth factors, such as BMP-2 and TGF-β3 (Simmons et al., 2004). The use of such growth factor delivery strategies could potentially overcome the need for expensive *in vitro* cell culture protocols. In addition, alginate can be subjected to gamma-irradiation to accelerate degradation rates *in vivo*, and can be covalently modified with RGD-containing peptides to control cell behaviour. Both modifications might be expected to lead to enhanced vascularization and/or endochondral bone formation *in vivo*. The fact that no such strategies (for example, incorporation of growth factors and/or gamma-irradiation of alginate) were utilised in this thesis for bone tissue engineering purposes could be considered a limitation of the work.

In this thesis, engineered osteochondral constructs were implanted into a subcutaneous environment. The fact that such constructs were not implanted into a load-bearing orthotopic environment could be considered a limitation of the work. The treatment and regeneration of damaged synovial joints in the body would require the use of tissue engineered grafts capable of withstanding a certain load threshold. Therefore, testing of osteochondral engineered grafts in a load-bearing orthotopic environment would be desirable. The fact that osteochondral constructs were implanted into nude mice is also a limitation of the work. Larger animal studies would be desirable in the future, ideally using a host that was not immunocompromised.

From a clinical perspective, the 6 week *in vitro* culture period used for priming scaled-up osteochondral constructs could be considered too long a waiting time before implantation of the tissue engineered implant (and could therefore be considered a limitation). Strategies to shorten this timeframe (or eliminate it completely) will likely be attempted in the future (see future work section). Ideally,

only one surgery would be required to implant a tissue engineered joint replacement construct.

8.7 Conclusions

- Dynamic compression can significantly increase sGAG synthesis in solid chondrocyte (CC) seeded agarose hydrogels, but the introduction of nutrient channels has a detrimental effect on cartilage formation within constructs.
- When normalized to wet weight, self-assembled constructs exhibit significantly higher levels of collagen accumulation compared to agarose hydrogels. Furthermore, self-assembly appears to lead to the faster generation of a more hyaline-like tissue, with a tissue architecture and a ratio of collagen to sGAG content more closely resembling native articular cartilage.
- As an alternative to using CCs, cartilage-like grafts can be engineered through self-assembly of infrapatellar fat pad-derived mesenchymal stem cells (FPSCs), with such grafts forming a dense cartilaginous tissue with cartilage ECM accumulation approaching native cartilage values.
- Co-culture of CCs and mesenchymal stem cells (MSCs) can lead to increased proliferation and cartilage matrix synthesis compared to monoculture controls.
- Chondrogenically primed MSC seeded alginate hydrogels can support endochondral bone formation within an osteochondral construct *in vivo*, and furthermore, a phenotypically stable layer of articular cartilage can be engineered over this bony tissue using self-assembly of CCs and MSCs.
- This osteochondral approach can be scaled-up in order to create anatomically shaped osteochondral constructs of a clinically relevant size, mimicking the geometry of medial femorotibial joint replacement prostheses (generated from moulds fabricated by rapid prototyping).
- This thesis provides a novel framework for tissue engineering biological joint replacement prostheses that could potentially regenerate damaged joints. If certain challenges can be overcome, it opens up the potential of a therapeutic solution for the millions of people suffering from OA worldwide.

8.8 Future Work

A key question that remains unanswered is how these scaled-up osteochondral constructs would fare within a load bearing orthotopic environment, as opposed to the ectopic environment presented in this thesis. Future work should include confirmation of efficacy of this approach within such a load bearing orthotopic environment.

The osseous layer of osteochondral constructs was generated by promoting endochondral ossification within an MSC seeded alginate hydrogel. Using gamma-irradiation on alginate has been shown to decrease the size of the polymer chains (and decrease the molecular weight) thus leading to increased degradation rates *in vivo* (Simmons et al., 2004). More rapidly degrading gels typically lead to increased bone formation, both in terms of quality and quantity (Alsberg et al., 2003). Future work should therefore attempt to tailor the degradation kinetics of alginate hydrogels (through gamma-irradiation) to accelerate degradation *in vivo* (Alsberg et al., 2003, Simmons et al., 2004) in the hope that this in turn will facilitate more rapid vascularisation and endochondral bone formation *in vivo*.

Future studies should also attempt to reinforce the osseous hydrogel base before implantation into a load bearing environment. One option for this would be to utilise 3D bioprinting technologies to first create a "skeleton" of polycaprolactone (PCL) fibres (or another biocompatible polymer) forming the outline of an anatomically shaped construct, and to then to fill this scaled-up PCL scaffold with an interpenetrating network of MSC seeded alginate hydrogel using layer-by-layer deposition. The alginate would be allowed to cross-link in the presence of calcium chloride. The 3D-Bioplotter® System (EnvisionTEC) is one rapid prototyping tool which could be used to create cell seeded printed composite constructs in this manner. These PCL reinforced alginate constructs would be able to withstand much larger initial forces *in vivo* and this would allow implantation of these constructs within a shorter timeframe (as opposed to the current 6 week *in vitro* culture period). Future studies should also involve the controlled spatial release of growth factors *in vivo*, in an attempt to improve bone and cartilage formation. This could be achieved through the incorporation of gelatin microspheres throughout osteochondral

constructs containing various growth factors (BMP-2, VEGF and TGF-β3 for example). This approach could also shorten the time required pre-implantation for *in vitro* priming of constructs.

In this study, porcine bone marrow-derived MSCs were used to form bone in the osseous alginate base, whilst these cells in combination with porcine CCs were used to form the scaled-up chondral layer of osteochondral constructs. Future work should involve implementation of this approach using diseased human adult MSCs.

CCs in OA cartilage typically produce cartilage-degrading enzymes, such as MMP13 and aggrecanases (Van der Kraan and Van den Berg, 2012). Future studies should investigate if a co-culture of MSCs and CCs from a diseased joint can reduce expression of these cartilage-degrading enzymes compared to CC only culture.

The non-uniform shape of self-assembled tissue led to varying and possible unreliable mechanical testing results in pilot studies, and such tests were not undertaken as part of the main studies. Future studies should use labelled cells as markers of deformation during micro-mechanical testing to determine the local levels of strain and hence determine the spatial mechanical properties of these engineered tissues.

Future studies should also explore whether cartilage grafts with zonal features typical of normal articular cartilage are generated using the strategies proposed in this thesis. For example, it would be important to investigate if lubricin is present in the superficial zone of self-assembled constructs. Also, scanning electron microscopy (SEM) should be performed to investigate the matrix organization of self-assembled tissues, and to compare this to native articular cartilage.

References

2008. Manual (MarcA)

ACHARYA, C., ADESIDA, A., ZAJAC, P., MUMME, M., RIESLE, J., MARTIN, I. & BARBERO, A. 2012. Enhanced chondrocyte proliferation and mesenchymal stromal cells chondrogenesis in coculture pellets mediate improved cartilage formation. *Journal of Cellular Physiology,* 227**,** 88-97.

ADKISSON IV, H. D., GILLIS, M. P., DAVIS, E. C., MALONEY, W. & HRUSKA, K. A. 2001. In vitro generation of scaffold independent neocartilage. *Clinical Orthopaedics and Related Research***,** S280-S294.

AHMED, N., DREIER, R., GÖPFERICH, A., GRIFKA, J. & GRÄSSEL, S. 2007. Soluble signalling factors derived from differentiated cartilage tissue affect chondrogenic differentiation of rat adult marrow stromal cells. *Cellular Physiology and Biochemistry,* 20**,** 665-678.

ALBRO, M. B., LI, R., BANERJEE, R. E., HUNG, C. T. & ATESHIAN, G. A. 2010b. Validation of theoretical framework explaining active solute uptake in dynamically loaded porous media. *Journal of Biomechanics,* 43**,** 2267-2273.

ALHADLAQ, A., ELISSEEFF, J. H., HONG, L., WILLIAMS, C. G., CAPLAN, A. I., SHARMA, B., KOPHER, R. A., TOMKORIA, S., LENNON, D. P., LOPEZ, A. & MAO, J. J. 2004. Adult stem cell driven genesis of human-shaped articular condyle. *Annals of Biomedical Engineering,* 32**,** 911-923.

ALHADLAQ, A. & MAO, J. J. 2005. Tissue-engineered osteochondral constructs in the shape of an articular condyle. *Journal of Bone and Joint Surgery - Series A,* 87**,** 936-944.

ALLON, A. A., AUROUER, N., YOO, B. B., LIEBENBERG, E. C., BUSER, Z. & LOTZ, J. C. 2010. Structured coculture of stem cells and disc cells prevent disc degeneration in a rat model. *Spine Journal,* 10**,** 1089-1097.

ALSBERG, E., KONG, H. J., HIRANO, Y., SMITH, M. K., ALBEIRUTI, A. & MOONEY, D. J. 2003. Regulating bone formation via controlled scaffold degradation. *Journal of Dental Research,* 82**,** 903-908.

ANDO, W., TATEISHI, K., HART, D. A., KATAKAI, D., TANAKA, Y., NAKATA, K., HASHIMOTO, J., FUJIE, H., SHINO, K., YOSHIKAWA, H. & NAKAMURA, N. 2007. Cartilage repair using an in vitro generated scaffold-free tissue-engineered construct derived from porcine synovial mesenchymal stem cells. *Biomaterials,* 28**,** 5462-5470.

ANDO, W., TATEISHI, K., KATAKAI, D., HART, D. A., HIGUCHI, C., NAKATA, K., HASHIMOTO, J., FUJIE, H., SHINO, K., YOSHIKAWA, H. & NAKAMURA, N. 2008. In vitro generation of a scaffold-free tissue-engineered construct (TEC) derived from human synovial mesenchymal stem cells: Biological and mechanical properties and further chondrogenic potential. *Tissue Eng Part A* 14**,** 2041-2049.

ANGELE, P., SCHUMANN, D., ANGELE, M., KINNER, B., ENGLERT, C., HENTE, R., FUCHTMEIER, B., NERLICH, M., NEUMANN, C. & KUJAT, R. 2004. Cyclic, mechanical compression enhances chondrogenesis

of mesenchymal progenitor cells in tissue engineering scaffolds. *Biorheology,* 41, 335-46.

APPELMAN, T. P., MIZRAHI, J., ELISSEEFF, J. H. & SELIKTAR, D. 2009. The differential effect of scaffold composition and architecture on chondrocyte response to mechanical stimulation. *Biomaterials,* 30, 518-525.

APPELMAN, T. P., MIZRAHI, J., ELISSEEFF, J. H. & SELIKTAR, D. 2011. The influence of biological motifs and dynamic mechanical stimulation in hydrogel scaffold systems on the phenotype of chondrocytes. *Biomaterials,* 32, 1508-1516.

ARCHER, C. W., DOWTHWAITE, G. P. & FRANCIS-WEST, P. 2003. Development of synovial joints. *Birth Defects Research Part C - Embryo Today: Reviews,* 69, 144-155.

ATESHIAN, G. A. 2009. The role of interstitial fluid pressurization in articular cartilage lubrication. *Journal of Biomechanics,* 42, 1163-1176.

ATHANASIOU, K. A., ESWARAMOORTHY, R., HADIDI, P. & HU, J. C. 2013. Self-organization and the self-assembling process in tissue engineering. *Annu Rev Biomed Eng,* 15, 115-36.

ATHANASIOU, K. A., ROSENWASSER, M. P., BUCKWALTER, J. A., MALININ, T. I. & MOW, V. C. 1991. Interspecies comparisons of in situ intrinsic mechanical properties of distal femoral cartilage. *Journal of Orthopaedic Research,* 9, 330-340.

AUGST, A. D., KONG, H. J. & MOONEY, D. J. 2006. Alginate hydrogels as biomaterials. *Macromolecular Bioscience,* 6, 623-633.

AULTHOUSE, A. L., BECK, M., GRIFFEY, E., SANFORD, J., ARDEN, K., MACHADO, M. A. & HORTON, W. A. 1989. Expression of the human chondrocyte phenotype in vitro. *In Vitro Cellular and Developmental Biology - Animal,* 25, 659-668.

AUNG, A., GUPTA, G., MAJID, G. & VARGHESE, S. 2011. Osteoarthritic chondrocyte-secreted morphogens induce chondrogenic differentiation of human mesenchymal stem cells. *Arthritis and Rheumatism,* 63, 148-158.

BAKER, B. M., SHAH, R. P., HUANG, A. H. & MAUCK, R. L. 2011. Dynamic tensile loading improves the functional properties of mesenchymal stem cell-laden nanofiber-based fibrocartilage. *Tissue Engineering - Part A,* 17, 1445-1455.

BARBERO, A., GROGAN, S., SCHÄFER, D., HEBERER, M., MAINIL-VARLET, P. & MARTIN, I. 2004. Age related changes in human articular chondrocyte yield, proliferation and post-expansion chondrogenic capacity. *Osteoarthritis and Cartilage,* 12, 476-484.

BEKKERS, J. E. J., CREEMERS, L. B., TSUCHIDA, A. I., VAN RIJEN, M. H. P., CUSTERS, R. J. H., DHERT, W. J. A. & SARIS, D. B. F. 2013a. One-stage focal cartilage defect treatment with bone marrow mononuclear cells and chondrocytes leads to better macroscopic cartilage regeneration compared to microfracture in goats. *Osteoarthritis and Cartilage,* 21, 950-956.

BEKKERS, J. E. J., TSUCHIDA, A. I., VAN RIJEN, M. H. P., VONK, L. A., DHERT, W. J. A., CREEMERS, L. B. & SARIS, D. B. F. 2013b. Single-stage cell-based cartilage regeneration using a combination of chondrons and mesenchymal stromal cells: Comparison with microfracture. *American Journal of Sports Medicine,* 41, 2158-2166.

BENYA, P. D. & SHAFFER, J. D. 1982. Dedifferentiated chondrocytes reexpress the differentiated collagen phenotype when cultured in agarose gels. *Cell,* 30, 215-224.

BENZ, K., BREIT, S., LUKOSCHEK, M., MAU, H. & RICHTER, W. 2002. Molecular analysis of expansion, differentiation, and growth factor treatment of human chondrocytes identifies differentiation markers and growth-related genes. *Biochemical and Biophysical Research Communications,* 293, 284-292.

BETRE, H., ONG, S. R., GUILAK, F., CHILKOTI, A., FERMOR, B. & SETTON, L. A. 2006. Chondrocytic differentiation of human adipose-derived adult stem cells in elastin-like polypeptide. *Biomaterials,* 27, 91-99.

BIAN, L., ANGIONE, S. L., NG, K. W., LIMA, E. G., WILLIAMS, D. Y., MAO, D. Q., ATESHIAN, G. A. & HUNG, C. T. 2009a. Influence of decreasing nutrient path length on the development of engineered cartilage. *Osteoarthritis and Cartilage,* 17, 677-685.

BIAN, L., CRIVELLO, K. M., NG, K. W., XU, D., WILLIAMS, D. Y., ATESHIAN, G. A. & HUNG, C. T. 2009c. Influence of temporary chondroitinase ABC-induced glycosaminoglycan suppression on maturation of tissue-engineered cartilage. *Tissue Eng Part A* 15, 2065-2072.

BIAN, L., ZHAI, D. Y., MAUCK, R. L. & BURDICK, J. A. 2011. Coculture of human mesenchymal stem cells and articular chondrocytes reduces hypertrophy and enhances functional properties of engineered cartilage. *Tissue Engineering - Part A,* 17, 1137-1145.

BRITTBERG, M. 2008. Autologous chondrocyte implantation-Technique and long-term follow-up. *Injury,* 39, 40-49.

BRITTBERG, M. 2010. Cell carriers as the next generation of cell therapy for cartilage repair: A review of the matrix-induced autologous chondrocyte implantation procedure. *American Journal of Sports Medicine,* 38, 1259-1271.

BRITTBERG, M., LINDAHL, A., NILSSON, A., OHLSSON, C., ISAKSSON, O. & PETERSON, L. 1994. Treatment of deep cartilage defects in the knee with autologous chondrocyte transplantation. *N Engl J Med,* 331, 889-95.

BROWNE, J. A., BECHTOLD, C. D., BERRY, D. J., HANSSEN, A. D. & LEWALLEN, D. G. 2010. Failed metal-on-metal hip arthroplasties: A spectrum of clinical presentations and operative findings. *Clinical Orthopaedics and Related Research,* 468, 2313-2320.

BRYANT, S. J., ANSETH, K. S., LEE, D. A. & BADER, D. L. 2004a. Crosslinking density influences the morphology of chondrocytes photoencapsulated in PEG hydrogels during the application of compressive strain. *Journal of Orthopaedic Research,* 22, 1143-1149.

BRYANT, S. J., CHOWDHURY, T. T., LEE, D. A., BADER, D. L. & ANSETH, K. S. 2004b. Crosslinking density influences chondrocyte metabolism in dynamically loaded photocrosslinked poly(ethylene glycol) hydrogels. *Annals of Biomedical Engineering,* 32, 407-417.

BRYANT, S. J., NICODEMUS, G. D. & VILLANUEVA, I. 2008. Designing 3D photopolymer hydrogels to regulate biomechanical cues and tissue growth for cartilage tissue engineering. *Pharmaceutical Research,* 25, 2379-2386.

BUCKLEY, C. T. & KELLY, D. J. 2012. Expansion in the presence of FGF-2 enhances the functional development of cartilaginous tissues engineered

using infrapatellar fat pad derived MSCs. *Journal of the Mechanical Behavior of Biomedical Materials,* 11, 102-111.

BUCKLEY, C. T., MEYER, E. G. & KELLY, D. J. 2012. The influence of construct scale on the composition and functional properties of cartilaginous tissues engineered using bone marrow-derived mesenchymal stem cells. *Tissue Engineering - Part A,* 18, 382-396.

BUCKLEY, C. T., THORPE, S. D. & KELLY, D. J. 2009a. Engineering of large cartilaginous tissues through the use of microchanneled hydrogels and rotational culture. *Tissue Engineering - Part A,* 15, 3213-3220.

BUCKLEY, C. T., THORPE, S. D. & KELLY, D. J. 2009b. Engineering of large cartilaginous tissues through the use of microchanneled hydrogels and rotational culture. *Tissue Eng Part A* 15, 3213-3220.

BUCKLEY, C. T., THORPE, S. D., O'BRIEN, F. J., ROBINSON, A. J. & KELLY, D. J. 2009c. The effect of concentration, thermal history and cell seeding density on the initial mechanical properties of agarose hydrogels. *Journal of the Mechanical Behavior of Biomedical Materials,* 2, 512-521.

BUCKLEY, C. T., VINARDELL, T. & KELLY, D. J. 2010a. Oxygen tension differentially regulates the functional properties of cartilaginous tissues engineered from infrapatellar fat pad derived MSCs and articular chondrocytes. *Osteoarthritis and Cartilage,* 18, 1345-1354.

BUCKLEY, C. T., VINARDELL, T., THORPE, S. D., HAUGH, M. G., JONES, E., MCGONAGLE, D. & KELLY, D. J. 2010b. Functional properties of cartilaginous tissues engineered from infrapatellar fat pad-derived mesenchymal stem cells. *Journal of Biomechanics,* 43, 920-926.

BUCKLEY, C. T., VINARDELL, T., THORPE, S. D., HAUGH, M. G., JONES, E., MCGONAGLE, D. & KELLY, D. J. 2010c. Functional properties of cartilaginous tissues engineered from infrapatellar fat pad-derived mesenchymal stem cells. *J Biomech* 43, 920-926.

BUCKWALTER, J. A. 1982. The fine structure of human intervertebral disc. *In:* WHITE, A. A. & GORDON, S. L. (eds.) *The American Academy of Orthopaedic Surgeons, Symposium on Idiopathic Low Back Pain.* St. Louis, Mosby, 108-143.

.

BUCKWALTER, J. A. 1983. Articular cartilage. *Instr Course Lect,* 32, 349-70.

BUCKWALTER, J. A. & MANKIN, H. J. 1997. Articular cartilage. Part I: Tissue design and chondrocyte-matrix interactions. *Journal of Bone and Joint Surgery - Series A,* 79, 600-611.

BUCKWALTER, J. A. & MARTIN, J. A. 2006. Osteoarthritis. *Advanced Drug Delivery Reviews,* 58, 150-167.

BUCKWALTER, J. A., MOW, V. C. & RATCLIFFE, A. 1994. Restoration of Injured or Degenerated Articular Cartilage. *J Am Acad Orthop Surg,* 2, 192-201.

BUSCHMANN, M. D., GLUZBAND, Y. A., GRODZINSKY, A. J. & HUNZIKER, E. B. 1995a. Mechanical compression modulates matrix biosynthesis in chondrocyte/agarose culture. *Journal of Cell Science,* 108, 1497-1508.

BUSCHMANN, M. D., GLUZBAND, Y. A., GRODZINSKY, A. J. & HUNZIKER, E. B. 1995b. Mechanical compression modulates matrix

biosynthesis in chondrocyte/agarose culture. *J Cell Sci,* 108 (Pt 4), 1497-508.

BUSCHMANN, M. D., GLUZBAND, Y. A., GRODZINSKY, A. J., KIMURA, J. H. & HUNZIKER, E. B. 1992a. Chondrocytes in agarose culture synthesize a mechanically functional extracellular matrix. *J Orthop Res,* 10, 745-58.

BUSCHMANN, M. D., GLUZBAND, Y. A., GRODZINSKY, A. J., KIMURA, J. H. & HUNZIKER, E. B. 1992b. Chondrocytes in agarose culture synthesize a mechanically functional extracellular matrix. *Journal of Orthopaedic Research,* 10, 745-758.

BUSCHMANN, M. D., KIM, Y. J., WONG, M., FRANK, E., HUNZIKER, E. B. & GRODZINSKY, A. J. 1999. Stimulation of aggrecan synthesis in cartilage explants by cyclic loading is localized to regions of high interstitial fluid flow. *Archives of Biochemistry and Biophysics,* 366, 1-7.

BUXTON, A. N., BAHNEY, C. S., YOO, J. U. & JOHNSTONE, B. 2011. Temporal exposure to chondrogenic factors modulates human mesenchymal stem cell chondrogenesis in hydrogels. *Tissue Eng Part A,* 17, 371-80.

BYERS, B. A., MAUCK, R. L., CHIANG, I. E. & TUAN, R. S. 2008. Transient exposure to transforming growth factor beta 3 under serum-free conditions enhances the biomechanical and biochemical maturation of tissue-engineered cartilage. *Tissue Eng Part A,* 14, 1821-34.

CAMPBELL, J. J., LEE, D. A. & BADER, D. L. 2006. Dynamic compressive strain influences chondrogenic gene expression in human mesenchymal stem cells. *Biorheology,* 43, 455-470.

CAO, T., HO, K. H. & TEOH, S. H. 2003. Scaffold design and in vitro study of osteochondral coculture in a three-dimensional porous polycaprolactone scaffold fabricated by fused deposition modeling. *Tissue Engineering,* 9, S103-S112.

CAPLAN, A. I. 2005. Review: mesenchymal stem cells: cell-based reconstructive therapy in orthopedics. *Tissue Eng,* 11, 1198-211.

CAPLAN, A. I. 2007. Adult mesenchymal stem cells for tissue engineering versus regenerative medicine. *J Cell Physiol,* 213, 341-7.

CAPLAN, A. I. & DENNIS, J. E. 2006. Mesenchymal stem cells as trophic mediators. *Journal of Cellular Biochemistry,* 98, 1076-1084.

CHANG, C. H., LIN, F. H., LIN, C. C., CHOU, C. H. & LIU, H. C. 2004. Cartilage tissue engineering on the surface of a novel gelatin-calcium- phosphate biphasic scaffold in a double-chamber bioreactor. *Journal of Biomedical Materials Research - Part B Applied Biomaterials,* 71, 313-321.

CHANG, R. W., FALCONER, J., STULBERG, S. D., ARNOLD, W. J., MANHEIM, L. M. & DYER, A. R. 1993. A randomized, controlled trial of arthroscopic surgery versus closed- needle joint lavage for patients with osteoarthritis of the knee. *Arthritis and Rheumatism,* 36, 289-296.

CHAO, P. H. G., GRAYSON, W. & VUNJAK-NOVAKOVIC, G. 2007. Engineering cartilage and bone using human mesenchymal stem cells. *Journal of Orthopaedic Science,* 12, 398-404.

CHEN, J., CHEN, H., LI, P., DIAO, H., ZHU, S., DONG, L., WANG, R., GUO, T., ZHAO, J. & ZHANG, J. 2011. Simultaneous regeneration of articular cartilage and subchondral bone in vivo using MSCs induced by a spatially controlled gene delivery system in bilayered integrated scaffolds. *Biomaterials,* 32, 4793-4805.

CHEN, X. C., WANG, R., ZHAO, X., WEI, Y. Q., HU, M., WANG, Y. S., ZHANG, X. W., ZHANG, R., ZHANG, L., YAO, B., WANG, L., JIA, Y. Q., ZENG, T. T., YANG, J. L., TIAN, L., KAN, B., LIN, X. J., LEI, S., DENG, H. X., WEN, Y. J., MAO, Y. Q. & LI, J. 2006. Prophylaxis against carcinogenesis in three kinds of unestablished tumor models via IL12-gene-engineered MSCs. *Carcinogenesis,* 27, 2434-2441.

CHIANG, H. & JIANG, C. C. 2009. Repair of articular cartilage defects: Review and perspectives. *Journal of the Formosan Medical Association,* 108, 87-101.

CHOWDHURY, T. T., BADER, D. L. & LEE, D. A. 2001. Dynamic compression inhibits the synthesis of nitric oxide and PGE2 by IL-1β-stimulated chondrocytes cultured in agarose constructs. *Biochemical and Biophysical Research Communications,* 285, 1168-1174.

CONNELLY, J. T., VANDERPLOEG, E. J., MOUW, J. K., WILSON, C. G. & LEVENSTON, M. E. 2010. Tensile loading modulates bone marrow stromal cell differentiation and the development of engineered fibrocartilage constructs. *Tissue Engineering - Part A,* 16, 1913-1923.

CONVERY, F. R., AKESON, W. H. & KEOWN, G. H. 1972. The repair of large osteochondral defects. An experimental study in horses. *Clinical Orthopaedics and Related Research,* 82, 253-262.

COOK, J. L., WILLIAMS, N., KREEGER, J. M., PEACOCK, J. T. & TOMLINSON, J. L. 2003. Biocompatibility of three-dimensional chondrocyte grafts in large tibial defects of rabbits. *Am J Vet Res,* 64, 12-20.

COOKE, M. E., ALLON, A. A., CHENG, T., KUO, A. C., KIM, H. T., VAIL, T. P., MARCUCIO, R. S., SCHNEIDER, R. A., LOTZ, J. C. & ALLISTON, T. 2011. Structured three-dimensional co-culture of mesenchymal stem cells with chondrocytes promotes chondrogenic differentiation without hypertrophy. *Osteoarthritis and Cartilage,* 19, 1210-1218.

COWIN, S. C. 2002. Mechanosensation and fluid transport in living bone. *Journal of Musculoskeletal Neuronal Interactions,* 2, 256-260.

COWIN, S. C. 2007. The significance of bone microstructure in mechanotransduction. *Journal of Biomechanics,* 40, S105-S109.

COYLE, C. H., IZZO, N. J. & CHU, C. R. 2009. Sustained hypoxia enhances chondrocyte matrix synthesis. *Journal of Orthopaedic Research,* 27, 793-799.

CUSHING, M. C. & ANSETH, K. S. 2007. Hydrogel cell cultures. *Science,* 316, 1133-1134.

DAHLIN, R. L., KINARD, L. A., LAM, J., NEEDHAM, C. J., LU, S., KASPER, F. K. & MIKOS, A. G. 2014a. Articular chondrocytes and mesenchymal stem cells seeded on biodegradable scaffolds for the repair of cartilage in a rat osteochondral defect model. *Biomaterials,* 35, 7460-7469.

DAHLIN, R. L., NI, M., MERETOJA, V. V., KASPER, F. K. & MIKOS, A. G. 2014b. TGF-β3-induced chondrogenesis in co-cultures of chondrocytes and mesenchymal stem cells on biodegradable scaffolds. *Biomaterials,* 35, 123-132.

DARLING, E. M. & ATHANASIOU, K. A. 2005. Rapid phenotypic changes in passaged articular chondrocyte subpopulations. *Journal of Orthopaedic Research,* 23, 425-432.

DE UGARTE, D. A., MORIZONO, K., ELBARBARY, A., ALFONSO, Z., ZUK, P. A., ZHU, M., DRAGOO, J. L., ASHJIAN, P., THOMAS, B., BENHAIM, P., CHEN, I., FRASER, J. & HEDRICK, M. H. 2003. Comparison of multi-lineage cells from human adipose tissue and bone marrow. *Cells Tissues Organs,* 174, 101-109.

DE VRIES-VAN MELLE, M. L., TIHAYA, M. S., KOPS, N., KOEVOET, W. J. L. M., MARY MURPHY, J., VERHAAR, J. A. N., ALINI, M., EGLIN, D. & VAN OSCH, G. J. V. M. 2014. Chondrogenic differentiation of human bone marrow-derived mesenchymal stem cells in a simulated osteochondral environment is hydrogel dependent. *European Cells and Materials,* 27, 112-123.

DIAZ-ROMERO, J., GAILLARD, J. P., GROGAN, S. P., NESIC, D., TRUB, T. & MAINIL-VARLET, P. 2005. Immunophenotypic analysis of human articular chondrocytes: changes in surface markers associated with cell expansion in monolayer culture. *J Cell Physiol,* 202, 731-42.

DICKHUT, A., GOTTWALD, E., STECK, E., HEISEL, C. & RICHTE, W. 2008. Chondrogenesis of mesenchymal stem cells in gel-like biomaterials in vitro and in vivo. *Frontiers in Bioscience,* 13, 4517-4528.

DICKHUT, A., PELTTARI, K., JANICKI, P., WAGNER, W., ECKSTEIN, V., EGERMANN, M. & RICHTER, W. 2009. Calcification or dedifferentiation: Requirement to lock mesenchymal stem cells in a desired differentiation stage. *Journal of Cellular Physiology,* 219, 219-226.

DIDUCH, D. R., JORDAN, L. C. M., MIERISCH, C. M. & BALIAN, G. 2000. Marrow stromal cells embedded in alginate for repair of osteochondral defects. *Arthroscopy,* 16, 571-577.

DIMITRIOU, R., TSIRIDIS, E. & GIANNOUDIS, P. V. 2005. Current concepts of molecular aspects of bone healing. *Injury,* 36, 1392-1404.

DING, C., QIAO, Z., JIANG, W., LI, H., WEI, J., ZHOU, G. & DAI, K. 2013. Regeneration of a goat femoral head using a tissue-specific, biphasic scaffold fabricated with CAD/CAM technology. *Biomaterials,* 34, 6706-6716.

DODGE, G. R., DIAZ, A., SANZ-RODRIGUEZ, C., REGINATO, A. M. & JIMENEZ, S. A. 1998. Effects of interferon-γ and tumor necrosis factor α on the expression of the genes encoding aggrecan, biglycan, and decorin core proteins in cultured human chondrocytes. *Arthritis and Rheumatism,* 41, 274-283.

DOMM, C., SCHÜNKE, M., CHRISTESEN, K. & KURZ, B. 2002. Redifferentiation of dedifferentiated bovine articular chondrocytes in alginate culture under low oxygen tension. *Osteoarthritis and Cartilage,* 10, 13-22.

DRAGOO, J. L., SAMIMI, B., ZHU, M., HAME, S. L., THOMAS, B. J., LIEBERMAN, J. R., HEDRICK, M. H. & BENHAIM, P. 2003. Tissue-engineered cartilage and bone using stem cells from human infrapatellar fat pads. *J Bone Joint Surg Br,* 85, 740-7.

DRURY, J. L. & MOONEY, D. J. 2003. Hydrogels for tissue engineering: Scaffold design variables and applications. *Biomaterials,* 24, 4337-4351.

DUPLOMB, L., DAGOUASSAT, M., JOURDON, P. & HEYMANN, D. 2007. Concise review: Embryonic stem cells: A new tool to study osteoblast and osteoclast differentiation. *Stem Cells,* 25, 544-552.

EINHORN, T. A. 1998. The cell and molecular biology of fracture healing. *Clinical Orthopaedics and Related Research*, S7-S21.

ELDER, B. D. & ATHANASIOU, K. A. 2008a. Effects of confinement on the mechanical properties of self-assembled articular cartilage constructs in the direction orthogonal to the confinement surface. *J Orthop Res,* 26, 238-46.

ELDER, B. D. & ATHANASIOU, K. A. 2008b. Effects of confinement on the mechanical properties of self-assembled articular cartilage constructs in the direction orthogonal to the confinement surface. *Journal of Orthopaedic Research,* 26, 238-246.

ELDER, B. D. & ATHANASIOU, K. A. 2008c. Synergistic and additive effects of hydrostatic pressure and growth factors on tissue formation. *PLoS ONE,* 3.

ELDER, B. D. & ATHANASIOU, K. A. 2009a. Effects of temporal hydrostatic pressure on tissue-engineered bovine articular cartilage constructs. *Tissue Eng Part A* 15, 1151-1158.

ELDER, B. D. & ATHANASIOU, K. A. 2009b. Systematic assessment of growth factor treatment on biochemical and biomechanical properties of engineered articular cartilage constructs. *Osteoarthritis and Cartilage,* 17, 114-123.

ELDER, B. D. & ATHANASIOU, K. A. 2009c. Systematic assessment of growth factor treatment on biochemical and biomechanical properties of engineered articular cartilage constructs. *Osteoarthritis Cartilage,* 17, 114-23.

ELDER, S. H., COOLEY, A. J., BORAZJANI, A., SOWELL, B. L., TO, H. & TRAN, S. C. 2009. Production of hyaline-like cartilage by bone marrow mesenchymal stem cells in a self-assembly model. *Tissue Eng Part A,* 15, 3025-3036.

ELDER, S. H., SANDERS, S. W., MCCULLEY, W. R., MARR, M. L., SHIM, J. W. & HASTY, K. A. 2006. Chondrocyte response to cyclic hydrostatic pressure in alginate versus pellet culture. *Journal of Orthopaedic Research,* 24, 740-747.

ELISSEEFF, J., PULEO, C., YANG, F. & SHARMA, B. 2005. Advances in skeletal tissue engineering with hydrogels. *Orthodontics & craniofacial research,* 8, 150-161.

ENGLISH, A., JONES, E. A., CORSCADDEN, D., HENSHAW, K., CHAPMAN, T., EMERY, P. & MCGONAGLE, D. 2007. A comparative assessment of cartilage and joint fat pad as a potential source of cells for autologous therapy development in knee osteoarthritis. *Rheumatology,* 46, 1676-1683.

ENOBAKHARE, B. O., BADER, D. L. & LEE, D. A. 1996. Quantification of sulfated glycosaminoglycans in chondrocyte/alginate cultures, by use of 1,9-dimethylmethylene blue. *Analytical Biochemistry,* 243, 189-191.

ERICKSON, I. E., HUANG, A. H., CHUNG, C., LI, R. T., BURDICK, J. A. & MAUCK, R. L. 2009. Differential maturation and structure-function relationships in mesenchymal stem cell- and chondrocyte-seeded hydrogels. *Tissue Eng Part A,* 15, 1041-52.

ERICKSON, I. E., VAN VEEN, S. C., SENGUPTA, S., KESTLE, S. R. & MAUCK, R. L. 2011. Cartilage matrix formation by bovine mesenchymal stem cells in three-dimensional culture is age-dependent. *Clin Orthop Relat Res* 469, 2744-2753.

ESTRADA, L. E., DODGE, G. R., RICHARDSON, D. W., FAROLE, A. & JIMENEZ, S. A. 2001. Characterization of a biomaterial with cartilage-like properties expressing type X collagen generated in vitro using neonatal

porcine articular and growth plate chondrocytes. *Osteoarthritis Cartilage,* 9, 169-177.

FARRELL, E., BOTH, S. K., ODORFER, K. I., KOEVOET, W., KOPS, N., O'BRIEN, F. J., BAATENBURG DE JONG, R. J., VERHAAR, J. A., CUIJPERS, V., JANSEN, J., ERBEN, R. G. & VAN OSCH, G. J. 2011. In-vivo generation of bone via endochondral ossification by in-vitro chondrogenic priming of adult human and rat mesenchymal stem cells. *BMC Musculoskelet Disord,* 12, 31.

FARRELL, E., VAN DER JAGT, O. P., KOEVOET, W., KOPS, N., VAN MANEN, C. J., HELLINGMAN, C. A., JAHR, H., O'BRIEN, F. J., VERHAAR, J. A., WEINANS, H. & VAN OSCH, G. J. 2009. Chondrogenic priming of human bone marrow stromal cells: a better route to bone repair? *Tissue Eng Part C Methods,* 15, 285-95.

FEDELE, A. O., WHITELAW, M. L. & PEET, D. J. 2002. Regulation of gene expression by the hypoxia-inducible factors. *Molecular interventions,* 2, 229-243.

FEDOROVICH, N. E., SCHUURMAN, W., WIJNBERG, H. M., PRINS, H. J., VAN WEEREN, P. R., MALDA, J., ALBLAS, J. & DHERT, W. J. 2012. Biofabrication of osteochondral tissue equivalents by printing topologically defined, cell-laden hydrogel scaffolds. *Tissue Eng Part C Methods,* 18, 33-44.

FISCHER, J., DICKHUT, A., RICKERT, M. & RICHTER, W. 2010. Human articular chondrocytes secrete parathyroid hormone-related protein and inhibit hypertrophy of mesenchymal stem cells in coculture during chondrogenesis. *Arthritis and Rheumatism,* 62, 2696-2706.

FOTY, R. A. & STEINBERG, M. S. 2005. The differential adhesion hypothesis: A direct evaluation. *Developmental Biology,* 278, 255-263.

FREED, L. E., HOLLANDER, A. P., MARTIN, I., BARRY, J. R., LANGER, R. & VUNJAK-NOVAKOVIC, G. 1998. Chondrogenesis in a cell-polymer-bioreactor system. *Exp Cell Res,* 240, 58-65.

FRIEDENSTEIN, A. J., CHAILAKHJAN, R. K. & LALYKINA, K. S. 1970. The development of fibroblast colonies in monolayer cultures of guinea-pig bone marrow and spleen cells. *Cell and Tissue Kinetics,* 3, 393-403.

FRIEDENSTEIN, A. J., LATZINIK, N. V., GORSKAYA YU, F., LURIA, E. A. & MOSKVINA, I. L. 1992. Bone marrow stromal colony formation requires stimulation by haemopoietic cells. *Bone and Mineral,* 18, 199-213.

FURUKAWA, T., EYRE, D. R., KOIDE, S. & GLIMCHER, M. J. 1980. Biochemical studies on repair cartilage resurfacing experimental defects in the rabbit knee. *Journal of Bone and Joint Surgery - Series A,* 62, 79-89.

FURUMATSU, T., MATSUMOTO, E., KANAZAWA, T., FUJII, M., LU, Z., KAJIKI, R. & OZAKI, T. 2013. Tensile strain increases expression of CCN2 and COL2A1 by activating TGF-β-Smad2/3 pathway in chondrocytic cells. *Journal of Biomechanics,* 46, 1508-1515.

GANNON, A. R., NAGEL, T. & KELLY, D. J. 2012. The role of the superficial region in determining the dynamic properties of articular cartilage. *Osteoarthritis and Cartilage,* 20, 1417-1425.

GAO, J., DENNIS, J. E., SOLCHAGA, L. A., AWADALLAH, A. S., GOLDBERG, V. M. & CAPLAN, A. I. 2001. Tissue-engineered fabrication

of an osteochondral composite graft using rat bone marrow-derived mesenchymal stem cells. *Tissue Engineering,* 7, 363-371.

GELSE, K., MÜHLE, C., FRANKE, O., PARK, J., JEHLE, M., DURST, K., GÖKEN, M., HENNIG, F., VON DER MARK, K. & SCHNEIDER, H. 2008. Cell-based resurfacing of large cartilage defects: Long-term evaluation of grafts from autologous transgene-activated periosteal cells in a porcine model of osteoarthritis. *Arthritis and Rheumatism,* 58, 475-488.

GEMMITI, C. V. & GULDBERG, R. E. 2006. Fluid flow increases type II collagen deposition and tensile mechanical properties in bioreactor-grown tissue-engineered cartilage. *Tissue Engineering,* 12, 469-479.

GEORGE, M. & ABRAHAM, T. E. 2006. Polyionic hydrocolloids for the intestinal delivery of protein drugs: Alginate and chitosan - a review. *Journal of Controlled Release,* 114, 1-14.

GERSTENFELD, L. C., CULLINANE, D. M., BARNES, G. L., GRAVES, D. T. & EINHORN, T. A. 2003. Fracture healing as a post-natal developmental process: Molecular, spatial, and temporal aspects of its regulation. *Journal of Cellular Biochemistry,* 88, 873-884.

GIOVANNINI, S., DIAZ-ROMERO, J., AIGNER, T., HEINI, P., MAINIL-VARLET, P. & NESIC, D. 2010. Micromass co-culture of human articular chondrocytes and human bone marrow mesenchymal stem cells to investigate stable neocartilage tissue formation in vitro. *European Cells and Materials,* 20, 245-259.

GOLDSTEIN, A. S., JUAREZ, T. M., HELMKE, C. D., GUSTIN, M. C. & MIKOS, A. G. 2001. Effect of convection on osteoblastic cell growth and function in biodegradable polymer foam scaffolds. *Biomaterials,* 22, 1279-1288.

GOMBOTZ, W. R. & WEE, S. F. 1998. Protein release from alginate matrices. *Advanced Drug Delivery Reviews,* 31, 267-285.

GRANT, G. T., MORRIS, E. R., REES, D. A., SMITH, P. J. C. & THOM, D. 1973. Biological interactions between polysaccharides and divalent cations: The egg-box model. *FEBS Letters,* 32, 195-198.

GRAYSON, W. L., BHUMIRATANA, S., GRACE CHAO, P. H., HUNG, C. T. & VUNJAK-NOVAKOVIC, G. 2010. Spatial regulation of human mesenchymal stem cell differentiation in engineered osteochondral constructs: effects of pre-differentiation, soluble factors and medium perfusion. *Osteoarthritis Cartilage,* 18, 714-23.

GRAYSON, W. L., CHAO, P. H., MAROLT, D., KAPLAN, D. L. & VUNJAK-NOVAKOVIC, G. 2008. Engineering custom-designed osteochondral tissue grafts. *Trends Biotechnol,* 26, 181-9.

GRIMAUD, E., HEYMANN, D. & RÉDINI, F. 2002. Recent advances in TGF-β effects on chondrocyte metabolism potential therapeutic roles of TGF-β in cartilage disorders. *Cytokine and Growth Factor Reviews,* 13, 241-257.

GRODZINSKY, A. J., LEVENSTON, M. E., JIN, M. & FRANK, E. H. 2000. Cartilage tissue remodeling in response to mechanical forces. *Annu Rev Biomed Eng,* 2, 691-713.

GU, W. Y., LAI, W. M. & MOW, V. C. 1998. A mixture theory for charged-hydrated soft tissues containing multi- electrolytes: Passive transport and swelling behaviors. *Journal of Biomechanical Engineering,* 120, 169-180.

GU, W. Y., YAO, H., HUANG, C. Y. & CHEUNG, H. S. 2003. New insight into deformation-dependent hydraulic permeability of gels and cartilage, and dynamic behavior of agarose gels in confined compression. *J Biomech,* 36, 593-8.

GUILAK, F. 2010. Homing in on a biological joint replacement. *Stem Cell Research and Therapy,* 1.

GUO, X., LIAO, J., PARK, H., SARAF, A., RAPHAEL, R. M., TABATA, Y., KASPER, F. K. & MIKOS, A. G. 2010. Effects of TGF-β3 and preculture period of osteogenic cells on the chondrogenic differentiation of rabbit marrow mesenchymal stem cells encapsulated in a bilayered hydrogel composite. *Acta Biomaterialia,* 6, 2920-2931.

GUO, X., PARK, H., LIU, G., LIU, W., CAO, Y., TABATA, Y., KASPER, F. K. & MIKOS, A. G. 2009. In vitro generation of an osteochondral construct using injectable hydrogel composites encapsulating rabbit marrow mesenchymal stem cells. *Biomaterials,* 30, 2741-2752.

GUO, X., WANG, C., DUAN, C., DESCAMPS, M., ZHAO, Q., DONG, L., LÜ, S., ANSELME, K., LU, J. & SONG, Y. Q. 2004. Repair of osteochondral defects with autologous chondrocytes seeded onto bioceramic scaffold in sheep. *Tissue Engineering,* 10, 1830-1840.

HAASPER, C., COLDITZ, M., KIRSCH, L., TSCHERNIG, T., VIERING, J., GRAUBNER, G., RUNTEMUND, A., ZEICHEN, J., MELLER, R., GLASMACHER, B., WINDHAGEN, H., KRETTEK, C., HURSCHLER, C. & JAGODZINSKI, M. 2008. A system for engineering an osteochondral construct in the shape of an articular surface: Preliminary results. *Annals of Anatomy,* 190, 351-359.

HARADA, N., WATANABE, Y., SATO, K., ABE, S., YAMANAKA, K., SAKAI, Y., KANEKO, T. & MATSUSHITA, T. 2014. Bone regeneration in a massive rat femur defect through endochondral ossification achieved with chondrogenically differentiated MSCs in a degradable scaffold. *Biomaterials,* 35, 7800-7810.

HAYES, A. J., HALL, A., BROWN, L., TUBO, R. & CATERSON, B. 2007. Macromolecular organization and in vitro growth characteristics of scaffold-free neocartilage grafts. *Journal of Histochemistry and Cytochemistry,* 55, 853-866.

HEATH, C. A. & MAGARI, S. R. 1996. Mini-review: Mechanical factors affecting cartilage regeneration in vitro. *Biotechnology and Bioengineering,* 50, 430-437.

HELLINGMAN, C. A., KOEVOET, W., KOPS, N., FARRELL, E., JAHR, H., LIU, W., DE JONG, R. J. B., FRENZ, D. A. & VAN OSCH, G. J. V. M. 2010. Fibroblast growth factor receptors in in vitro and in vivo chondrogenesis: Relating tissue engineering using adult mesenchymal stem cells to embryonic development. *Tissue Engineering - Part A,* 16, 545-556.

HENDRIKS, J., RIESLE, J. & VAN BLITTERSWIJK, C. A. 2007. Co-culture in cartilage tissue engineering. *Journal of Tissue Engineering and Regenerative Medicine,* 1, 170-178.

HILDNER, F., CONCARO, S., PETERBAUER, A., WOLBANK, S., DANZER, M., LINDAHL, A., GATENHOLM, P., REDL, H. & VAN GRIENSVEN, M. 2009. Human adipose-derived stem cells contribute to chondrogenesis in

coculture with human articular chondrocytes. *Tissue Engineering - Part A,* 15, 3961-3969.

HOBEN, G. M., HU, J. C., JAMES, R. A. & ATHANASIOU, K. A. 2007. Self-assembly of fibrochondrocytes and chondrocytes for tissue engineering of the knee meniscus. *Tissue Eng,* 13, 939-46.

HU, J. C. & ATHANASIOU, K. A. 2006a. The effects of intermittent hydrostatic pressure on self-assembled articular cartilage constructs. *Tissue Engineering,* 12, 1337-1344.

HU, J. C. & ATHANASIOU, K. A. 2006b. A self-assembling process in articular cartilage tissue engineering. *Tissue Eng,* 12, 969-79.

HUANG, A. H., FARRELL, M. J., KIM, M. & MAUCK, R. L. 2010a. Long-term dynamic loading improves the mechanical properties of chondrogenic mesenchymal stem cell-laden hydrogels. *European Cells and Materials,* 19, 72-85.

HUANG, A. H., STEIN, A. & MAUCK, R. L. 2010b. Evaluation of the complex transcriptional topography of mesenchymal stem cell chondrogenesis for cartilage tissue engineering. *Tissue Engineering - Part A,* 16, 2699-2708.

HUANG, A. H., STEIN, A., TUAN, R. S. & MAUCK, R. L. 2009. Transient exposure to transforming growth factor beta 3 improves the mechanical properties of mesenchymal stem cell-laden cartilage constructs in a density-dependent manner. *Tissue Eng Part A,* 15, 3461-3472.

HUANG, C. Y., HAGAR, K. L., FROST, L. E., SUN, Y. & CHEUNG, H. S. 2004a. Effects of cyclic compressive loading on chondrogenesis of rabbit bone-marrow derived mesenchymal stem cells. *Stem Cells,* 22, 313-23.

HUANG, C. Y. C., REUBEN, P. M. & CHEUNG, H. S. 2005. Temporal expression patterns and corresponding protein inductions of early responsive genes in rabbit bone marrow-derived mesenchymal stem cells under cyclic compressive loading. *Stem Cells,* 23, 1113-1121.

HUANG, C. Y. C., REUBEN, P. M., D'PPOLITO, G., SCHILLER, P. C. & CHEUNG, H. S. 2004b. Chondrogenesis of Human Bone Marrow-Derived Mesenchymal Stem Cells in Agarose Culture. *Anatomical Record - Part A Discoveries in Molecular, Cellular, and Evolutionary Biology,* 278, 428-436.

HUANG, J. I., DURBHAKULA, M. M., ANGELE, P., JOHNSTONE, B. & YOO, J. U. 2006. Lunate arthroplasty with autologous mesenchymal stem cells in a rabbit model. *Journal of Bone and Joint Surgery - Series A,* 88, 744-752.

HUANG, Q., GOH, J. C. H., HUTMACHER, D. W. & LEE, E. H. 2002. In vivo mesenchymal cell recruitment by a scaffold loaded with transforming growth factor β1 and the potential for in situ chondrogenesis. *Tissue Engineering,* 8, 469-482.

HUNG, C. T., LIMA, E. G., MAUCK, R. L., TAKAI, E., LEROUX, M. A., LU, H. H., STARK, R. G., GUO, X. E. & ATESHIAN, G. A. 2003. Anatomically shaped osteochondral constructs for articular cartilage repair. *J Biomech,* 36, 1853-64.

HUNG, C. T., MAUCK, R. L., WANG, C. C. B., LIMA, E. G. & ATESHIAN, G. A. 2004. A paradigm for functional tissue engineering of articular cartilage via applied physiologic deformational loading. *Annals of Biomedical Engineering,* 32, 35-49.

HUNTER, C., MOUW, J. K. & LEVENSTON, M. E. 2004. Dynamic compression of chondrocyte-seeded fibrin gels: Effects on matrix accumulation and mechanical stiffness. *Osteoarthritis and Cartilage,* 12, 117-130.

HUNZIKER, E. B. 1999. Articular cartilage repair: Are the intrinsic biological constraints undermining this process insuperable? *Osteoarthritis and Cartilage,* 7, 15-28.

HUNZIKER, E. B. 2002. Articular cartilage repair: basic science and clinical progress. A review of the current status and prospects. *Osteoarthritis Cartilage,* 10, 432-63.

HUNZIKER, E. B. 2009. The elusive path to cartilage regeneration. *Advanced Materials,* 21, 3419-3424.

HUNZIKER, E. B. & KAPFINGER, E. 1998. Removal of proteoglycans from the surface of defects in articular cartilage transiently enhances coverage by repair cells. *Journal of Bone and Joint Surgery - Series B,* 80, 144-150.

HUNZIKER, E. B., KAPFINGER, E. & GEISS, J. 2007. The structural architecture of adult mammalian articular cartilage evolves by a synchronized process of tissue resorption and neoformation during postnatal development. *Osteoarthritis and Cartilage,* 15, 403-413.

HUNZIKER, E. B., QUINN, T. M. & HAUSELMANN, H. J. 2002a. Quantitative structural organization of normal adult human articular cartilage. *Osteoarthritis Cartilage,* 10, 564-72.

HUNZIKER, E. B., QUINN, T. M. & HÄUSELMANN, H. J. 2002b. Quantitative structural organization of normal adult human articular cartilage. *Osteoarthritis and Cartilage,* 10, 564-572.

HUTMACHER, D. W. 2000. Scaffolds in tissue engineering bone and cartilage. *Biomaterials,* 21, 2529-2543.

HUTMACHER, D. W. 2001. Scaffold design and fabrication technologies for engineering tissues - State of the art and future perspectives. *Journal of Biomaterials Science, Polymer Edition,* 12, 107-124.

HUTMACHER, D. W., SCHANTZ, T., ZEIN, I., NG, K. W., TEOH, S. H. & TAN, K. C. 2001. Mechanical properties and cell cultural response of polycaprolactone scaffolds designed and fabricated via fused deposition modeling. *Journal of Biomedical Materials Research,* 55, 203-216.

HWANG, N. S., VARGHESE, S., PULEO, C., ZHANG, Z. & ELISSEEFF, J. 2007. Morphogenetic signals from chondrocytes promote chondrogenic and osteogenic differentiation of mesenchymal stem cells. *Journal of Cellular Physiology,* 212, 281-284.

IGARASHI, T., IWASAKI, N., KASAHARA, Y. & MINAMI, A. 2010. A cellular implantation system using an injectable ultra-purified alginate gel for repair of osteochondral defects in a rabbit model. *Journal of Biomedical Materials Research - Part A,* 94, 844-855.

IGNAT'EVA, N. Y., DANILOV, N. A., AVERKIEV, S. V., OBREZKOVA, M. V., LUNIN, V. V. & SOBOL, E. N. 2007. Determination of hydroxyproline in tissues and the evaluation of the collagen content of the tissues. *J Anal Chem,* 62, 51-57.

JAKOB, M., DÉMARTEAU, O., SCHÄFER, D., STUMM, M., HEBERER, M. & MARTIN, I. 2003. Enzymatic digestion of adult human articular cartilage yields a small fraction of the total available cells. *Connective Tissue Research,* 44, 173-180.

JANICKI, P., KASTEN, P., KLEINSCHMIDT, K., LUGINBUEHL, R. & RICHTER, W. 2010. Chondrogenic pre-induction of human mesenchymal stem cells on β-TCP: Enhanced bone quality by endochondral heterotopic bone formation. *Acta Biomaterialia,* 6, 3292-3301.

JEON, O., ALT, D. S., AHMED, S. M. & ALSBERG, E. 2012. The effect of oxidation on the degradation of photocrosslinkable alginate hydrogels. *Biomaterials,* 33, 3503-3514.

JIANG, J., TANG, A., ATESHIAN, G. A., EDWARD GUO, X., HUNG, C. T. & LU, H. H. 2010. Bioactive stratified polymer ceramic-hydrogel scaffold for integrative osteochondral repair. *Annals of Biomedical Engineering,* 38, 2183-2196.

JOHNSTONE, B., HERING, T. M., CAPLAN, A. I., GOLDBERG, V. M. & YOO, J. U. 1998. In vitro chondrogenesis of bone marrow-derived mesenchymal progenitor cells. *Experimental Cell Research,* 238, 265-272.

JONES, D. G. & PETERSON, L. 2006. Autologous chondrocyte implantation. *Journal of Bone and Joint Surgery - Series A,* 88, 2502-2520.

JUKES, J. M., BOTH, S. K., LEUSINK, A., STERK, L. M. T., VAN BLITTERSWIJK, C. A. & DE BOER, J. 2008. Endochondral bone tissue engineering using embryonic stem cells. *Proceedings of the National Academy of Sciences of the United States of America,* 105, 6840-6845.

JURGENS, W. J. F. M., VAN DIJK, A., DOULABI, B. Z., NIESSEN, F. B., RITT, M. J. P. F., VAN MILLIGEN, F. J. & HELDER, M. N. 2009. Freshly isolated stromal cells from the infrapatellar fat pad are suitable for a one-step surgical procedure to regenerate cartilage tissue. *Cytotherapy,* 11, 1052-1064.

KAFIENAH, W., MISTRY, S., DICKINSON, S. C., SIMS, T. J., LEARMONTH, I. & HOLLANDER, A. P. 2007. Three-dimensional cartilage tissue engineering using adult stem cells from osteoarthritis patients. *Arthritis and Rheumatism,* 56, 177-187.

KAFIENAH, W. & SIMS, T. J. 2004. Biochemical methods for the analysis of tissue-engineered cartilage. *Methods Mol Biol,* 238, 217-30.

KALSON, N. S., GIKAS, P. D. & BRIGGS, T. W. R. 2010. Current strategies for knee cartilage repair. *International Journal of Clinical Practice,* 64, 1444-1452.

KANDEL, R. A., GRYNPAS, M., PILLIAR, R., LEE, J., WANG, J., WALDMAN, S., ZALZAL, P. & HURTIG, M. 2006. Repair of osteochondral defects with biphasic cartilage-calcium polyphosphate constructs in a Sheep model. *Biomaterials,* 27, 4120-4131.

KANG, N., LIU, X., GUAN, Y., WANG, J., GONG, F., YANG, X., YAN, L., WANG, Q., FU, X., CAO, Y. & XIAO, R. 2012. Effects of co-culturing BMSCs and auricular chondrocytes on the elastic modulus and hypertrophy of tissue engineered cartilage. *Biomaterials,* 33, 4535-4544.

KEENEY, J. A., EUNICE, S., PASHOS, G., WRIGHT, R. W. & CLOHISY, J. C. 2011. What is the evidence for total knee arthroplasty in young patients?: A systematic review of the literature. *Clinical Orthopaedics and Related Research,* 469, 574-583.

KELLY, D. J. & PRENDERGAST, P. J. 2005. Mechano-regulation of stem cell differentiation and tissue regeneration in osteochondral defects. *J Biomech,* 38, 1413-22.

KELLY, T. A., NG, K. W., WANG, C. C. B., ATESHIAN, G. A. & HUNG, C. T. 2006. Spatial and temporal development of chondrocyte-seeded agarose constructs in free-swelling and dynamically loaded cultures. *Journal of Biomechanics,* 39, 1489-1497.

KELLY, T. A. N., NG, K. W., ATESHIAN, G. A. & HUNG, C. T. 2009. Analysis of radial variations in material properties and matrix composition of chondrocyte-seeded agarose hydrogel constructs. *Osteoarthritis and Cartilage,* 17, 73-82.

KELLY, T. A. N., WANG, C. C. B., MAUCK, R. L., ATESHIAN, G. A. & HUNG, C. T. 2004. Role of cell-associated matrix in the development of free-swelling and dynamically loaded chondrocyte-seeded agarose gels. *Biorheology,* 41, 223-237.

KERIN, C., MALHOTRA, A., SPENCER-JONES, R. & COOL, W. P. 2011. When do total knee replacements fail? *Journal of Long-Term Effects of Medical Implants,* 21, 51-54.

KHAN, W. S., ADESIDA, A. B. & HARDINGHAM, T. E. 2007. Hypoxic conditions increase hypoxia-inducible transcription factor 2alpha and enhance chondrogenesis in stem cells from the infrapatellar fat pad of osteoarthritis patients. *Arthritis Res Ther,* 9, R55.

KHARKAR, P. M., KIICK, K. L. & KLOXIN, A. M. 2013. Designing degradable hydrogels for orthogonal control of cell microenvironments. *Chemical Society Reviews,* 42, 7335-7372.

KHEIR, E. & SHAW, D. 2009. Hyaline articular cartilage. *Orthopaedics and Trauma,* 23, 450-455.

KIM, M., KRAFT, J. J., VOLK, A. C., PUGARELLI, J., PLESHKO, N. & DODGE, G. R. 2011. Characterization of a cartilage-like engineered biomass using a self-aggregating suspension culture model: Molecular composition using FT-IRIS. *J Orthop Res* 29, 1881-1887.

KIM, Y. J., SAH, R. L., DOONG, J. Y. & GRODZINSKY, A. J. 1988. Fluorometric assay of DNA in cartilage explants using Hoechst 33258. *Anal Biochem,* 174, 168-76.

KIM, Y. J., SAH, R. L. Y., GRODZINSKY, A. J., PLAAS, A. H. K. & SANDY, J. D. 1994. Mechanical regulation of cartilage biosynthetic behavior: Physical stimuli. *Archives of Biochemistry and Biophysics,* 311, 1-12.

KISIDAY, J. D., FRISBIE, D. D., MCILWRAITH, C. W. & GRODZINSKY, A. J. 2009. Dynamic compression stimulates proteoglycan synthesis by mesenchymal stem cells in the absence of chondrogenic cytokines. *Tissue Engineering - Part A,* 15, 2817-2824.

KLEIN, T. J., MALDA, J., SAH, R. L. & HUTMACHER, D. W. 2009. Tissue engineering of articular cartilage with biomimetic zones. *Tissue Eng Part B Rev,* 15, 143-57.

KO, H. C. H., MILTHORPE, B. K. & MCFARLAND, C. D. 2007. Engineering thick tissues - The vascularisation problem. *European Cells and Materials,* 14, 1-18.

KOCK, L., VAN DONKELAAR, C. C. & ITO, K. 2012. Tissue engineering of functional articular cartilage: The current status. *Cell and Tissue Research,* 347, 613-627.

KOLAMBKAR, Y. M., BOERCKEL, J. D., DUPONT, K. M., BAJIN, M., HUEBSCH, N., MOONEY, D. J., HUTMACHER, D. W. & GULDBERG,

R. E. 2011a. Spatiotemporal delivery of bone morphogenetic protein enhances functional repair of segmental bone defects. *Bone,* 49, 485-492.

KOLAMBKAR, Y. M., DUPONT, K. M., BOERCKEL, J. D., HUEBSCH, N., MOONEY, D. J., HUTMACHER, D. W. & GULDBERG, R. E. 2011b. An alginate-based hybrid system for growth factor delivery in the functional repair of large bone defects. *Biomaterials,* 32, 65-74.

KON, E., GOBBI, A., FILARDO, G., DELCOGLIANO, M., ZAFFAGNINI, S. & MARCACCI, M. 2009. Arthroscopic second-generation autologous chondrocyte implantation compared with microfracture for chondral lesions of the knee: Prospective nonrandomized study at 5 years. *American Journal of Sports Medicine,* 37, 33-41.

KRAFT, J. J., JEONG, C., NOVOTNY, J. E., SEACRIST, T., CHAN, G., DOMZALSKI, M., TURKA, C. M., RICHARDSON, D. W. & DODGE, G. R. 2011. Effects of hydrostatic loading on a self-aggregating, suspension culture-derived cartilage tissue analog. *Cartilage,* 2, 254-264.

KREKLAU, B., SITTINGER, M., MENSING, M. B., VOIGT, C., BERGER, G., BURMESTER, G. R., RAHMANZADEH, R. & GROSS, U. 1999. Tissue engineering of biphasic joint cartilage transplants. *Biomaterials,* 20, 1743-1749.

KRONENBERG, H. M. 2003. Developmental regulation of the growth plate. *Nature,* 423, 332-336.

KUO, C. K. & MA, P. X. 2001. Ionically crosslinked alginate hydrogels as scaffolds for tissue engineering: Part 1. Structure, gelation rate and mechanical properties. *Biomaterials,* 22, 511-521.

KURTZ, S. M., LAU, E., ONG, K., ZHAO, K., KELLY, M. & BOZIC, K. J. 2009. Future young patient demand for primary and revision joint replacement: National projections from 2010 to 2030. *Clinical Orthopaedics and Related Research,* 467, 2606-2612.

LEE, C. H., COOK, J. L., MENDELSON, A., MOIOLI, E. K., YAO, H. & MAO, J. J. 2010. Regeneration of the articular surface of the rabbit synovial joint by cell homing: A proof of concept study. *The Lancet,* 376, 440-448.

LEE, C. H., MARION, N. W., HOLLISTER, S. & MAO, J. J. 2009. Tissue formation and vascularization in anatomically shaped human joint condyle ectopically in vivo. *Tissue Engineering - Part A,* 15, 3923-3930.

LEE, D. A. & BADER, D. L. 1997. Compressive strains at physiological frequencies influence the metabolism of chondrocytes seeded in agarose. *Journal of Orthopaedic Research,* 15, 181-188.

LEE, D. A., FREAN, S. P., LEES, P. & BADER, D. L. 1998. Dynamic mechanical compression influences nitric oxide production by articular chondrocytes seeded in agarose. *Biochemical and Biophysical Research Communications,* 251, 580-585.

LEE, D. A., NOGUCHI, T., FREAN, S. P., LEES, P. & BADER, D. L. 2000. The influence of mechanical loading on isolated chondrocytes seeded in agarose constructs. *Biorheology,* 37, 149-161.

LEE, J. S. & IM, G. I. 2010. Influence of chondrocytes on the chondrogenic differentiation of adipose stem cells. *Tissue Engineering - Part A,* 16, 3569-3577.

LEE, K. Y. & MOONEY, D. J. 2012. Alginate: Properties and biomedical applications. *Progress in Polymer Science (Oxford),* 37, 106-126.

LEE, K. Y. & YUK, S. H. 2007. Polymeric protein delivery systems. *Progress in Polymer Science (Oxford),* 32, 669-697.

LEE, S. Y., NAKAGAWA, T. & REDDI, A. H. 2008. Induction of chondrogenesis and expression of superficial zone protein (SZP)/lubricin by mesenchymal progenitors in the infrapatellar fat pad of the knee joint treated with TGF-beta1 and BMP-7. *Biochem Biophys Res Commun,* 376, 148-53.

LEE, W. D., HURTIG, M. B., KANDEL, R. A. & STANFORD, W. L. 2011. Membrane culture of bone marrow stromal cells yields better tissue than pellet culture for engineering cartilage-bone substitute biphasic constructs in a two-step process. *Tissue Eng Part C Methods,* 17, 939-948.

LEIJTEN, J. C. H., GEORGI, N., WU, L., VAN BLITTERSWIJK, C. A. & KARPERIEN, M. 2013. Cell sources for articular cartilage repair strategies: Shifting from monocultures to cocultures. *Tissue Engineering - Part B: Reviews,* 19, 31-40.

LENNON, D. P. & CAPLAN, A. I. 2006. Isolation of human marrow-derived mesenchymal stem cells. *Exp Hematol,* 34, 1604-5.

LETTRY, V., HOSOYA, K., TAKAGI, S. & OKUMURA, M. 2010. Coculture of equine mesenchymal stem cells and mature equine articular chondrocytes results in improved chondrogenic differentiation of the stem cells. *Japanese Journal of Veterinary Research,* 58, 5-15.

LI, X., PENG, J., WU, M., YE, H., ZHENG, C., WU, G., XU, H., CHEN, X. & LIU, X. 2011. BMP2 promotes chondrocyte proliferation via the Wnt/β-catenin signaling pathway. *Molecular Medicine Reports,* 4, 621-626.

LI, Y. J., BATRA, N. N., YOU, L., MEIER, S. C., COE, I. A., YELLOWLEY, C. E. & JACOBS, C. R. 2004. Oscillatory fluid flow affects human marrow stromal cell proliferation and differentiation. *Journal of Orthopaedic Research,* 22, 1283-1289.

LIMA, E. G., BIAN, L., MAUCK, R. L., BYERS, B. A., TUAN, R. S., ATESHIAN, G. A. & HUNG, C. T. The effect of applied compressive loading on tissue-engineered cartilage constructs cultured with TGF-β3. 2006. 779-782.

LIMA, E. G., BIAN, L., NG, K. W., MAUCK, R. L., BYERS, B. A., TUAN, R. S., ATESHIAN, G. A. & HUNG, C. T. 2007. The beneficial effect of delayed compressive loading on tissue-engineered cartilage constructs cultured with TGF-beta 3. *Osteoarthritis and Cartilage,* 15, 1025-1033.

LITTLE, C. J., BAWOLIN, N. K. & CHEN, X. 2011. Mechanical properties of natural cartilage and tissue-engineered constructs. *Tissue Engineering - Part B: Reviews,* 17, 213-227.

LIU, X. & MA, P. X. 2004. Polymeric scaffolds for bone tissue engineering. *Annals of Biomedical Engineering,* 32, 477-486.

LIU, X., SUN, H., YAN, D., ZHANG, L., LV, X., LIU, T., ZHANG, W., LIU, W., CAO, Y. & ZHOU, G. 2010. In vivo ectopic chondrogenesis of BMSCs directed by mature chondrocytes. *Biomaterials,* 31, 9406-9414.

LIU, Y., BUCKLEY, C. T., ALMEIDA, H. V., MULHALL, K. J. & KELLY, D. J. 2014. Infrapatellar Fat Pad-Derived Stem Cells Maintain Their Chondrogenic Capacity in Disease and Can be Used to Engineer Cartilaginous Grafts of Clinically Relevant Dimensions. *Tissue Eng Part A.*

LIU, Y., BUCKLEY, C. T., DOWNEY, R., MULHALL, K. J. & KELLY, D. J. 2012. The Role of Environmental Factors in Regulating the Development of

Cartilaginous Grafts Engineered Using Osteoarthritic Human Infrapatellar Fat Pad-Derived Stem Cells. *Tissue Eng Part A*.

LYONS, F. G., AL-MUNAJJED, A. A., KIERAN, S. M., TONER, M. E., MURPHY, C. M., DUFFY, G. P. & O'BRIEN, F. J. 2010. The healing of bony defects by cell-free collagen-based scaffolds compared to stem cell-seeded tissue engineered constructs. *Biomaterials,* 31, 9232-9243.

MA, H.-M., LU, Y.-C., HO, F.-Y. & HUANG, C.-H. 2005. Long-Term Results of Total Condylar Knee Arthroplasty. *The Journal of Arthroplasty,* 20, 580-584.

MA, H. L., HUNG, S. C., LIN, S. Y., CHEN, Y. L. & LO, W. H. 2003. Chondrogenesis of human mesenchymal stem cells encapsulated in alginate beads. *Journal of Biomedical Materials Research - Part A,* 64, 273-281.

MACKIE, E. J. 2003. Osteoblasts: Novel roles in orchestration of skeletal architecture. *International Journal of Biochemistry and Cell Biology,* 35, 1301-1305.

MACKIE, E. J., AHMED, Y. A., TATARCZUCH, L., CHEN, K. S. & MIRAMS, M. 2008. Endochondral ossification: How cartilage is converted into bone in the developing skeleton. *International Journal of Biochemistry and Cell Biology,* 40, 46-62.

MAHMOUDIFAR, N. & DORAN, P. M. 2005. Tissue engineering of human cartilage and osteochondral composites using recirculation bioreactors. *Biomaterials,* 26, 7012-7024.

MALDA, J., VAN BLITTERSWIJK, C. A., GROJEC, M., MARTENS, D. E., TRAMPER, J. & RIESLE, J. 2003. Expansion of Bovine Chondrocytes on Microcarriers Enhances Redifferentiation. *Tissue Engineering,* 9, 939-948.

MANKIN, H. J. 1982. The response of articular cartilage to mechanical injury. *Journal of Bone and Joint Surgery - Series A,* 64, 460-466.

MANO, J. F. & REIS, R. L. 2007. Osteochondral defects: Present situation and tissue engineering approaches. *Journal of Tissue Engineering and Regenerative Medicine,* 1, 261-273.

MARCACCI, M., BERRUTO, M., BROCCHETTA, D., DELCOGLIANO, A., GHINELLI, D., GOBBI, A., KON, E., PEDERZINI, L., ROSA, D., SACCHETTI, G. L., STEFANI, G. & ZANASI, S. 2005. Articular cartilage engineering with Hyalograft® C: 3-Year clinical results. *Clinical Orthopaedics and Related Research*, 96-105.

MARQUASS, B., SCHULZ, R., HEPP, P., ZSCHARNACK, M., AIGNER, T., SCHMIDT, S., STEIN, F., RICHTER, R., OSTERHOFF, G., AUST, G., JOSTEN, C. & BADER, A. 2011. Matrix-associated implantation of predifferentiated mesenchymal stem cells versus articular chondrocytes: In vivo results of cartilage repair after 1 year. *American Journal of Sports Medicine,* 39, 1401-1412.

MARSANO, A., MILLWARD-SADLER, S. J., SALTER, D. M., ADESIDA, A., HARDINGHAM, T., TOGNANA, E., KON, E., CHIARI-GRISAR, C., NEHRER, S., JAKOB, M. & MARTIN, I. 2007. Differential cartilaginous tissue formation by human synovial membrane, fat pad, meniscus cells and articular chondrocytes. *Osteoarthritis and Cartilage,* 15, 48-58.

MARTEL-PELLETIER, J. 2004. Pathophysiology of osteoarthritis. *Osteoarthritis and Cartilage,* 12, S31-S33.

MARTIN, I., MIOT, S., BARBERO, A., JAKOB, M. & WENDT, D. 2007. Osteochondral tissue engineering. *J Biomech,* 40, 750-65.

MARTIN, I., OBRADOVIC, B., TREPPO, S., GRODZINSKY, A. J., LANGER, R., FREED, L. E. & VUNJAK-NOVAKOVIC, G. 2000. Modulation of the mechanical properties of tissue engineered cartilage. *Biorheology,* 37, 141-7.

MARTIN, I., WENDT, D. & HEBERER, M. 2004a. The role of bioreactors in tissue engineering. *Trends Biotechnol,* 22, 80-6.

MARTIN, I., WENDT, D. & HEBERER, M. 2004b. The role of bioreactors in tissue engineering. *Trends in Biotechnology,* 22, 80-86.

MASON, J. M., GRANDE, D. A., BARCIA, M., GRANT, R., PERGOLIZZI, R. G. & BREITBART, A. S. 1998. Expression of human bone morphogenic protein 7 in primary rabbit periosteal cells: Potential utility in gene therapy for osteochondral repair. *Gene Therapy,* 5, 1098-1104.

MAUCK, R. L., BYERS, B. A., YUAN, X. & TUAN, R. S. 2007. Regulation of cartilaginous ECM gene transcription by chondrocytes and MSCs in 3D culture in response to dynamic loading. *Biomechanics and Modeling in Mechanobiology,* 6, 113-125.

MAUCK, R. L., HUNG, C. T. & ATESHIAN, G. A. 2003a. Modeling of Neutral Solute Transport in a Dynamically Loaded Porous Permeable Gel: Implications for Articular Cartilage Biosynthesis and Tissue Engineering. *Journal of Biomechanical Engineering,* 125, 602-614.

MAUCK, R. L., NICOLL, S. B., SEYHAN, S. L., ATESHIAN, G. A. & HUNG, C. T. 2003b. Synergistic action of growth factors and dynamic loading for articular cartilage tissue engineering. *Tissue Eng,* 9, 597-611.

MAUCK, R. L., SEYHAN, S. L., ATESHIAN, G. A. & HUNG, C. T. 2002a. Influence of seeding density and dynamic deformational loading on the developing structure/function relationships of chondrocyte-seeded agarose hydrogels. *Ann Biomed Eng,* 30, 1046-56.

MAUCK, R. L., SEYHAN, S. L., ATESHIAN, G. A. & HUNG, C. T. 2002b. Influence of seeding density and dynamic deformational loading on the developing structure/function relationships of chondrocyte-seeded agarose hydrogels. *Annals of Biomedical Engineering,* 30, 1046-1056.

MAUCK, R. L., SOLTZ, M. A., WANG, C. C., WONG, D. D., CHAO, P. H., VALHMU, W. B., HUNG, C. T. & ATESHIAN, G. A. 2000a. Functional tissue engineering of articular cartilage through dynamic loading of chondrocyte-seeded agarose gels. *J Biomech Eng,* 122, 252-60.

MAUCK, R. L., SOLTZ, M. A., WANG, C. C. B., WONG, D. D., CHAO, P. H. G., VALHMU, W. B., HUNG, C. T. & ATESHIAN, G. A. 2000b. Functional tissue engineering of articular cartilage through dynamic loading of chondrocyte-seeded agarose gels. *Journal of Biomechanical Engineering,* 122, 252-260.

MAUCK, R. L., WANG, C. C. B., OSWALD, E. S., ATESHIAN, G. A. & HUNG, C. T. 2003c. The role of cell seeding density and nutrient supply for articular cartilage tissue engineering with deformational loading. *Osteoarthritis Cartilage,* 11, 879-890.

MAUCK, R. L., WANG, C. C. B., OSWALD, E. S., ATESHIAN, G. A. & HUNG, C. T. 2003d. The role of cell seeding density and nutrient supply for articular cartilage tissue engineering with deformational loading. *Osteoarthritis and Cartilage,* 11, 879-890.

MAUCK, R. L., YUAN, X. & TUAN, R. S. 2006. Chondrogenic differentiation and functional maturation of bovine mesenchymal stem cells in long-term agarose culture. *Osteoarthritis Cartilage,* 14, 179-89.

MCDEVITT, C. A. & MUIR, H. 1976. Biochemical changes in the cartilage of the knee in experimental and natural osteoarthritis in the dog. *Journal of Bone and Joint Surgery - Series B,* 58, 94-101.

MCKIBBIN, B. 1978. The biology of fracture healing in long bones. *Journal of Bone and Joint Surgery - Series B,* 60 B, 150-162.

MEHLHORN, A. T., SCHMAL, H., KAISER, S., LEPSKI, G., FINKENZELLER, G., STARK, G. B. & SÜDKAMP, N. P. 2006. Mesenchymal stem cells maintain TGF-β-mediated chondrogenic phenotype in alginate bead culture. *Tissue Engineering,* 12, 1393-1403.

MEIJER, G. J., DE BRUIJN, J. D., KOOLE, R. & VAN BLITTERSWIJK, C. A. 2008. Cell based bone tissue engineering in jaw defects. *Biomaterials,* 29, 3053-3061.

MERCERON, C., VINATIER, C., PORTRON, S., MASSON, M., AMIAUD, J., GUIGAND, L., CHÉREL, Y., WEISS, P. & GUICHEUX, J. 2010. Differential effects of hypoxia on osteochondrogenic potential of human adipose-derived stem cells. *American Journal of Physiology - Cell Physiology,* 298, C355-C364.

MERETOJA, V. V., DAHLIN, R. L., KASPER, F. K. & MIKOS, A. G. 2012. Enhanced chondrogenesis in co-cultures with articular chondrocytes and mesenchymal stem cells. *Biomaterials,* 33, 6362-6369.

MERETOJA, V. V., DAHLIN, R. L., WRIGHT, S., KASPER, F. K. & MIKOS, A. G. 2013. The effect of hypoxia on the chondrogenic differentiation of co-cultured articular chondrocytes and mesenchymal stem cells in scaffolds. *Biomaterials,* 34, 4266-4273.

MESALLATI, T., BUCKLEY, C. T. & KELLY, D. J. 2014a. A comparison of self-assembly and hydrogel encapsulation as a means to engineer functional cartilaginous grafts using culture expanded chondrocytes. *Tissue Eng Part C Methods,* 20, 52-63.

MESALLATI, T., BUCKLEY, C. T. & KELLY, D. J. 2014b. Engineering articular cartilage-like grafts by self-assembly of infrapatellar fat pad-derived stem cells. *Biotechnol Bioeng,* 111, 1686-98.

MESALLATI, T., BUCKLEY, C. T., NAGEL, T. & KELLY, D. J. 2011. Introducing microchannels into chondrocyte-seeded agarose hydrogels influences matrix accumulation in response to dynamic compression and TGF-β3 stimulation. 30 IFMBE, 26-30.

MESALLATI, T., BUCKLEY, C. T., NAGEL, T. & KELLY, D. J. 2013. Scaffold architecture determines chondrocyte response to externally applied dynamic compression. *Biomech Model Mechanobiol,* 12, 889-99.

MEYER, E. G., BUCKLEY, C. T., STEWARD, A. J. & KELLY, D. J. 2011. The effect of cyclic hydrostatic pressure on the functional development of cartilaginous tissues engineered using bone marrow derived mesenchymal stem cells. *Journal of the Mechanical Behavior of Biomedical Materials,* 4, 1257-1265.

MIAO, C., MU, S., DUAN, P., LIANG, X., YANG, B., ZHOU, G. & TANG, S. 2009. Effects of chondrogenic microenvironment on construction of

cartilage tissues using marrow stromal cells in vitro. *Artificial Cells, Blood Substitutes, and Biotechnology,* 37, 214-221.

MITROVIC, D., QUINTERO, M., STANKOVIC, A. & RYCKEWAERT, A. 1983. Cell density of adult human femoral condylar articular cartilage. Joints with normal and fibrillated surfaces. *Laboratory Investigation,* 49, 309-316.

MO, X. T., GUO, S. C., XIE, H. Q., DENG, L., ZHI, W., XIANG, Z., LI, X. Q. & YANG, Z. M. 2009. Variations in the ratios of co-cultured mesenchymal stem cells and chondrocytes regulate the expression of cartilaginous and osseous phenotype in alginate constructs. *Bone,* 45, 42-51.

MOCHIZUKI, T., MUNETA, T., SAKAGUCHI, Y., NIMURA, A., YOKOYAMA, A., KOGA, H. & SEKIYA, I. 2006. Higher chondrogenic potential of fibrous synovium- and adipose synovium-derived cells compared with subcutaneous fat-derived cells: distinguishing properties of mesenchymal stem cells in humans. *Arthritis Rheum,* 54, 843-53.

MOUW, J. K., CONNELLY, J. T., WILSON, C. G., MICHAEL, K. E. & LEVENSTON, M. E. 2007. Dynamic compression regulates the expression and synthesis of chondrocyte-specific matrix molecules in bone marrow stromal cells. *Stem Cells,* 25, 655-663.

MOW, V. C. & GUO, X. E. 2002. Mechano-electrochemical properties of articular cartilage: Their inhomogeneities and anisotropies. *Annual Review of Biomedical Engineering,* 4, 175-209.

MOW, V. C. & HUNG, C. T. 2001. Biomechanics of articular cartilage

In: NORDIN, M. & FRANKEL, V. H. (eds.) *Basic biomechanics of the musculoskeletal system.* 3rd ed. Philadelphia: Lippincott Williams & Wilkins, 60-101.

MOW, V. C., RATCLIFFE, A. & ROBIN POOLE, A. 1992. Cartilage and diarthrodial joints as paradigms for hierarchical materials and structures. *Biomaterials,* 13, 67-97.

MOW, V. C., WANG, C. C. & HUNG, C. T. 1999. The extracellular matrix, interstitial fluid and ions as a mechanical signal transducer in articular cartilage. *Osteoarthritis and Cartilage,* 7, 41-58.

MUIR, H. 1983. Proteoglycans as organizers of the intercellular matrix. *Biochemical Society Transactions,* 11, 613-622.

MURDOCH, A. D., GRADY, L. M., ABLETT, M. P., KATOPODI, T., MEADOWS, R. S. & HARDINGHAM, T. E. 2007. Chondrogenic differentiation of human bone marrow stem cells in transwell cultures: Generation of scaffold-free cartilage. *Stem Cells,* 25, 2786-2796.

MURPHY, J. M., DIXON, K., BECK, S., FABIAN, D., FELDMAN, A. & BARRY, F. 2002. Reduced chondrogenic and adipogenic activity of mesenchymal stem cells from patients with advanced osteoarthritis. *Arthritis and Rheumatism,* 46, 704-713.

MUSCHLER, G. F., NAKAMOTO, C. & GRIFFITH, L. G. 2004. Engineering principles of clinical cell-based tissue engineering. *Journal of Bone and Joint Surgery - Series A,* 86, 1541-1558.

NAKANO, T., WANG, Y. W., OZIMEK, L. & SIM, J. S. 2004. Chemical composition of the infrapatellar fat pad of swine. *J Anat,* 204, 301-6.

NAUMANN, A., DENNIS, J. E., AIGNER, J., COTICCHIA, J., ARNOLD, J., BERGHAUS, A., KASTENBAUER, E. R. & CAPLAN, A. I. 2004. Tissue

engineering of autologous cartilage grafts in three-dimensional in vitro macroaggregate culture system. *Tissue Eng,* 10, 1695-1706.

NEJADNIK, H., HUI, J. H., CHOONG, E. P. F., TAI, B. C. & ENG HIN, L. 2010. Autologous bone marrow-derived mesenchymal stem cells versus autologous chondrocyte implantation: An observational cohort study. *American Journal of Sports Medicine,* 38, 1110-1116.

NEWMAN, A. P. 1998. Articular cartilage repair. *American Journal of Sports Medicine,* 26, 309-324.

NG, K. W., MAUCK, R. L., STATMAN, L. Y., LIN, E. Y., ATESHIAN, G. A. & HUNG, C. T. 2006. Dynamic deformational loading results in selective application of mechanical stimulation in a layered, tissue-engineered cartilage construct. *Biorheology,* 43, 497-507.

NG, K. W., O'CONOR, C. J., KUGLER, L. E., COOK, J. L., ATESHIAN, G. A. & HUNG, C. T. 2011. Transient supplementation of anabolic growth factors rapidly stimulates matrix synthesis in engineered cartilage. *Annals of Biomedical Engineering,* 39, 2491-2500.

NG, K. W., WANG, C. C. B., MAUCK, R. L., KELLY, T. A. N., CHAHINE, N. O., COSTA, K. D., ATESHIAN, G. A. & HUNG, C. T. 2005. A layered agarose approach to fabricate depth-dependent inhomogeneity in chondrocyte-seeded constructs. *Journal of Orthopaedic Research,* 23, 134-141.

NIEDERAUER, G. G., SLIVKA, M. A., LEATHERBURY, N. C., KORVICK, D. L., HARROFF, H. H., EHLER, W. C., DUNN, C. J. & KIESWETTER, K. 2000. Evaluation of multiphase implants for repair of focal osteochondral defects in goats. *Biomaterials,* 21, 2561-74.

NISHIMURA, K., SOLCHAGA, L. A., CAPLAN, A. I., YOO, J. U., GOLDBERG, V. M. & JOHNSTONE, B. 1999. Chondroprogenitor cells of synovial tissue. *Arthritis and Rheumatism,* 42, 2631-2637.

NOVOTNY, J. E., TURKA, C. M., JEONG, C., WHEATON, A. J., LI, C., PRESEDO, A., RICHARDSON, D. W., REDDY, R. & DODGE, G. R. 2006. Biomechanical and magnetic resonance characteristics of a cartilage-like equivalent generated in a suspension culture. *Tissue Eng,* 12, 2755-2764.

O'BRIEN, F. J. 2011. Biomaterials & scaffolds for tissue engineering. *Materials Today,* 14, 88-95.

O'DRISCOLL, S. W. 1998. The healing and regeneration of articular cartilage. *J Bone Joint Surg Am,* 80, 1795-812.

O'SHEA, T. M. & MIAO, X. 2008. Bilayered scaffolds for osteochondral tissue engineering. *Tissue Engineering - Part B: Reviews,* 14, 447-464.

OFEK, G., REVELL, C. M., HU, J. C., ALLISON, D. D., GRANDE-ALLEN, K. J. & ATHANASIOU, K. A. 2008. Matrix development in self-assembly of articular cartilage. *PLoS One,* 3, e2795.

OLIVEIRA, J. M., RODRIGUES, M. T., SILVA, S. S., MALAFAYA, P. B., GOMES, M. E., VIEGAS, C. A., DIAS, I. R., AZEVEDO, J. T., MANO, J. F. & REIS, R. L. 2006. Novel hydroxyapatite/chitosan bilayered scaffold for osteochondral tissue-engineering applications: Scaffold design and its performance when seeded with goat bone marrow stromal cells. *Biomaterials,* 27, 6123-6137.

PARK, D. J., CHOI, B. H., ZHU, S. J., HUH, J. Y., KIM, B. Y. & LEE, S. H. 2005. Injectable bone using chitosan-alginate gel/mesenchymal stem cells/BMP-2 composites. *Journal of Cranio-Maxillofacial Surgery,* 33, 50-54.

PAVONE, V., BOETTNER, F., FICKERT, S. & SCULCO, T. P. 2001. Total condylar knee arthroplasty: A long-term followup. *Clinical Orthopaedics and Related Research*, 18-25.

PAYNE, K. A., DIDIANO, D. M. & CHU, C. R. 2010. Donor sex and age influence the chondrogenic potential of human femoral bone marrow stem cells. *Osteoarthritis and Cartilage,* 18, 705-713.

PEI, M., HE, F., BOYCE, B. M. & KISH, V. L. 2009. Repair of full-thickness femoral condyle cartilage defects using allogeneic synovial cell-engineered tissue constructs. *Osteoarthritis and Cartilage,* 17, 714-722.

PEI, M., HE, F. & VUNJAK-NOVAKOVIC, G. 2008. Synovium-derived stem cell-based chondrogenesis. *Differentiation,* 76, 1044-56.

PELTTARI, K., STECK, E. & RICHTER, W. 2008a. The use of mesenchymal stem cells for chondrogenesis. *Injury,* 39 Suppl 1, S58-65.

PELTTARI, K., STECK, E. & RICHTER, W. 2008b. The use of mesenchymal stem cells for chondrogenesis. *Injury-International Journal of the Care of the Injured,* 39, S58-S65.

PELTTARI, K., WINTER, A., STECK, E., GOETZKE, K., HENNIG, T., OCHS, B. G., AIGNER, T. & RICHTER, W. 2006. Premature induction of hypertrophy during in vitro chondrogenesis of human mesenchymal stem cells correlates with calcification and vascular invasion after ectopic transplantation in SCID mice. *Arthritis and Rheumatism,* 54, 3254-3266.

PHELPS, E. A. & GARCIA, A. J. 2009. Update on therapeutic vascularization strategies. *Regenerative Medicine,* 4, 65-80.

PITTENGER, M. F., MACKAY, A. M., BECK, S. C., JAISWAL, R. K., DOUGLAS, R., MOSCA, J. D., MOORMAN, M. A., SIMONETTI, D. W., CRAIG, S. & MARSHAK, D. R. 1999. Multilineage potential of adult human mesenchymal stem cells. *Science,* 284, 143-7.

PITTENGER, M. F., MOSCA, J. D. & MCINTOSH, K. R. 2000. Human mesenchymal stem cells: progenitor cells for cartilage, bone, fat and stroma. *Curr Top Microbiol Immunol,* 251, 3-11.

POOLE, A. R., KOJIMA, T., YASUDA, T., MWALE, F., KOBAYASHI, M. & LAVERTY, S. 2001. Composition and structure of articular cartilage: A template for tissue repair. *Clinical Orthopaedics and Related Research*, S26-S33.

POOLE, C. A. 1997. Articular cartilage chondrons: Form, function and failure. *Journal of Anatomy,* 191, 1-13.

POOLE, C. A., FLINT, M. H. & BEAUMONT, B. W. 1987. Chondrons in cartilage: Ultrastructural analysis of the pericellular microenvironment in adult human articular cartilages. *Journal of Orthopaedic Research,* 5, 509-522.

PRENDERGAST, P. J., HUISKES, R. & SØBALLE, K. 1997. Biophysical stimuli on cells during tissue differentiation at implant interfaces. *Journal of Biomechanics,* 30, 539-548.

RALSTON, S. H. 2009. Bone structure and metabolism. *Medicine,* 37, 469-474.

RE'EM, T., WITTE, F., WILLBOLD, E., RUVINOV, E. & COHEN, S. 2012. Simultaneous regeneration of articular cartilage and subchondral bone

induced by spatially presented TGF-beta and BMP-4 in a bilayer affinity binding system. *Acta Biomaterialia,* 8, 3283-3293.

REGINATO, A. M., IOZZO, R. V. & JIMENEZ, S. A. 1994. Formation of nodular structures resembling mature articular cartilage in long-term primary cultures of human fetal epiphyseal chondrocytes on a hydrogel substrate. *Arthritis Rheum,* 37, 1338-1349.

REVELL, C. M., REYNOLDS, C. E. & ATHANASIOU, K. A. 2008. Effects of initial cell seeding in self assembly of articular cartilage. *Ann Biomed Eng* 36, 1441-1448.

RICHTER, W. 2009. Mesenchymal stem cells and cartilage in situ regeneration. *Journal of Internal Medicine,* 266, 390-405.

ROBINS, J. C., AKENO, N., MUKHERJEE, A., DALAL, R. R., ARONOW, B. J., KOOPMAN, P. & CLEMENS, T. L. 2005. Hypoxia induces chondrocyte-specific gene expression in mesenchymal cells in association with transcriptional activation of Sox9. *Bone,* 37, 313-322.

RODRIGUES, M. T., GOMES, M. E. & REIS, R. L. 2011. Current strategies for osteochondral regeneration: From stem cells to pre-clinical approaches. *Current Opinion in Biotechnology,* 22, 726-733.

RODRIGUES, M. T., LEE, S. J., GOMES, M. E., REIS, R. L., ATALA, A. & YOO, J. J. 2012. Bilayered constructs aimed at osteochondral strategies: The influence of medium supplements in the osteogenic and chondrogenic differentiation of amniotic fluid-derived stem cells. *Acta Biomaterialia,* 8, 2795-2806.

ROY, R., BOSKEY, A. L. & BONASSAR, L. J. 2008. Non-enzymatic glycation of chondrocyte-seeded collagen gels for cartilage tissue engineering. *Journal of Orthopaedic Research,* 26, 1434-1439.

SABATINO, M. A., SANTORO, R., GUEVEN, S., JAQUIERY, C., WENDT, D. J., MARTIN, I., MORETTI, M. & BARBERO, A. 2012. Cartilage graft engineering by co-culturing primary human articular chondrocytes with human bone marrow stromal cells. *Journal of Tissue Engineering and Regenerative Medicine.*

SAKIYAMA-ELBERT, S. E. & HUBBELL, J. A. 2001. Functional biomaterials: Design of novel biomaterials. *Annual Review of Materials Science,* 31, 183-201.

SAMPAT, S. R., O'CONNELL, G. D., FONG, J. V., ALEGRE-AGUARON, E., ATESHIAN, G. A. & HUNG, C. T. 2011. Growth factor priming of synovium-derived stem cells for cartilage tissue engineering. *Tissue Eng Part A,* 17, 2259-65.

SANTO, V. E., GOMES, M. E., MANO, J. F. & REIS, R. L. 2013a. Controlled release strategies for bone, cartilage, and osteochondral engineering-part i: Recapitulation of native tissue healing and variables for the design of delivery systems. *Tissue Engineering - Part B: Reviews,* 19, 308-326.

SANTO, V. E., GOMES, M. E., MANO, J. F. & REIS, R. L. 2013b. Controlled release strategies for bone, cartilage, and osteochondral engineering-part ii: Challenges on the evolution from single to multiple bioactive factor delivery. *Tissue Engineering - Part B: Reviews,* 19, 327-352.

SANTORO, R., OLIVARES, A. L., BRANS, G., WIRZ, D., LONGINOTTI, C., LACROIX, D., MARTIN, I. & WENDT, D. 2010. Bioreactor based

engineering of large-scale human cartilage grafts for joint resurfacing. *Biomaterials,* 31, 8946-8952.

SANTOS, M. I. & REIS, R. L. 2010. Vascularization in bone tissue engineering: Physiology, current strategies, major hurdles and future challenges. *Macromolecular Bioscience,* 10, 12-27.

SARAF, A. & MIKOS, A. G. 2006. Gene delivery strategies for cartilage tissue engineering. *Advanced Drug Delivery Reviews,* 58, 592-603.

SCHAEFER, D., MARTIN, I., JUNDT, G., SEIDEL, J., HEBERER, M., GRODZINSKY, A., BERGIN, I., VUNJAK-NOVAKOVIC, G. & FREED, L. E. 2002. Tissue-engineered composites for the repair of large osteochondral defects. *Arthritis Rheum,* 46, 2524-34.

SCHAEFER, D., MARTIN, I., SHASTRI, P., PADERA, R. F., LANGER, R., FREED, L. E. & VUNJAK-NOVAKOVIC, G. 2000. In vitro generation of osteochondral composites. *Biomaterials,* 21, 2599-2606.

SCHEK, R. M., TABOAS, J. M., SEGVICH, S. J., HOLLISTER, S. J. & KREBSBACH, P. H. 2004. Engineered osteochondral grafts using biphasic composite solid free-form fabricated scaffolds. *Tissue Engineering,* 10, 1376-1385.

SCHINDELER, A., MCDONALD, M. M., BOKKO, P. & LITTLE, D. G. 2008. Bone remodeling during fracture repair: The cellular picture. *Seminars in Cell and Developmental Biology,* 19, 459-466.

SCHINHAN, M., GRUBER, M., VAVKEN, P., DOROTKA, R., SAMOUH, L., CHIARI, C., GRUEBL-BARABAS, R. & NEHRER, S. 2011. Critical-size defect induces unicompartmental osteoarthritis in a stable ovine knee. *Journal of Orthopaedic Research.*

SCHNABEL, M., MARLOVITS, S., ECKHOFF, G., FICHTEL, I., GOTZEN, L., VÉCSEI, V. & SCHLEGEL, J. 2002. Dedifferentiation-associated changes in morphology and gene expression in primary human articular chondrocytes in cell culture. *Osteoarthritis and Cartilage,* 10, 62-70.

SCHUMACHER, B. L., HUGHES, C. E., KUETTNER, K. E., CATERSON, B. & AYDELOTTE, M. B. 1999. Immunodetection and partial cDNA sequence of the proteoglycan, superficial zone protein, synthesized by cells lining synovial joints. *Journal of Orthopaedic Research,* 17, 110-120.

SCOTTI, C., PICCININI, E., TAKIZAWA, H., TODOROV, A., BOURGINE, P., PAPADIMITROPOULOS, A., BARBERO, A., MANZ, M. G. & MARTIN, I. 2013. Engineering of a functional bone organ through endochondral ossification. *Proceedings of the National Academy of Sciences of the United States of America,* 110, 3997-4002.

SCOTTI, C., TONNARELLI, B., PAPADIMITROPOULOS, A., SCHERBERICH, A., SCHAEREN, S., SCHAUERTE, A., LOPEZ-RIOS, J., ZELLER, R., BARBERO, A. & MARTIN, I. 2010. Recapitulation of endochondral bone formation using human adult mesenchymal stem cells as a paradigm for developmental engineering. *Proceedings of the National Academy of Sciences of the United States of America,* 107, 7251-7256.

SEIL, R. & PAPE, D. 2011. Causes of failure and etiology of painful primary total knee arthroplasty. *Knee Surgery, Sports Traumatology, Arthroscopy,* 19, 1418-1432.

SELMI, T. A. S., NEYRET, P., VERDONK, P. C. M. & BARNOUIN, L. 2007. Autologous chondrocyte transplantation in combination with an alginate-

agarose based hydrogel (Cartipatch). *Techniques in Knee Surgery,* 6, 253-258.

SELMI, T. A. S., VERDONK, P., CHAMBAT, P., DUBRANA, F., POTEL, J. F., BARNOUIN, L. & NEYRET, P. 2008. Autologous chondrocyte implantation in a novel alginate-agarose hydrogel: Outcome at two years. *Journal of Bone and Joint Surgery - Series B,* 90, 597-604.

SETTON, L. 2008. Polymer therapeutics: reservoir drugs. *Nature materials,* 7, 172-174.

SETTON, L. A., TOHYAMA, H. & MOW, V. C. 1998. Swelling and curling behaviors of articular cartilage. *Journal of Biomechanical Engineering,* 120, 355-361.

SHEEHY, E. J., BUCKLEY, C. T. & KELLY, D. J. 2011. Chondrocytes and bone marrow-derived mesenchymal stem cells undergoing chondrogenesis in agarose hydrogels of solid and channelled architectures respond differentially to dynamic culture conditions. *Journal of Tissue Engineering and Regenerative Medicine,* 5, 747-758.

SHEEHY, E. J., BUCKLEY, C. T. & KELLY, D. J. 2012. Oxygen tension regulates the osteogenic, chondrogenic and endochondral phenotype of bone marrow derived mesenchymal stem cells. *Biochemical and Biophysical Research Communications,* 417, 305-310.

SHEEHY, E. J., VINARDELL, T., BUCKLEY, C. T. & KELLY, D. J. 2013. Engineering osteochondral constructs through spatial regulation of endochondral ossification. *Acta Biomaterialia,* 9, 5484-5492.

SHEN, B., WEI, A., TAO, H., DIWAN, A. D. & MA, D. D. F. 2009. BMP-2 enhances TGF-β3-mediated chondrogenic differentiation of human bone marrow multipotent mesenchymal stromal cells in alginate bead culture. *Tissue Engineering - Part A,* 15, 1311-1320.

SHERWOOD, J. K., RILEY, S. L., PALAZZOLO, R., BROWN, S. C., MONKHOUSE, D. C., COATES, M., GRIFFITH, L. G., LANDEEN, L. K. & RATCLIFFE, A. 2002. A three-dimensional osteochondral composite scaffold for articular cartilage repair. *Biomaterials,* 23, 4739-4751.

SHIRASAWA, S., SEKIYA, I., SAKAGUCHI, Y., YAGISHITA, K., ICHINOSE, S. & MUNETA, T. 2006. In vitro chondrogenesis of human synovium-derived mesenchymal stem cells: optimal condition and comparison with bone marrow-derived cells. *J Cell Biochem,* 97, 84-97.

SHU, B., ZHANG, M., XIE, R., WANG, M., JIN, H., HOU, W., TANG, D., HARRIS, S. E., MISHINA, Y., O'KEEFE, R. J., HILTON, M. J., WANG, Y. & CHEN, D. 2011. BMP2, but not BMP4, is crucial for chondrocyte proliferation and maturation during endochondral bone development. *Journal of Cell Science,* 124, 3428-3440.

SIEMINSKI, A. L. & GOOCH, K. J. 2000. Biomaterial-microvasculature interactions. *Biomaterials,* 21, 2233-2241.

SILVA, M. M. C. G., CYSTER, L. A., BARRY, J. J. A., YANG, X. B., OREFFO, R. O. C., GRANT, D. M., SCOTCHFORD, C. A., HOWDLE, S. M., SHAKESHEFF, K. M. & ROSE, F. R. A. J. 2006. The effect of anisotropic architecture on cell and tissue infiltration into tissue engineering scaffolds. *Biomaterials,* 27, 5909-5917.

SIMMONS, C. A., ALSBERG, E., HSIONG, S., KIM, W. J. & MOONEY, D. J. 2004. Dual growth factor delivery and controlled scaffold degradation

enhance in vivo bone formation by transplanted bone marrow stromal cells. *Bone,* 35, 562-569.

SOLTZ, M. A. & ATESHIAN, G. A. 1998. Experimental verification and theoretical prediction of cartilage interstitial fluid pressurization at an impermeable contact interface in confined compression. *Journal of Biomechanics,* 31, 927-934.

SOMMERFELDT, D. & RUBIN, C. 2001. Biology of bone and how it orchestrates the form and function of the skeleton. *European Spine Journal,* 10, S86-S95.

SPILLER, K. L., MAHER, S. A. & LOWMAN, A. M. 2011. Hydrogels for the repair of articular cartilage defects. *Tissue Engineering - Part B: Reviews,* 17, 281-299.

ST-PIERRE, J. P., GAN, L., WANG, J., PILLIAR, R. M., GRYNPAS, M. D. & KANDEL, R. A. 2012. The incorporation of a zone of calcified cartilage improves the interfacial shear strength between in vitro-formed cartilage and the underlying substrate. *Acta Biomaterialia,* 8, 1603-1615.

STEINBERG, M. S. 1970. Does differential adhesion govern self-assembly processes in histogenesis? Equilibrium configurations and the emergence of a hierarchy among populations of embryonic cells. *Journal of Experimental Zoology,* 173, 395-433.

STEWART, A. A., BYRON, C. R., PONDENIS, H. & STEWART, M. C. 2007. Effect of fibroblast growth factor-2 on equine mesenchymal stem cell monolayer expansion and chondrogenesis. *American Journal of Veterinary Research,* 68, 941-945.

SUN, D., AYDELOTTE, M. B. & MALDONADO, B. 1986. Clonal analysis of the population of chondrocytes from the Swarm rat chondrosarcoma in agarose culture. *J Orthop Res,* 4, 427-436.

SUN, W. & LAL, P. 2002. Recent development on computer aided tissue engineering - A review. *Computer Methods and Programs in Biomedicine,* 67, 85-103.

SUNDELACRUZ, S. & KAPLAN, D. L. 2009. Stem cell- and scaffold-based tissue engineering approaches to osteochondral regenerative medicine. *Seminars in Cell and Developmental Biology,* 20, 646-655.

TACCHETTI, C., QUARTO, R., NITSCH, L., HARTMANN, D. J. & CANCEDDA, R. 1987. In vitro morphogenesis of chick embryo hypertrophic cartilage. *Journal of Cell Biology,* 105, 999-1006.

TALLHEDEN, T., BENGTSSON, C., BRANTSING, C., SJO?GREN-JANSSON, E., CARLSSON, L., PETERSON, L., BRITTBERG, M. & LINDAHL, A. 2005. Proliferation and differentiation potential of chondrocytes from osteoarthritic patients. *Arthritis research & therapy.,* 7, R560-568.

TEMENOFF, J. S. & MIKOS, A. G. 2000a. Injectable biodegradable materials for orthopedic tissue engineering. *Biomaterials,* 21, 2405-2412.

TEMENOFF, J. S. & MIKOS, A. G. 2000b. Review: Tissue engineering for regeneration of articular cartilage. *Biomaterials,* 21, 431-440.

TERRACIANO, V., HWANG, N., MORONI, L., PARK, H. B., ZHANG, Z., MIZRAHI, J., SELIKTAR, D. & ELISSEEFF, J. 2007. Differential response of adult and embryonic mesenchymal progenitor cells to mechanical compression in hydrogels. *Stem Cells,* 25, 2730-2738.

THEODOROPOULOS, J. S., DE CROOS, J. N. A., PARK, S. S., PILLIAR, R. & KANDEL, R. A. 2011. Integration of tissue-engineered cartilage with host

cartilage: An in vitro model. *Clinical Orthopaedics and Related Research,* 469, 2785-2795.

THOMAS, R. S., CLARKE, A. R., DUANCE, V. C. & BLAIN, E. J. 2011. Effects of Wnt3A and mechanical load on cartilage chondrocyte homeostasis. *Arthritis Res Ther,* 13, R203.

THORPE, S. D., BUCKLEY, C. T., VINARDELL, T., O'BRIEN, F. J., CAMPBELL, V. A. & KELLY, D. J. 2008. Dynamic compression can inhibit chondrogenesis of mesenchymal stem cells. *Biochemical and Biophysical Research Communications,* 377, 458-462.

THORPE, S. D., BUCKLEY, C. T., VINARDELL, T., O'BRIEN, F. J., CAMPBELL, V. A. & KELLY, D. J. 2010a. The response of bone marrow-derived mesenchymal stem cells to dynamic compression following tgf-β3 induced chondrogenic differentiation. *Annals of Biomedical Engineering,* 38, 2896-2909.

THORPE, S. D., BUCKLEY, C. T., VINARDELL, T., O'BRIEN, F. J., CAMPBELL, V. A. & KELLY, D. J. 2010b. The Response of Bone Marrow-Derived Mesenchymal Stem Cells to Dynamic Compression Following TGF-β3 Induced Chondrogenic Differentiation. *Annals of Biomedical Engineering*, 1-14.

THORPE, S. D., NAGEL, T., CARROLL, S. F. & KELLY, D. J. 2013. Modulating gradients in regulatory signals within mesenchymal stem cell seeded hydrogels: a novel strategy to engineer zonal articular cartilage. *PLoS One,* 8, e60764.

TORTELLI, F., TASSO, R., LOIACONO, F. & CANCEDDA, R. 2010. The development of tissue-engineered bone of different origin through endochondral and intramembranous ossification following the implantation of mesenchymal stem cells and osteoblasts in a murine model. *Biomaterials,* 31, 242-249.

TOYODA, T., SEEDHOM, B. B., KIRKHAM, J. & BONASS, W. A. 2002. Upregulation of aggrecan and type II collagen mRNA expression in bovine chondrocytes by the application of hydrostatic pressure. *Biorheology,* 40, 79-85.

TOYODA, T., SEEDHOM, B. B., YAO, J. Q., KIRKHAM, J., BROOKES, S. & BONASS, W. A. 2003. Hydrostatic Pressure Modulates Proteoglycan Metabolism in Chondrocytes Seeded in Agarose. *Arthritis and Rheumatism,* 48, 2865-2872.

TRAN-KHANH, N., HOEMANN, C. D., MCKEE, M. D., HENDERSON, J. E. & BUSCHMANN, M. D. 2005. Aged bovine chondrocytes display a diminished capacity to produce a collagen-rich, mechanically functional cartilage extracellular matrix. *J Orthop Res,* 23, 1354-1362.

TRAN, S. C., COOLEY, A. J. & ELDER, S. H. 2011. Effect of a mechanical stimulation bioreactor on tissue engineered, scaffold-free cartilage. *Biotechnology and Bioengineering,* 108, 1421-1429.

TREMBLAY, P. L., HUDON, V., BERTHOD, F., GERMAIN, L. & AUGER, F. A. 2005. Inosculation of tissue-engineered capillaries with the host's vasculature in a reconstructed skin transplanted on mice. *American Journal of Transplantation,* 5, 1002-1010.

TSUCHIYA, K., CHEN, G., USHIDA, T., MATSUNO, T. & TATEISHI, T. 2004. The effect of coculture of chondrocytes with mesenchymal stem cells on

their cartilaginous phenotype in vitro. *Materials Science and Engineering C,* 24, 391-396.

VAN DER KRAAN, P. M. & VAN DEN BERG, W. B. 2012. Chondrocyte hypertrophy and osteoarthritis: Role in initiation and progression of cartilage degeneration? *Osteoarthritis and Cartilage,* 20, 223-232.

VAN DER STOK, J., KOOLEN, M. K. E., JAHR, H., KOPS, N., WAARSING, J. H., WEINANS, H. & VAN DER JAGT, O. P. 2014. Chondrogenically differentiated mesenchymal stromal cell pellets stimulate endochondral bone regeneration in critical-sized bone defects. *European Cells and Materials,* 27, 137-148.

VAN VLIERBERGHE, S., DUBRUEL, P. & SCHACHT, E. 2011. Biopolymer-based hydrogels as scaffolds for tissue engineering applications: A review. *Biomacromolecules,* 12, 1387-1408.

VILLANUEVA, I., GLADEM, S. K., KESSLER, J. & BRYANT, S. J. 2010. Dynamic loading stimulates chondrocyte biosynthesis when encapsulated in charged hydrogels prepared from poly(ethylene glycol) and chondroitin sulfate. *Matrix Biology,* 29, 51-62.

VILLANUEVA, I., HAUSCHULZ, D. S., MEJIC, D. & BRYANT, S. J. 2008. Static and dynamic compressive strains influence nitric oxide production and chondrocyte bioactivity when encapsulated in PEG hydrogels of different crosslinking densities. *Osteoarthritis and Cartilage,* 16, 909-918.

VINARDELL, T., BUCKLEY, C. T., THORPE, S. D. & KELLY, D. J. 2010. Composition-function relations of cartilaginous tissues engineered from chondrocytes and mesenchymal stem cells isolated from bone marrow and infrapatellar fat pad. *J Tissue Eng Regen Med.*

VINARDELL, T., BUCKLEY, C. T., THORPE, S. D. & KELLY, D. J. 2011. Composition-function relations of cartilaginous tissues engineered from chondrocytes and mesenchymal stem cells isolated from bone marrow and infrapatellar fat pad. *J Tissue Eng Regen Med* 5, 673-683.

VINARDELL, T., SHEEHY, E. J., BUCKLEY, C. T. & KELLY, D. J. 2012a. A comparison of the functionality and in vivo phenotypic stability of cartilaginous tissues engineered from different stem cell sources. *Tissue Engineering - Part A,* 18, 1161-1170.

VINARDELL, T., SHEEHY, E. J., BUCKLEY, C. T. & KELLY, D. J. 2012b. A comparison of the functionality and in vivo phenotypic stability of cartilaginous tissues engineered from different stem cell sources. *Tissue Eng Part A,* 18, 1161-70.

VINARDELL, T., THORPE, S. D., BUCKLEY, C. T. & KELLY, D. J. 2009. Chondrogenesis and integration of mesenchymal stem cells within an in vitro cartilage defect repair model. *Annals of Biomedical Engineering,* 37, 2556-2565.

VINATIER, C., MRUGALA, D., JORGENSEN, C., GUICHEUX, J. & NOÃ«L, D. 2009. Cartilage engineering: a crucial combination of cells, biomaterials and biofactors. *Trends in Biotechnology,* 27, 307-314.

WALDMAN, S. D., COUTO, D. C., GRYNPAS, M. D., PILLIAR, R. M. & KANDEL, R. A. 2006. A single application of cyclic loading can accelerate matrix deposition and enhance the properties of tissue-engineered cartilage. *Osteoarthritis and Cartilage,* 14, 323-330.

WALDMAN, S. D., SPITERI, C. G., GRYNPAS, M. D., PILLIAR, R. M., HONG, J. & KANDEL, R. A. 2003a. Effect of biomechanical conditioning on cartilaginous tissue formation in vitro. *J Bone Joint Surg Am,* 85-A Suppl 2, 101-5.

WALDMAN, S. D., SPITERI, C. G., GRYNPAS, M. D., PILLIAR, R. M. & KANDEL, R. A. 2003b. Long-term intermittent shear deformation improves the quality of cartilaginous tissue formed in vitro. *J Orthop Res,* 21, 590-6.

WANG, A., DE LA MOTTE, C., LAUER, M. & HASCALL, V. 2011. Hyaluronan matrices in pathobiological processes. *FEBS Journal,* 278, 1412-1418.

WANG, C. C. B., CHAHINE, N. O., HUNG, C. T. & ATESHIAN, G. A. 2003. Optical determination of anisotropic material properties of bovine articular cartilage in compression. *Journal of Biomechanics,* 36, 339-353.

WANG, D. W., FERMOR, B., GIMBLE, J. M., AWAD, H. A. & GUILAK, F. 2005. Influence of oxygen on the proliferation and metabolism of adipose derived adult stem cells. *Journal of Cellular Physiology,* 204, 184-191.

WANG, Q. G., MAGNAY, J. L., NGUYEN, B., THOMAS, C. R., ZHANG, Z., EL HAJ, A. J. & KUIPER, N. J. 2009. Gene expression profiles of dynamically compressed single chondrocytes and chondrons. *Biochemical and Biophysical Research Communications,* 379, 738-742.

WANG, X., GROGAN, S. P., RIESER, F., WINKELMANN, V., MAQUET, V., LA BERGE, M. & MAINIL-VARLET, P. 2004. Tissue engineering of biphasic cartilage constructs using various biodegradable scaffolds: An in vitro study. *Biomaterials,* 25, 3681-3688.

WARMAN, M. L. 2000. Human genetic insights into skeletal development, growth, and homeostasis. *Clinical Orthopaedics and Related Research,* S40-S54.

WENDT, D., JAKOB, M. & MARTIN, I. 2005. Bioreactor-based engineering of osteochondral grafts: from model systems to tissue manufacturing. *J Biosci Bioeng,* 100, 489-94.

WENG, Y., WANG, M., LIU, W., HU, X., CHAI, G., YAN, Q., ZHU, L., CUI, L. & CAO, Y. 2006. Repair of experimental alveolar bone defects by tissue-engineered bone. *Tissue Engineering,* 12, 1503-1513.

WICKHAM, M. Q., ERICKSON, G. R., GIMBLE, J. M., VAIL, T. P. & GUILAK, F. 2003a. Multipotent stromal cells derived from the infrapatellar fat pad of the knee. *Clin Orthop Relat Res,* 196-212.

WICKHAM, M. Q., ERICKSON, G. R., GIMBLE, J. M., VAIL, T. P. & GUILAK, F. 2003b. Multipotent stromal cells derived from the infrapatellar fat pad of the knee. *Clinical Orthopaedics and Related Research,* 196-212.

WIDUCHOWSKI, W., WIDUCHOWSKI, J. & TRZASKA, T. 2007. Articular cartilage defects: Study of 25,124 knee arthroscopies. *Knee,* 14, 177-182.

WOODFIELD, T. B., MALDA, J., DE WIJN, J., PETERS, F., RIESLE, J. & VAN BLITTERSWIJK, C. A. 2004. Design of porous scaffolds for cartilage tissue engineering using a three-dimensional fiber-deposition technique. *Biomaterials,* 25, 4149-61.

WOODFIELD, T. B. F., GUGGENHEIM, M., VON RECHENBERG, B., RIESLE, J., VAN BLITTERSWIJK, C. A. & WEDLER, V. 2009. Rapid prototyping of anatomically shaped, tissue-engineered implants for restoring congruent articulating surfaces in small joints. *Cell Proliferation,* 42, 485-497.

WU, L., CAI, X., ZHANG, S., KARPERIEN, M. & LIN, Y. 2013a. Regeneration of articular cartilage by adipose tissue derived mesenchymal stem cells:

Perspectives from stem cell biology and molecular medicine. *Journal of Cellular Physiology,* 228, 938-944.

WU, L., LEIJTEN, J., VAN BLITTERSWIJK, C. A. & KARPERIEN, M. 2013b. Fibroblast growth factor-1 is a mesenchymal stromal cell-secreted factor stimulating proliferation of osteoarthritic chondrocytes in co-culture. *Stem Cells and Development,* 22, 2356-2367.

WU, L., LEIJTEN, J. C. H., GEORGI, N., POST, J. N., VAN BLITTERSWIJK, C. A. & KARPERIEN, M. 2011. Trophic effects of mesenchymal stem cells increase chondrocyte proliferation and matrix formation. *Tissue Engineering - Part A,* 17, 1425-1436.

WU, L., PRINS, H. J., HELDER, M. N., VAN BLITTERSWIJK, C. A. & KARPERIEN, M. 2012. Trophic effects of mesenchymal stem cells in chondrocyte co-cultures are independent of culture conditions and cell sources. *Tissue Eng Part A,* 18, 1542-51.

XU, L., WANG, Q., XU, F., YE, Z., ZHOU, Y. & TAN, W. S. 2013. Mesenchymal stem cells downregulate articular chondrocyte differentiation in noncontact coculture systems: Implications in cartilage tissue regeneration. *Stem Cells and Development,* 22, 1657-1669.

YAMAOKA, H., ASATO, H., OGASAWARA, T., NISHIZAWA, S., TAKAHASHI, T., NAKATSUKA, T., KOSHIMA, I., NAKAMURA, K., KAWAGUCHI, H., CHUNG, U. I., TAKATO, T. & HOSHI, K. 2006. Cartilage tissue engineering using human auricular chondrocytes embedded in different hydrogel materials. *Journal of Biomedical Materials Research - Part A,* 78, 1-11.

YANG, H. N., PARK, J. S., NA, K., WOO, D. G., KWON, Y. D. & PARK, K. H. 2009. The use of green fluorescence gene (GFP)-modified rabbit mesenchymal stem cells (rMSCs) co-cultured with chondrocytes in hydrogel constructs to reveal the chondrogenesis of MSCs. *Biomaterials,* 30, 6374-6385.

YANG, W., YANG, F., WANG, Y., BOTH, S. K. & JANSEN, J. A. 2013. In vivo bone generation via the endochondral pathway on three-dimensional electrospun fibers. *Acta Biomaterialia,* 9, 4505-4512.

YU, H., GRYNPAS, M. & KANDEL, R. A. 1997. Composition of cartilagenous tissue with mineralized and non-mineralized zones formed in vitro. *Biomaterials,* 18, 1425-1431.

ZEIN, I., HUTMACHER, D. W., TAN, K. C. & TEOH, S. H. 2002. Fused deposition modeling of novel scaffold architectures for tissue engineering applications. *Biomaterials,* 23, 1169-1185.

ZHANG, B., YANG, S., SUN, Z., ZHANG, Y., XIA, T., XU, W. & YE, S. 2011. Human mesenchymal stem cells induced by growth differentiation factor 5: an improved self-assembly tissue engineering method for cartilage repair. *Tissue Eng Part C Methods,* 17, 1189-99.

ZHANG, L., SU, P., XU, C., YANG, J., YU, W. & HUANG, D. 2010. Chondrogenic differentiation of human mesenchymal stem cells: A comparison between micromass and pellet culture systems. *Biotechnol Lett* 32, 1339-1346.

Appendices

Appendix I: Introducing Microchannels into Chondrocyte-Seeded Agarose Hydrogels Influences Matrix Accumulation in Response to Dynamic Compression and TGF-β3 Stimulation

Abstract

Tissue engineering technologies combining cells with scaffolds are promising strategies for cartilage repair. A recurring problem with scaffold-based therapies is the formation of superior peripheral tissue, resulting in an inhomogeneous tissue construct. Nutrient transfer limitations to the centre of the construct are believed to be responsible for the phenomena. The introduction of channels into a scaffold or hydrogel, or using mechanical loading to improve nutrient transfer, are two potential approaches to overcome this limitation. If both approaches are combined, the mechanical environment within dynamically compressed hydrogels will be modified by the introduction of microchannels into the construct. The objective of this study was to investigate how chondrocytes would respond to this altered mechanical environment.

Isolated porcine chondrocytes were suspended in 2% agarose. Microchanneled and solid construct cylinders (Ø 6 x 4 mm) were fabricated and maintained in supplemented media containing TGF-β3 (10ηg/ml). Loaded solid and channeled constructs were subjected to a compressive strain amplitude of 10%, for 2 hours/day, 5 days/week, for a duration of 6 weeks.

In the presence of TGF-β3, dynamic compressive loading in solid constructs resulted in an increase in *sulphated glycosaminoglycan* (sGAG) accumulation. There was a trend towards greater sGAG synthesis in microchanneled constructs; however sGAG accumulation was lower in these groups. While the introduction of microchannels alone may not result in the development of engineered tissue suitable for implantation, it does represent a unique model to investigate chondrocyte mechanobiology.

Introduction

Tissue engineering strategies aim to repair cartilaginous defects through the use of porous scaffold or hydrogel based systems which provide a 3D environment allowing cells to maintain their differentiated phenotype and deposit extracellular matrix (ECM). Agarose hydrogels are commonly used for cartilage tissue engineering applications, as they have been found to support the chondrogenic phenotype and the synthesis of cartilage ECM (Benya and Shaffer, 1982, Buschmann et al., 1992b). In addition they have been shown to provide a well characterized mechanical environment (Buckley et al., 2009c), suitable for investigating cellular responses to biophysical stimuli. The biosynthetic activity of chondrocytes during in vitro cultivation is known to depend on both the biochemical and biophysical stimuli experienced by the cells. Previous studies have shown that the application of dynamic compressive loading to chondrocyte-seeded agarose hydrogels enhances cartilage specific matrix synthesis (Mauck et al., 2000b, Buschmann et al., 1995a, Mauck et al., 2002b).

However a recurring problem with these agarose constructs is the heterogeneous deposition of ECM within them, with typically greater matrix accumulation in the peripheral regions of the construct (Kelly et al., 2009). Kelly et al. (Kelly et al., 2006) reported a greater stiffness in the periphery of both free-swelling and dynamically loaded constructs. Ng et al. (Ng et al., 2005) also observed a heterogeneous development of material properties in free swelling chondrocyte-seeded agarose disks. It has been suggested that nutrient diffusion limitations are a possible reason for these heterogeneous constructs (Martin et al., 2004b). Dynamic compression can enhance nutrient transport within agarose constructs (Albro et al., 2010a). Altering the architecture of the constructs is another possible way to overcome nutrient transport limitations. Bian et al. (Bian et al., 2009a) obtained a more homogeneous cartilaginous tissue upon the introduction of macroscopic channels throughout the depth of the construct. Buckley et al. (Buckley et al., 2009a) found that the introduction of microchannels, in addition to rotational

culture, resulted in sGAG accumulation levels in the core similar to those measured in the periphery of solid constructs.

The objective of this study is to investigate the influence of construct architecture and dynamic loading on matrix accumulation within chondrocyte seeded agarose hydrogels. Channels were transversely introduced into cylindrical agarose gels, and constructs were subjected to dynamic loading over a 42 day period. In addition solid, non-channeled constructs were cultured in parallel. My original hypothesis was that dynamic compressive loading of channeled constructs would enhance nutrient delivery and fluid flow, and therefore lead to a greater and more homogeneous deposition of matrix throughout the construct compared to solid gels or free swelling conditions.

Materials and Methods

A. Cell isolation, expansion and hydrogel encapsulation

Articular cartilage was aseptically harvested from the femoropatellar joints of two 4-month old porcine donors (~50kg). Isolated chondrocytes were plated at a seeding density of 8.75×10^6 cells/cm^2 and expanded to passage one (P1). Chondrocytes were then suspended in DMEM/F12 and mixed with 4% agarose (Type VII, Sigma-Aldrich, Arklow, Ireland) at ~40°C, to yield a final gel concentration of 2% and a cell density of 15×10^6 cells/ml. The agarose/cell suspension was cast in a polytetrafluoroethylene (PTFE) mould, and solid construct cylinders were removed using a 6mm biopsy punch. An equal number of channeled construct cylinders were fabricated via a moulding process as previously described (Buckley et al., 2009a). Channels were of 500μm diameter, with a centre-centre spacing of 1mm. Constructs were maintained in 6-well plates in a chemically defined chondrogenic medium (CDM) consisting of DMEM GlutaMAX supplemented with penicillin (100U/ml)-streptomycin (100μg/ml) (all GIBCO, Biosciences, Ireland), 1.5 mg/ml bovine serum albumin (BSA), 100μg/ml sodium pyruvate, 40μg/ml L-proline, 4.7 μg/ml

linoleic acid, 50 μg/ml L-ascorbic acid-2-phosphate, 1× insulin-transferrin-selenium, 2.5 μg/ml amphotericin B, and 100nM dexamethasone (all Sigma-Aldrich, Ireland). Media was also supplemented with 10ng/ml TGF-β3 (R&D Systems, Abingdon, UK). After cell encapsulation, constructs were left in free swelling conditions for 72 hours before the addition of TGF-β3, and the initiation of dynamic loading (Day 0). Medium was fully replaced twice a week, with 500μl samples taken from wells for each group (n=2-3) at each medium exchange.

B. Dynamic compression application

Intermittent dynamic compression (DC) was carried out in a custom pneumatic based compression bioreactor housed within an incubator as previously described (Thorpe et al., 2010b). The compression protocol consisted of ~10% strain amplitude superimposed on a 0.01 N/construct preload at a frequency of 1Hz. Constructs were loaded each day for 2 consecutive hours, 5days/week over 42 days. Free swelling (FS) controls were maintained adjacent to the bioreactor during loading periods, in the same amount of medium. Both solid and microchanneled constructs were subjected to both culturing regimes, and constructs were assessed at 0, 21, and 42 days.

C. Biochemical analysis

The biochemical content of constructs was assessed at each time point. All constructs were cored using a 3mm biopsy punch and separated from the annulus. The wet mass of both the core and annulus was recorded and all samples were subsequently frozen at -85°C for later analyses. Samples were digested with papain (125μg/ml) in 0.1M sodium acetate, 5mM L-cysteine-HCL, 0.05 M EDTA, pH 6 (all Sigma-Aldrich, Ireland) under constant rotation at 60°C for 18 hours. DNA content was quantified using the Hoechst Bisbenzimide 33258 dye assay. Proteoglycan content was estimated by quantifying the amount of sGAG in each hydrogel core/annulus using the dimethylmethylene blue dye binding assay (Blyscan, Biocolor Ltd., Northern Ireland), with a shark chondroitin sulphate standard. sGAG secreted to culture media was also analysed for each group, with

total media volume accounted for. Total collagen content was determined by measuring the hydroxyproline content, using a hydroxyproline to collagen ratio of 1:7.69.

D. Histology and immunohistochemistry

At each time point, two or more samples per group were formalin fixed, dehydrated, and embedded in paraffin. Sectioning at 5μm produced a cross section perpendicular to the disc face. Sections were stained with 1% alcian blue 8GX (Sigma-Aldrich, Arklow, Ireland) in 0.1M HCL for sGAG accumulation. Samples were stained with picro-sirius red for collagen deposition. Collagen type I and II deposition were identified by immunohistochemical analysis. A mouse monoclonal collagen type I antibody (1:200; 1.4 mg/ml; Abcam, UK) and mouse monoclonal anti-collagen type II antibody (1:80; 1mg/ml; Abcam) were used as primary antibodies for collagen types I and II respectively. An anti-mouse IgG biotin secondary antibody (1:200; 1mg/ml; Sigma-Aldrich) was used for the detection of both primary antibodies.

E. Statistical Analysis

Statistical analyses were performed using the software package MINITAB 15.1 (Minitab Ltd., Coventry, UK). Groups were analysed for significant differences using a general linear model for analysis of variance with factors of culture time, architecture, dynamic compression, and interactions between these factors examined. Tukey's test for multiple comparisons was used to compare conditions. Significance was accepted at a level of $p<0.05$. Numerical and graphical results are presented as mean ± SD (n=3-4 for each group at each time point).

Results

sGAG accumulation was observed to significantly increase in all experimental groups (Figure S1A). By day 42 dynamically compressed solid groups (DCS) were found to have significantly greater sGAG content (534.7±38.7 μg) compared to all other groups. Dynamically compressed microchanneled groups (DCM) accumulated comparable levels of sGAG as compared to free swelling microchanneled groups (FSM) (307.18±10.64 μg vs. 304.4±22.2 μg). It was also noted that there was no significant difference in sGAG levels between the four groups at the final time point when normalized to DNA (Figure S1D). DNA content was found to be significantly greater in DCS groups (11.029±1.135 μg), when compared to free swelling solid (FSS) groups (7.566±0.44 μg) after 42 days in culture (Figure S1C).

I next compared core and annulus accumulation at day 42 (Figure S3A). All groups were found to have significantly greater sGAG levels in the annulus compared to their corresponding core (μg). This is to be expected as the annulus represents a volume three times that of the core. When normalized to wet weight however (data not shown), each group produced significantly more sGAG in the core than their corresponding annulus. I also found that the FSS, FSM, and DCS groups produced significantly more sGAG in the core than their corresponding annulus at day 42 when normalized to DNA.

At day 42, DCM constructs were found to release the greatest amount of sGAG (1026.6±49.6 μg) to the media ($p<0.05$). I also found at this time point that DCS constructs released significantly more sGAG (921±37.5 μg) to the media than either FSM (812.7±24.4 μg) or FSS (654.08±8.02 μg) constructs ($p<0.05$). Taking into account sGAG both accumulated and released per construct over the 42 day culture period, I calculated that DCM constructs produced the greatest overall sGAG amounts when normalized to DNA (156.3743±15.97704 μg/μg) (Figure S1F), although the differences were not statistically significant.

Collagen accumulation was observed to increase at each time point (Figure S1B). DCS groups produced the highest levels of collagen (239.77±21.99 μg) at day

42 ($p<0.05$). Loading was also seen to enhance collagen accumulation in microchanneled groups. When collagen was normalized to DNA, I found no significant difference between groups at day 42 (Figure S1E).

Construct sections from all experimental groups stained positively with Alcian blue (Figure S2). DCS constructs exhibited slightly more intense staining for sGAG than FSS constructs, while staining was comparable between the DCM and FSM groups. Less intense staining was observed around the periphery of the constructs. This corresponded to our sGAG biochemical results (%w/w). I also observed that the staining seemed to decrease in intensity further into the core of the construct. A more homogeneous sGAG distribution was observed around DCM constructs. Immunohistochemistry for type II collagen revealed a more homogenous distribution in loaded constructs (Figure S2).

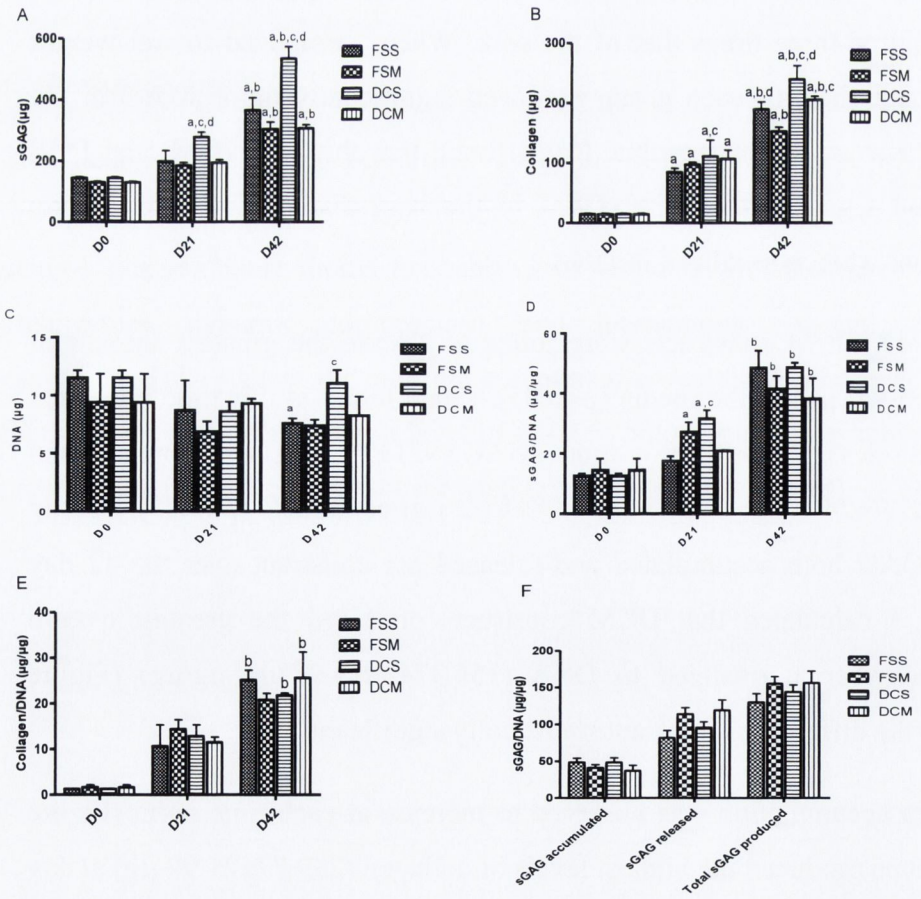

Figure S1: Biochemical composition of constructs for FSS, FSM, DCS, and DCM groups. (A) sGAG content (μg); (B) Collagen content (μg); (C) DNA content (μg); (D) sGAG/DNA (μg/μg); (E) Collagen/DNA (μg/μg); (F) Total sGAG/DNA accumulated, released, and produced at day 42 (μg/μg). a: $p<0.05$ vs. Day 0; b: $p<0.05$ vs. Day 21; c: $p<0.05$ vs. different culturing conditions with same architecture at same time point; d: $p<0.05$ vs. different architecture with same culturing conditions at same time point.

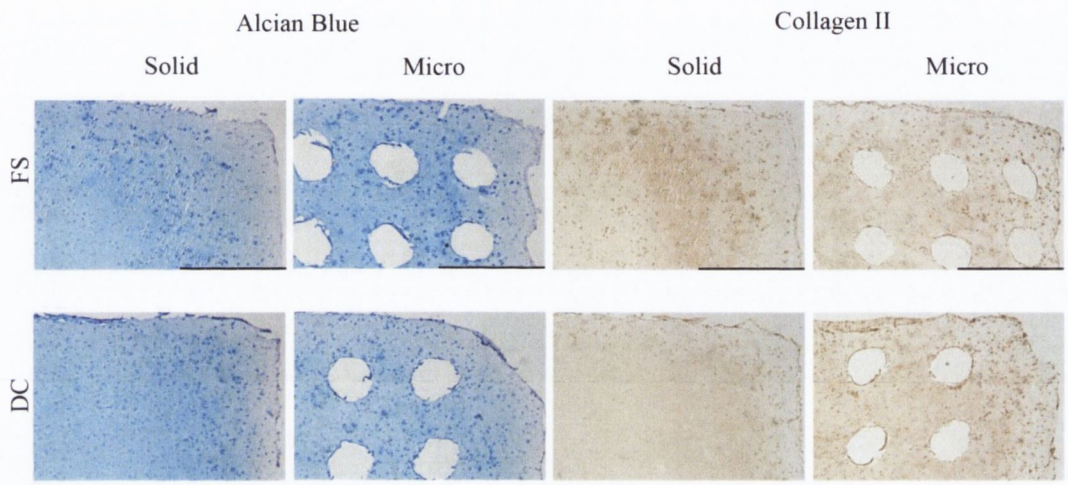

Figure S2: Alcian Blue staining and type II collagen immunohistochemistry staining of solid and microchanneled constructs subjected to dynamic compression (DC) and free swelling (FS) conditions. Scale bar 1mm. Sections are representative of ¼ of a construct.

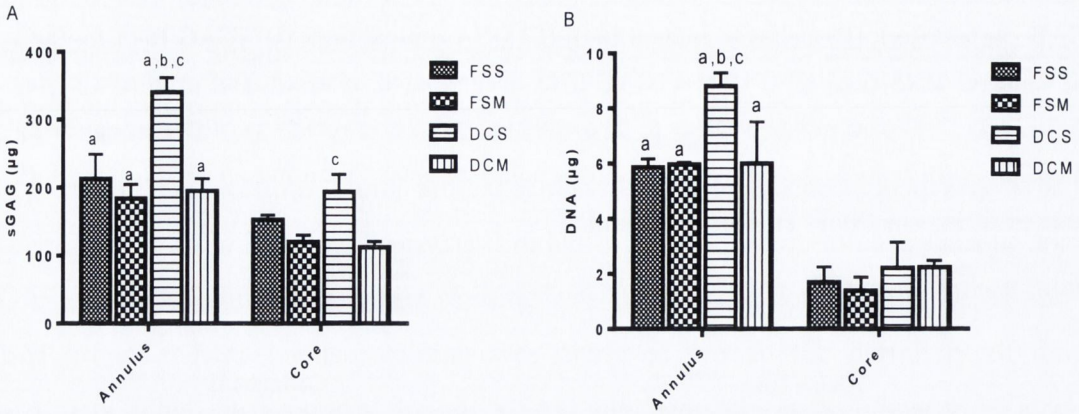

Figure S3: Biochemical composition of core and annular regions for FSS, FSM, DCS, and DCM groups at D42. (A) sGAG content (µg); (B) DNA content (µg). a: $p<0.05$ vs. core; b: $p<0.05$ vs. different culturing conditions with same architecture in same region; c: $p<0.05$ vs. different architecture with same culturing conditions in same region.

Discussion

The purpose of this study was to investigate the influence of dynamic compressive loading and modified construct architecture on the *in vitro* development of engineered cartilage tissue. It has been previously shown that the biosynthetic activity of chondrocytes depends on the biophysical stimuli experienced by the cells (Buschmann et al., 1995a). I also observed greater sGAG accumulation in loaded solid constructs compared to all other groups, but I did not find that loading enhanced matrix accumulation in DCM groups. It was seen that loading enhanced cell proliferation in solid gels at day 42, when compared to FSS constructs (Figure S1C). Comparable sGAG synthesis rates (sGAG/DNA) between all groups at this time point (Figure S1D) indicate that this superior sGAG accumulation in DCS constructs was due to a higher cell number. The fact that loading maintains cell viability and/or promotes proliferation in solid constructs and not in microchannel constructs may be due to higher levels of fluid flow in loaded channeled constructs. From previous finite element biphasic models for solid and channeled constructs, we predicted high levels of strain and fluid flow at the edges of channels, with pore pressure greatest in the radial spaces separating the channels.

A more homogeneous distribution of sGAG was observed throughout DCM and FSM hydrogels (Figure S2), suggesting that a modified scaffold architecture can result in a more homogeneous construct. This corresponded to our biochemical results (%w/w), with the DCM and FSM groups presenting the least heterogeneous spatial distribution of sGAG (data not shown). From our histological sections we can see that a significant amount of sGAG is diffusing out into the media, with poor staining around the periphery of the constructs. The fact that both solid and microchannel constructs are releasing sGAG in this manner, for both culturing conditions indicates that agarose may not be an efficient scaffold for retaining ECM. A high oxygen environment at the periphery of the constructs could also be inhibiting chondrogenesis. I also observed that staining seemed to decrease in intensity the further into the core of the solid construct one passed, once one proceeded past the initial peripheral region, indicating that there may be some nutrient transport limitations towards the core.

Greater sGAG release to the media was observed in loaded constructs, with DCM constructs releasing the greatest amount of sGAG (μg). This can be explained by the microchannels providing a conduit for the diffusion of ECM components into the surrounding media. Taking into account sGAG both accumulated and released per construct over the 42 day culture period (Figure S1F), we observe a trend towards greater sGAG synthesis in microchanneled constructs, when normalized to DNA. However, total sGAG accumulation was lower in this group. This indicates that while the introduction of microchannels may lead to greater ECM synthesis in constructs, the additional ECM components seem to be lost to the surrounding media and not retained by the constructs. Overall the total sGAG accumulation in the construct is reduced by the introduction of channels.

In conclusion this study presents an approach to modifying the local mechanical environment of chondrocytes, in order to understand their basic cellular mechanobiology and engineer cartilaginous tissues. Although a modified architecture may increase the total production of ECM, it does not lead to a greater overall retention in the engineered construct. Further work must look to develop novel approaches to retain sGAG within the developing tissue.

Appendix II: Finite Element Analysis Methods (Chapter 3)

Finite element analysis was carried out by Dr. Thomas Nagel in the Trinity Centre for Bioengineering. Linear biphasic models were created for both architecture types (channeled- three dimensional model; solid- axisymmetric model) to quantify the spatial variation in biophysical stimuli due to the different architectures. Finite element (FE) models were created using the commercial FE software package MARC (Version 2008r1, MSC Software Corporation, USA). The implementation of a binary mixture within the SOIL model in MARC was used (for further details see (2008)). Models for the channeled constructs were created using a channel diameter of 500μm, with centre-centre spacing of 1mm (Fig. 1f). Care was taken to provide mesh refinements in regions of expected high gradients of mechanical variables. The mesh contained approximately 12,000 elements. 20 noded hexahedral elements with triquadratic interpolation of displacements and trilinear shape functions for

pore pressure were used. A two field variational approach was adopted with the governing nonlinear weak formulation of the initial-boundary value problem consistently linearised for an incremental-iterative solution within a full Newton-Raphson algorithm. Both architecture types (channeled and solid) were modeled in unconfined compression between impermeable platens, with frictionless contact applied between constructs and the compression plate. Accordingly, zero pressure boundary conditions were applied at the free cylindrical surface and the channel surfaces. The nonlinear permeability was modelled as described by (Gu et al., 2003) according to Eqn. 1.

$$\kappa = \kappa_0 \left(\frac{\phi_0^W + e}{\phi_0^W} \right)^n \qquad \textbf{(Eqn. 1)}$$

With κ_0 the initial permeability, ϕ_0^W initial porosity and e the dilatational strain. The values for these parameters and the exponent n were taken from (Gu et al., 2003) and are presented in Table S1. A global axial strain of 10% was applied to mimic the strain applied by the bioreactor. For the model, one representative cycle was modelled with a load-time curve derived directly from the bioreactor protocol. It should be noted that the mean values of the field variables will change during the initial cyclic loading phase due to fluid phase associated relaxation phenomena. The contour and graphical plots generated from the finite element models represent the central cross-sections at the peak of the generated stimulus.

Table S1 Material parameters used to define linear poroelastic models of agarose constructs.

Parameter	Symbol	Value
Young's modulus	E_Y	10 kPa
Poisson's ratio	v	0.1
Initial Porosity	ϕ_0^W	0.98
Initial hydraulic permeability	κ_0	6.61 x 10^{-13} m^4/Ns
Non-linear permeability exponent	n	3.236
Viscosity	μ	10^{-3} Ns/m^2

Appendix III: Supplementary Figures (Chapter 3)

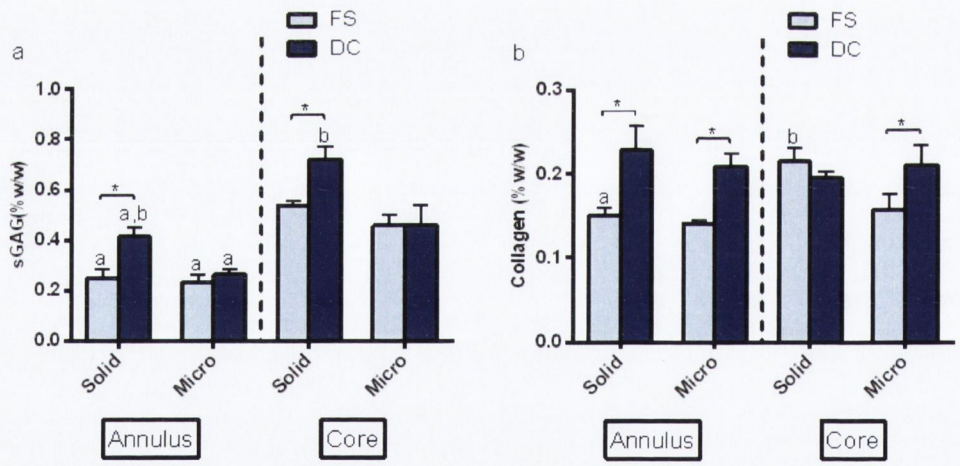

Figure S4: Biochemical composition of core and annular regions for free swelling (FS) and dynamically compressed (DC) solid and microchanneled constructs at day 42 with non-FGF-2 expanded chondrocytes. (a) sGAG content (%w/w); (b) Collagen content (%w/w). a: $p<0.05$ vs. core of same group; b: $p<0.05$ vs. microchannel with same loading conditions in same region. * denotes significant difference with $p<0.05$.

Appendix IV: Supplementary Figures (Chapter 5)

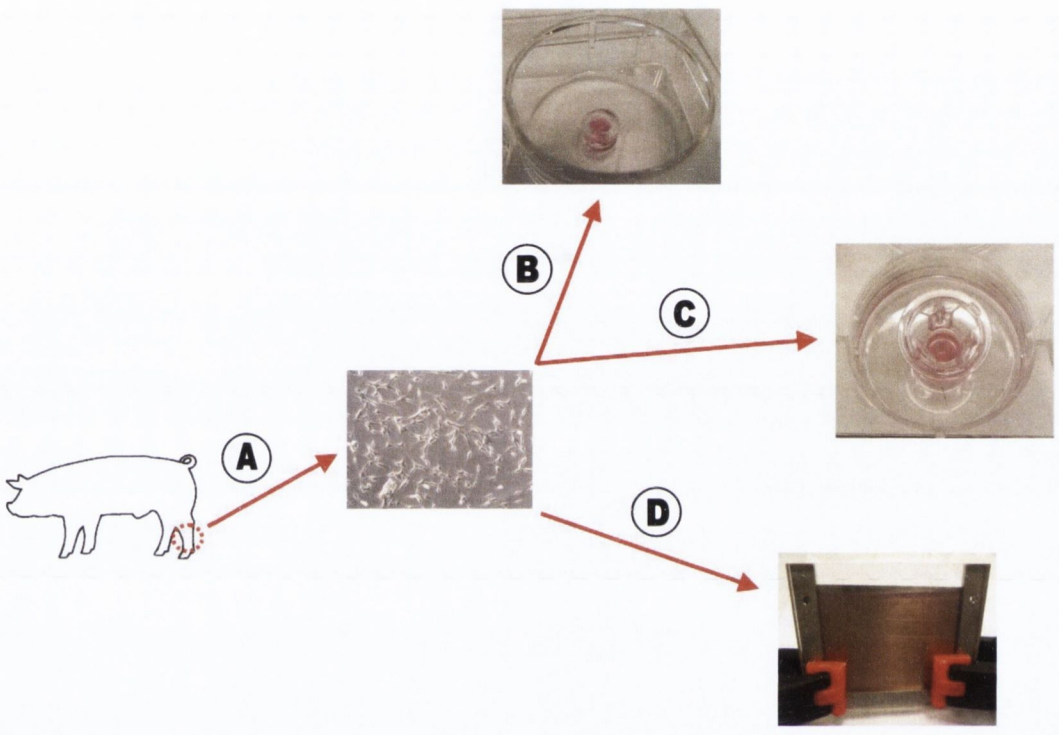

Figure S5: Methodology used for engineering of the constructs. (A) Infrapatellar fat pad-derived stem cells (FPSCs) were isolated from porcine femoropatellar joints. (B) Self-assembled cartilaginous tissues were engineered by geometrically confining FPSCs within PDMS moulds on tissue culture plastic. (C) The study was repeated by using cell culture transwell inserts. (D) Corresponding FPSC encapsulated agarose hydrogels were formed using stainless steel moulds.

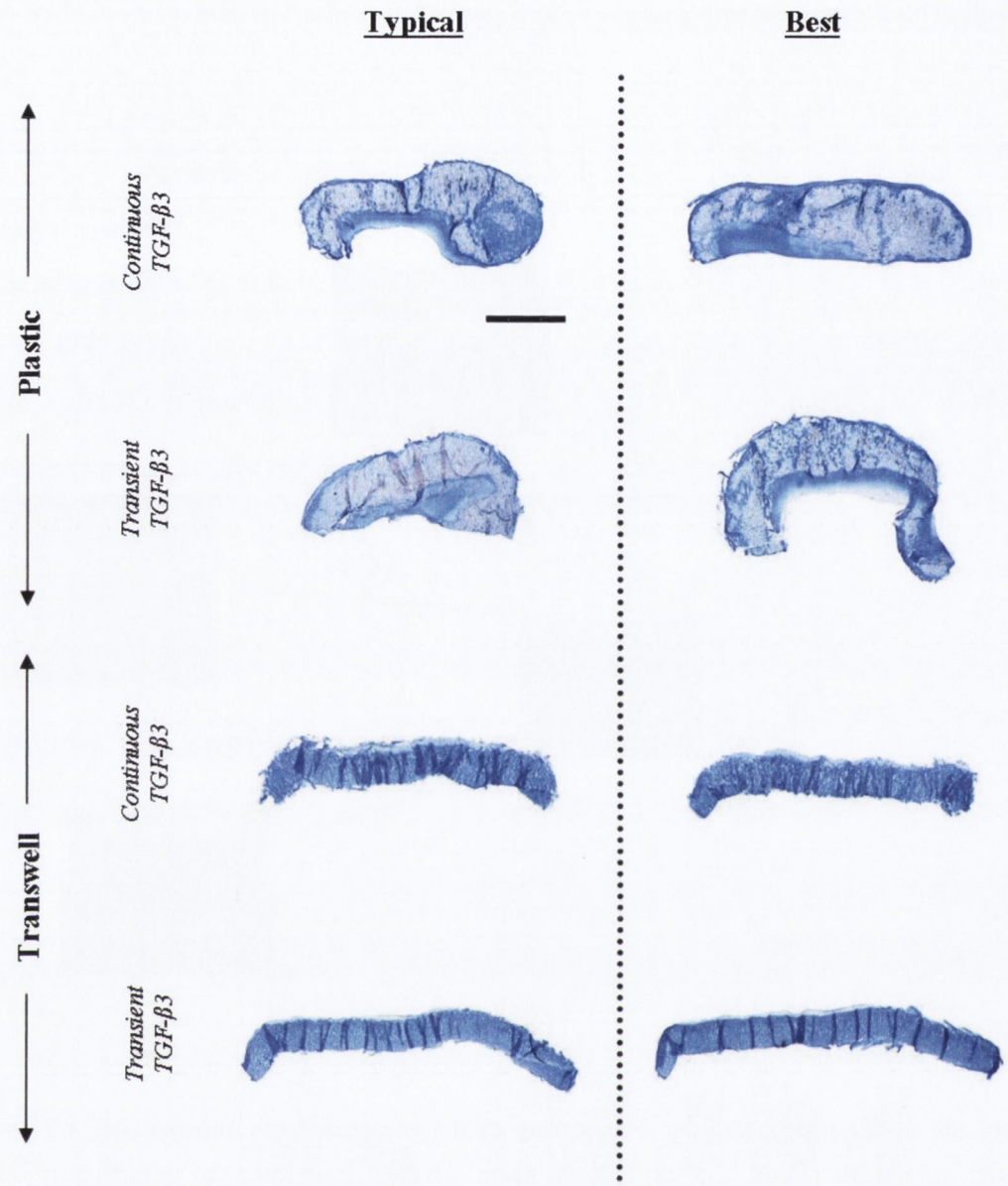

Figure S6: Comparison of typical SA constructs formed and best from each group, for both plastic and transwell studies. Scale bar = 1 mm.

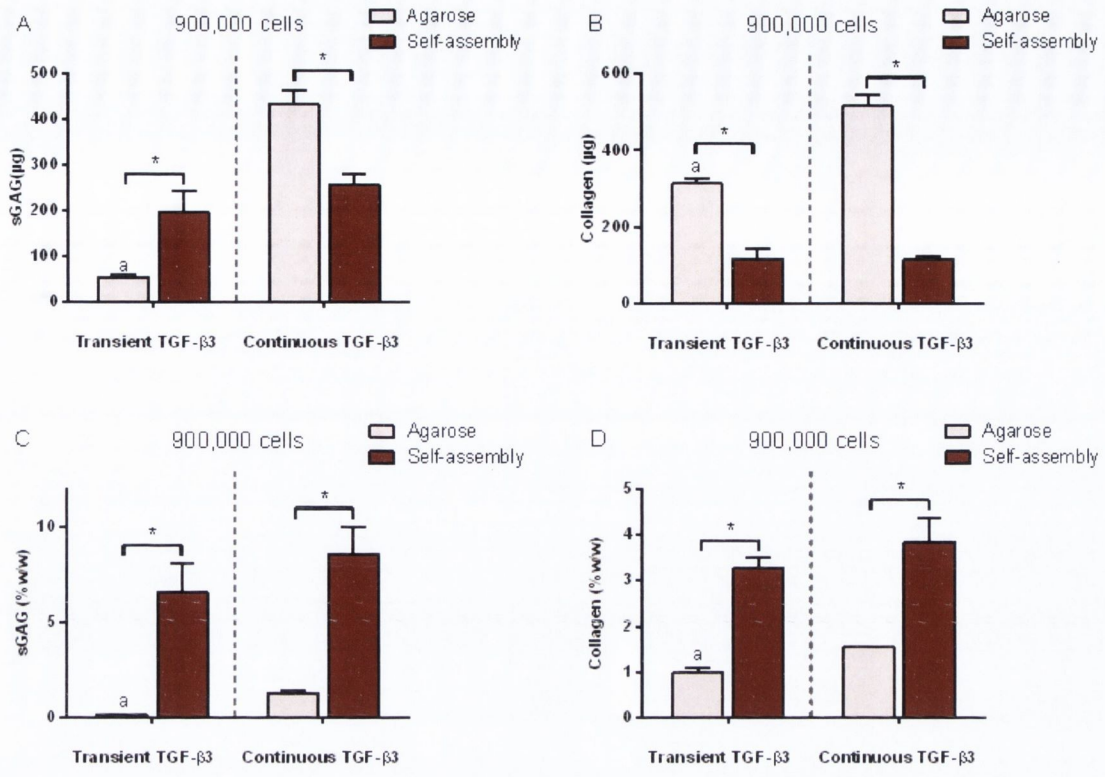

Figure S7: sGAG and collagen content of agarose and self-assembled constructs formed on plastic at day 42 at low seeding density for both transient and continuous TGF-β3 supplementation. (A) sGAG content (µg); (B) collagen content (µg) (C) sGAG content normalized to wet weight (%w/w); (D) collagen content normalized to wet weight (%w/w). [a] $p<0.05$ versus continuous TGF-β3 with same scaffold. *Denotes significant difference with $p<0.05$ (n=4).

Appendix V: Supplementary Figures (Chapter 6)

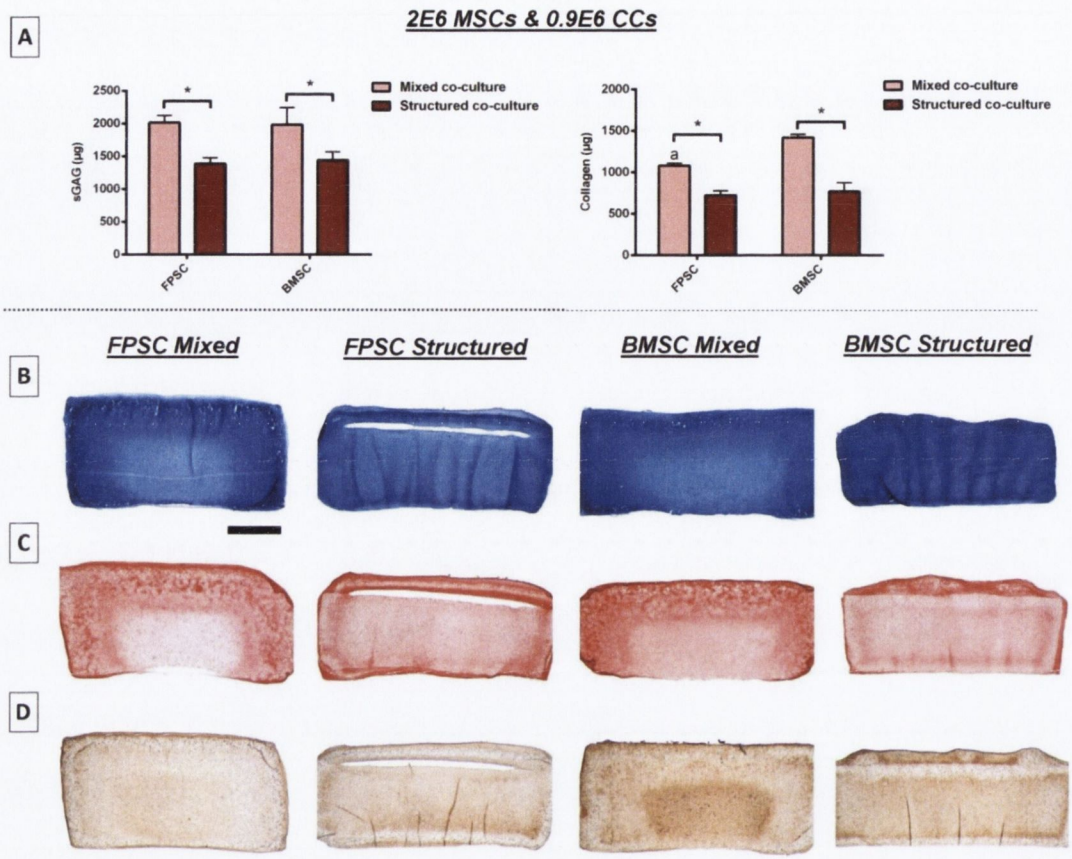

Figure S8: Comparison of mixed to structured co-culture for FPSCs and BMSCs at the 2E6 MSC seeding density at week 5. (A) sGAG and collagen accumulation (µg). (B) Alcian Blue staining for sGAG production. (C) Picrosirius red staining for collagen production. (D) Type II collagen immunohistochemistry staining. [a] $p<0.05$ versus corresponding BMSC group. * denotes significant difference with $p < 0.05$. Scale bar = 1 mm.

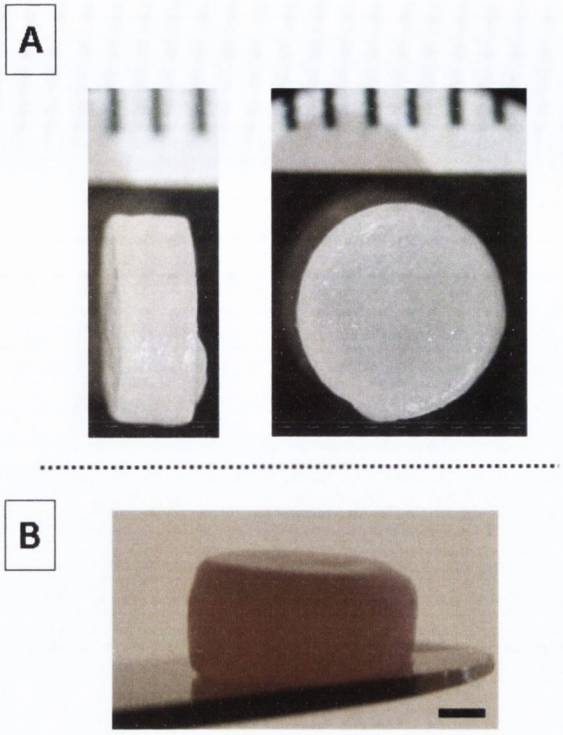

Figure S9: Macroscopic images of structured co-culture constructs at week 5. (A) Structured co-culture construct with 2E6 FPSCs self-assembled on a CC seeded agarose hydrogel. (B) Structured co-culture construct with 4E6 FPSCs self-assembled on a CC seeded agarose hydrogel. Scale bar = 1 mm.

Appendix VI: Supplementary Figures (Chapter 7)

Figure S10: Macroscopic image showing retrieval of osteochondral constructs (5mm diameter) 6 weeks post-implantation (chondral layer formed using self-assembly).

Figure S11: Macroscopic image of nude mouse containing scaled-up osteochondral construct in the shape of the tibial plateau (2cm diameter) 8 weeks post-implantation.